ARTEMISININ - FROM TRADITIONAL CHINESE MEDICINE TO ARTEMISININ COMBINATION THERAPIES; FOUR DECADES OF RESEARCH ON THE BIOCHEMISTRY, PHYSIOLOGY, AND BREEDING OF ARTEMISIA ANNUA

EDITED BY: Tomasz Czechowski, Ian A. Graham, Pamela J. Weathers, Peter E. Brodelius and Geoffrey Duncan Brown

PUBLISHED IN: Frontiers in Plant Science and Frontiers in Bioengineering and Biotechnology

frontiers Research Topics

frontiers

ISSN 1664-8714
ISBN 978-2-88966-158-9
DOI 10.3389/978-2-88966-158-9

About Frontiers

Frontiers is more than just an open-access publisher of scholarly articles: it is a pioneering approach to the world of academia, radically improving the way scholarly research is managed. The grand vision of Frontiers is a world where all people have an equal opportunity to seek, share and generate knowledge. Frontiers provides immediate and permanent online open access to all its publications, but this alone is not enough to realize our grand goals.

Frontiers Journal Series

The Frontiers Journal Series is a multi-tier and interdisciplinary set of open-access, online journals, promising a paradigm shift from the current review, selection and dissemination processes in academic publishing. All Frontiers journals are driven by researchers for researchers; therefore, they constitute a service to the scholarly community. At the same time, the Frontiers Journal Series operates on a revolutionary invention, the tiered publishing system, initially addressing specific communities of scholars, and gradually climbing up to broader public understanding, thus serving the interests of the lay society, too.

Dedication to Quality

Each Frontiers article is a landmark of the highest quality, thanks to genuinely collaborative interactions between authors and review editors, who include some of the world's best academicians. Research must be certified by peers before entering a stream of knowledge that may eventually reach the public - and shape society; therefore, Frontiers only applies the most rigorous and unbiased reviews.
Frontiers revolutionizes research publishing by freely delivering the most outstanding research, evaluated with no bias from both the academic and social point of view. By applying the most advanced information technologies, Frontiers is catapulting scholarly publishing into a new generation.

What are Frontiers Research Topics?

Frontiers Research Topics are very popular trademarks of the Frontiers Journals Series: they are collections of at least ten articles, all centered on a particular subject. With their unique mix of varied contributions from Original Research to Review Articles, Frontiers Research Topics unify the most influential researchers, the latest key findings and historical advances in a hot research area! Find out more on how to host your own Frontiers Research Topic or contribute to one as an author by contacting the Frontiers Editorial Office: researchtopics@frontiersin.org

ARTEMISININ - FROM TRADITIONAL CHINESE MEDICINE TO ARTEMISININ COMBINATION THERAPIES; FOUR DECADES OF RESEARCH ON THE BIOCHEMISTRY, PHYSIOLOGY, AND BREEDING OF ARTEMISIA ANNUA

Topic Editors:
Tomasz Czechowski, University of York, United Kingdom
Ian A. Graham, University of York, United Kingdom
Pamela J. Weathers, Worcester Polytechnic Institute, United States
Peter E. Brodelius, Linnaeus University, Sweden
Geoffrey Duncan Brown, University of Reading, United Kingdom

Citation: Czechowski, T., Graham, I. A., Weathers, P. J., Brodelius, P. E., Brown, G. D., eds. (2020). Artemisinin - From Traditional Chinese Medicine to Artemisinin Combination Therapies; Four Decades of Research on the Biochemistry, Physiology, and Breeding of Artemisia annua. Lausanne: Frontiers Media SA. doi: 10.3389/978-2-88966-158-9

Table of Contents

frontiers in Plant Science

EDITORIAL
published: 18 September 2020
doi: 10.3389/fpls.2020.594565

Editorial: Artemisinin—From Traditional Chinese Medicine to Artemisinin Combination Therapies; Four Decades of Research on the Biochemistry, Physiology, and Breeding of *Artemisia annua*

Tomasz Czechowski[1], *Pamela J. Weathers*[2], *Peter E. Brodelius*[3], *Geoffrey D. Brown*[4] *and Ian A. Graham*[1*]

[1] Centre for Novel Agricultural Products, Department of Biology, University of York, York, United Kingdom, [2] Department of Biology and Biotechnology, Worcester Polytechnic Institute, Worcester, MA, United States, [3] Department of Chemistry and Biomedical Sciences, Linnaeus University, Kalmar, Sweden, [4] Department of Chemistry, University of Reading, Reading, United Kingdom

Keywords: ***Artemisia annua*, artemisinin, semi-synthetics, molecular breeding, malaria**

OPEN ACCESS

Edited and reviewed by:
Zeng-Yu Wang,
Qingdao Agricultural University, China

***Correspondence:**
Ian A. Graham
ian.graham@york.ac.uk

Specialty section:
This article was submitted to Plant Biotechnology, a section of the journal Frontiers in Plant Science

Received: *13 August 2020*
Accepted: *08 September 2020*
Published: *18 September 2020*

Citation:
Czechowski T, Weathers PJ, Brodelius PE, Brown GD and Graham IA (2020) Editorial: Artemisinin—From Traditional Chinese Medicine to Artemisinin Combination Therapies; Four Decades of Research on the Biochemistry, Physiology, and Breeding of Artemisia annua. Front. Plant Sci. 11:594565. doi: 10.3389/fpls.2020.594565

Editorial on the Research Topic

Artemisinin—From Traditional Chinese Medicine to Artemisinin Combination Therapies; Four Decades of Research on the Biochemistry, Physiology, and Breeding of *Artemisia annua*

The 2015 Nobel Prize in Physiology or Medicine was awarded to Tu Youyou for her "discoveries concerning a novel therapy against malaria". Educated in pharmaceutical sciences, Tu was recruited to Chinese military research Program 523, with the aim of finding new drugs for the treatment of malaria. A malaria epidemic during the Vietnam War had led Ho Chí Minh, the Prime Minister of North Vietnam, to request medical help from China. In response, Chairman Mao approved Project 523, which involved over 500 scientists, military personnel, and medical practitioners and ran from 1967 to 1980. Whilst reviewing written records of traditional Chinese medicine, Tu noticed a mention of Qinghao (*Artemisia annua*) for alleviation of malaria fevers in Ge Hong's "A handbook of prescriptions for emergencies", which has been dated to around 317–420 A.D. She next found that an ethyl ether extract from *A. annua* leaves strongly inhibited malaria, leading Tu and two other members of her team to test the Qinghao plant extract for safety and side-effects on themselves. In 1972, Tu´s team obtained the pure active substance from this extract and determined its chemical structure, naming it as qinghaosu, or artemisinin, as it became more commonly known in the West. A series of chemical derivatives of artemisinin were subsequently developed by Project 523, including dihydroartemisinin, artemether, and artesunate. These compounds have become part of the artemisinin combination therapies (ACTs), currently the World Health Organisation (WHO)-recommended first-line drugs to combat malaria.

Almost fifty years after Tu´s discovery, malaria still poses a global threat, with an estimated 228 million cases occurring worldwide in 2018 causing 405,000 deaths – two thirds of them among children under 5 years old in sub-Saharan Africa (World malaria report, 2019). The introduction of ACTs (it is estimated that 3 billion treatment courses have been procured worldwide between 2010

and 2018), rapid diagnostic tests (RDTs) and malaria vector controls, including insecticide-treated mosquito nets, reduced the number of cases significantly over the past 10 years (World malaria report, 2019). However, artemisinin resistance conferred by genetic mutations in *Plasmodium falciparum* recently emerged in the Greater Mekong sub-region (Ariey et al., 2014) together with *Pfhrp2/3* gene deletions that render parasites undetectable by RDT (Owusu et al., 2018), represent major new threats in the global fight against malaria.

A. annua remains the sole global source of the drug at the time of writing, despite significant efforts to develop alternative production platforms, as discussed herein. National malaria programmes delivered 214 million ACT treatment courses in 2018 (WHO Malaria report, 2019), equating to around 100 metric tonnes of pure artemisinin obtained from *A. annua* (assuming 0.5 g artemisinin per treatment). The plant-sourced drug demand stimulated breeding efforts to improve yields. Widely practiced phenotypic selection of open pollination varieties has been supplemented by modern molecular breeding approaches, resulting in *A. annua* F1 hybrids that yield almost 55 kg of artemisinin per hectare with a content reaching 1.44% of leaf dry weight (Artemisia F1 Seed). Several publications herein suggest that natural variation within *A. annua* populations may have even more to offer in terms of further improving yields. Wetzstein et al. show that further yield improvements can be achieved through the use of phenotypic-based selection and clonally propagating high-yielding genotypes. Work from Ferreira et al. shows the importance of a thorough understanding of seasonal variation of artemisinin content in the *A. annua* crop when planning harvest and maximising artemisinin returns from plantations. That work also highlights existing differences in response to photoperiod among different chemotypes of *A. annua*. Czechowski et al. shed new light on the molecular basis of the existence of high- and low- artemisinin producing chemotypes, providing candidate targets for yield improvement through molecular breeding.

Transgenic routes, also being explored for further artemisinin yield improvement in *A. annua*, have resulted in the elucidation of much of the artemisinin biosynthetic pathway and the identification of multiple transcriptional regulators of biosynthetic genes, as reviewed by Ikram and Simonsen The same work also reviews transgenic approaches that have succeeded in achieving an artemisinin content of 2.6% leaf dry weight by overexpressing biosynthetic genes; and over 3%, when metabolic pathways competing for the five-carbon isoprenoid precursors are blocked. Ma et al. and Tang et al. report on further transgenic approaches that identify additional genes involved in the regulation of artemisinin biosynthesis in *A. annua*. Fu et al. present work adding to the sparse knowledge of the transport systems potentially involved in regulation of artemisinin biosynthesis, which may prove to be a valuable alternate route for genetic improvement of artemisinin production. A number of the transgenic approaches to improve artemisinin yield appear to come at the cost of plant biomass and fitness, highlighting the need for extensive field trials to validate laboratory and glasshouse data. Regulatory approval will be required before release of these GMOs, which remains a challenge for this high-profile medicinal plant. Transgenics is, of course, also an extremely valuable experimental tool for characterisation of *in planta* gene function, yielding knowledge that is useful for both genome editing and molecular breeding. In this context, Zhang et al. report on the characterisation of genes involved in the supply of isoprene precursors from the MEP-pathway and Catania et al. report on the effects of silencing the first committed step in artemisinin biosynthesis using an RNAi approach. This latter study also opens up the prospect of using *A. annua* as a production platform for other high value sesquiterpenes.

Attempts to transfer artemisinin production to other plant and microbial hosts are reviewed by Ikram and Simonsen and Kung et al. Achievements of the Keasling group in engineering *Saccharomyces cerevisiae* that produces the artemisinin precursor, artemisinic acid, at yields of 25 g/L remains an exemplar for successful metabolic engineering (Paddon et al., 2013). However, costs associated with the non-enzymatic photochemical conversion of artemisinic acid to artemisinin have proved too expensive to allow the semi-synthetic route to compete with plant-based production, where both enzymatic and non-enzymatic steps are conducted in glandular secretory trichomes, which are specialized 10-cell structures found on the surface of the leaf, stems and flower buds (Peplow, 2016). Kung et al. discuss recent developments in the chemical conversions of artemisinic acid to artemisinin potentially replacing costly photochemical processes developed by Sanofi, raising the prospect once again of an alternative source of artemisinin that would help stabilise supply.

Ikram and Simonsen review the prospect of engineering plant heterologous systems for artemisinin production and report a proof-of-concept in *Nicotiana* species, albeit at yields significantly less than for *A. annua* itself. The presence of endogenous glycosyltransferases in *Nicotiana* species that are able to glycosylate the engineered artemisinin precursors, rendering them unsuitable for further spontaneous conversions into artemisinin, makes the use of these species as production hosts particularly challenging. In an effort to find an alternative host with less glycosyltransferase activity, Ikram et al. have evaluated the non-vascular plant, *Physcomitrella patens*. The artemisinin levels achieved in this moss species were significantly higher than those from *Nicotania* species, but still around 100-times lower than those found in *A. annua*.

The use of monotherapies that rely on artemisinin or its derivatives as the sole antimalarial agents is not recommended by the World Health Organisation since this practice significantly increases the risk of the emergence of parasite resistance. Some previous literature has supported the use of *A. annua* herbal remedies as cost-effective alternatives to ACTs with the suggestion that artemisinin works in combination with other compounds, such as flavonoids (for example Weathers et al., 2014). Czechowski et al. used *in vitro* assays with whole plant extracts from a series of *A. annua* mutants, deficient in either the production of artemisinin or flavonoids, to demonstrate that artemisinin is the sole metabolite from *A. annua* with *in vitro* anti-plasmodial activity. The possibility of other compounds having *in vivo* effects was also discussed as it is recognised that *in vitro* and *in vivo* studies do not always recapitulate

one another in therapeutics development. This study has recently been cited as evidence in a WHO position paper that does not support the promotion or use of Artemisia plant material in any form for the prevention or treatment of malaria (WHO, 2019).

AUTHOR CONTRIBUTIONS

All authors contributed to the production of the Research Topic and/or the editorial.

REFERENCES

Ariey, F., Witkowski, B., Amaratunga, C., Beghain, J., Langlois, A. C., Khim, N., et al. (2014). A molecular marker of artemisinin-resistant Plasmodium falciparum malaria. *Nature* 505 (7481), 50–55. doi: 10.1038/nature12876

Artemisia F1 Seed. Available at: https://www.artemisiaf1seed.org (Accessed July 21, 2020).

Owusu, E. D. A., Djonor, S. K., Brown, C. A., Grobusch, M. P., and Mens, P. F. (2018). Plasmodium falciparum diagnostic tools in HIV-positive under-5-year-olds in two ART clinics in Ghana: are there missed infections? *Malar J.* 17 (1), 92. doi: 10.1186/s12936-018-2231-7

Paddon, C. J., Westfall, P. J., Pitera, D. J., Benjamin, K., Fisher, K., McPhee, D., et al. (2013). High-level semi-synthetic production of the potent antimalarial artemisinin. *Nature* 496 (7446), 528–532. doi: 10.1038/nature12051

Peplow, M. (2016). Synthetic biology's first malaria drug meets market resistance. *Nature* 530 (7591), 389–390. doi: 10.1038/530390a

Weathers, P. J., Towler, M., Hassanali, A., Lutgen, P., and Engeu, P. O. (2014). Dried-leaf Artemisia annua: A practical malaria therapeutic for developing countries? *World J. Pharmacol.* 3 (4), 39–55. doi: 10.5497/wjp.v3.i4.39

WHO (2019). *The use of non-pharmaceutical forms of Artemisia* (Geneva: World Health Organization). Licence: CC BY-NC-SA 3.0 IGO.

World malaria report 2019 (2019). *Licence: CC BY-NC-SA 3.0 IGO* (Geneva: World Health Organization).

Conflict of Interest: The authors declare that the research was conducted in the absence of any commercial or financial relationships that could be construed as a potential conflict of interest.

frontiers in Bioengineering and Biotechnology

ORIGINAL RESEARCH
published: 15 August 2017
doi: 10.3389/fbioe.2017.00047

Stable Production of the Antimalarial Drug Artemisinin in the Moss *Physcomitrella patens*

*Nur Kusaira Binti Khairul Ikram[1,2,3], Arman Beyraghdar Kashkooli[4], Anantha Vithakshana Peramuna[3], Alexander R. van der Krol[4], Harro Bouwmeester[5] and Henrik Toft Simonsen[3]**

[1] Faculty of Science, Institute of Biological Sciences, University of Malaya, Kuala Lumpur, Malaysia, [2] Department of Plant and Environmental Sciences, University of Copenhagen, Frederiksberg, Denmark, [3] Department of Biotechnology and Biomedicine, Technical University of Denmark, Kongens Lyngby, Denmark, [4] Laboratory of Plant Physiology, Wageningen University, Wageningen, Netherlands, [5] Plant Hormone Biology Lab, Swammerdam Institute for Life Sciences, University of Amsterdam, Amsterdam, Netherlands

Malaria is a real and constant danger to nearly half of the world's population of 7.4 billion people. In 2015, 212 million cases were reported along with 429,000 estimated deaths. The World Health Organization recommends artemisinin-based combinatorial therapies, and the artemisinin for this purpose is mainly isolated from the plant *Artemisia annua*. However, the plant supply of artemisinin is irregular, leading to fluctuation in prices. Here, we report the development of a simple, sustainable, and scalable production platform of artemisinin. The five genes involved in artemisinin biosynthesis were engineered into the moss *Physcomitrella patens via* direct *in vivo* assembly of multiple DNA fragments. *In vivo* biosynthesis of artemisinin was obtained without further modifications. A high initial production of 0.21 mg/g dry weight artemisinin was observed after only 3 days of cultivation. Our study shows that *P. patens* can be a sustainable and efficient production platform of artemisinin that without further modifications allow for industrial-scale production. A stable supply of artemisinin will lower the price of artemisinin-based treatments, hence become more affordable to the lower income communities most affected by malaria; an important step toward containment of this deadly disease threatening millions every year.

Keywords: ***Physcomitrella patens*, malaria, artemisinin, *in vivo* assembly, bioengineering**

OPEN ACCESS

Edited by:
Pamela J. Weathers, Worcester Polytechnic Institute, United States

Reviewed by:
Fumihiko Sato, Kyoto University, Japan
Kashmir Singh, Panjab University, India

****Correspondence:***
Henrik Toft Simonsen
hets@dtu.dk

Specialty section:
This article was submitted to Plant Biotechnology, a section of the journal Frontiers in Bioengineering and Biotechnology

Received: *19 April 2017*
Accepted: *28 July 2017*
Published: *15 August 2017*

Citation:
Khairul Ikram NKB, Beyraghdar Kashkooli A, Peramuna AV, van der Krol AR, Bouwmeester H and Simonsen HT (2017) Stable Production of the Antimalarial Drug Artemisinin in the Moss Physcomitrella patens. Front. Bioeng. Biotechnol. 5:47. doi: 10.3389/fbioe.2017.00047

INTRODUCTION

Physcomitrella patens is a non-vascular plant that has been well established as a model organism to be used in basic research and in applied biotechnology (Simonsen et al., 2009; Buttner-Mainik et al., 2011; Ikram et al., 2015; Reski et al., 2015). The genome is fully sequenced and the haploid life cycle and efficient homologous recombination makes *P. patens* an attractive industrial production system compared to other plant hosts (Schaefer and Zrÿd, 1997; Reski, 1998). Additionally, a novel transformation technology involving *in vivo* assembly of multiple DNA fragments in *P. patens* has been established, further increasing the potential as a photosynthetic chassis for synthetic biology (King et al., 2016). Currently, several recombinant pharmaceutical proteins and molecules of commercial value are being produced in this system (Anterola et al., 2009; Zhan et al., 2014; Pan et al., 2015; Reski et al., 2015).

Artemisinin originates from the plant *Artemisinia annua* and is the first-choice treatment for malaria (Novotny et al., 1966). Chemically, artemisinin is a sesquiterpene lactone bearing a unique endoperoxide structure and its complex structure makes it difficult and not economically feasible to be chemically synthesized (Pandey and Pandey-Rai, 2016). Several efforts have been made to obtain artemisinin from a stable source, such as yeast (Ro et al., 2006), where a production of artemisinic acid followed by a three-step chemical synthesis to artemisinin was established (Paddon and Keasling, 2014). It was previously shown that artemisinin could be mass-produced by cultivation of *A. annua* or semi-synthetically in microorganisms producing artemisinic acid (Paddon and Keasling, 2014). Besides these efforts, extensive bioengineering of modified *Nicotiana* plants (Malhotra et al., 2016; Wang et al., 2016) has provided limited production of artemisinin. However, these have not yet been used for large-scale production. Currently, there are no reports on the stable heterologous biosynthesis of artemisinin in photosynthetic organisms that can be grown in bioreactors.

In order to produce artemisinin in *P. patens*, we introduced the five genes responsible for the biosynthesis of dihydroartemisinic acid (**Figure 1**), where amorpha-4,11-diene synthase, *ADS* (Komatsu et al., 2010) catalyzes the first step. This was followed by the second step, the cytochrome P450, *CYP71AV1* (Ro et al., 2006) which we linked with the third step, the alcohol dehydrogenase 1 (*ADH1*) (Paddon et al., 2013) by the hybrid LP4/2A peptide linker (François et al., 2004). Finally, we introduced the fourth step catalyzed by double-bond reductase 2 (*DBR2*) (Zhang et al., 2008) and the fifth step, being the aldehyde dehydrogenase 1 (*ALDH1*) (Teoh et al., 2009). These five genes would yield dihydroartemisinic acid. The final conversion of dihydroartemisinic acid into artemisinin is thought to occur by photooxidation (Sy and Brown, 2002), thus the enzymatic end product is dihydroartemisinic acid. The five genes were transformed into *P. patens* using *in vivo* homologous recombination that allows multiple DNA fragments to be transformed at once into the genome (King et al., 2016). Here, we show that engineered *P. patens* can produce significant levels of artemisinin. This could become a sustainable and efficient production platform of artemisinin, which could potentially help to stabilize the supply of artemisinin and aid in containing malaria.

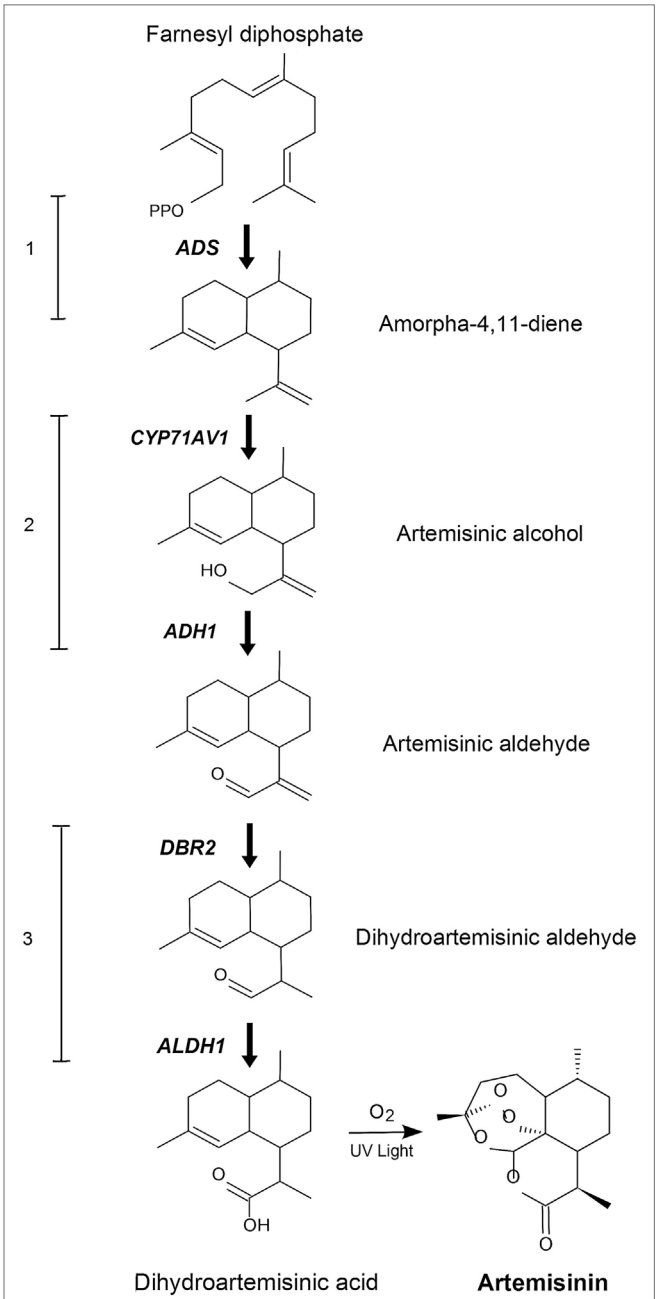

FIGURE 1 | Schematic representation of the engineered artemisinin biosynthetic pathway in *Physcomitrella patens*. The five genes that encode the dihydroartemisinic acid biosynthetic pathway are *ADS*, amorphadiene synthase; *CYP71AV1*, amorphadiene oxidase; *ADH1*, alcohol dehydrogenase 1; *DBR2*, artemisinic aldehyde double-bond reductase; *ALDH1*, aldehyde dehydrogenase 1. The numbers 1–3 indicates transformation sets.

MATERIALS AND METHODS

P. patens Material and Growth Conditions

Physcomitrella patens (Gransden ecotype, International Moss Stock Center #40001) was grown on solid and liquid PhyB media under sterile conditions, at 25°C with continuous 20–50 W/m^2 light intensity. For PhyB media mix 800 mg $Ca(NO_3)_2$, 250 mg $MgSO_4{\cdot}7H_2O$, 12.5 mg $FeSO_4{\cdot}7H_20$, 0.5 g $(NH_4)_2C_4H_4O$, 10 mL KH_2PO_4 buffer (25 g KH_2PO_4 per liter and adjusted to pH 6.5 with 4 M KOH), and 0.25 mL trace element solution (110 mg $CuSO_4{\cdot}5H_20$, 110 mg $ZnSO_4{\cdot}7H_2O$, 1,228 mg H_3BO_3, 778 mg $MnCl_2{\cdot}4H_2O$, 110 mg $CoCl_2{\cdot}6H_2O$, 53 mg KI, 50 mg $Na_2MoO_4{\cdot}2H_2O$ per liter). The medium can be solidified with 0.7% (w/v) agar and is sterilized by autoclaving at 121°C (Bach et al., 2014).

Transformation of *P. patens*

A detailed description of *P. patens* transformation was previously published (Bach et al., 2014). Five days cultured *P. patens* with approximately 1.5 g (fresh weight) was digested

by adding 1 mL of 0.5% DriselaseR enzyme solution in 8.5% mannitol (Sigma D9515) for every 40 mg of *P. patens* tissue. The tissue was incubated at room temperature with occasional gentle shaking for 30–60 min before filtering through a 100-µm pored mesh-filter. The filtrate was collected by centrifugation at 150–200 × *g* for 4 min with slow breaking. The pellet was washed twice with protoplast wash solution (8.5% mannitol, 10 mM $CaCl_2$). Protoplast density was measured using a hemocytometer, and resuspended in MMM solution (9.1% D-mannitol, 10% MES, and 15 mM $MgCl_2$) at a concentration of 1.6×10^6 protoplasts/mL. 300 µL of the protoplast suspension and 300 µL of PEG solution were added to a 15-mL tube containing 10 µg total DNA followed by incubation in a water bath for 5 min at 45°C and another 5 min at room temperature. 300 µL of 8.5% D-mannitol were added five times followed by another five times dilutions with 1 mL of 8.5% D-mannitol. Transformed protoplasts were pelleted by centrifugation and resuspended in 500 µL of 8.5% D-mannitol and 2.5 mL of protoplast regeneration media (top layer; PRMT). 1 mL of the mixture was dispensed on three plates containing protoplast regeneration media (bottom layer; PRMB) overlaid with cellophane. The plates were incubated in continuous light for 5–7 days at 25°C. The cellophane and regenerating protoplasts were then transferred to PhyB media containing the appropriate selection marker for 2 weeks, before transferring on PhyB media without antibiotics for another 2 weeks. This process was repeated twice, after which the stable transformants was kept on PhyB media with biweekly subcultivation including blending in sterile water until further use.

DNA Fragments and Genes

The Pp108 locus homologous recombination flanking regions were amplified from *P. patens* genomic DNA. The *ADS* gene was a kind gift from Assoc. Prof. Dae Kyun Ro, University of Calgary, Canada. The synthetic genes *CYP71AV1* (DQ268763), *ADH1* (JF910157.1), *DBR2* (EU704257.1), and *ALDH1* (FJ809784.1) were codon-optimized according to the *P. patens* codon usage by GenScript, USA. The Ubiquitin promoter and Ubiquitin terminator from *Arabidopsis thaliana* (CP002686.1) synthetic genes were also purchased from GenScript. The Maize Ubiquitin 1 promoter and G418 selection cassettes were obtained from the pMP1355 vector, a kind gift from Prof. Mark Estelle, University of California San Diego, USA. The rice actin promoter and hygromycin selection cassette were obtained from the pZAG1 vector, a kind gift from Assoc. Prof. Yuji Hiwatashi from Miyagi University, Japan.

PCR, DNA Purification and Concentration

The DNA fragments were amplified using PhusionR High-Fidelity DNA Polymerase (New England Biolabs). The primers used are listed in Table S1 in Supplementary Material. PCR conditions and annealing temperatures were modified depending on primers and templates used in the reaction. PCR reactions using plasmid DNA as template were digested with DpnI (NEB, USA) for 1 h at 37°C followed by inactivation at 65°C for 20 min to lower background after transformation. PCR products were purified using QIAquick PCR Purification Kit (QIAGEN GmbH, Germany). The DNA fragments for transformations were concentrated *via* ethanol precipitation to a final concentration of ~1 µg/µL, determined using NanoDrop2000 (Thermo Fisher Scientific).

GC–MS Analysis of Amorpha-4,11-Diene

Amorpha-4,11-diene production was measured using a Shimadzu GCMS-QP2010 Plus (GC-2010). The initial screening was performed by HS-SPME (Headspace-Solid Phase Micro-Extraction) (Drew et al., 2012; Andersen et al., 2015). Quantification of amorpha-4,11-diene was performed according to a published protocol (Rodriguez et al., 2014). One-week-old *P. patens* was blended in sterile water using a Polytron (PT 1200 E, Kinematic AG) to a final concentration of 0.2 g/mL (fresh weight). Two milliliters of the blended *P. patens* were inoculated into 20 mL liquid PhyB media and cultivated on a shaker under standard conditions for 4 days. Then, 2 mL of decane were added into the *P. patens* culture and cultivation was continued for up to 2 weeks. After 2 weeks, 100 µL of decane was harvested and diluted twice in ethyl acetate spiked with an internal standard (trans-caryophyllene), and analyzed by GC–MS. 1 µL of the extract was injected in split mode and separated with HP-5MS UI column (20.0 m × 0.18 mm × 0.18 µm) with hydrogen as a carrier gas. The GC program was as follows, injection temperature of 250°C, oven temperatures of 60°C for 3 min and 60–320°C at 40°C/min. The amorpha-4,11-diene concentration was calculated based on the calibration curve of the internal standard run in parallel (Rodriguez et al., 2014).

P. patens Growth and Biomass Measurements

Physcomitrella patens lines were blended in sterile water and subcultivated onto PhyB. After 1 week, the *P. patens* was blended for 30 s in sterile water, normalized to a concentration of 0.2 g/mL (fresh weight) as previously described (Zhan et al., 2014; Pan et al., 2015). 2 mL of the blended *P. patens* was inoculated into 20 mL liquid PhyB media and cultivated on a horizontal shaker under standard conditions without aeration. The *P. patens* cultures were prepared in 3 replicates and harvested in 3, 6, 12, 15, and 18 days. The harvested *P. patens* tissue was dried overnight in an oven at 90°C and weighed.

Metabolite Extraction and UPLC-MRM-MS Analysis

Physcomitrella patens lines were blended in sterile water and subcultivated onto PhyB. After 1 week the fresh *P. patens* samples were harvested, snap-frozen, and ground into a fine powder. Samples of 3,000 mg were extracted with 3 mL citrate phosphate buffer, pH 5.4, followed by vortexing and sonication for 15 min. 1 mL Viscozyme (Sigma V2010) was added and samples were incubated at 37°C. The whole mixture was then extracted three times with 3 mL ethyl acetate, concentrated to a volume of 1 mL, and stored at −20°C. For liquid culture extracts, 500 mL of liquid culture was harvested, passed through a filter paper and extracted with 200 mL of ethyl acetate in a separation funnel. Ethyl acetate was concentrated to a volume of 1 mL and stored at −20°C. Ethyl

acetate of both liquid culture and *P. patens* sample extracts were then dried under a flow of N_2 and resuspended into 300 µL of 75% MeOH:H_2O (V:V). Extracts were passed through a 0.45-µm membrane filter (Minisart® RC4, Sartorius, Germany) before analysis.

Artemisinin and artemisinin biosynthesis pathway intermediates were measured in a targeted approach by using a Waters Xevo tandem quadrupole mass spectrometer equipped with an electrospray ionization source and coupled to an Acuity UPLC system (Waters), essentially as described before (Ting et al., 2013). A BEH C18 column (100 mm × 2.1 mm × 1.7 µm; Waters) was used for chromatographic separation by applying a water:acetonitrile gradient. The gradient started with 5% (v/v) acetonitrile in water with formic acid [1:1,000 (v/v)] for 1.25 min, then raised to 50% in 2.35 min and further raised to 90% at 3.65 min. This was kept for 0.75 min before returning to the 5% acetonitrile/water (v/v) with formic acid [1:1,000 (v/v)] by using a 0.15-min gradient. The same solvent composition was used to equilibrate the column for 1.85 min. The flow rate was 0.5 mL/min, and the column temperature was maintained at 50°C. Injection volume was set to 10 µL. Desolvation and cone gas flow were set to 1,000 and 50 L/h, and the mass spectrometer was operated in positive ionization mode. Capillary voltage was set at 3.0 kV. Desolvation and source temperatures were set at 650 and 150°C, respectively. The cone voltage was optimized for all metabolites using the Waters IntelliStart MS Console. Fragmentation by collision-induced dissociation was done in the ScanWave collision cell using argon. Multiple Reaction Monitoring (MRM) was used for detection and quantification of artemisinin. MRM transitions for artemisinin and pathway intermediates measurement settings were optimized for MRM channels, which are presented in (Table S2 in Supplementary Material). Artemisinin and dihydroartemisinic acid were gifts from Dafra Pharma (Belgium). Other precursors were synthesized from dihydroartemisinic acid by Chiralix (Nijmegen, the Netherlands) and were then examined by NMR (>98% purity). External calibration curves were measured by using reference standards. The metabolite profiling was performed twice with 2 months apart, using the same original cell lines that had been subcultivated four times on PhyB media in between the analysis.

Analysis of Conjugated Artemisinin Biosynthesis Pathway Intermediates by LC-QTOF-MS

In order to analyze the putative conjugated forms of artemisinin biosynthesis pathway intermediates, *P. patens* lines were blended in sterile water and subcultivated onto PhyB. After 1 week, 100 mg of fresh *P. patens* was ground in liquid nitrogen and extracted with 300 µL MeOH:formic acid [1,000:1 (v/v)]. Samples were briefly vortexed and sonicated for 15 min, followed by 15 min centrifugation at 13,000 × *g*. Extracts were passed through a 0.45-µm membrane filter (Minisart® RC4, Sartorius, Germany) before analysis on a Water alliance 2795 HPLC connected to a QTOF Ultima V 4.00.00 mass spectrometer (Waters. MS technologies, UK). The mass spectrometer was operated in negative ionization mode. A precoloumn of 2.0 mm × 4 mm (Phenomenex, USA) was connected to the C18 analytical column (Luna 3 µm C18/2 100A; 2.0 mm × 150 mm; Phenomenex, USA). Degassed eluent A and B were HPLC-grade water:formic acid [1,000:1 (v/v)] and acetonitrile:formic acid [1,000:1 (v/v)], respectively. The flow rate was 19 mL/min. The HPLC gradient started from 5% eluent B and linearly increased to 75% in 45 min. after that the column was equilibrated for 15 min with 5% eluent B. 5 µL of each sample was used for injection.

P. patens Cell Components Isolation and Extraction

Physcomitrella patens protoplasts were isolated according to a previously published protocol (Bach et al., 2014). The *P. patens* lines were blended in sterile water and subcultivated onto PhyB. After 1 week, protoplast were isolated and pelleted by centrifugation at 150–200 × *g* for 4 min with slow breaking. Supernatant, which contained the apoplast (AP) was harvested and 10 mL of ultra-pure water was added to the pelleted protoplast to lyse the cells. Lysed cells were centrifuged at 6,000 × *g* for 10 min, and 7 mL of the supernatant was mixed with an equal amount of sucrose to a final concentration of 0.3 M. The mixture was loaded into an ultracentrifuge tube with a 2 mL over-lay of water and centrifuged at 135,000 × *g* for 40 min at room temperature using a swinging bucket rotor. The bottom layers containing the cytoplasm (CT) and the cell pellet (CP) was harvested. The top layer (1.5 mL) containing neutral lipid bodies (LBs) was transferred to another centrifuge tube, mixed with sucrose to a final concentration of 0.3 M, overlaid with 2 mL of water as before, and 1 mL of the top-most layer of the LBs after centrifugation at 135,000 x *g* for 40 min. The harvested samples; AP, CT, LBs, and CP was then extracted with 3 mL ethyl acetate and concentrated to a volume of 1 mL and stored at −20°C. The samples were then dried under a flow of N_2 and resuspended into 300 µL of 75% MeOH:H_2O (V:V). Extracts were passed through a 0.45-µm membrane filter (Minisart® RC4, Sartorius, Germany) before analysis.

RESULTS AND DISCUSSIONS

Engineering of *P. patens*

We introduced *ADS* under the control of the strong constitutively expressed promoter, Ubiquitin1 from *Zea mays* with geneticin (G418) as resistance cassette. After two rounds of selection the *ADS* product amorpha-4,11-diene was detected in 11 lines with an average content of 200 mg/L, which is higher than in *A. annua* (Ma et al., 2009), *Nicotiana tabacum* (Wallaart et al., 2001), *E. coli* (Martin et al., 2003), and yeast (Ro et al., 2006). An encouraging initial result was achieved without further optimization of terpenoid biosynthesis. The best producing line was selected for further transformation with *CYP71AV1* and *ADH1*. The *CYP71AV1*-LP4/2A-*ADH1* construct was controlled by the rice actin promoter with hygromycin resistance cassette. The genome homologous overhang was targeted to remove the previously integrated G418 cassette during the recombination event. Of 47 transformed lines, 11 were chemo- and genotyped and one line was selected for transformation with the final genes, *DBR2* and *ALDH1*. The *DBR2*-LP4/2A-*ALDH1* construct was

controlled by the Arabidopsis Ubiquitin promoter and the G418 selection cassette was used again. The hygromycin cassette was targeted for recombination to remove this selection marker. Three independent transformants were recovered, and genotyping showed that the five genes in the biosynthesis of dihydroartemisinic acid were integrated into the genome (Figure S1 in Supplementary Material). PCR analysis showed there was no untargeted integration for the selected lines. This showed that the selected *P. patens* lines have a uniform integration of the five genes and one copy of each.

Metabolite Profiling and Growth of Engineered Strains

Extracts of the transgenic *P. patens* lines containing all five genes were analyzed using ultra-high performance liquid chromatography coupled with a triple quadrupole mass spectrometer operated in MRM mode (MRM) (UPLC-MRM-MS). MRM traces identical with the artemisinin standard were detected in the *P. patens* extracts, but not in the liquid culture medium or in extracts of wild-type *P. patens* (WT) (**Figure 2**; Figure S2 in Supplementary Material). The analysis was performed twice with 2 months apart in triplicates each time. The presence of artemisinin, but no intermediates, in *P. patens* was confirmed by comparison with an artemisinin standard (Figure S2 in Supplementary Material). Quantification using external calibration showed that the artemisinin yield was 0.21 mg/g dry weight (DW), which is in the range of native *A. annua* (0.001–1.54 mg/g DW) (Bhakuni et al., 2001) and in cross-bred plants (up to 10 mg/g DW) and higher in genetically engineered (up to 30 mg/g DW) (Tang et al., 2014). The amount of artemisinin in our *P. patens* lines is higher than what was initially obtained *via* heterologous expression in *N. tabacum* (0.0068 mg/g DW) (Farhi et al., 2011) and in *Nicotiana benthamiana* (0.003 mg/g DW) (Wang et al., 2016). Recent efforts of targeting the biosynthesis to the chloroplast elevated the yield in *N. tabacum* to 0.8 mg/g DW (Malhotra et al., 2016), since glycosylation of the precursors was avoided. Glycosylation and glutathione conjugation was previously shown to influence the yield in *N. benthamiana* (Mukanganyama et al., 2001; van Herpen et al., 2010; Ting et al., 2013; Liu et al., 2014). We also explored the presence of sugar and glutathione conjugated products by liquid chromatography coupled to quadrupole time-of-flight mass spectrometry (LC-QTOF-MS). However, no glycosylated or glutathione conjugated products were detected in the culture medium nor in the *P. patens* extracts. The lack of glycosides may be explained by the fact that *P. patens* only has 20 glycosyltransferase 1 (*GT1*) genes that encode for enzymes involved in deactivation or detoxification of secondary metabolites, while higher vascular plants usually have hundreds (Yonekura-Sakakibara and Hanada, 2011). As no pathway intermediates (conjugated or not) were detected in our extracts, we conclude that the pathway operates efficiently in *P. patens*.

A slight reduction in growth rate was observed after day 12, resulting in 11% lower biomass in the transgenic line after 18 days (**Figure 3A**). This indicates that there is just a small disruption of other metabolic pathways responsible for *P. patens* growth and fitness. The effect of artemisinin biosynthesis on *P. patens* growth is less, but follows and suggests the same pattern as was previously observed (Simonsen et al., 2009; Zhan et al., 2014; Pan et al., 2015). The lesser growth is likely due to toxicity of the product and to depletion of nutrients in the media, but this

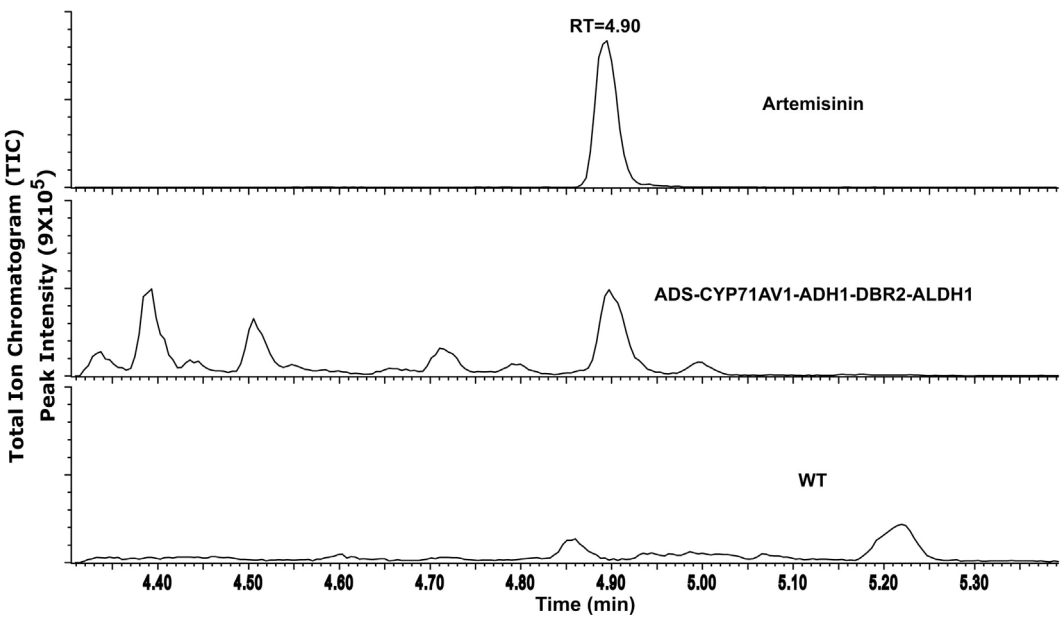

FIGURE 2 | UPLC-MRM-MS analysis of artemisinin produced from transgenic *Physcomitrella patens*, an internal standard (artemisinin) and WT as control with retention time. TIC represents the sum of multiple reaction monitoring channels used for the detection of artemisinin: *m/z* 283.19 > 219.21; 283.19 > 247.19; and 283.19 > 265.22.

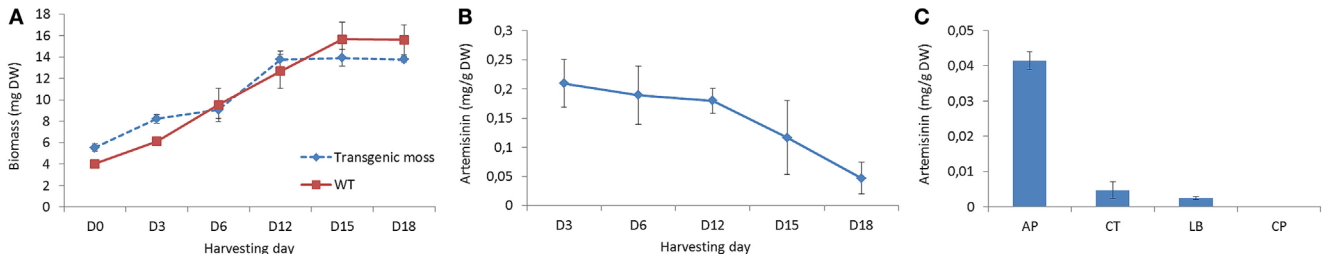

FIGURE 3 | Growth and production of artemisinin in *Physcomitrella patens*. **(A)** Time course analysis of growth of transgenic and WT *P. patens* in liquid culture. D0 indicates the initial sub-culturing day. **(B)** Time course analysis of artemisinin production in *P. patens*. Error bars denote the SE of triplicate shake-flask liquid culture. **(C)** Production of artemisinin after 18 days of cultivation in different cellular component of AP, apoplast; CT, cytoplasm; LBs, lipid bodies; and CP, cell pellet.

requires further studies in semi-continuous cultures. The highest concentration (0.21 mg/g DW) of artemisinin was observed after 3 days of cultivation (**Figure 3B**), whereas the highest accumulative amount of artemisinin (2.5 mg artemisinin) was observed at day 12. This is mainly due to the increase in biomass. This show that the primary production of artemisinin in *P. patens* happens within the first 2 weeks after subcultivation. This rapid production of artemisinin is very valuable for future industrial production and suggests that a semi-continuous batch cultivation with weekly extraction and disruption of the cells can provide high amounts of artemisinin.

Conversion of dihydroartemisinic acid to artemisinin in *A. annua* has been suggested to occur *via* photooxidation and induced by oxygen (Sy and Brown, 2002). In the present study, *P. patens* was grown under 24-h light and ambient air, which seems to facilitate the conversion to artemisinin as dihydroartemisinic acid was not detected in the extract. The reduction in artemisinin content from day 12 to day 18 might be due to chemical degradation of the compound, but no obvious breakdown products was found in the analysis; thus, this drop requires further studies.

Storage of Artemisinin in *P. patens*

Artemisinin biosynthesis occurs in the glandular trichomes of *A. annua,* but *P. patens* does not have trichomes. To identify the storage location of artemisinin in our transgenic *P. patens,* extracts of the AP, CT, LBs, and CPs were analyzed by UPLC-MRM-MS. Artemisinin was detected in all the extracts except for the CPs (**Figure 3C**). The highest accumulation was in the AP at 0.04 mg/g DW (after 18 days of cultivation, analyzed at 18 days to obtain enough biomass for the analysis) with 10- and 20-fold less in the CT and LBs. In the native plant *A. annua,* dihydroartemisinic acid is transported to the subcuticular space of the glandular trichomes before photooxidation into artemisinin (Brown, 2010). The high accumulation of artemisinin in the *P. patens* AP indicates a transport of pathway products over the cell membrane, as also shown *N. benthamiana* (Wang et al., 2016).

This work demonstrates a stable production of artemisinin in a photosynthetic organism that allows for large-scale industrial production. The production will not be affected by environmental and ecological variables and overall have a lower environmental impact than field production (water usages, fertilizers, petrol usages, etc.). It should be noted that besides using codon-optimized sequences, no other enhancement, e.g. increasing terpenoid precursor supply or multi copy gene integration was applied. The high flux through the terpenoid pathway is likely to be due to the metabolic robustness of *P. patens* (Schaefer and Zrÿd, 1997). In contrast, yeast needed extensive and complex precursor pathway engineering prior to the introduction of the artemisinic acid pathway genes. Further optimization of the metabolic network in *P. patens* has been shown to optimize sesquiterpenoid production (Zhan et al., 2014) and possibly also artemisinin production. Possible targets include overexpression of the key enzymes, 3-hydroxy-3-methylglutaryl-CoA reductase (*HMGR*), and farnesyl diphosphate synthase (*FPS*), which improved terpenoid production in other plants (van Herpen et al., 2010) and microbial (Ro et al., 2006; Paddon et al., 2013) hosts. Another possibility is targeting biosynthesis to different cellular compartments, which has also been shown to improve artemisinin and other sesquiterpenoid yield up to 1,000-fold in *N. tabacum* (Wu et al., 2006; Malhotra et al., 2016), which alone in *P. patens* would lead to a yield of 210 mg/g DW.

Optimization of artemisinin yield in *P. patens* can potentially result in a stable, sustainable, environmentally friendly, and commercially viable production platform. A considerable advantage of *P. patens* as an artemisinin production platform is that the extract only requires simple purification steps (**Figure 2**). This is different from the current yeast production platform that requires further chemical synthesis to yield artemisinin (Paddon et al., 2013; Turconi et al., 2014) and the production in *N. tabacum* was only described as semi-pure extracts (Malhotra et al., 2016). The use of *P. patens* could lead to a reduced price for artemisinin-based treatments, allowing lower income communities most affected by malaria, to contain malaria. Furthermore, scaling up the production of artemisinin in plant-based bioreactors would expand the use of plant cells in bioreactors.

CONCLUSION

All five artemisinin biosynthetic pathway genes were engineered into the moss *P. patens*. *In vivo* biosynthesis of artemisinin was

obtained without further modifications and a high initial production of 0.21 mg/g DW artemisinin was observed after only 3 days of cultivation. This bioengineering achievement expands the frontiers of synthetic biotechnology, offering a genetically robust plant-based platform, which can be scaled up for industrial production of other complex high-value plant-based compounds. *P. patens* uses light as an energy source, thus is potentially more cost effective than other carbon supplemented biotechnological platforms.

AUTHOR CONTRIBUTIONS

NI planned and performed the experiments, analyzed the data, and wrote the manuscript. ABK performed the UPLC-MRM-MS and LC-QTOF-MS, analyzed the data, and reviewed the manuscript. AP performed the *P. patens* cell components isolation experiments and reviewed the manuscript. ARvdK and HB reviewed the manuscript. HS planned the experiment and supervised and reviewed the manuscript.

ACKNOWLEDGMENTS

NI was supported by a grant from the Ministry of Higher Education, Malaysia and the University of Malaya. AP and HS was supported by The Danish Council for Independent Research (#4005-00158B). The authors would like to thank Professor Mark Estelle, Assoc. Prof. Yuji Hiwatashi, and Assoc. Prof. Dae Kyun Ro for kindly providing the pMP1355, and PZAG1 vector, and the ADS template.

SUPPLEMENTARY MATERIAL

The Supplementary Material for this article can be found online at http://journal.frontiersin.org/article/10.3389/fbioe.2017.00047/full#supplementary-material.

REFERENCES

Andersen, T. B., Cozzi, F., and Simonsen, H. T. (2015). Optimization of biochemical screening methods for volatile and unstable sesquiterpenoids using HS-SPME-GC-MS. *Chromatography* 2, 277–292. doi:10.3390/chromatography2020277

Anterola, A., Shanle, E., Perroud, P.-F., and Quatrano, R. (2009). Production of taxa-4(5),11(12)-diene by transgenic *Physcomitrella patens*. *Transgenic Res.* 18, 655–660. doi:10.1007/s11248-009-9252-5

Bach, S. S., King, B. C., Zhan, X., Simonsen, H. T., and Hamberger, B. (2014). "Heterologous stable expression of terpenoid biosynthetic genes using the moss *Physcomitrella patens*," in *Plant Isoprenoids*, ed. M. Rodríguez-Concepción (New York, USA: Springer), 257–271.

Bhakuni, R., Jain, D., Sharma, R., and Kumar, S. (2001). Secondary metabolites of *Artemisia annua* and their biological activity. *Curr. Sci.* 80, 35–48.

Brown, G. D. (2010). The biosynthesis of artemisinin (Qinghaosu) and the phytochemistry of *Artemisia annua* L.(Qinghao). *Molecules* 15, 7603–7698. doi:10.3390/molecules15117603

Buttner-Mainik, A., Parsons, J., Jerome, H., Hartmann, A., Lamer, S., Schaaf, A., et al. (2011). Production of biologically active recombinant human factor H in *Physcomitrella*. *Plant Biotechnol. J.* 9, 373–383. doi:10.1111/j.1467-7652.2010.00552.x

Drew, D. P., Rasmussen, S. K., Avato, P., and Simonsen, H. T. (2012). A comparison of headspace solid-phase microextraction and classic hydrodistillation for the identification of volatile constituents from *Thapsia* spp. provides insights into guaianolide biosynthesis in Apiaceae. *Phytochem. Anal.* 23, 44–51. doi:10.1002/pca.1323

Farhi, M., Marhevka, E., Ben-Ari, J., Algamas-Dimantov, A., Liang, Z., Zeevi, V., et al. (2011). Generation of the potent anti-malarial drug artemisinin in tobacco. *Nat. Biotechnol.* 29, 1072–1074. doi:10.1038/nbt.2054

François, I. E. J. A., Van Hemelrijck, W., Aerts, A. M., Wouters, P. F. J., Proost, P., Broekaert, W. F., et al. (2004). Processing in *Arabidopsis thaliana* of a heterologous polyprotein resulting in differential targeting of the individual plant defensins. *Plant Sci.* 166, 113–121. doi:10.1016/j.plantsci.2003.09.001

Ikram, N. K. B. K., Zhan, X., Pan, X., King, B. C., and Simonsen, H. T. (2015). Stable heterologous expression of biologically active terpenoids in green plant cells. *Front. Plant Sci.* 6:129. doi:10.3389/fpls.2015.00129

King, B. C., Vavitsas, K., Ikram, N. K. B. K., Schrøder, J., Scharff, L. B., Hamberger, B., et al. (2016). In vivo assembly of DNA-fragments in the moss, *Physcomitrella patens*. *Sci. Rep.* 6, 25030. doi:10.1038/srep25030

Komatsu, M., Uchiyama, T., Ōmura, S., Cane, D. E., and Ikeda, H. (2010). Genome-minimized *Streptomyces* host for the heterologous expression of secondary metabolism. *Proc. Natl. Acad. Sci. U.S.A.* 107, 2646–2651. doi:10.1073/pnas.0914833107

Liu, Q., Manzano, D., Tanic, N., Pesic, M., Bankovic, J., Pateraki, I., et al. (2014). Elucidation and in planta reconstitution of the parthenolide biosynthetic pathway. *Metab. Eng.* 23, 145–153. doi:10.1016/j.ymben.2014.03.005

Ma, C., Wang, H., Lu, X., Wang, H., Xu, G., and Liu, B. (2009). Terpenoid metabolic profiling analysis of transgenic *Artemisia annua* L. by comprehensive two-dimensional gas chromatography time-of-flight mass spectrometry. *Metabolomics* 5, 497–506. doi:10.1007/s11306-009-0170-6

Malhotra, K., Subramaniyan, M., Rawat, K., Kalamuddin, M., Qureshi, M. I., Malhotra, P., et al. (2016). Compartmentalized metabolic engineering for artemisinin biosynthesis and effective malaria treatment by oral delivery of plant cells. *Mol. Plant.* 9, 1464–1477. doi:10.1016/j.molp.2016.09.013

Martin, V. J., Pitera, D. J., Withers, S. T., Newman, J. D., and Keasling, J. D. (2003). Engineering a mevalonate pathway in *Escherichia coli* for production of terpenoids. *Nat. Biotechnol.* 21, 796–802. doi:10.1038/nbt833

Mukanganyama, S., Naik, Y. S., Widersten, M., Mannervik, B., and Hasler, J. A. (2001). Proposed reductive metabolism of artemisinin by glutathione transferases in vitro. *Free Radic. Res.* 35, 427–434. doi:10.1080/10715760100300941

Novotny, L., Samek, Z., and Sorm, F. (1966). The Structure of bisabolangelone a sesquiterpenic ketoalcohol from *Angelica silvestris* L. seeds. *Tetrahedron Lett.* 7, 3541–46. doi:10.1016/S0040-4039(01)82825-2

Paddon, C. J., and Keasling, J. D. (2014). Semi-synthetic artemisinin: a model for the use of synthetic biology in pharmaceutical development. *Nat. Rev. Microbiol.* 12, 355–367. doi:10.1038/nrmicro3240

Paddon, C. J., Westfall, P. J., Pitera, D. J., Benjamin, K., Fisher, K., Mcphee, D., et al. (2013). High-level semi-synthetic production of the potent antimalarial artemisinin. *Nature* 496, 528–532. doi:10.1038/nature12051

Pan, X.-W., Han, L., Zhang, Y.-H., Chen, D.-F., and Simonsen, H. (2015). Sclareol production in the moss *Physcomitrella patens* and observations on growth and terpenoid biosynthesis. *Plant Biotechnol. Rep.* 9, 1–11. doi:10.1007/s11816-015-0353-8

Pandey, N., and Pandey-Rai, S. (2016). Updates on artemisinin: an insight to mode of actions and strategies for enhanced global production. *Protoplasma* 253, 15–30. doi:10.1007/s00709-015-0805-6

Reski, R. (1998). Development, genetics and molecular biology of mosses. *Plant Biol.* 111, 1–15. doi:10.1111/j.1438-8677.1998.tb00670.x

Reski, R., Parsons, J., and Decker, E. L. (2015). Moss-made pharmaceuticals: from bench to bedside. *Plant Biotechnol. J.* 13, 1191–1198. doi:10.1111/pbi.12401

Ro, D. K., Paradise, E. M., Ouellet, M., Fisher, K. J., Newman, K. L., Ndungu, J. M., et al. (2006). Production of the antimalarial drug precursor artemisinic acid in engineered yeast. *Nature* 440, 940–943. doi:10.1038/nature04640

Rodriguez, S., Kirby, J., Denby, C. M., and Keasling, J. D. (2014). Production and quantification of sesquiterpenes in *Saccharomyces cerevisiae*, including extraction, detection and quantification of terpene products and key related metabolites. *Nat. Protoc.* 9, 1980–1996. doi:10.1038/nprot.2014.132

Schaefer, D. G., and Zrÿd, J. P. (1997). Efficient gene targeting in the moss *Physcomitrella patens*. *Plant J.* 11, 1195–1206. doi:10.1046/j.1365-313X.1997.11061195.x

Simonsen, H. T., Drew, D. P., and Lunde, C. (2009). Perspectives on using *Physcomitrella Patens* as an alternative production platform for thapsigargin and other terpenoid drug candidates. *Perspect. Medicin. Chem.* 3, 1–6.

Sy, L.-K., and Brown, G. D. (2002). The mechanism of the spontaneous autoxidation of dihydroartemisinic acid. *Tetrahedron* 58, 897–908. doi:10.1016/S0040-4020(01)01192-9

Tang, K., Shen, Q., Yan, T., and Fu, X. (2014). Transgenic approach to increase artemisinin content in *Artemisia annua* L. *Plant Cell Rep.* 33, 605–615. doi:10.1007/s00299-014-1566-y

Teoh, K. H., Polichuk, D. R., Reed, D. W., and Covello, P. S. (2009). Molecular cloning of an aldehyde dehydrogenase implicated in artemisinin biosynthesis in *Artemisia annua*. *Botany* 87, 635–642. doi:10.1139/B09-032

Ting, H.-M., Wang, B., Rydén, A.-M., Woittiez, L., Van Herpen, T., Verstappen, F. W. A., et al. (2013). The metabolite chemotype of *Nicotiana benthamiana* transiently expressing artemisinin biosynthetic pathway genes is a function of CYP71AV1 type and relative gene dosage. *New Phytol.* 199, 352–366. doi:10.1111/nph.12274

Turconi, J., Griolet, F., Guevel, R., Oddon, G., Villa, R., Geatti, A., et al. (2014). Semisynthetic artemisinin, the chemical path to industrial production. *Org. Process Res. Dev.* 18, 417–422. doi:10.1021/op5001397

van Herpen, T. W., Cankar, K., Nogueira, M., Bosch, D., Bouwmeester, H. J., and Beekwilder, J. (2010). *Nicotiana benthamiana* as a production platform for artemisinin precursors. *PLoS ONE* 5:e14222. doi:10.1371/journal.pone.0014222

Wallaart, T. E., Bouwmeester, H. J., Hille, J., Poppinga, L., and Maijers, N. C. (2001). Amorpha-4,11-diene synthase: cloning and functional expression of a key enzyme in the biosynthetic pathway of the novel antimalarial drug artemisinin. *Planta* 212, 460–465. doi:10.1007/s004250000428

Wang, B., Kashkooli, A. B., Sallets, A., Ting, H.-M., De Ruijter, N. C., Olofsson, L., et al. (2016). Transient production of artemisinin in *Nicotiana benthamiana* is boosted by a specific lipid transfer protein from *A. annua*. *Metab. Eng.* 38, 159–169. doi:10.1016/j.ymben.2016.07.004

Wu, S., Schalk, M., Clark, A., Miles, R. B., Coates, R., and Chappell, J. (2006). Redirection of cytosolic or plastidic isoprenoid precursors elevates terpene production in plants. *Nat. Biotechnol.* 24, 1441–1447. doi:10.1038/nbt1251

Yonekura-Sakakibara, K., and Hanada, K. (2011). An evolutionary view of functional diversity in family 1 glycosyltransferases. *Plant J.* 66, 182–193. doi:10.1111/j.1365-313X.2011.04493.x

Zhan, X., Zhang, Y., Chen, D., and Simonsen, H. T. (2014). Metabolic engineering of the moss *Physcomitrella patens* to produce the sesquiterpenoids patchoulol and α/β-santalene. *Front. Plant Sci.* 5:636. doi:10.3389/fpls.2014.00636

Zhang, Y., Teoh, K. H., Reed, D. W., Maes, L., Goossens, A., Olson, D. J., et al. (2008). The molecular cloning of artemisinic aldehyde Δ11(13) reductase and its role in glandular trichome-dependent biosynthesis of artemisinin in *Artemisia annua*. *J. Biol. Chem.* 283, 21501–21508. doi:10.1074/jbc.M803090200

Conflict of Interest Statement: All authors declare that they have no conflict of interest. HS is co-founder of Mosspiration Biotech IVS that aim to produce fragrances in *P. patens*, but not artemisinin.

frontiers in Plant Science

REVIEW
published: 15 November 2017
doi: 10.3389/fpls.2017.01966

A Review of Biotechnological Artemisinin Production in Plants

*Nur K. B. K. Ikram[1] and Henrik T. Simonsen[2]**

[1] Institute of Biological Sciences, Faculty of Science, University of Malaya, Kuala Lumpur, Malaysia, [2] Department of Biotechnology and Biomedicine, Technical University of Denmark, Kongens Lyngby, Denmark

Malaria is still an eminent threat to major parts of the world population mainly in sub-Saharan Africa. Researchers around the world continuously seek novel solutions to either eliminate or treat the disease. Artemisinin, isolated from the Chinese medicinal herb *Artemisia annua*, is the active ingredient in artemisinin-based combination therapies used to treat the disease. However, naturally artemisinin is produced in small quantities, which leads to a shortage of global supply. Due to its complex structure, it is difficult chemically synthesize. Thus to date, *A. annua* remains as the main commercial source of artemisinin. Current advances in genetic and metabolic engineering drives to more diverse approaches and developments on improving *in planta* production of artemisinin, both in *A. annua* and in other plants. In this review, we describe efforts in bioengineering to obtain a higher production of artemisinin in *A. annua* and stable heterologous *in planta* systems. The current progress and advancements provides hope for significantly improved production in plants.

Keywords: plant biotechnology, malaria, artemisinin, *Artemisia annua*, bioengineering

OPEN ACCESS

Edited by:
Tomasz Czechowski, University of York, United Kingdom

Reviewed by:
Patrick Smithers Covello, National Research Council Plant Biotechnology Institute, Canada
Deyu Xie, North Carolina State University, United States

****Correspondence:***
Henrik T. Simonsen
hets@dtu.dk

Specialty section:
This article was submitted to Plant Biotechnology, a section of the journal Frontiers in Plant Science

Received: *15 August 2017*
Accepted: *31 October 2017*
Published: *15 November 2017*

Citation:
Ikram NKBK and Simonsen HT (2017) A Review of Biotechnological Artemisinin Production in Plants. Front. Plant Sci. 8:1966. doi: 10.3389/fpls.2017.01966

INTRODUCTION

Malaria is still a global concern with around 214 million annual cases and 430,000 annual deaths, mainly among of children younger than 5 (World Health Organization [WHO], 2016). This fatal disease is caused by *Plasmodium* sp. particularly *Plasmodium falciparum* that proliferate in female *Anopheles* mosquitoes (Cox, 2010). Since the 1940s there has been continuous attempts to halt the spread of the disease and this has succeeded in Europe, North America, and parts of Asia and Latin America (Carter and Mendis, 2002). However, not in Sub-Saharan Africa where 80% of the annual malaria patients are found. Besides measures such as vector control and insecticide-treated nets, research and development has led to new drugs and a vaccine. The current preferred therapy is artemisinin combination therapy (ACT) (Banek et al., 2014; Lalloo et al., 2016) that is based on artemisinin produced in the natural source *Artemisia annua*. Artemisinin can also be produced heterologously in the plants *Nicotiana benthamiana* and *Physcomitrella patens* (Han et al., 2016; Wang et al., 2016; Ikram et al., 2017). The vaccine toward *Plasmodium* is called PfSPZ and can be produced in *N. benthamiana* and *P. patens* plants (Rosales-Mendoza et al., 2014, 2017; Boes et al., 2016; Epstein et al., 2017).

Malaria drugs have contributed significantly to the reductions in malaria mortality and morbidity. The focus for many years has been to screen traditional medicine to find new antimalarial drugs (Simonsen et al., 2001; Adia et al., 2016; Nondo et al., 2017). The malaria drug artemisinin is an example of this and originates from *A. annua*, a Chinese medicinal

plant (Qinghao), commonly known as sweet wormwood. It was discovered by the Chinese researcher You-You Tu and her team in 1972, and was named Qinghaosu (Klayman, 1985; Tu, 2011). Chemically, artemisinin is a sesquiterpene lactone with a unique endoperoxide structure, without the nitrogen containing heterocyclic ring like other antimalarial compounds (Luo and Shen, 1987). The *in planta* accumulation of artemisinin is 0.01–1.4% dry weight depending on the plant variety and artemisinin is stored in the glandular trichomes of *A. annua* (Duke et al., 1994; Van Agtmael et al., 1999; Bhakuni et al., 2001; Muangphrom et al., 2016). The current production using plants with a "low" content of artemisinin can only just cover the global need, which have led to an increase in price (Peplow, 2016). In 2006, World Health Organization (WHO) recommended artemisinin as the first-choice treatment for malaria. Rapid emergence of antimalarial drug resistance drew attention to formulation of artemisinin-based combination therapy (ACT) with artemisinin as the primary substance and is now the preferred treatment (World Health Organization [WHO], 2015).

To secure the global need of artemisinin, there are continuous and extensive efforts to enhance the production of artemisinin in the native plant *A. annua*. *A. annua* is currently the primary commercial source of artemisinin and significant breeding programs has contributed to higher artemisinin content in the plant (Ma et al., 2015; Pulice et al., 2016; Xie et al., 2016), including establishment of mutant libraries (Pandey et al., 2016). Several plant-breeding techniques have been applied to create superior cultivars of *A. annua*. For example, conventional breeding by crossing *A. annua* with high artemisinin content in wild population has led to hybrid lines with 2% artemisinin d.w (Delabays et al., 2001; Cockram et al., 2012). A detailed genetic map of *A. annua* comprising of genes and markers controlling artemisinin yield has been established to generate robust high yielding crops (Graham et al., 2010). Identification of *A. annua* superior parental lines with desired traits from these genetic maps has provided two high-yielding hybrids and diallel crossing of the parental lines and the hybrids has showed consistent results for the development of improved *A. annua* hybrids (Townsend et al., 2013). Doubling the number of chromosomes generated a new variety of tetraploid cultivar with higher artemisinin content and this might become a new elite line (Banyai et al., 2010b). The overall production of the new cultivars from various laboratories have increased the level of artemisinin to about 1 to 2% d.w. (Delabays et al., 1993; Ferreira et al., 2005; Graham et al., 2010; Brisibe et al., 2012), but not all the established plant lines are stable over generations (Delabays et al., 2001).

Efforts in plant breeding have been challenging due to the heterozygous nature of *A. annua,* which results in transgenic plants with varying degrees of artemisinin content even though they were generated in the same laboratory (Delabays et al., 2001; Graham et al., 2010; Larson et al., 2013). This variation is due to the segregation of the heterozygous wild type progeny leading to a different genetic background than the parent plant. Although several high content lines have been created, the unstable yield in the progeny of these cultivars were insufficient to increase the global supply of artemisinin (Shretta and Yadav, 2012; Paddon et al., 2013).

Accumulation of artemisinin in *A. annua* is limited to the small 10 cell glandular trichomes (GT) mostly on leaves and other aerial parts (Ferreira and Janick, 1995; Lommen et al., 2006; Ling et al., 2016). Low GT numbers are correlated to low artemisinin content (Graham et al., 2010; Kjær et al., 2012). Attempts to increase the number of GTs by physical and chemical stress have not been successful (Kjær et al., 2012). One study expressed the β glucosidase (*bgl*1) gene in *A. annua* through *Agrobacterium*-mediated transformation, which resulted in an increase of GT density by 20% on leaves and 66% on flowers and an increase in artemisinin content of 1.4% in leaves and 2.56% in flowers (d.w). Manipulating GT density together with biosynthetic pathway engineering may further increase artemisinin content in *A. annua*. In depth understanding of *A. annua* GT generation at the molecular level, will broaden the opportunities of increasing the artemisinin production. This approximately though require a greater acceptance of GMO crops in open fields to ensure the global supply.

Plant tissue culture has also been investigated to establish a production of artemisinin in *A. annua* hairy root or cell suspension cultures (Nair et al., 1986; Baldi and Dixit, 2008). Several manipulations of the growth conditions such as different sugar supply, light irradiation, UV-B radiation and chilling treatment have led to production of artemisinin in *A. annua* tissue cultures (Woerdenbag et al., 1993; Liu et al., 2002; Wang and Weathers, 2007; Baldi and Dixit, 2008; Yin et al., 2008; Pandey and Pandey-Rai, 2014). Generating somaclonal variants tolerant against salt stress through gamma-rays irradiation has resulted in 13 somaclonal variants (ASV1 to ASV13) of which one of the variants, ASV12 is a stable salt-tolerant line with a higher expression profile of artemisinin key genes (ADS, CYP71AV1, DBR2, and ALDH1) and a higher artemisinin content as compared to wild type. In addition, treatments with elicitors such as methyl jasmonate has significantly increased artemisinin production by up to 49% including up-regulating the expression of artemisinin biosynthesis genes as well as increased GT index (0.128) (Baldi and Dixit, 2008; Wang et al., 2010; Dangash et al., 2014; Xiang et al., 2015). Other elicitors such as chitosan, gibberellic acid, and salicylic acid also aid in the accumulation of artemisinin (Guo et al., 2010; Banyai et al., 2011). Combinations of various cultivation and elicitation methods are currently being geared for a mass production of artemisinin in *A. annua* hairy roots via bioreactors with 6.3 g/L dry weight (37.50 g fresh weight) biomass and 0.32 mg/g artemisinin content after 25 days (Patra and Srivastava, 2017).

Other efforts to enhance artemisinin production have been attempted through genetic engineering of the artemisinin biosynthetic pathway genes in microbial heterologous hosts. Extensive work on the development of microbial production of artemisinin precursors led to semi-synthesis of artemisinin, but this is only partly commercially successful (Benjamin et al., 2016; Peplow, 2016; Singh et al., 2017). In this review, the progress and recent bioengineering advances in artemisinin production in stable heterologous *in planta* systems including genetic modifications of *A. annua* is summarized.

ARTEMISININ BIOSYNTHESIS IN *Artemisia annua*

The biosynthesis of Artemisinin (**Figure 1**) has been explored for many years. However, not every detail about the regulation and biosynthesis is completely understood, but the discovery that the whole biosynthesis is located in the glandular trichomes of *A. annua* has facilitated in-depth regulatory studies (Olsson et al., 2009; Olofsson et al., 2011). Derived from the general terpenoid biosynthesis, two molecules of isopentenyl diphosphate (IPP) and one dimethylallyl diphosphate (DMAPP) are condensed by farnesyl diphosphate synthase (FPPS/FPS) into farnesyl diphosphate (FPP, farnesyl pyrophosphate), the C15 sesquiterpenoid precursor (Weathers et al., 2006; Brown, 2010; Wen and Yu, 2011). Overexpression of FPS in *A. annua* resulted in an increase of artemisinin production (Han et al., 2006; Banyai et al., 2010a), which confirms the role of FPS and availability of the substrates in the regulation of artemisinin biosynthesis similar to other sesquiterpene lactones (Simonsen et al., 2013).

FPP is converted to amorpha-4,11-diene by amorpha-4,11-diene synthase (ADS) via carbocation formation and cyclization (Bouwmeester et al., 1999; Mercke et al., 2000; Picaud et al., 2005, 2006). In the following two oxidization steps, amorpha-4,11-diene is hydroxylated into artemisinic alcohol and oxidized to artemisinic aldehyde by amorphadiene monooxygenase (CYP71AV1), a cytochrome P450 enzyme (Teoh et al., 2006; Wang et al., 2011). The activity of the CYP71AV1 has also been confirmed through a knock-out of the endogenous gene in *A. annua* showing that these plants do not produce any downstream products of amorphadiene (Czechowski et al., 2016). It has later been discovered that the alcohol dehydrogenase (ADH1, a dehydrogenase/reductase enzyme) is specific toward artemisinin alcohol and oxidizes this to the aldehyde. This specificity and strong expression in *A. annua* glandular trichomes confirms that ADH1 is responsible for oxidation of artemisinic alcohol to artemisinic aldehyde (Olofsson et al., 2011; Paddon et al., 2013; He et al., 2017). Artemisinic aldehyde is further reduced to dihydroartemisinic aldehyde by artemisinic aldehyde Δ11 (13) reductase (DBR2) and subsequently oxidized to dihydroartemisinic acid by aldehyde dehydrogenase (ALDH1), which is also expressed in the trichomes (Zhang et al., 2008; Teoh et al., 2009; Rydén et al., 2010; Liu et al., 2016). Besides catalyzing the oxidation of dihydroartemisinic aldehyde to the acid, ALDH1 also catalyzes the oxidation of artemisinic aldehyde to artemisinic acid (a reaction that in yeast is catalyzed by CYP71AV1) (Teoh et al., 2006, 2009). Another enzyme, dihydroartemisinic aldehyde reductase (RED1) converts dihydroartemisinic aldehyde to dihydroartemisinic alcohol, a "dead end" substance, which

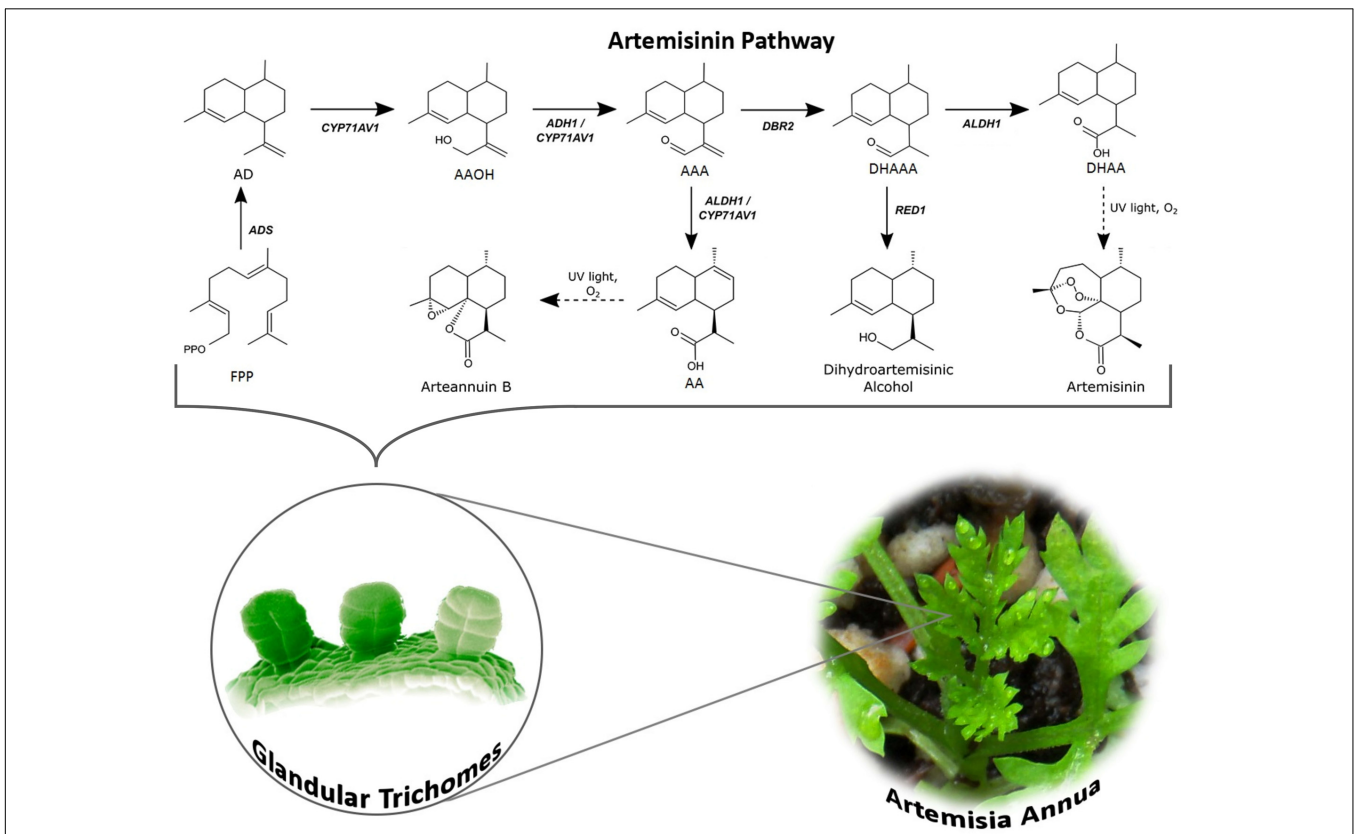

FIGURE 1 | Artemisinin biosynthesis pathway occurs in the glandular trichomes of *Artemisia annua*. The pathway intermediates are defined as FPP, farnesyl diphosphate; AD, amorpha-4,11-diene; AAOH, artemisinic alcohol; AAA, artemisinic aldehyde; AA, artemisinic acid; DHAAA, dihydroartemisinic aldehyde; DHAA, dihydroartemisinic acid. The full name of the enzymes is stated in the text.

affects the production yield of artemisinin (Rydén et al., 2010). The final step is a light-induced non-enzymatic spontaneous reaction converting dihydroartemisinic acid to artemisinin and artemisinic acid to arteannuin B (Sy and Brown, 2002; Teoh et al., 2006; Czechowski et al., 2016).

BIOENGINEERING OF ARTEMISININ PRODUCTION IN GREEN PLANT CELLS

Bioengineering of Biosynthetic Genes in *Artemisia annua*

Characterization of enzymes in the artemisinin biosynthetic pathway provides new tools and advances the possibility of engineering the production of artemisinin. This can be achieved by enhancing the general terpenoid metabolism and through overexpression of several genes involved in artemisinin biosynthesis in *A. annua* (Tang et al., 2014). Overexpression of key terpenoid genes encoding for the enzymes IDI, FPS, HMGR, the plastid targeted DXR and HDR have increased production significantly (some by 2 to 3 fold) in many different studies in *A. annua* (Han et al., 2006; Aquil et al., 2009; Banyai et al., 2010a; Nafis et al., 2011; Xiang et al., 2012; Ma et al., 2017a). Co-expression of FPS, CYP71AV1 and its redox partner, POR (cytochrome P450 reductase) increased production by 3.6 fold, whereas combining four genes ADS, CYP71AV1, ALDH1, and POR from *A. annua* yielded a 3.4 fold increase in the artemisinin levels (Chen et al., 2013; Shi et al., 2017). Additionally, the production also increased by overexpression of ADS, CYP71AV1, and HMGR (Ma et al., 2009; Alam et al., 2016). The expression of several genes in the pathway clearly have an effect on the artemisinin level and do increase the amount of biomass obtained (Shen et al., 2012; Alam et al., 2016). Thus, utilizing genetic engineering to target the expression of both upstream and specific artemisinin genes should be pursued.

The overexpression of DBR2 clearly showed that this is a key enzyme that regulates the production of artemisinin by guiding the metabolic flow from artemisinic acid toward dihydroartemisinic acid. Without the activity of DBR2 the plants solely make artemisinic acid and thereby arteannuin B (Zhang et al., 2008), thus showing that overexpression of this enzyme will enhance artemisinin production. Collectively, the overexpression studies have provided insights into the understanding of the pathway and how to upregulate it.

Another strategy in bioengineering is to block competing reactions such as the squalene synthase (SQS) and β-caryophyllene synthase, enzymes consuming FPP for sterol and β-caryophyllene biosynthesis. This has been proven to elevate artemisinin production by 3.14 and 5.49 fold, respectively

TABLE 1 | Genetic engineering to improve the production of artemisinin in *Artemisia Annua.*

Type	Overexpressed enzymes	Artemisinin yield	Reference
Upstream key enzymes	FPS	13.0 mg/g (DW)	Han et al., 2006 Banyai et al., 2010a Chen et al., 2000
	HMGR	1.7 mg/g (DW)	Aquil et al., 2009
		0.6 mg/g (DW)	Nafis et al., 2011
	AaIPP1	2.5 mg/g (DW)	Ma et al., 2017a
	AaHDR1	0.09 mg/g (FW)	Ma et al., 2017b
Artemisinin biosynthesis enzymes	DXR	1.21 mg/g (DW)	Xiang et al., 2012
with related key enzymes	CYP71AV1 and POR	0.98 mg/g (FW)	Shen et al., 2012
	HMGR and ADS	1.73 mg/g (DW)	Alam and Abdin, 2011
	FPS and ADS	26 mg/g (DW)	Han et al., 2016
	FPS, CYP71AV1, POR	2.90 mg/g (FW)	Chen et al., 2013
	ADS, CYP71AV1, ALDH1, and POR		Shi et al., 2017
	ADS, CYP71AV1, POR	15.1 mg/g (DW)	Lu et al., 2013a
	DBR2	22.35 mg/g (DW)	Tang et al., 2012b
	ALDH1	25.34 mg/g (DW)	Tang et al., 2012a
Competitive pathway enzymes	SQS	31.0 mg/g (DW)	Zhang et al., 2009
	CPS	3.56 mg/g (DW)	Chen et al., 2011
Transcription factors	AaWRKY	14.2 mg/g (DW)	Jiang et al., 2016
	AaERF1 and AaERF2	9.1 and 8.1 mg/g (DW)	Yu et al., 2012
	AaORA	11.9 mg/g (DW)	Lu et al., 2013b
	AaMYC2	15.3 mg/g (DW)	Shen et al., 2016a
	AaNAC1	23.5 mg/g (DW)	Lv et al., 2016
Others	Rol B	7.30 ug/g (DW)	
	Rol C	3.33 ug/g (DW)	Dilshad et al., 2015b
	AaPYL9	1.80 mg/g (FW)	Zhang et al., 2013
	AtCRY1	1.65 mg/g (DW)	Hong et al., 2009

TABLE 2 | Compilation of bioengineering works in heterologous *in planta* host producing artemisinin and artemisinic acid.

Construct	Strain	Artemisinin	Artemisinic acid	Reference
Mega vector consisting HMGR, CYP71AV1, CPR, DBR2, cytosolic-targeting ADS and mitochondria-targeting ADS	*Nicotiana tabacum*	0.0068 mg/g DW	–	Farhi et al., 2011
Transient expression of ADS, CYP71AV1, DBR2, ALDH1 with co-expression of lipid transfer proteins from *A. annua*	*Nicotiana benthamiana*	0.0030 μg/g DW	–	Wang et al., 2016
FPS, ADS, CYP71AV1, CPR targeted at the chloroplast followed by combinatorial supertransformation of CYPB5, ADH1, ALDH1, DBR2	*Nicotiana tabacum*	–	120 μg/g FW	Fuentes et al., 2016
Six MVA pathway genes, AACT, HMGS, HMGR, MVK, PMK, PMD transformed into chloroplast and subcellular targeting DBR2, CYP71AV1 and CPR via chloroplast transient peptide	*Nicotiana tabacum*	0.8 mg/g DW	–	Malhotra et al., 2016
Five artemisinin pathway genes, ADS, CYP71AV1, ADH1, DBR2, ALDH1 stably transformed into *Physcomitrella patens* via a novel *in vivo* DNA assembly method	*Physcomitrella patens*	0.21 mg/g DW	–	Ikram et al., 2017

(Zhang et al., 2009; Chen et al., 2011). Since RED1 competes with ALDH1 in artemisinin biosynthesis of *A. annua*, removing RED1 could also lead to the increase of artemisinin production in *A. annua* (Rydén et al., 2010).

FPS in general has a higher k_{cat} value than sesquiterpene synthases and this is true for the FPS and ADS in *A. annua*. Thus, it has been investigated whether a fusion of the two enzymes would increase the turnover of FPP to amorphadiene (Han et al., 2016). The findings that such fusion can facilitate metabolite channeling through a biosynthesis pathway has recently been shown for other metabolites (Laursen et al., 2016). The metabolite channeling from FPS to ADS is supported by a 2–3 fold increase of amorphadiene in plants where these two genes are fused (Han et al., 2016). The dynamic artemisinin content in the transgenic and wild type plants is associated with the expression of these genes involved in the artemisinin pathway. **Table 1** summarizes the work on genetic manipulation in *A. annua* to improve the production of artemisinin.

Bioengineering the Regulation of Artemisinin Biosynthesis

Over the last 20 years *Agrobacterium rol* A, B, and C genes have been shown to increase the biosynthesis of stress response metabolites in different plant families (Bulgakov, 2008). *Rol* genes are a potential activator of secondary metabolites which directly upregulate artemisinin production by induction of the gene expression, leading to higher amounts of enzymes and thus more products. Transformation of *rol* genes in other *Artemisia* sp. resulted not only in the overexpression of artemisinin pathway genes, but also artemisinin content in the plant (Dilshad et al., 2015a,b; Amanullah et al., 2016). Integration of individual and combined *rol* B and C genes in *A. annua* increases the production of artemisinin by up to ninefold (Ghosh et al., 1997; Dilshad et al., 2015a,b).

Identifying transcription factors involved in regulating artemisinin production has also contributed to a higher production of artemisinin and was recently reviewed (Shen et al., 2016b). Overexpression of the transcription factor AaWRKY1 shows a 4.4 fold increase of artemisinin compared to the control plant. Overexpression of another transcription factor jasmonate-responsive AP2/ERF-type; AaERF1 and AaERF2 increases the gene expression levels of ADS, CYP71AV1, and DBR2 resulting in a higher accumulation of artemisinin and artemisinic acid in *A. annua* (Shen et al., 2016b). What is clear from recent work is that there are parts of the artemisinin pathway, which have promoters that are specific for trichomes (Chen et al., 2017). Therefore changing these to a strong constitutive promoter might be a novel engineering target with CRISPR/Cas9 technology.

Metabolic Engineering in *Nicotiana* spp.

Introducing artemisinin pathway genes in heterologous plants has been successful in both stable and transient expression but the artemisinin yield is relatively low (Farhi et al., 2011; Zhang et al., 2011; Ting et al., 2013). Currently, only *Nicotiana* spp. has been used as the plant alternative in the artemisinin research as it is cheap, well-established with rapid growth and high biomass. The expression of ADS in *Nicotiana tabacum* resulted in an increased production of the first product amorpha-4,11-diene (Wallaart et al., 2001). The addition of CYP71AV1, DBR2, and ALDH1 produced 4 mg/g fresh weight of amorph-4,11-adiene in leaves followed by 0.01 mg/g dry weight of artemisinic alcohol (Zhang et al., 2011). Stable expression of five multiple genes from the MVA and artemisinin pathway constructed in a single vector into *N. tabacum* produces 0.48–6.8 μg/g dry weight of artemisinin (Farhi et al., 2011). However, transient expression combining ADS, FPS, HMGR, and CYP71AV1 in *N. benthamiana* produced artemisinic acid that was further modified by endogenous glycosyl transferase into artemisinic acid-12-β-diglucoside (Van Herpen et al., 2010). There is a high production of glycosylated artemisinin precursors with the expression of artemisinin genes in *N. benthamiana* (Ting et al., 2013).

Glycosylation is a problem in the *Nicotiana* spp. (Van Herpen et al., 2010; Ting et al., 2013). To overcome this, attempts were made to target the biosynthesis into different cellular compartments such as the chloroplast. Fuentes et al. (2016) introduced the artemisinin pathway into *N. tabacum* chloroplast via a stable plastid genome transformation followed

by a combinatorial transformation resulting in a transformation of transplastomic recipient lines (COSTREL) that produces 120 μg/g artemisinic acid.

Another group aimed to engineer two mega-metabolic pathways separately into two different cellular compartments. They first elevated the IPP pools by introducing six genes from MVA pathway into *N. tabacum* chloroplast followed by the artemisinin pathway genes into the nuclear genome with subcellular targeting at DBR2, CPR, and CYP71AV1 via chloroplast transit peptide. The lines produced ∼0.8 mg/g dry weight of artemisinin (Malhotra et al., 2016). While various methods were explored in order to enhance artemisinin production in *Nicotiana*, the production levels remain minimal due to the complex nature of the gene expression and regulation in artemisinin biosynthesis pathway as well as the complex glycosylation response in *Nicotiana*.

Metabolic Engineering in *Physcomitrella* Patens

A new production platform is being established in a non-vascular plant, the moss *P. patens* (Simonsen et al., 2009; Buttner-Mainik et al., 2011; Ikram et al., 2015; Reski et al., 2015). Having unique molecular tools of highly efficient homologous recombination and a fully sequenced genome, *P. patens* is an attractive production system when compared to other plant production hosts (Schaefer and Zrÿd, 1997; Reski, 1998; Frank et al., 2005). Additionally, a novel transformation technology involving *in vivo* assembly of multiple DNA fragments in *P. patens* has been established, further increasing its attractiveness as a promising photosynthetic chassis for synthetic biology (King et al., 2016). This is also supported by several works utilizing *P. patens* as a "green factory," for example, the expression of taxadiene synthase in *P. patens* produces taxadiene without any phenotypic change, making it a capable host for the production of paclitaxel (Anterola et al., 2009). In addition, three important sesquiterpenoids in the fragrance industry, patchoulol, β-santalene, and sclareol was also successfully produced in *P. patens* with productivity up to 1.3, 0.039, and 2.84 mg/g dry weight respectively (Zhan et al., 2014; Pan et al., 2015). We recently reported the successful production of artemisinin in *P. patens* (Ikram et al., 2017). All five artemisinin pathway genes were introduced into *P. patens* via the *in vivo* assembly of multiple DNA fragments method and the transgenic *P. patens* lines produces 0.21 mg/g DW of artemisinin, a significant level at only 3 days of culturing. A considerable advantage of *P. patens* as an artemisinin production platform is the absence of pathway intermediates (glycosylation and glutathione conjugation). *P. patens* has less glycosyltransferases as compared to higher plants that may lead to the possibility of lower risk of endogenous modifications to xenobiotic metabolites. Further research in bioengineering of *P. patens* for a higher artemisinin production is ongoing and could potentially help stabilize the supply of artemisinin and aid in containing malaria. Bioengineering of artemisinin biosynthesis pathway in heterologous *in planta* host with successful production of artemisinic acid and artemisinin is summarized in **Table 2**.

PERSPECTIVES

Current advances in genetic and metabolic engineering drive a more diverse research and development approach on improving *in planta* production of artemisinin. The successes achieved in heterologous plant hosts and engineering of *A. annua* remains are of great importance. Microbial engineering of artemisinic acid shows some potential, but the added costs for later chemical synthesis of artemisinin is a detracting factor for replacing *A. Annua* as the main artemisinin source. Progress in plant engineering and synthetic biology has significantly improved the awareness of using plant as production hosts leading to great efforts in the implementation and enhancement of artemisinin production in both *in vivo* and *in vitro* production. Furthermore, heterologous *in planta* production seems to be more cost effective and environmentally friendly than other current biotechnological platforms. Advances in multigene transformation, transcription factors along with targeting of cellular compartment techniques will enable elevation of production levels in future engineered plants bringing us closer to industrial scale plant factories for artemisinin production. Perhaps the continuous production of artemisinin and other valuable plant metabolites in suspended bioreactor cultures with *in situ* extraction to avoid cell toxicity is not too far in the future. This will avoid the regulatory restrictions on in field GMO plants, and allow for stable continues production of drugs.

AUTHOR CONTRIBUTIONS

NI and HS collectively wrote the manuscript and initiated the work behind it. NI contributed with major parts of the literature research.

ACKNOWLEDGMENT

NI was supported by a grant from the Ministry of Higher Education, Malaysia and the University of Malaya.

REFERENCES

Adia, M. M., Emami, S. N., Byamukama, R., Faye, I., and Borg-Karlson, A.-K. (2016). Antiplasmodial activity and phytochemical analysis of extracts from selected Ugandan medicinal plants. *J. Ethnopharmacol.* 186, 14–19. doi: 10.1016/j.jep.2016.03.047

Alam, P., and Abdin, M. Z. (2011). Over-expression of HMG-CoA reductase and amorpha-4,11-diene synthase genes in *Artemisia annua* L. and its influence on artemisinin content. *Plant Cell Rep.* 30, 1919–1928. doi: 10.1007/s00299-011-1099-6

Alam, P., Kamaluddin, Sharaf-Eldin, M. A., Elkholy, S. F., and Abdin, M. Z. (2016). The effect of over-expression of rate limiting enzymes on the yield of

artemisinin in *Artemisia annua*. *Rendiconti Lincei* 27, 311–319. doi: 10.1007/s12210-015-0481-7

Amanullah, B. M., Rizvi, Z. F., and Zia, M. (2016). Production of artemisinin and its derivatives in hairy roots of *Artemisia dubia* induced by rola gene transformation. *Pak. J. Bot.* 48, 699–706.

Anterola, A., Shanle, E., Perroud, P.-F., and Quatrano, R. (2009). Production of taxa-4(5),11(12)-diene by transgenic *Physcomitrella patens*. *Transgenic Res.* 18, 655–660. doi: 10.1007/s11248-009-9252-5

Aquil, S., Husaini, A. M., Abdin, M. Z., and Rather, G. M. (2009). Overexpression of the HMG-CoA reductase gene leads to enhanced artemisinin biosynthesis in transgenic *Artemisia annua* plants. *Planta Med.* 75, 1453–1458. doi: 10.1055/s-0029-1185775

Baldi, A., and Dixit, V. K. (2008). Yield enhancement strategies for artemisinin production by suspension cultures of *Artemisia annua*. *Bioresour. Technol.* 99, 4609–4614. doi: 10.1016/j.biortech.2007.06.061

Banek, K., Lalani, M., Staedke, S. G., and Chandramohan, D. (2014). Adherence to artemisinin-based combination therapy for the treatment of malaria: a systematic review of the evidence. *Malar. J.* 13:7. doi: 10.1186/1475-2875-13-7

Banyai, W., Kirdmanee, C., Mii, M., and Supaibulwatana, K. (2010a). Overexpression of farnesyl pyrophosphate synthase (FPS) gene affected artemisinin content and growth of *Artemisia annua* L. *Plant Cell Tissue Organ Cult.* 103, 255–265. doi: 10.1007/s11240-010-9775-8

Banyai, W., Sangthong, R., Karaket, N., Inthima, P., Mii, M., and Supaibulwatana, K. (2010b). Overproduction of artemisinin in tetraploid *Artemisia annua* L. *Plant Biotechnol. J.* 27, 427–433. doi: 10.5511/plantbiotechnology.10.0726a

Banyai, W., Mii, M., and Supaibulwatana, K. (2011). Enhancement of artemisinin content and biomass in *Artemisia annua* by exogenous GA3 treatment. *Plant Growth Regul.* 63, 45–54. doi: 10.1007/s10725-010-9510-9

Benjamin, K. R., Silva, I. R., Cherubim, J. O. P., Mcphee, D., and Paddon, C. J. (2016). Developing commercial production of semi-synthetic artemisinin, and of ^{2}-farnesene, an isoprenoid produced by fermentation of Brazilian sugar. *J. Braz. Chem. Soc.* 27, 1339–1345. doi: 10.5935/0103-5053.20160119

Bhakuni, R., Jain, D., Sharma, R., and Kumar, S. (2001). Secondary metabolites of *Artemisia annua* and their biological activity. *Curr. Sci.* 80, 35–48.

Boes, A., Reimann, A., Twyman, R. M., Fischer, R., Schillberg, S., and Spiegel, H. (2016). "A plant-based transient expression system for the rapid production of malaria vaccine candidates," in *Vaccine Design: Methods and Protocols: Vaccines for Veterinary Diseases*, Vol. 2, ed. S. Thomas (New York, NY: Springer), 597–619.

Bouwmeester, H. J., Wallaart, T. E., Janssen, M. H., Van Loo, B., Jansen, B. J., Posthumus, M. A., et al. (1999). Amorpha-4, 11-diene synthase catalyses the first probable step in artemisinin biosynthesis. *Phytochemistry* 52, 843–854. doi: 10.1016/S0031-9422(99)00206-X

Brisibe, E. A., Udensi, O., Chukwurah, P. N., De Magalhäes, P. M., Figueira, G. M., and Ferreira, J. F. (2012). Adaptation and agronomic performance of *Artemisia annua* L. under lowland humid tropical conditions. *Ind. Crops Prod.* 39, 190–197. doi: 10.1016/j.indcrop.2012.02.018

Brown, G. D. (2010). The biosynthesis of artemisinin (Qinghaosu) and the phytochemistry of *Artemisia annua* L. (Qinghao). *Molecules* 15, 7603–7698. doi: 10.3390/molecules15117603

Bulgakov, V. P. (2008). Functions of rol genes in plant secondary metabolism. *Biotechnol. Adv.* 26, 318–324. doi: 10.1016/j.biotechadv.2008.03.001

Buttner-Mainik, A., Parsons, J., Jerome, H., Hartmann, A., Lamer, S., Schaaf, A., et al. (2011). Production of biologically active recombinant human factor H in *Physcomitrella*. *Plant Biotechnol. J.* 9, 373–383. doi: 10.1111/j.1467-7652.2010.00552.x

Carter, R., and Mendis, K. N. (2002). Evolutionary and historical aspects of the burden of malaria. *Clin. Microbiol. Rev.* 15, 564–594. doi: 10.1128/CMR.15.4.564-594.2002

Chen, D., Ye, H., and Li, G. (2000). Expression of a chimeric farnesyl diphosphate synthase gene in *Artemisia annua* L. transgenic plants via *Agrobacterium tumefaciens*-mediated transformation. *Plant Sci.* 155, 179–185. doi: 10.1016/S0168-9452(00)00217-X

Chen, J.-L., Fang, H.-M., Ji, Y.-P., Pu, G.-B., Guo, Y.-W., Huang, L.-L., et al. (2011). Artemisinin biosynthesis enhancement in transgenic *Artemisia annua* plants by downregulation of the β-caryophyllene synthase gene. *Planta Med.* 77, 1759–1765. doi: 10.1055/s-0030-1271038

Chen, M., Yan, T., Shen, Q., Lu, X., Pan, Q., Huang, Y., et al. (2017). GLANDULAR TRICHOME-SPECIFIC WRKY 1 promotes artemisinin biosynthesis in *Artemisia annua*. *New Phytol.* 214, 304–316. doi: 10.1111/nph.14373

Chen, Y., Shen, Q., Wang, Y., Wang, T., Wu, S., Zhang, L., et al. (2013). The stacked over-expression of FPS, CYP71AV1 and CPR genes leads to the increase of artemisinin level in *Artemisia annua* L. *Plant Biotechnol. Rep.* 7, 287–295. doi: 10.1007/s11816-012-0262-z

Cockram, J., Hill, C., Burns, C., Arroo, R. R., Woolley, J. G., Flockart, I., et al. (2012). Screening a diverse collection of *Artemisia annua* germplasm accessions for the antimalarial compound, artemisinin. *Plant Genet. Resour.* 10, 152–154. doi: 10.1017/S1479262112000159

Cox, F. (2010). History of the discovery of the malaria parasites and their vectors. *Parasit. Vectors* 3:5. doi: 10.1186/1756-3305-3-5

Czechowski, T., Larson, T. R., Catania, T. M., Harvey, D., Brown, G. D., and Graham, I. A. (2016). *Artemisia annua* mutant impaired in artemisinin synthesis demonstrates importance of nonenzymatic conversion in terpenoid metabolism. *Proc. Natl. Acad. Sci. U.S.A.* 113, 15150–15155. doi: 10.1073/pnas.1611567113

Dangash, A., Pandya, N., Bharillya, A., Jhala, A., and Jain, D. (2014). Impact of exogenous elicitors on artemisinin production and trichome density in *Artemisia annua* L. under subtropical conditions. *Not. Sci. Biol.* 6, 349–353. doi: 10.15835/nsb.6.3.9109

Delabays, N., Collet, G., and Benakis, A. (1993). Selection and breeding for high artemisinin (Qinghaosu) yielding strains of *Artemisia annua*. *Acta Hortic.* 330, 203–208. doi: 10.17660/ActaHortic.1993.330.24

Delabays, N., Simonnet, X., and Gaudin, M. (2001). The genetics of artemisinin content in *Artemisia annua* L. and the breeding of high yielding cultivars. *Curr. Med. Chem.* 8, 1795–1801. doi: 10.2174/0929867013371635

Dilshad, E., Cusido, R. M., Estrada, K. R., Bonfill, M., and Mirza, B. (2015a). Genetic transformation of *Artemisia carvifolia* buch with rol genes enhances artemisinin accumulation. *PLOS ONE* 10:e0140266. doi: 10.1371/journal.pone.0140266

Dilshad, E., Cusido, R. M., Palazon, J., Estrada, K. R., Bonfill, M., and Mirza, B. (2015b). Enhanced artemisinin yield by expression of rol genes in *Artemisia annua*. *Malar. J.* 14, 424. doi: 10.1186/s12936-015-0951-5

Duke, M. V., Paul, R. N., Elsohly, H. N., Sturtz, G., and Duke, S. O. (1994). Localization of artemisinin and artemisitene in foliar tissues of glanded and glandless biotypes of *Artemisia annua* L. *Int. J. Plant Sci.* 155, 365–372. doi: 10.1086/297173

Epstein, J. E., Paolino, K. M., Richie, T. L., Sedegah, M., Singer, A., Ruben, A. J., et al. (2017). Protection against *Plasmodium falciparum* malaria by PfSPZ vaccine. *JCI Insight* 2:e89154. doi: 10.1172/jci.insight.89154

Farhi, M., Marhevka, E., Ben-Ari, J., Algamas-Dimantov, A., Liang, Z., Zeevi, V., et al. (2011). Generation of the potent anti-malarial drug artemisinin in tobacco. *Nat. Biotechnol.* 29, 1072–1074. doi: 10.1038/nbt.2054

Ferreira, J. F., and Janick, J. (1995). Floral morphology of *Artemisia annua* with special reference to trichomes. *Int. J. Plant Sci.* 156, 807–815. doi: 10.1086/297304

Ferreira, J. F., Laughlin, J., Delabays, N., and De Magalhães, P. M. (2005). Cultivation and genetics of *Artemisia annua* L. for increased production of the antimalarial artemisinin. *Plant Genet. Resour.* 3, 206–229. doi: 10.1079/PGR200585

Frank, W., Decker, E., and Reski, R. (2005). Molecular tools to study *Physcomitrella patens*. *Plant Biol.* 7, 220–227. doi: 10.1055/s-2005-865645

Fuentes, P., Zhou, F., Erban, A., Karcher, D., Kopka, J., and Bock, R. (2016). A new synthetic biology approach allows transfer of an entire metabolic pathway from a medicinal plant to a biomass crop. *eLife* 5:e13664. doi: 10.7554/eLife.13664

Ghosh, B., Mukherjee, S., and Jha, S. (1997). Genetic transformation of *Artemisia annua* by *Agrobacterium tumefaciens* and artemisinin synthesis in transformed cultures. *Plant Sci.* 122, 193–199. doi: 10.4103/0973-1296.127372

Graham, I. A., Besser, K., Blumer, S., Branigan, C. A., Czechowski, T., Elias, L., et al. (2010). The genetic map of *Artemisia annua* L. identifies loci affecting yield of the antimalarial drug artemisinin. *Science* 327, 328–331. doi: 10.1126/science.1182612

Guo, X.-X., Yang, X.-Q., Yang, R.-Y., and Zeng, Q.-P. (2010). Salicylic acid and methyl jasmonate but not Rose Bengal enhance artemisinin production through invoking burst of endogenous singlet oxygen. *Plant Sci.* 178, 390–397. doi: 10.1016/j.plantsci.2010.01.014

Han, J., Wang, H., Kanagarajan, S., Hao, M., Lundgren, A., and Brodelius, P. E. (2016). Promoting artemisinin biosynthesis in *Artemisia annua* plants by substrate channeling. *Mol. Plant* 9, 946–948. doi: 10.1016/j.molp.2016.03.004

Han, J. L., Liu, B. Y., Ye, H. C., Wang, H., Li, Z. Q., and Li, G. F. (2006). Effects of overexpression of the endogenous farnesyl diphosphate synthase on the artemisinin content in *Artemisia annua* L. *J. Integr. Plant Biol.* 48, 482–487. doi: 10.1111/j.1744-7909.2006.00208.x

He, Q., Fu, X., Shi, P., Liu, M., Shen, Q., and Tang, K. (2017). Glandular trichome-specific expression of alcohol dehydrogenase 1 (ADH1) using a promoter-GUS fusion in *Artemisia annua* L. *Plant Cell Tissue Organ Cult.* 130, 61–72. doi: 10.1007/s11240-017-1204-9

Hong, G.-J., Hu, W.-L., Li, J.-X., Chen, X.-Y., and Wang, L.-J. (2009). Increased accumulation of artemisinin and anthocyanins in *Artemisia annua* expressing the *Arabidopsis* blue light receptor *CRY1*. *Plant Mol. Biol. Rep.* 27, 334–341. doi: 10.1007/s11105-008-0088-6

Ikram, N. K. B., Beyraghdar Kashkooli, A., Peramuna, A. V., Van Der Krol, A. R., Bouwmeester, H., and Simonsen, H. T. (2017). Stable production of the antimalarial drug artemisinin in the moss *Physcomitrella patens*. *Front. Bioeng. Biotechnol.* 5:47. doi: 10.3389/fbioe.2017.00047

Ikram, N. K., Zhan, X., Pan, X., King, B. C., and Simonsen, H. T. (2015). Stable heterologous expression of biologically active terpenoids in green plant cells. *Front. Plant Sci.* 6:129. doi: 10.3389/fpls.2015.00129

Jiang, W., Fu, X., Pan, Q., Tang, Y., Shen, Q., Lv, Z., et al. (2016). Overexpression of AaWRKY1 leads to an enhanced content of artemisinin in *Artemisia annua*. *Biomed Res. Int.* 2016:7314971. doi: 10.1155/2016/7314971

King, B. C., Vavitsas, K., Ikram, N. K. B. K., Schrøder, J., Scharff, L. B., Hamberger, B., et al. (2016). In vivo assembly of DNA-fragments in the moss, *Physcomitrella patens*. *Sci. Rep.* 6:25030. doi: 10.1038/srep25030

Kjær, A., Grevsen, K., and Jensen, M. (2012). Effect of external stress on density and size of glandular trichomes in full-grown *Artemisia annua*, the source of anti-malarial artemisinin. *AoB Plants* 2012:ls018. doi: 10.1093/aobpla/pls018

Klayman, D. L. (1985). Qinghaosu (artemisinin): an antimalarial drug from China. *Science* 228, 1049–1055. doi: 10.1126/science.3887571

Lalloo, D. G., Shingadia, D., Bell, D. J., Beeching, N. J., Whitty, C. J. M., and Chiodini, P. L. (2016). UK malaria treatment guidelines 2016. *J. Infect.* 72, 635–649. doi: 10.1016/j.jinf.2016.02.001

Larson, T. R., Branigan, C., Harvey, D., Penfield, T., Bowles, D., and Graham, I. A. (2013). A survey of artemisinic and dihydroartemisinic acid contents in glasshouse and global field-grown populations of the artemisinin-producing plant *Artemisia annua* L. *Ind. Crops Prod.* 45, 1–6. doi: 10.1016/j.indcrop.2012.12.004

Laursen, T., Borch, J., Knudsen, C., Bavishi, K., Torta, F., Martens, H. J., et al. (2016). Characterization of a dynamic metabolon producing the defense compound dhurrin in sorghum. *Science* 354, 890–893. doi: 10.1126/science.aag2347

Ling, X., Hexin, T., and Lei, Z. (2016). *Artemisia annua* glandular secretory trichomes: the biofactory of antimalarial agent artemisinin. *Sci. Bull.* 61, 26–36. doi: 10.1007/s11434-015-0980-z

Liu, C.-Z., Guo, C., Wang, Y.-C., and Ouyang, F. (2002). Effect of light irradiation on hairy root growth and artemisinin biosynthesis of *Artemisia annua* L. *Proc. Biochem.* 38, 581–585. doi: 10.1016/S0032-9592(02)00165-6

Liu, M., Shi, P., Fu, X., Brodelius, P. E., Shen, Q., Jiang, W., et al. (2016). Characterization of a trichome-specific promoter of the aldehyde dehydrogenase 1 (ALDH1) gene in *Artemisia annua*. *Plant Cell Tissue Organ Cult.* 126, 469–480. doi: 10.1007/s11240-016-1015-4

Lommen, W., Schenk, E., Bouwmeester, H., and Verstappen, F. (2006). Trichome dynamics and artemisinin accumulation during development and senescence of *Artemisia annua* leaves. *Planta Med.* 72, 336–345. doi: 10.1055/s-2005-916202

Lu, X., Shen, Q., Zhang, L., Zhang, F., Jiang, W., Lv, Z., et al. (2013a). Promotion of artemisinin biosynthesis in transgenic *Artemisia annua* by overexpressing *ADS*, *CYP71AV1* and *CPR* genes. *Ind. Crops Prod.* 49, 380–385. doi: 10.1016/j.indcrop.2013.04.045

Lu, X., Zhang, L., Zhang, F., Jiang, W., Shen, Q., Zhang, L., et al. (2013b). AaORA, a trichome-specific AP2/ERF transcription factor of *Artemisia annua*, is a positive regulator in the artemisinin biosynthetic pathway and in disease resistance to *Botrytis cinerea*. *New Phytol.* 198, 1191–1202. doi: 10.1111/nph.12207

Luo, X. D., and Shen, C. C. (1987). The chemistry, pharmacology, and clinical applications of qinghaosu (artemisinin) and its derivatives. *Med. Res. Rev.* 7, 29–52. doi: 10.1002/med.2610070103

Lv, Z., Wang, S., Zhang, F., Chen, L., Hao, X., Pan, Q., et al. (2016). Overexpression of a Novel NAC domain-containing transcription factor gene (AaNAC1) enhances the content of artemisinin and increases tolerance to drought and *Botrytis cinerea* in *Artemisia annua*. *Plant Cell Physiol.* 57, 1961–1971. doi: 10.1093/pcp/pcw118

Ma, C., Wang, H., Lu, X., Wang, H., Xu, G., and Liu, B. (2009). Terpenoid metabolic profiling analysis of transgenic *Artemisia annua* L. by comprehensive two-dimensional gas chromatography time-of-flight mass spectrometry. *Metabolomics* 5, 497–506. doi: 10.1007/s11306-009-0170-6

Ma, D., Li, G., Alejos-Gonzalez, F., Zhu, Y., Xue, Z., Wang, A., et al. (2017a). Overexpression of a type I isopentenyl pyrophosphate isomerase of *Artemisia annua* in the cytosol leads to high arteannuin B production and artemisinin increase. *Plant J.* 91, 466–479. doi: 10.1111/tpj.13583

Ma, D., Li, G., Zhu, Y., and Xie, D.-Y. (2017b). Overexpression and suppression of *Artemisia annua* 4-hydroxy-3-methylbut-2-enyl diphosphate reductase 1 gene (*AaHDR1*) differentially regulate artemisinin and terpenoid biosynthesis. *Front. Plant Sci.* 8:77. doi: 10.3389/fpls.2017.00077

Ma, D.-M., Wang, Z., Wang, L., Alejos-Gonzales, F., Sun, M.-A., and Xie, D.-Y. (2015). A genome-wide scenario of terpene pathways in self-pollinated *Artemisia annua*. *Mol. Plant* 8, 1580–1598. doi: 10.1016/j.molp.2015.07.004

Malhotra, K., Subramaniyan, M., Rawat, K., Kalamuddin, M., Qureshi, M. I., Malhotra, P., et al. (2016). Compartmentalized metabolic engineering for artemisinin biosynthesis and effective malaria treatment by oral delivery of plant Cells. *Mol. Plant* 9, 1464–1477. doi: 10.1016/j.molp.2016.09.013

Mercke, P., Bengtsson, M., Bouwmeester, H. J., Posthumus, M. A., and Brodelius, P. E. (2000). Molecular cloning, expression, and characterization of amorpha-4,11-diene synthase, a key enzyme of artemisinin biosynthesis in *Artemisia annua* L. *Arch. Biochem. Biophys.* 381, 173–180. doi: 10.1006/abbi.2000.1962

Muangphrom, P., Seki, H., Fukushima, E. O., and Muranaka, T. (2016). Artemisinin-based antimalarial research: application of biotechnology to the production of artemisinin, its mode of action, and the mechanism of resistance of *Plasmodium* parasites. *J. Nat. Med.* 70, 318–334. doi: 10.1007/s11418-016-1008-y

Nafis, T., Akmal, M., Ram, M., Alam, P., Ahlawat, S., Mohd, A., et al. (2011). Enhancement of artemisinin content by constitutive expression of the HMG-CoA reductase gene in high-yielding strain of *Artemisia annua* L. *Plant Biotechnol. Rep.* 5, 53–60. doi: 10.1007/s11816-010-0156-x

Nair, M. S. R., Acton, N., Klayman, D. L., Kendrick, K., Basile, D. V., and Mante, S. (1986). Production of artemisinin in tissue cultures of *Artemisia Annua*. *J. Nat. Prod.* 49, 504–507. doi: 10.1021/np50045a021

Nondo, R. S. O., Moshi, M. J., Erasto, P., Masimba, P. J., Machumi, F., Kidukuli, A. W., et al. (2017). Anti-plasmodial activity of norcaesalpin D and extracts of four medicinal plants used traditionally for treatment of malaria. *BMC Complement. Altern. Med.* 17:167. doi: 10.1186/s12906-017-1673-8

Olofsson, L., Engstrom, A., Lundgren, A., and Brodelius, P. (2011). Relative expression of genes of terpene metabolism in different tissues of *Artemisia annua* L. *BMC Plant Biol.* 11:45. doi: 10.1186/1471-2229-11-45

Olsson, M. E., Olofsson, L. M., Lindahl, A.-L., Lundgren, A., Brodelius, M., and Brodelius, P. E. (2009). Localization of enzymes of artemisinin biosynthesis to the apical cells of glandular secretory trichomes of *Artemisia annua* L. *Phytochemistry* 70, 1123–1128. doi: 10.1016/j.phytochem.2009.07.009

Paddon, C. J., Westfall, P., Pitera, D., Benjamin, K., Fisher, K., Mcphee, D., et al. (2013). High-level semi-synthetic production of the potent antimalarial artemisinin. *Nature* 496, 528–532. doi: 10.1038/nature12051

Pan, X.-W., Han, L., Zhang, Y.-H., Chen, D.-F., and Simonsen, H. T. (2015). Sclareol production in the moss *Physcomitrella* patens and observations on growth and terpenoid biosynthesis. *Plant Biotechnol. Rep.* 9, 149–159. doi: 10.1007/s11816-015-0353-8

Pandey, N., Meena, R. P., Rai, S. K., and Pandey-Rai, S. (2016). In vitro generation of high artemisinin yielding salt tolerant somaclonal variant and development of SCAR marker in *Artemisia annua* L. *Plant Cell Tissue Organ Cult.* 127, 301–314. doi: 10.1007/s11240-016-1050-1

Pandey, N., and Pandey-Rai, S. (2014). Short term UV-B radiation-mediated transcriptional responses and altered secondary metabolism of in vitro

propagated plantlets of *Artemisia annua* L. *Plant Cell Tissue Organ Cult.* 116, 371–385. doi: 10.1007/s11240-013-0413-0

Patra, N., and Srivastava, A. K. (2017). "Mass production of artemisinin using hairy root cultivation of *Artemisia annua* in bioreactor," in *Bioprocessing of Plant in Vitro Systems*, eds A. Pavlov and T. Bleys (Cham: Springer International Publishing), 1–17.

Peplow, M. (2016). Synthetic malaria drug meets market resistance: first commercial deployment of synthetic biology for medicine has modest impact. *Nature* 530, 389–391. doi: 10.1038/530390a

Picaud, S., Mercke, P., He, X., Sterner, O., Brodelius, M., Cane, D. E., et al. (2006). Amorpha-4,11-diene synthase: mechanism and stereochemistry of the enzymatic cyclization of farnesyl diphosphate. *Arch. Biochem. Biophys.* 448, 150–155. doi: 10.1016/j.abb.2005.07.015

Picaud, S., Olofsson, L., Brodelius, M., and Brodelius, P. E. (2005). Expression, purification, and characterization of recombinant amorpha-4,11-diene synthase from *Artemisia annua* L. *Arch. Biochem. Biophys.* 436, 215–226. doi: 10.1016/j.abb.2005.02.012

Pulice, G., Pelaz, S., and Matías-Hernández, L. (2016). Molecular Farming in *Artemisia annua*, a promising approach to improve anti-malarial drug production. *Front. Plant Sci.* 7:329. doi: 10.3389/fpls.2016.00329

Reski, R. (1998). Development, genetics and molecular biology of mosses. *Bot. Acta* 111, 1–15. doi: 10.1111/j.1438-8677.1998.tb00670.x

Reski, R., Parsons, J., and Decker, E. L. (2015). Moss-made pharmaceuticals: from bench to bedside. *Plant Biotechnol. J.* 13, 1191–1198. doi: 10.1111/pbi.12401

Rosales-Mendoza, S., Nieto-Gómez, R., and Angulo, C. (2017). A perspective on the development of plant-made vaccines in the fight against Ebola virus. *Front. Immunol.* 8:252. doi: 10.3389/fimmu.2017.00252

Rosales-Mendoza, S., Orellana-Escobedo, L., Romero-Maldonado, A., Decker, E. L., and Reski, R. (2014). The potential of *Physcomitrella patens* as a platform for the production of plant-based vaccines. *Expert Rev. Vaccines* 13, 203–212. doi: 10.1586/14760584.2014.872987

Rydén, A.-M., Ruyter-Spira, C., Quax, W. J., Osada, H., Muranaka, T., Kayser, O., et al. (2010). The molecular cloning of dihydroartemisinic aldehyde reductase and its implication in artemisinin biosynthesis in *Artemisia annua*. *Planta Med.* 76, 1778–1783. doi: 10.1055/s-0030-1249930

Schaefer, D. G., and Zrÿd, J. P. (1997). Efficient gene targeting in the moss *Physcomitrella patens*. *Plant J.* 11, 1195–1206. doi: 10.1046/j.1365-313X.1997.11061195.x

Shen, Q., Chen, Y., Wang, T., Wu, S., Lu, X., Zhang, L., et al. (2012). Overexpression of the cytochrome P450 monooxygenase (cyp71av1) and cytochrome P450 reductase (cpr) genes increased artemisinin content in *Artemisia annua* (Asteraceae). *Genet. Mol. Res.* 11, 3298–3309. doi: 10.4238/2012.September.12.13

Shen, Q., Lu, X., Yan, T., Fu, X., Lv, Z., Zhang, F., et al. (2016a). The jasmonate-responsive AaMYC2 transcription factor positively regulates artemisinin biosynthesis in *Artemisia annua*. *New Phytol.* 210, 1269–1281. doi: 10.1111/nph.13874

Shen, Q., Yan, T., Fu, X., and Tang, K. (2016b). Transcriptional regulation of artemisinin biosynthesis in *Artemisia annua* L. *Sci. Bull.* 61, 18–25. doi: 10.1007/s11434-015-0983-9

Shi, P., Fu, X., Liu, M., Shen, Q., Jiang, W., Li, L., et al. (2017). Promotion of artemisinin content in *Artemisia annua* by overexpression of multiple artemisinin biosynthetic pathway genes. *Plant Cell Tissue Organ Cult.* 129, 251–259. doi: 10.1007/s11240-017-1173-z

Shretta, R., and Yadav, P. (2012). Stabilizing supply of artemisinin and artemisinin-based combination therapy in an era of wide-spread scale-up. *Malar. J.* 11:399. doi: 10.1186/1475-2875-11-399

Simonsen, H. T., Drew, D. P., and Lunde, C. (2009). Perspectives on using *Physcomitrella patens* as an alternative production platform for thapsigargin and other terpenoid drug candidates. *Perspect. Medicin. Chem.* 3, 1–6. doi: 10.4137/PMC.S2220

Simonsen, H. T., Nordskjold, J. B., Smitt, U. W., Nyman, U., Palpu, P., Joshi, P., et al. (2001). In vitro screening of Indian medicinal plants for antiplasmodial activity. *J. Ethnopharmacol.* 74, 195–204. doi: 10.1016/S0378-8741(00)00369-X

Simonsen, H. T., Weitzel, C., and Christensen, S. B. (2013). "Guaianolide sesquiterpenoids - Their pharmacology and biosynthesis," in *Handbook of Natural Products - Phytochemistry, Botany and Metabolism of Alkaloids, Phenolics and Terpenes*, eds K. G. Ramawat and J. M. Merillon (Berlin: Springer-Verlag), 3069–3098.

Singh, D., Mcphee, D., Paddon, C. J., Cherry, J., Maurya, G., Mahale, G., et al. (2017). Amalgamation of synthetic biology and chemistry for high-throughput nonconventional synthesis of the antimalarial drug artemisinin. *Org. Process Res. Dev.* 21, 551–558. doi: 10.1021/acs.oprd.6b00414

Sy, L.-K., and Brown, G. D. (2002). The mechanism of the spontaneous autoxidation of dihydroartemisinic acid. *Tetrahedron* 58, 897–908. doi: 10.1016/S0040-4020(01)01193-0

Tang, K., Chen, Y., Shen, Q., Wang, T., Wu, S., and Wang, G. (2012a). Overexpression ALDH1 gene increased artemisinin content in *Artemisia annua* L. China Patent Application CN201210014242.

Tang, K., Shen, Q., Chen, Y., Wang, T., Wu, S., and Lu, X. (2012b). Overexpression DBR2 gene increased artemisinin content in *Artemisia annua* L. China Patent Application CN201210014227.

Tang, K., Shen, Q., Yan, T., and Fu, X. (2014). Transgenic approach to increase artemisinin content in *Artemisia annua* L. *Plant Cell Rep.* 33, 605–615. doi: 10.1007/s00299-014-1566-y

Teoh, K. H., Polichuk, D. R., Reed, D. W., and Covello, P. S. (2009). Molecular cloning of an aldehyde dehydrogenase implicated in artemisinin biosynthesis in *Artemisia annua*. *Botany* 87, 635–642. doi: 10.1139/B09-032

Teoh, K. H., Polichuk, D. R., Reed, D. W., Nowak, G., and Covello, P. S. (2006). *Artemisia annua* L. (Asteraceae) trichome-specific cDNAs reveal CYP71AV1, a cytochrome P450 with a key role in the biosynthesis of the antimalarial sesquiterpene lactone artemisinin. *FEBS Lett.* 580, 1411–1416. doi: 10.1016/j.febslet.2006.01.065

Ting, H. M., Wang, B., Rydén, A. M., Woittiez, L., Herpen, T., Verstappen, F. W., et al. (2013). The metabolite chemotype of *Nicotiana benthamiana* transiently expressing artemisinin biosynthetic pathway genes is a function of CYP71AV1 type and relative gene dosage. *New Phytol.* 199, 352–366. doi: 10.1111/nph.12274

Townsend, T., Segura, V., Chigeza, G., Penfield, T., Rae, A., Harvey, D., et al. (2013). The use of combining ability analysis to identify elite parents for *Artemisia annua* F1 hybrid production. *PLOS ONE* 8:e61989. doi: 10.1371/journal.pone.0061989

Tu, Y. (2011). The discovery of artemisinin (qinghaosu) and gifts from Chinese medicine. *Nat. Med.* 17, 1217–1220. doi: 10.1038/nm.2471

Van Agtmael, M. A., Eggelte, T. A., and Van Boxtel, C. J. (1999). Artemisinin drugs in the treatment of malaria: from medicinal herb to registered medication. *Trends Pharmacol. Sci.* 20, 199–205. doi: 10.1016/S0165-6147(99)01302-4

Van Herpen, T. W., Cankar, K., Nogueira, M., Bosch, D., Bouwmeester, H. J., and Beekwilder, J. (2010). *Nicotiana benthamiana* as a production platform for artemisinin precursors. *PLOS ONE* 5:e14222. doi: 10.1371/journal.pone.0014222

Wallaart, T. E., Bouwmeester, H. J., Hille, J., Poppinga, L., and Maijers, N. C. (2001). Amorpha-4,11-diene synthase: cloning and functional expression of a key enzyme in the biosynthetic pathway of the novel antimalarial drug artemisinin. *Planta* 212, 460–465. doi: 10.1007/s004250000428

Wang, B., Kashkooli, A. B., Sallets, A., Ting, H.-M., De Ruijter, N. C., Olofsson, L., et al. (2016). Transient production of artemisinin in *Nicotiana benthamiana* is boosted by a specific lipid transfer protein from *A. annua*. *Metab. Eng.* 38, 159–169. doi: 10.1016/j.ymben.2016.07.004

Wang, H., Ma, C., Li, Z., Ma, L., Wang, H., Ye, H., et al. (2010). Effects of exogenous methyl jasmonate on artemisinin biosynthesis and secondary metabolites in *Artemisia annua* L. *Ind. Crops Prod.* 31, 214–218. doi: 10.1016/j.indcrop.2009.10.008

Wang, Y., and Weathers, P. (2007). Sugars proportionately affect artemisinin production. *Plant Cell Rep.* 26, 1073–1081. doi: 10.1007/s00299-006-0295-2

Wang, Y., Yang, K., Jing, F., Li, M., Deng, T., Huang, R., et al. (2011). Cloning and characterization of trichome-specific promoter of cpr71av1 gene involved in artemisinin biosynthesis in *Artemisia annua* L. *Mol. Biol.* 45, 751. doi: 10.1134/S0026893311040145

Weathers, P. J., Elkholy, S., and Wobbe, K. K. (2006). Artemisinin: the biosynthetic pathway and Its regulation in *Artemisia annua*, a terpenoid-rich species. *In Vitro Cell Dev. Biol. Plant* 42, 309–317. doi: 10.1079/IVP2006782

Wen, W., and Yu, R. (2011). Artemisinin biosynthesis and its regulatory enzymes: progress and perspective. *Pharmacogn. Rev.* 5, 189–194. doi: 10.4103/0973-7847.91118

Woerdenbag, H., Lüers, J. J., Van Uden, W., Pras, N., Malingré, T., and Alfermann, A. W. (1993). Production of the new antimalarial drug artemisinin in shoot cultures of *Artemisia annua* L. *Plant Cell Tissue Organ Cult.* 32, 247–257. doi: 10.1007/BF00029850

World Health Organization [WHO] (2015). *Guidelines for the Treatment of Malaria*, 3rd Edn. Geneva: WHO.

World Health Organization [WHO] (2016). *World Malaria Report*. Geneva: WHO.

Xiang, L., Zeng, L. X., Yuan, Y., Chen, M., Wang, F., Liu, X. Q., et al. (2012). Enhancement of artemisinin biosynthesis by overexpressing dxr, cyp71av1 and cpr in the plants of *Artemisia annua* L. *Plant Omics* 5, 503–507.

Xiang, L., Zhu, S., Zhao, T., Zhang, M., Liu, W., Chen, M., et al. (2015). Enhancement of artemisinin content and relative expression of genes of artemisinin biosynthesis in *Artemisia annua* by exogenous MeJA treatment. *Plant Growth Regul.* 75, 435–441. doi: 10.1007/s10725-014-0004-z

Xie, D.-Y., Ma, D.-M., Judd, R., and Jones, A. L. (2016). Artemisinin biosynthesis in *Artemisia annua* and metabolic engineering: questions, challenges, and perspectives. *Phytochem. Rev.* 15, 1093–1114. doi: 10.1007/s11101-016-9480-2

Yin, L., Zhao, C., Huang, Y., Yang, R.-Y., and Zeng, Q.-P. (2008). Abiotic stress-induced expression of artemisinin biosynthesis genes in *Artemisia annua* L. *Chin. J. Appl. Environ. Biol.* 14, 1–15.

Yu, Z.-X., Li, J.-X., Yang, C.-Q., Hu, W.-L., Wang, L.-J., and Chen, X.-Y. (2012). The jasmonate-responsive AP2/ERF transcription factors AaERF1 and AaERF2 positively regulate artemisinin biosynthesis in *Artemisia annua* L. *Mol. Plant* 5, 353–365. doi: 10.1093/mp/ssr087

Zhan, X., Zhang, Y.-H., Chen, D.-F., and Simonsen, H. T. (2014). Metabolic engineering of the moss *Physcomitrella patens* to produce the sesquiterpenoids patchoulol and α/β-santalene. *Front. Plant Sci.* 5:636. doi: 10.3389/fpls.2014.00636

Zhang, F., Lu, X., Lv, Z., Zhang, L., Zhu, M., Jiang, W., et al. (2013). Overexpression of the *Artemisia* orthologue of ABA receptor, AaPYL9, enhances ABA sensitivity and improves artemisinin content in *Artemisia annua* L. *PLOS ONE* 8:e56697. doi: 10.1371/journal.pone.0056697

Zhang, L., Jing, F., Li, F., Li, M., Wang, Y., Wang, G., et al. (2009). Development of transgenic *Artemisia annua* (Chinese wormwood) plants with an enhanced content of artemisinin, an effective anti-malarial drug, by hairpin-RNA-mediated gene silencing. *Biotechnol. Appl. Biochem.* 52, 199–207. doi: 10.1042/BA20080068

Zhang, Y., Nowak, G., Reed, D. W., and Covello, P. S. (2011). The production of artemisinin precursors in tobacco. *Plant Biotechnol. J.* 9, 445–454. doi: 10.1111/j.1467-7652.2010.00556.x

Zhang, Y., Teoh, K. H., Reed, D. W., Maes, L., Goossens, A., Olson, D. J., et al. (2008). The molecular cloning of artemisinic aldehyde Δ11(13) reductase and its role in glandular trichome-dependent biosynthesis of artemisinin in *Artemisia annua*. *J. Biol. Chem.* 283, 21501–21508. doi: 10.1074/jbc.M803090200

Conflict of Interest Statement: The authors declare that the research was conducted in the absence of any commercial or financial relationships that could be construed as a potential conflict of interest.

frontiers in Plant Science

MINI REVIEW
published: 31 January 2018
doi: 10.3389/fpls.2018.00087

Approaches and Recent Developments for the Commercial Production of Semi-synthetic Artemisinin

*Stephanie H. Kung, Sean Lund, Abhishek Murarka, Derek McPhee and Chris J. Paddon**

Amyris Inc., Emeryville, CA, United States

The antimalarial drug artemisinin is a natural product produced by the plant *Artemisia annua*. Extracts of *A. annua* have been used in Chinese herbal medicine for over two millennia. Following the re-discovery of *A. annua* extract as an effective antimalarial, and the isolation and structural elucidation of artemisinin as the active agent, it was recommended as the first-line treatment for uncomplicated malaria in combination with another effective antimalarial drug (Artemisinin Combination Therapy) by the World Health Organization (WHO) in 2002. Following the WHO recommendation, the availability and price of artemisinin fluctuated greatly, ranging from supply shortfalls in some years to oversupply in others. To alleviate these supply and price issues, a second source of artemisinin was sought, resulting in an effort to produce artemisinic acid, a late-stage chemical precursor of artemisinin, by yeast fermentation, followed by chemical conversion to artemisinin (i.e., semi-synthesis). Engineering to enable production of artemisinic acid in yeast relied on the discovery of *A. annua* genes encoding artemisinic acid biosynthetic enzymes, and synthetic biology to engineer yeast metabolism. The progress of this effort, which resulted in semi-synthetic artemisinin entering commercial production in 2013, is reviewed with an emphasis on recent publications and opportunities for further development. Aspects of both the biology of artemisinin production in *A. annua*, and yeast strain engineering are discussed, as are recent developments in the chemical conversion of artemisinic acid to artemisinin.

Keywords: artemisinic acid, artemisinin, semi-synthetic, *Saccharomyces cerevisiae*, synthetic biology, *Artemisia annua*

OPEN ACCESS

Edited by:
Peter E. Brodelius,
Linnaeus University, Sweden

Reviewed by:
Hikaru Seki,
Osaka University, Japan
Ryo Nakabayashi,
RIKEN, Japan

***Correspondence:**
Chris J. Paddon
paddon@amyris.com

Specialty section:
This article was submitted to Plant Biotechnology, a section of the journal Frontiers in Plant Science

Received: *06 November 2017*
Accepted: *15 January 2018*
Published: *31 January 2018*

Citation:
Kung SH, Lund S, Murarka A, McPhee D and Paddon CJ (2018) Approaches and Recent Developments for the Commercial Production of Semi-synthetic Artemisinin. Front. Plant Sci. 9:87. doi: 10.3389/fpls.2018.00087

INTRODUCTION

Artemisia annua has been known to traditional Chinese medicine for two millennia, but its modern history dates back to the 1970s when Chinese scientists rediscovered its antimalarial properties, and shortly thereafter isolated artemisinin, the active compound, and elucidated its structure (Tu, 2016, 2017). In 2002 the World Health Organization designated Artemisinin Combination Therapy (ACTs) as the first-line treatment for uncomplicated malaria (Paddon and Keasling, 2014). Following this decision there were significant swings in both the availability and price of artemisinin, which led to the concept of developing a second, non-plant derived, source to stabilize the availability and cost, and ultimately to decrease its cost (Hale et al., 2007). The semi-synthetic

artemisinin project that sprang from this concept envisaged production of a late-stage precursor (artemisinic acid) by microbial fermentation, followed by its isolation from the fermentation medium and chemical conversion to artemisinin (**Figure 1A**; Hale et al., 2007).

The semi-synthetic artemisinin project that led to the industrial production of artemisinic acid and its chemical conversion to artemisinin has been reviewed (Paddon and Keasling, 2014). Briefly, brewer's yeast (*Saccharomyces cerevisiae*) was engineered to overexpress the enzymes of the mevalonate pathway along with *A. annua* amorphadiene synthase, leading to the production of over 40 g/L amorphadiene (the hydrocarbon precursor of artemisinic acid) in fed-batch fermentors fed with ethanol (presumed to feed directly into cytosolic acetyl-CoA production) (Westfall et al., 2012). The cytochrome P450 enzyme (CYP71AV1) and its cognate reductase (*Aa*CPR) responsible for the oxidation of amorphadiene had been identified earlier (Ro et al., 2006), but conversion of amorphadiene to artemisinic acid was poor when expressed in yeast (Westfall et al., 2012). High-level production of artemisinic acid (25 g/L) by yeast fermentation at 2 L scale was achieved by decreasing the expression of *Aa*CPR to (presumably) alter the stoichiometry of the CYP71AV1:*Aa*CPR interaction, and co-expression of other enzymes (cytochrome b5 and two dehydrogenases) involved in the three oxidation reactions that convert amorphadiene to artemisinic acid (**Figure 1B**; Paddon et al., 2013). Following the development of an industrial process for the chemical conversion of artemisinic acid to artemisinin, commercial production of semi-synthetic artemisinin began in 2013 (Paddon and Keasling, 2014; Peplow, 2016).

The strain engineering and processes for production for amorphadiene and artemisinic acid at laboratory scale (Westfall et al., 2012; Paddon et al., 2013) were completed in 2008, almost a decade ago. Much has changed technologically in the intervening years, allowing the prospect of significantly improving the production of semi-synthetic artemisinin to decrease its cost. Developments have been made in several relevant areas including improved production of terpenes by yeast, understanding of cytochrome P450 oxidation reactions, advancements in understanding of the enzymology and physiology of artemisinin production in *A. annua* trichomes (Czechowski et al., 2016), and finally advances in the chemistry for conversion of artemisinic acid to artemisinin. These developments are described below. For comparison, advances in the biotechnological production of artemisinin in plants have been recently reviewed (Ikram and Simonsen, 2017), as has an overview of the engineering of cellular metabolism (Nielsen and Keasling, 2016).

DEVELOPING TERPENOID PRODUCTION DIRECTLY FROM SUGAR

Early descriptions of amorphadiene production by yeast were at concentrations of ∼100 mg/L (Ro et al., 2006), which was increased to 40 g/L following considerable strain engineering and the use of a pure ethanol feedstock in pulse-fed batch fermentations. However, this methodology is not industrially scalable owing to the excessively high oxygen demand, and the process difficulties that a pure ethanol feed would bring (Westfall et al., 2012). An ethanol–glucose feed could be industrially feasible, but decreases amorphadiene production to less than 20 g/L (Westfall et al., 2012). While strains were generated that produce amorphadiene constitutively in lab-scale fermentations, it is likely that the strain stability necessary in a large-scale industrial fermentation would require the use of a switch to turn on production. The most well-studied genetic switches rely on the addition of galactose to the fermentation medium, which is expensive and would add to the production cost. There has been considerable progress in the industrial production of terpenes by yeast in the decade following the amorphadiene work described above, though directed primarily at production of another sesquiterpene, β-farnesene (Benjamin et al., 2016; Leavell et al., 2016).

Regarding the industrial process of artemisinic aid production, the use of sugar as the primary feedstock (as opposed to a glucose/ethanol mix) would lead to feedstock cost saving, albeit somewhat limited. Of greater significance is that recently developed strains using sugar as feedstock have much higher flux to product, attaining over 100 g/L β-farnesene production in 6-day fed-batch fermentations (Meadows et al., 2016). Conversion of these improved β-farnesene strains to amorphadiene production by swapping β-farnesene synthase for amorphadiene synthase should enable production of much greater concentrations of amorphadiene as a substrate for biological oxidation in an industrially scalable manner. The use of a cost-effective switch (Sandoval et al., 2014) to turn on production at scale would likely improve genetic stability, extend the fermentation production run, and decrease cost. Another process approach to improve production of artemisinic acid could involve *in situ* product removal using oils such as isopropyl myristate which has been demonstrated to boost artemisinic acid production (Paddon et al., 2013). Expression of an *A. annua* transport system for export of artemisinic acid (Wang et al., 2016) may improve its secretion from yeast.

A fundamental biochemical challenge is to improve the oxidation of amorphadiene to artemisinic acid. The highest published fermentative production of artemisinic acid in a yeast strain expressing the full complement of *A. annua* enzymes for the oxidation of amorphadiene was 25 g/L (Paddon et al., 2013), grown under the same regimen as the parental strain that produced 40 g/L amorphadiene (Westfall et al., 2012), a conversion efficiency of 55 mol%; there is clearly room for improvement in the oxidation of amorphadiene to artemisinic acid. Given that expression of *A. annua* alcohol and aldehyde dehydrogenases in yeast strains producing amorphadiene and expressing optimized CYP71AV1/*Aa*CPR/cytochrome-b_5 ratios virtually eliminated buildup of artemisinic alcohol and aldehyde (Teoh et al., 2009; Paddon et al., 2013), it seems reasonable to conclude that the bottleneck in oxidation of amorphadiene lies in the activity of CYP71AV1 and associated proteins. It follows that improving oxidation of amorphadiene to artemisinic alcohol by CYP71AV1 and associated proteins would likely be a fruitful approach to improving the overall production of artemisinic acid.

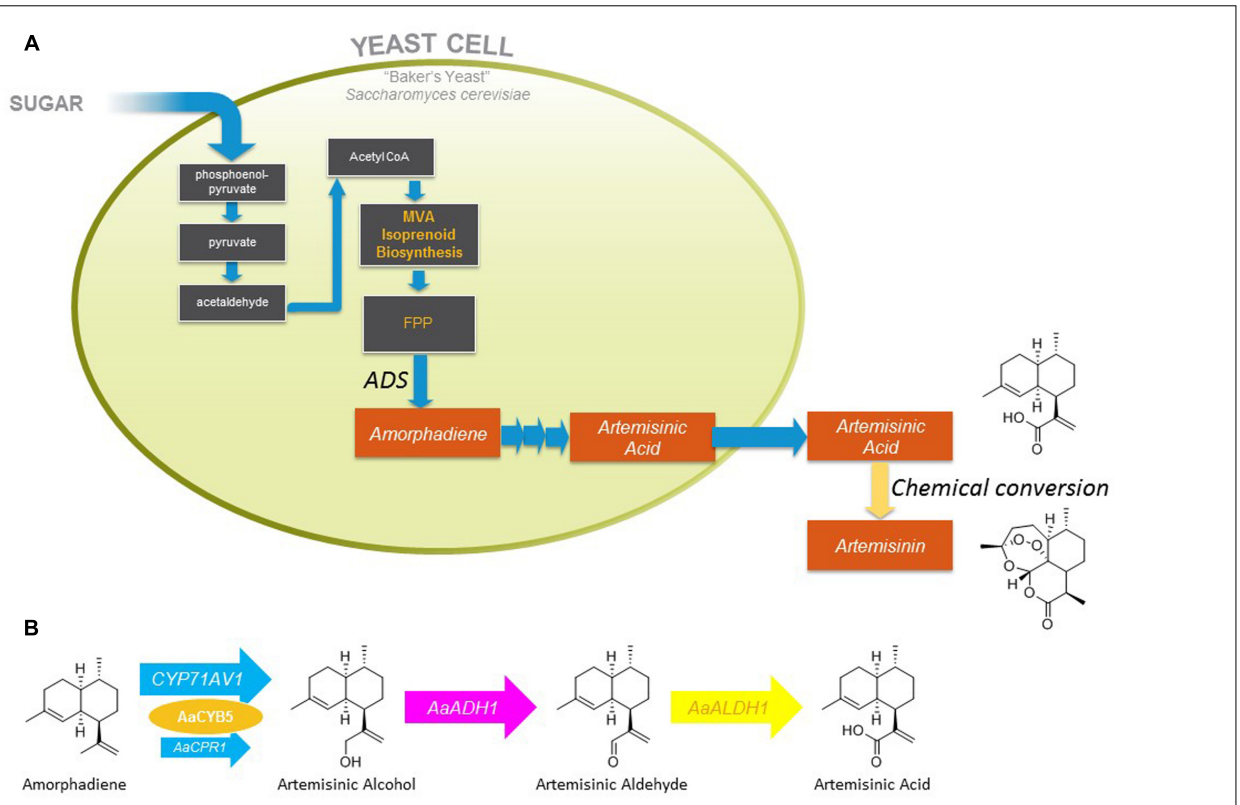

FIGURE 1 | Summary of yeast strain engineering underlying fermentative production of artemisinic acid and subsequent conversion to artemisinin. **(A)** Biosynthetic pathway engineered in yeast for production of amorphadiene, its oxidation to artemisinic acid, and subsequent chemical conversion to artemisinin. **(B)** *A. annua* enzymes expressed in yeast for oxidation of amorphadiene to artemisinic acid. MVA, mevalonate; FPP, farnesyl diphosphate; *Aa*ADH1, alcohol dehydrogenase; *Aa*ALDH1, aldehyde dehydrogenase.

INCREASING ACTIVITY OF HETEROLOGOUSLY EXPRESSED CYP71AV1

At the current level of production, the concentration of amorphadiene is approaching 200 mM in the fermentation tanks, which is well beyond the solubility limit. At such high concentrations of substrate, plant P450s harvested from nature are working well outside of the biological context in which they evolved, in addition to being heterologously expressed in yeast. While CYP71AV1 is remarkably able to accomplish such high conversions under the extreme concentrations of amorphadiene, a variety of approaches to engineer improved P450 conversion and generate even higher, economically relevant titers of artemisinic acid are required.

Engineering of the catalytic system directly could be accomplished on several fronts. Based on previous successes with titrating expression levels of *Aa*CPR and cytochrome-b_5, we know that modulation of the enzymes indirectly participating in catalysis can have a huge impact. While the interaction between CYP71AV1 and cytochrome-b_5 has not been characterized, our results (Paddon et al., 2013) are consistent with studies on the interaction between cytochrome-b_5 and CYP2B4, whereby cytochrome-b_5 provides the second electron of the oxidation reaction, the reaction being strongly influenced by the stoichiometry of the two proteins (Im and Waskell, 2011). Cytochrome-b_5 may also behave as an allosteric activator, as was suggested by its interaction with CYP3A4 (Zhao et al., 2012). *Aa*CPR has been shown to have relatively poor coupling to its cognate P450 compared to human CPRs and P450s (Simtchouk et al., 2013). This uncoupling likely produces large amounts of reactive oxygen species in addition to consuming valuable NADPH. Potential avenues to increase heterologous oxidation of amorphadiene would be to engineer the *Aa*CPR/CYP71AV1 coupling efficiency by altering the protein–protein interactions or weakening the binding of NADPH to *Aa*CPR when *Aa*CPR is not set up to transfer electrons to CYP71AV1. To reduce potential substrate or product inhibition that may be occurring under these abnormal conditions, engineering of CYP71AV1 directly through tightening of the active site or engineering of the substrate entrance channel could be undertaken. Such strategies would eliminate non-productive binding conformations observed in other P450s (Tietz et al., 2017). In addition to engineering the active site of P450s, engineering how P450s interact with the yeast endoplasmic reticulum has been fruitful for endeavors such as heterologous hydrocodone production (Galanie et al., 2015). Manipulation of the yeast genome may also be a means to improve heterologous P450 activity, for example it was recently

shown that a mutation (*Δ*pah1) resulting in expansion of yeast endoplasmic reticulum leads to an increase in the heterologous production of triterpenoid saponins (Arendt et al., 2017).

The approaches described above illustrate the need for development of rapid screening systems. Saturation mutagenesis of CYP71AV1, a protein of 496 amino acids, and testing production of oxidized product(s) from yeast producing amorphadiene with reasonable statistical coverage would require well over 10,000 assays to detect mutants with improved oxidation properties. Assays for quantification of artemisinic acid and other oxidized intermediates used to date are long [up to 30 min. (Paddon et al., 2013)], and too consuming of time and resources for high-throughput screening. A rapid methodology for detecting improved production of oxidized products of amorphadiene would be needed such as rapid mass spectrometry (Rohman and Wingfield, 2016) or surrogate assays based on spectrophotometric or fluorescent methods that could cut the time required to measure titers to 10 s or less per sample, albeit with the statistical reproducibility required to detect genuine improvements on artemisinic acid production from the background variability inherent in a high-throughput screen.

CHEMICAL CONVERSION OF ARTEMISINIC ACID TO ARTEMISININ

Following determination of the structure of artemisinin in 1977 (Tu, 2016, 2017), chemists quickly responded to the synthetic challenge presented by its sesquiterpene lactone structure, with seven chiral centers and a unique stable endoperoxide bond, and the first syntheses were reported soon thereafter. Broadly speaking, all these can be divided into two groups: total syntheses starting from a chiral pool compound and semi-syntheses from a terpene natural product precursor. The former is solely of academic interest, as they invariably involve too many steps to provide artemisinin at a price that can compete with extraction of the natural product from *A. annua* or the semi-synthetic approach described above. As there is no shortage of reviews that comprehensively cover both the earlier and more recent total and partial synthesis approaches (Jung, 1994; Haynes, 2006; Kim and Sasaki, 2006; Li et al., 2006; Wang et al., 2014; Corsello and Garg, 2015; Vil et al., 2017), here we shall only focus on reported industrial-scale partial synthesis routes or syntheses conceivably amenable to industrial scale-up that represent or could become commercially viable routes to artemisinin and by extension, the various derivatives used in ACTs. All semi-syntheses involve the steps shown in **Figure 2**, differing only in the reagents used to accomplish each step.

The first partial synthesis (Roth and Acton, 1989) started with a $NaBH_4/NiCl_2.6H_20$ ("nickel boride") reduction of the unsaturated carboxylic acid group of artemisinic acid, a relatively abundant *A. annua* natural product. This reduction afforded an 85:15 (*R*:*S*) mixture of 11,13-dihydroartemisinic acid isomers. 11-(*R*)-Dihydroartemisinic acid has also been reported as present (Wallaart et al., 1999) or not (Haynes and Vonwiller, 1991) in *A. annua*. This apparent contradiction has been explained by either differences in the plant cultivars analyzed or the inherent instability of the molecule, which reportedly quickly vanishes from the leaves after harvest (Kim and Kim, 1992). This would be consistent with a spontaneous transformation of 11-(*R*)-dihydroartemisinic acid into artemisinin on exposure to air and light, conditions likely found in nature (Czechowski et al., 2016) and mimicked by exposing the intermediate to photooxidation, followed by air oxidation in petroleum ether at room temperature for 4 days to give a 17% total yield of artemisinin (Roth and Acton, 1989).

Almost all other subsequent semi-syntheses have followed this route, with variations of the reagents and reaction conditions used in the various steps with the aim of improving the overall reaction yield. These include: (1) the use of asymmetric catalytic hydrogenation in the production of dihydroartemisinic acid aimed at improving the (*R*:*S*) ratio, as only the *R* isomer correctly forms artemisinin, while the "wrong" (*S*)-isomer undergoes an identical sequence of intermediate steps to give the undesired 9-(*S*)-isomer of the final target; (2) protection of the carboxylic acid function, typically as a simple ester. The advantages of esterification enabled a 23% yield of artemisinin using the methyl ester in place of the acid (Acton and Roth, 1992). Presumably the protection blocks the well-known oxidative lactonization of dihydroartemisinic acid to give dihydro-*epi*-deoxyarteannuin B [the latter is an advanced intermediate in an alternative semi-synthesis of artemisinin (Nowak and Lansbury, 1998), but in the sequence of **Figure 2** it is an unproductive byproduct]; (3) the use of pure oxygen instead of air in the final step, along with the addition of diverse catalysts, such as acid (Kim and Kim, 1992) or copper ion (Kim and Sasaki, 2006).

The first synthesis amenable to scale-up was developed by Amyris chemists in the context of the semi-synthetic artemisinin project described above. As the main details have been reported elsewhere (Paddon et al., 2013) only the highlights are summarized here: (1) the use of chlorotris (triphenylphosphonium) rhodium(I) ("Wilkinson's catalyst") in an asymmetric catalytic hydrogenation of artemisinic acid to afford a 90:10 ratio of (*R*) and (*S*)-dihydroartemisinic acid; (2) on the assumption that large-scale photochemistry would add significant capital costs to the project, the dye sensitized photogeneration of singlet oxygen was replaced by a chemical generation of this reactive species based on the group VI metal salt-induced disproportionation of concentrated H_2O_2 (Boehme and Brauer, 1992; Nardello et al., 2002); (3) for safety reasons the oxygen used in the last step was replaced by air, and (4) benzenesulfonic acid/Cu(II) Dowex resin was used as catalyst replacing the expensive copper triflate used in other syntheses. This 4-step synthesis gave the desired target in 40% overall yield, an improvement over the typical <30% overall yields previously reported in the literature.

After the technology transferred from Amyris to Sanofi, extensive work was undertaken between 2008 and 2013 to "industrialize" this process. Despite a series of notable improvements to the Amyris route that provided a safe and scalable process that even slightly improved upon the Amyris bench scale yields at pilot scale, it became apparent that this route had reached its performance limits and would not be

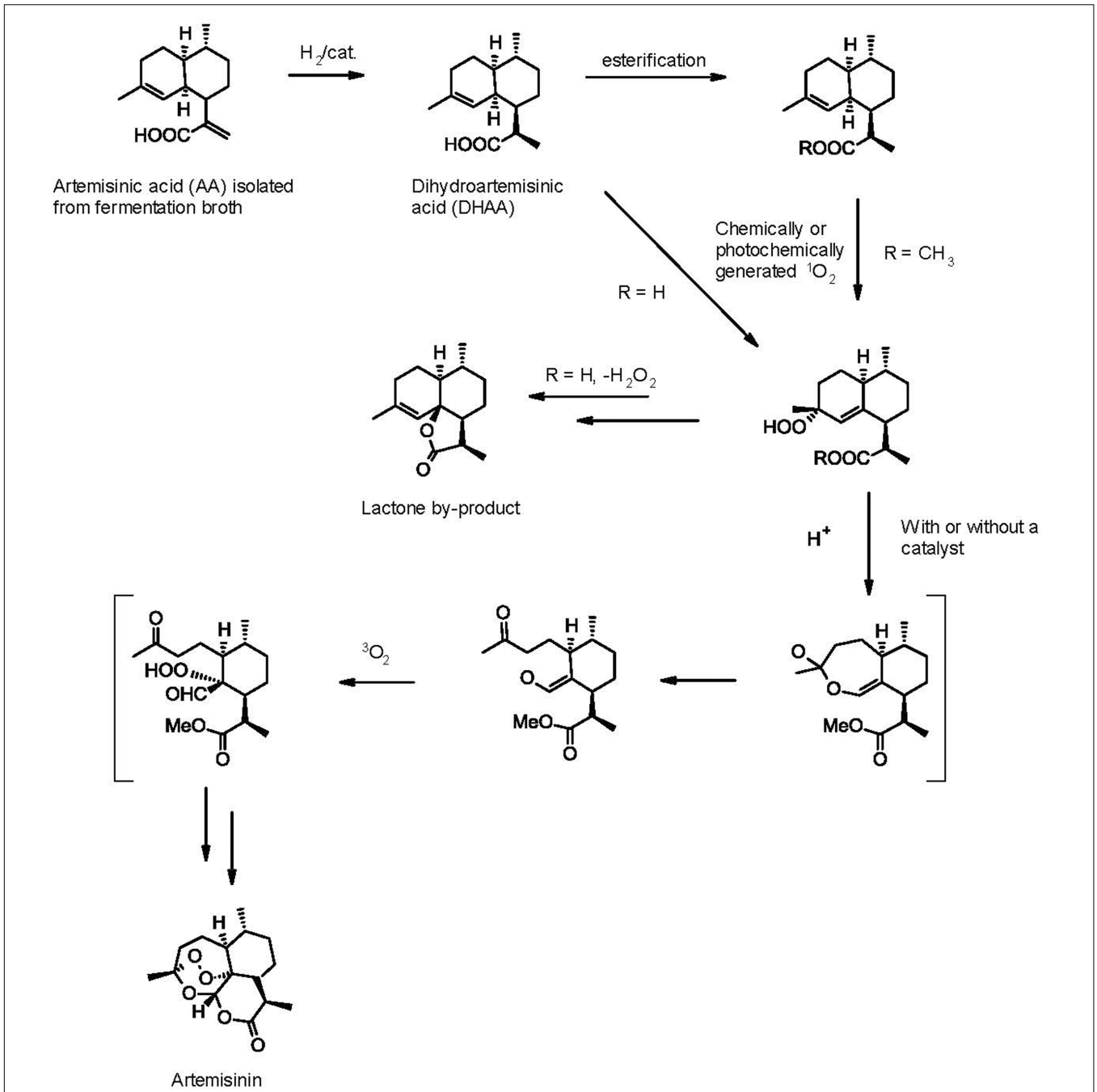

FIGURE 2 | Generic chemical synthesis of artemisinin from artemisinic acid.

cost-effective enough for commercial production. This led Sanofi chemists to reconsider the original photochemical approach. As the details of this work have been published (Turconi et al., 2014), including the optimization of the key photochemical generation of singlet oxygen (Burgard et al., 2016), they are not repeated here. The resulting semi-batch tetraphenylporphyrin dye sensitized photochemical process in a custom-designed photochemical reactor is currently being used to manufacture up to 60 MT/year of the target molecule in about 55% overall yield from artemisinic acid produced by fermentation of engineered *S. cerevisiae* strains in what is the only current industrial-scale semi-synthesis of artemisinin.

While as yet unproven as commercially viable syntheses of artemisinin, there have been developments that point the way to potential additional improvements that could break the existing cost/yield barrier. For example, although not part of the current manufacturing process, Sanofi chemists also developed an alternative high-yielding diimide reduction of artemisinic

acid to dihydroartemisinic acid that does not require catalytic hydrogenation with a chiral catalyst, yet still provides excellent chemical yields (>90% including all crystallization, isolation, and drying steps), in addition to high diastereoselectivities (≥97:3). Details of the pilot-scale optimization of this process have been published (Feth et al., 2013). In another area, the continuous-flow photochemical synthesis of artemisinin from dihydroartemisinic acid has been reported (Levesque and Seeberger, 2012; Kopetzki et al., 2013). Although to our knowledge this approach has not been scaled up, recent data (Porta et al., 2016) suggest that once the problems of large-scale generation of singlet oxygen in a flow system are overcome (Loponov et al., 2014), this could conceivably become the basis of a new industrial route. Meanwhile, other authors have followed up on the original Amyris "non-photochemical" route and claim similar yields of around 40% using the same molybdate catalyst/H_2O_2 route to generate singlet oxygen, but with a simplified and perhaps easier to scale overall process (Chen et al., 2013). Finally, very recently a route that differs in part from the previous approaches has been demonstrated. Chemists at IPCA have reported a novel large-scale synthesis of artemisinin from amorphadiene (Singh et al., 2017). The key step in this route is the functionalization of amorphadiene using simple and cheap chemistry to directly afford (*R*)-dihydroartemisinic acid (i.e., avoiding the need for a stereoselective reduction of artemisinic acid). The reported ca. 60% yield of pure artemisinin from dihydroartemisinic acid obtained also using an improved molybdate/peroxide route suggests that further yield breakthroughs may indeed be possible through additional process optimization of the key steps, namely the singlet oxygen generation and the Hoch cleavage and subsequent rearrangements.

CONCLUSION AND OUTLOOK

Malaria remains a major disease in the developing world, killing approximately 1500 people per day, the majority being children in sub-Saharan Africa (White et al., 2014). Artemisinin derivatives, administered as ACTs, remain the most effective antimalarial medications. The plant-derived supply of artemisinin has become more plentiful since initiation of the semi-synthetic artemisinin project, but is still subject to the vagaries of weather and agricultural economics; a second-source of artemisinin supply as described here is still required to stabilize the supply chain of this critically important drug. Industrial production of semi-synthetic artemisinin began in 2013, but technological advances described above in both biology and chemistry have opened opportunities to improve the process and decrease the cost of semi-synthetic artemisinin production. Developing these technologies could further safeguard the supply of artemisinin for those who need it most in the developing world.

AUTHOR CONTRIBUTIONS

All authors wrote different sections of the mini-review, and the completed manuscript was assembled and edited by the corresponding author (CP). All authors approved the submitted manuscript.

FUNDING

Funding for the semi-synthetic artemisinin project at Amyris, Inc. was provided by The Bill and Melinda Gates Foundation.

REFERENCES

Acton, N., and Roth, R. J. (1992). On the conversion of dihydroartemisinic acid into artemisinin. *J. Org. Chem*. 57, 3610–3614. doi: 10.1021/jo00039a020

Arendt, P., Miettinen, K., Pollier, J., De Rycke, R., Callewaert, N., and Goossens, A. (2017). An endoplasmic reticulum-engineered yeast platform for overproduction of triterpenoids. *Metab. Eng*. 40, 165–175. doi: 10.1016/j.ymben.2017.02.007

Benjamin, K. R., Silva, I. R., Cherubim, J. P., McPhee, D., and Paddon, C. J. (2016). Developing commercial production of semi-synthetic artemisinin, and of β-Farnesene, an isoprenoid produced by fermentation of Brazilian sugar. *J. Braz. Chem. Soc*. 27, 1339–1345. doi: 10.5935/0103-5053.20160119

Boehme, K., and Brauer, H.-D. (1992). Generation of singlet oxygen from hydrogen peroxide disproportionation catalyzed by molybdate ions. *Inorg. Chem*. 31, 3468–3471. doi: 10.1021/ic00042a024

Burgard, A., Gieshoff, T., Peschl, A., Hörstermann, D., Keleschovsky, C., Villa, R., et al. (2016). Optimisation of the photochemical oxidation step in the industrial synthesis of artemisinin. *Chem. Eng. J*. 294, 83–96. doi: 10.1016/j.cej.2016.02.085

Chen, H.-J., Han, W.-B., Hao, H.-D., and Wu, Y. (2013). A facile and scalable synthesis of qinghaosu (artemisinin). *Tetrahedron* 69, 1112–1114. doi: 10.1016/j.tet.2012.11.056

Corsello, M. A., and Garg, N. K. (2015). Synthetic chemistry fuels interdisciplinary approaches to the production of artemisinin. *Nat. Prod. Rep*. 32, 359–366. doi: 10.1039/c4np00113c

Czechowski, T., Larson, T. R., Catania, T. M., Harvey, D., Brown, G. D., and Graham, I. A. (2016). Artemisia annua mutant impaired in artemisinin synthesis demonstrates importance of nonenzymatic conversion in terpenoid metabolism. *Proc. Natl. Acad. Sci. U.S.A*. 113, 15150–15155. doi: 10.1073/pnas.1611567113

Feth, M. P., Rossen, K., and Burgard, A. (2013). Pilot plant PAT approach for the diastereoselective diimide reduction of artemisinic acid. *Org. Process Res. Dev*. 17, 282–293. doi: 10.1021/op300347w

Hale, V., Keasling, J. D., Renninger, N., and Diagana, T. T. (2007). Microbially derived artemisinin: a biotechnology solution to the global problem of access to affordable antimalarial drugs. *Am. J. Trop. Med. Hyg*. 77(Suppl. 6), 198–202.

Galanie, S., Thodey, K., Trenchard, I. J., Filsinger Interrante, M., and Smolke, C. D. (2015). Complete biosynthesis of opioids in yeast. *Science* 349, 1095–1100. doi: 10.1126/science.aac9373

Haynes, R. K. (2006). From artemisinin to new artemisinin antimalarials: biosynthesis, extraction, old and new derivatives, stereochemistry and medicinal chemistry requirements. *Curr. Top. Med. Chem*. 6, 509–537. doi: 10.2174/156802606776743129

Haynes, R. K., and Vonwiller, S. C. (1991). The development of new peroxidic antimalarials. *Chem. Austral*. 58, 64–67.

Ikram, N. K. B. K., and Simonsen, H. T. (2017). A review of biotechnological artemisinin production in plants. *Front. Plant Sci*. 8:1966. doi: 10.3389/fpls.2017.01966

Im, S.-C., and Waskell, L. (2011). The interaction of microsomal cytochrome P450 2B4 with its redox partners, cytochrome P450 reductase and cytochrome b5. *Arch. Biochem. Biophys*. 507, 144–153. doi: 10.1016/j.abb.2010.10.023

Jung, M. Y. (1994). Current developments in the chemistry of artemisinin and related compounds. *Curr. Med. Chem*. 1, 35–49.

Kim, B., and Sasaki, T. (2006). Recent progress in the synthesis of artemisinin and its derivatives. *Org. Prep. Proced. Int*. 38, 1–80. doi: 10.1080/00304940609355981

Kim, N. M., and Kim, S. U. (1992). Biosynthesis of artemisinin from 11,12-dihydroarteannuic acid. *J. Korean Agric. Chem. Soc*. 35, 106–109.

Kopetzki, D., Levesque, F., and Seeberger, P. H. (2013). A continuous-flow process for the synthesis of artemisinin. *Chemistry* 19, 5450–5456. doi: 10.1002/chem.201204558

Leavell, M. D., McPhee, D. J., and Paddon, C. J. (2016). Developing fermentative terpenoid production for commercial usage. *Curr. Opin. Biotechnol*. 37, 114–119. doi: 10.1016/j.copbio.2015.10.007

Levesque, F., and Seeberger, P. H. (2012). Continuous-Flow synthesis of the anti-malaria drug artemisinin. *Angew. Chem. Int. Ed. Engl*. 51, 1706–1709. doi: 10.1002/anie.201107446

Li, Y., Huang, H., and Wu, Y.-L. (2006). "Qinghaosu (Artemisinin)-a fatastic antimalarial drug from a traditional chinese medicine," in *Medicinal Chemistry of Bioactive natural Products*, eds X.-T. Liang and W.-S. Fang (New York, NY: John Wiley and Sons), 183–256. doi: 10.1002/0471739340.ch5

Loponov, K. N., Lopes, J., Barlog, M., Astrova, E. V., Malkov, A. V., and Lapkin, A. A. (2014). Optimization of a scalable photochemical reactor for reactions with singlet oxygen. *Org. Process Res. Dev*. 18, 1443–1454. doi: 10.1021/op500181z

Meadows, A. L., Hawkins, K. M., Tsegaye, Y., Antipov, E., Kim, Y., Raetz, L., et al. (2016). Rewriting yeast central carbon metabolism for industrial isoprenoid production. *Nature* 537, 694–697. doi: 10.1038/nature19769

Nardello, V., Bogaert, S., Alsters, P. L., and Aubry, J.-M. (2002). Singlet oxygen generation from H2O2/MoO42-: peroxidation of hydrophobic substrates in pure organic solvents. *Tetrahedron Lett*. 43, 8731–8734. doi: 10.1016/S0040-4039(02)02108-1

Nielsen, J., and Keasling, J. D. (2016). Engineering cellular metabolism. *Cell* 164, 1185–1197. doi: 10.1016/j.cell.2016.02.004

Nowak, D. M., and Lansbury, P. T. (1998). Synthesis of (+)-artemisinin and (+)-deoxoartemisinin from arteannuin B and arteannuic acid. *Tetrahedron* 54, 319–336. doi: 10.1016/S0040-4020(97)10286-1

Paddon, C. J., and Keasling, J. D. (2014). Semi-synthetic artemisinin: a model for the use of synthetic biology in pharmaceutical development. *Nat. Rev. Microbiol*. 12, 355–367. doi: 10.1038/nrmicro3240

Paddon, C. J., Westfall, P. J., Pitera, D. J., Benjamin, K., Fisher, K., McPhee, D., et al. (2013). High-level semi-synthetic production of the potent antimalarial artemisinin. *Nature* 496, 528–532. doi: 10.1038/nature12051

Peplow, M. (2016). Synthetic biology's first malaria drug meets market resistance. *Nature* 530, 389–390. doi: 10.1038/530390a

Porta, R., Benaglia, M., and Puglisi, A. (2016). Flow chemistry: recent developments in the synthesis of pharmaceutical products. *Org. Process Res. Dev*. 20, 2–25. doi: 10.1021/acs.oprd.5b00325

Ro, D. K., Paradise, E. M., Ouellet, M., Fisher, K. J., Newman, K. L., Ndungu, J. M., et al. (2006). Production of the antimalarial drug precursor artemisinic acid in engineered yeast. *Nature* 440, 940–943. doi: 10.1038/nature04640

Rohman, M., and Wingfield, J. (2016). "High-Throughput screening using mass spectrometry within drug discovery," in *High Throughput Screening: Methods and Protocols*, ed. W. P. Janzen (New York, NY: Springer), 47–63.

Roth, R. J., and Acton, N. (1989). A simple conversion of artemisinic acid into artemisinin. *J. Nat. Prod*. 52, 1183–1185. doi: 10.1021/np50065a050

Sandoval, C. M., Ayson, M., Moss, N., Lieu, B., Jackson, P., Gaucher, S. P., et al. (2014). Use of pantothenate as a metabolic switch increases the genetic stability of farnesene producing *Saccharomyces cerevisiae*. *Metab. Eng*. 25, 215–226. doi: 10.1016/j.ymben.2014.07.006

Simtchouk, S., Eng, J. L., Meints, C. E., Makins, C., and Wolthers, K. R. (2013). Kinetic analysis of cytochrome P450 reductase from *Artemisia annua* reveals accelerated rates of NADH-dependent flavin reduction. *FEBS J*. 280, 6627–6642. doi: 10.1111/febs.12567

Singh, D., McPhee, D., Paddon, C. J., Cherry, J., Maurya, G., Patel, Y., et al. (2017). Amalgamation of synthetic biology and chemistry for high-throughput nonconventional synthesis of the antimalarial drug artemisinin. *Org. Process Res. Dev*. 21, 551–558. doi: 10.1021/acs.oprd.6b00414

Teoh, K. H., Polichuk, D. R., Reed, D. W., and Covello, P. S. (2009). Molecular cloning of an aldehyde dehydrogenase implicated in artemisinin biosynthesis in *Artemisia annua*. *Botany* 87, 635–642. doi: 10.1139/B09-032

Tietz, D. R., Podust, L. M., Sherman, D. H., and Pochapsky, T. C. (2017). Solution conformations and dynamics of substrate-bound cytochrome P450 MycG. *Biochemistry* 56, 2701–2714. doi: 10.1021/acs.biochem.7b00291

Tu, Y. (2016). Artemisinin-A gift from traditional chinese medicine to the world (Nobel Lecture). *Angew. Chem. Int. Ed. Engl*. 55, 10210–10226. doi: 10.1002/anie.201601967

Tu, Y. (2017). *From Artemisia annua L. to Artemisinins. The Discovery and Development of Artemisinins and Antimalarial Agents*. London: Academic Press.

Turconi, J., Griolet, F., Guevel, R., Oddon, G., Villa, R., Geatti, A., et al. (2014). Semisynthetic artemisinin, the chemical path to industrial production. *Org. Process Res. Dev*. 18, 417–422. doi: 10.1021/op4003196

Vil, V. A., Yaremenko, I. A., Ilovaisky, A. I., and Terent'ev, A. O. (2017). Synthetic strategies for peroxide ring construction in artemisinin. *Molecules* 22:E117. doi: 10.3390/molecules22010117

Wallaart, T. E., van Uden, W., Lubberink, H. G., Woerdenbag, H. J., Pras, N., and Quax, W. J. (1999). Isolation and identification of dihydroartemisinic acid from artemisia annua and its possible role in the biosynthesis of artemisinin. *J. Nat. Prod*. 62, 430–433. doi: 10.1021/np980370p

Wang, B., Kashkooli, A. B., Sallets, A., Ting, H.-M., de Ruijter, N. C. A., Olofsson, L., et al. (2016). Transient production of artemisinin in *Nicotiana benthamiana* is boosted by a specific lipid transfer protein from *A. annua*. *Metab. Eng*. 38, 159–169. doi: 10.1016/j.ymben.2016.07.004

Wang, Z., Yang, L., Yang, X., and Zhang, X. (2014). Advances in the chemical synthesis of artemisinin. *Synth. Commun*. 44, 1987–2003. doi: 10.1080/00397911.2014.884225

Westfall, P. J., Pitera, D. J., Lenihan, J. R., Eng, D., Woolard, F. X., Regentin, R., et al. (2012). Production of amorphadiene in yeast, and its conversion to dihydroartemisinic acid, precursor to the antimalarial agent artemisinin. *Proc. Natl. Acad. Sci. U.S.A*. 109, E111–E118. doi: 10.1073/pnas.1110740109

White, N. J., Pukrittayakamee, S., Hien, T. T., Faiz, M. A., Mokuolu, O. A., and Dondorp, A. M. (2014). Malaria. *Lancet* 383, 723–735. doi: 10.1016/S0140-6736(13)60024-0

Zhao, C., Gao, Q., Roberts, A. G., Shaffer, S. A., Doneanu, C. E., Xue, S., et al. (2012). Cross-Linking mass spectrometry and mutagenesis confirm the functional importance of surface interactions between CYP3A4 and Holo/Apo cytochrome *b*5. *Biochemistry* 51, 9488–9500. doi: 10.1021/bi301069r

Conflict of Interest Statement: All authors have shares or stock options in Amyris, Inc.

frontiers in Plant Science

ORIGINAL RESEARCH
published: 27 March 2018
doi: 10.3389/fpls.2018.00358

Selection and Clonal Propagation of High Artemisinin Genotypes of *Artemisia annua*

Hazel Y. Wetzstein[1,2], Justin A. Porter[1], Jules Janick[1], Jorge F. S. Ferreira[3] and Theophilus M. Mutui[4]*

[1] Department of Horticulture and Landscape Architecture, Purdue University, West Lafayette, IN, United States, [2] Department of Horticulture, University of Georgia, Athens, GA, United States, [3] U.S. Salinity Laboratory, United States Department of Agriculture, Agricultural Research Service, Riverside, CA, United States, [4] Department of Seed, Crop and Horticultural Sciences, University of Eldoret, Eldoret, Kenya

Artemisinin, produced in the glandular trichomes of *Artemisia annua* L. is a vital antimalarial drug effective against *Plasmodium falciparum* resistant to quinine-derived medicines. Although work has progressed on the semi-synthetic production of artemisinin, field production of *A. annua* remains the principal commercial source of the compound. Crop production of artemisia must be increased to meet the growing worldwide demand for artemisinin combination therapies (ACTs) to treat malaria. Grower artemisinin yields rely on plants generated from seeds from open-pollinated parents. Although selection has considerably increased plant artemisinin concentration in the past 15 years, seed-generated plants have highly variable artemisinin content that lowers artemisinin yield per hectare. Breeding efforts to produce improved F_1 hybrids have been hampered by the inability to produce inbred lines due to self-incompatibility. An approach combining conventional hybridization and selection with clonal propagation of superior genotypes is proposed as a means to enhance crop yield and artemisinin production. Typical seed-propagated artemisia plants produce less than 1% (dry weight) artemisinin with yields below 25 kg/ha. Genotypes were identified producing high artemisinin levels of over 2% and possessing improved agronomic characteristics such as high leaf area and shoot biomass production. Field studies of clonally-propagated high-artemisinin plants verified enhanced plant uniformity and an estimated gross primary productivity of up to 70 kg/ha artemisinin, with a crop density of one plant m^{-2}. Tissue culture and cutting protocols for the mass clonal propagation of *A. annua* were developed for shoot regeneration, rooting, acclimatization, and field cultivation. Proof of concept studies showed that both tissue culture-regenerated plants and rooted cutting performed better than plants derived from seed in terms of uniformity, yield, and consistently high artemisinin content. Use of this technology to produce plants with homogeneously-high artemisinin can help farmers markedly increase the artemisinin yield per cultivated area. This would lead to increased profit to farmers and decreased prices of ACT.

Keywords: *Artemisia annua*, artemisinin, genotypes, malaria, tissue culture

OPEN ACCESS

Edited by:
Tomasz Czechowski, University of York, United Kingdom

Reviewed by:
Stephen Oscar Duke, United States Department of Agriculture, United States
Deyu Xie, North Carolina State University, United States

****Correspondence:***
Hazel Y. Wetzstein
hwetzste@purdue.edu

Specialty section:
This article was submitted to Plant Biotechnology, a section of the journal Frontiers in Plant Science

Received: *06 November 2017*
Accepted: *02 March 2018*
Published: *27 March 2018*

Citation:
Wetzstein HY, Porter JA, Janick J, Ferreira JFS and Mutui TM (2018) Selection and Clonal Propagation of High Artemisinin Genotypes of Artemisia annua. Front. Plant Sci. 9:358. doi: 10.3389/fpls.2018.00358

INTRODUCTION

Artemisia annua L. (known a sweet Annie, annual wormwood, qinghao) is native to China and a widely naturalized and cultivated medicinal plant (Ferreira and Janick, 1997). The plant is a source of artemisinin, a sesquiterpene lactone compound that is produced in the glandular trichomes of leaves and floral parts (Duke et al., 1994; Ferreira and Janick, 1995). Artemisinin is a vital antimalarial medicine effective against drug resistant *Plasmodium falciparum*. Artemisinin combination therapies (ACTs) are recommended as a first-line treatment for drug-resistant malaria that no longer responds to quinine-derived drugs such as chloroquine or mefloquine. Globally, the World Health Organization (World Malaria Report, 2016) attributed an estimated 212 million new cases and 429,000 deaths to malaria in 2015. At the start of 2016, nearly half of the world's population was at risk of malaria. An important additional feature is that *A. annua* compounds also exhibit antiinflammatory, antibacterial, antitumor, antiviral, and anthelmintic activities (Bhakuni et al., 2001).

Although work has progressed on the semi-synthetic production of artemisinin, field production of *A. annua* remains the principal commercial source of the compound. Satisfying the demand for artemisinin will require improved plant material containing consistently high artemisinin levels. The agricultural production of artemisia in developing countries afflicted by malaria is not only necessary, but also important to the economic well-being of farmers and their communities in these countries, where artemisia recently became a new pharmaceutical crop. Due to low and variable yield content of artemisinin the demand for artemisinin cannot be met with current plant yields (Alejos-Gonzalez et al., 2011). Artemisia growers rely on plants generated from seeds from open-pollinated plants. Thus, homogeneously high-artemisinin plants will decrease the need to expand *A. annua* cultivated land and will increase artemisinin yield per area, and possibly decrease costs of ACTs.

Although selection has considerably increased plant artemisinin concentration in the past 15 years, seed-generated plants have highly variable artemisinin content that lowers artemisinin yield per hectare. Open-pollinated cultivars produced by mass selection show variable plant-to-plant artemisinin content and biomass production due to genetic recombination. Breeding efforts to produce improved F_1 hybrids have been hampered by self-incompatibility, which prevents conventional back-crossing to produce inbred lines. So-called hybrid cultivars based on intercrosses of two heterozygous lines still exhibit high plant-to-plant variation. For example the leading hybrid, 'Artemis,' exhibited extensive variation for metabolic and agronomic traits; artemisinin content on a μg/mg dry basis for individual plants ranged 22 fold, plant fresh weight varied 28 fold, and leaf area ranged 9 fold (Graham et al., 2010).

Cultivar improvement to increase artemisinin production in *A. annua* has been limited. In a global field trial of 280 distinct lines, including commercial lines and test hybrids selected for high artemisinin production, artemisinin content ranged from 0.5 to 1.4% (Larson et al., 2013). Typically, average plant artemisinin concentrations were reported to range from 0.6 to 0.7% in China[1], and from 0.6 to 0.8% in Africa in 2013, with currently-used plants producing around 1% (Malcolm Cutler, personal communication). The bottleneck for the feasible production of artemisinin in developing countries is the lack of affordable high-quality plant material to produce consistently high artemisinin yield (Ferreira et al., 2005).

An approach combining conventional hybridization/selection with clonal propagation of superior genotypes is proposed as a means to enhance crop yield and artemisinin production. Agricultural production using improved clonal material is commonly used with many agricultural crops. Our objectives in this study were 2 fold: (1) to select *Artemisia* genotypes with high artemisinin content, and (2) to develop protocols effective for mass clonal propagation by either cuttings and/or micropropagation. Furthermore, proof-of-concept studies were conducted to assess the field performance of tissue culture-propagated plants to determine if they have consistent levels of artemisinin and acceptable agronomic characteristics in comparisons with cutting and seed-derived plants.

MATERIALS AND METHODS

Germplasm

Seed of *A. annua* were obtained from Brazil, China, and Purdue University, and their open-pollinated progeny were grown in the greenhouse and field. Selections were made over successive generations based on agronomic characteristics such as leaf area, biomass, flowering time, and artemisinin content. Selections were cloned by cuttings and maintained in a greenhouse under long days.

Artemisinin Chromatographic Analysis

Plant samples were oven dried at 50°C, ground to 0.5 mm particle size, extracted by refluxing in petroleum ether for 1 h, allowed to evaporate in a fume hood, then reconstituted in 20 ml of acetonitrile (two washes of 10 ml each), filtered through 0.2 μm PTFE luer-lock syringe filters and quantified (g/100 g leaf dry weight) for artemisinin, dihydroartemisinic acid, and artemisinic acid by HPLC-UV (Ferreira and Gonzalez, 2009).

Stock Plants for Propagation Studies

Greenhouse stock plants produced from cuttings were used as a source plants for propagation studies. *A. annua* is a short-day, monocarpic plant with extremely small flowers and seeds (Wetzstein et al., 2014). To prevent flowering under fall and winter day lengths, plants were given supplemental light to maintain a 16-h photoperiod. Plants were maintained in pots (19 cm diameter, 3.8 L) containing Fafard 3B medium (Conrad Fafard, Agawam, MA, United States) in a glass greenhouse set at 25°C. Propagation studies were performed before and concurrently with selections of elite germplasm, and included studies using a Brazilian genotype (3M, CPQBA) and field-selected clones (B4, B6, C1, C10, MP11, P63, P137) derived

[1]http://www.a2s2.org/market-data/a2s2-market-update-aug13.html

from crosses. All clones were selected for high-artemisinin concentration and biomass production.

Propagation by Cuttings

Various types of cuttings (terminal, lateral, one-node, and two-node) were obtained from greenhouse-grown clones of B4 and C10 clones. Preliminary rooting studies indicated that a 1500 ppm indole-3-butyric acid, potassium salt (KIBA) dip was effective for root development. Cuttings were dipped 5 s and inserted in growing media under mist. Rooting was evaluated after 14 days.

Initiation and Establishment of Aseptic Cultures

A range of explants types (shoot tips, leaves, nodes, floral bud, and seedling parts) were evaluated in preliminary experiments, and a series of different sterilization combinations were assessed. High numbers of clean, regenerable cultures were obtained with shoot tip explants using the following surface sterilization and culture initiation methods. Shoot tips (1 to 1.5 cm long) with young unexpanded leaves were collected from stock plants grown in the greenhouses. The basal, older leaves were removed, retaining leaves $\leq$ 0.5 cm long. Explants were washed for 30 min in tap water containing a two drops of antibacterial hand soap (SoftCIDE®, VWR, Suwanee, GA, United States), and then rinsed in water for 15 min. This was followed by sequential immersion in 70% ethanol for 20 s, 1.2% sodium hypochlorite containing 1–2 drops of Tween-20 surfactant for 10 min with agitation, and three rinses in sterile distilled water for 5 min each. After surface sterilization, shoot tips were placed on shoot induction medium consisting of Murashige and Skoog (MS) macro and micro salts (Murashige and Skoog, 1962), B5 vitamins (Gamborg et al., 1968), 0.1 mg L^{-1} myo-inositol, 0.2 mg^{-1} L 6-benzylaminopurine (BA), 0.05 mg L^{-1} kinetin (Kin), 30 g L^{-1} sucrose, and 4 g L^{-1} Gel-Gro (ICN Biochemicals, Aurora, OH, United States). The medium was adjusted to pH 6.0, dispensed in 20 mL aliquots into test tubes, and autoclaved at 121°C for 20 min. Cultures were maintained under a 16/8-h (light/dark) photoperiod under cool-white fluorescent lights (Osram Sylvania, Mississauga, ON, Canada) with 70 μmol m^2 s^{-1} irradiance at 25 ± 10°C. Cultures were transferred to fresh medium every 3 weeks and maintained in glass baby food jars (66 mm × 59 mm). These primary shoot cultures served as a source of explants for subsequent medium optimization studies for shoot proliferation and rooting.

In Vitro Shoot Regeneration Studies

Plant growth regulator screenings for shoot regeneration were conducted using material from stock cultures of the C10 clone. Small shoot clumps (1 cm × 1 cm) were inoculated on media containing different concentrations of BA (0, 0.89, 2.22, 4.44, and 8.88 μM) and naphthaleneacetic acid (NAA) (0, 0.27, 0.54 μM) to assess shoot proliferation and regeneration efficacy. The components of the media were the same as for culture initiation, except that plant growth regulators were modified. The media were dispensed into glass baby food jars with 30 ml of medium per jar. Treatments were replicated using 24 jars per medium type. Tissues were subcultured to fresh medium at 3 weeks. Shoot and callus were separated and fresh weights were recorded for plants from all jars after 6 weeks; tissues were oven dried to determine dry weights. Nine cultures were randomly selected to determine the average number of shoots per jar that were taller than 0.6 cm. Based on results of screening studies, further refinement studies were conducted to evaluate the effect of plant growth regulators on shoot and callus production. Shoot clumps (1 cm × 1 cm) from stock cultures of the 3M genotype were placed on media with different concentrations of BA (0, 0.89, 1.79, 2.67, or 3.56 μM) and NAA (0 or 0.27 μM). Except for the plant growth regulators, the components of the media, culture vessel, and growth conditions were the same as in preliminary screening studies. Twenty four jars per medium type were used for shoot and callus growth assessments; with nine jars were used for counting total numbers of shoots. The response of four different genotypes was evaluated using shoots initiated from 3M, C10, B6, and MP11. Shoot clumps (1 cm × 1 cm) were placed on media with BA (0.89, 1.79, or 3.56 μM) and NAA (0.27 μM) with 72 replicates for each plant growth regulator combination. Fresh weight and dry weight for both callus and shoots were determined after 6 weeks. A subset of 24 jars per treatment was used to determine the number of shoots per culture.

In Vitro Rooting

To evaluate rooting, shoots from stock cultures of clones C10 and MP11 genotypes were placed on MS medium with B5 vitamins (Gamborg et al., 1968), 0.1 mg L^{-1} myo-inositol, 30 g L^{-1} sucrose, and 4 g L^{-1} Gel-Gro (ICN Biochemicals, Aurora, OH, United States), supplemented with different concentrations of indole-3-butyric acid (IBA) (0, 2.4, 4.9, and 9.8 μM). Percent rooting, number of roots, and number of lateral roots were assessed after 4 weeks. Studies indicated that better quality shoots were obtained following a shoot elongation step when shoots were subcultured into Magenta boxes containing basal medium for 1 week prior to transfer onto rooting medium. The rooting performance of elongated shoots from several genotypes was assessed on rooting medium containing 9.8 μM IBA.

Field Performance of Tissue Culture-Derived Plants

The performance of plantlets derived from tissue culture was evaluated in field studies conducted in Athens, GA. Corresponding plant material from two genotypes, 3M and MP11, were propagated either via tissue culture or by cuttings and planted in field plots to compare the effect of propagation method on artemisinin concentration. In addition, seedling plants derived from open-pollinated seed collected from UGA research plots were transplanted into test plots to compare the performance and variability of vegetatively-propagated versus seed-produced plants. For the production of rooted cuttings, the base of shoot tip cuttings 10 cm tall from greenhouse stock plants were dipped into an aqueous solution of 1500 ppm KIBA for 5 s, planted in 72-cell plug trays in commercial potting mix (Fafard 3B; Conrad Fafard, Agawam, MA, United States), and covered

with clear plastic propagation domes (Humi-dome; Hummert, Earth City, MO, United States). Leaf samples from four plants of each propagation type were collected for artemisinin analysis as described below. Propagules were planted in the field on June 24 and harvested September 10. To compare plant growth characteristics, the total biomass of the MP11 genotype was determined using six plants per propagation method. At harvest, five leaves and stems were manually separated into component parts, and oven dried to determine plant dry weight.

Effect of Growing Conditions on Sesquiterpenes

Leaf concentrations of artemisinin, artemisinic acid, and dihydroartemisinic acid were quantified by HPLC-UV (Ferreira and Gonzalez, 2009) from clones grown under greenhouse, field, or tissue culture conditions. If artemisinin concentration can be accurately assessed from greenhouse-grown plants, this would streamline selection in that field screenings would not be necessary. Comparisons were made using three genotypes: 3M, MP11, and C10. Greenhouse plants were grown and maintained in pots as described under plant material. Tissue culture plants were regenerated from shoots collected from stock shoot cultures. Field material was from plants propagated by cuttings and grown in research plots.

RESULTS

Selection for Improved Genotypes

Hybridization and selection studies identified a number of excellent genotypes in terms of both artemisinin content and agronomic characteristics. Data from field trials of six promising genotypes are shown in **Table 1**. Artemisinin leaf concentration for the six genotypes (C1, C10, B6, P137, P63, and B4) had 2-year field averages ranging from 1.6 to 2.16%. Significant differences in plant height, plant width, and stem dry weight were observed. Two genotypes (P63 and B4) exhibited a smaller stature than the others, but size differences did not necessarily relate to artemisinin plant production. The six genotypes had marked differences in leaf size and morphology (**Figure 1**). In addition to artemisinin concentration, plant size, and leaf area are important factors as they directly influence total artemisinin production. The genotype with the highest artemisinin content, C1, had an average artemisinin content of 2.16% and, based on dry leaf biomass and crop density of 1.0 plant/m^2,had an estimated gross primary productivity of 69.6 kg of artemisinin/ha. Considering a commercial extraction efficiency of 75%, C1 would produce 52.2 kg of artemisinin/ha. P137 was the second highest yielding genotype due to its high leaf dry weight production. The six selections, particularly C1, C10, B6 and P137, represent substantial improvements in artemisinin production compared to current commercial plantings using seed of open-pollinated plants that typically produce approximately 1% artemisinin or less.

Propagation by Cuttings

Vegetative propagation methods were evaluated in order to assess if methods for mass clonal propagation could be developed. Stem cuttings were initiated using tip and nodal tissues given KIBA treatments to assess rooting. There were clonal differences observed with clone B4 rooting better than C1. Nonetheless, all cutting types rooted well with 74% rooting or higher obtained (**Table 2**). These results indicate that both tip and nodal cuttings can be rooted with an IBA-hormone dip combined with misting is a very effective way to mass propagate selected *A. annua* clones.

In Vitro Shoot Regeneration

Micropropagation was also explored for *A. annua*. In preliminary experiments, several explant types were evaluated including shoot tips, nodes, leaves, and parts from axenically-germinated seedling-regeneration experiments. Shoot tips proved to be extremely regenerable when initiated on media with BA, and had relatively low contamination rates (0 to 9%) using the protocols described. Depending on genotype, 68 to 89% of explants responded on initiation medium producing shoot cultures that were used as stock cultures for shoot regeneration studies. Leaves and nodes did not perform as well (data not shown). Highest shoot growth was achieved with 2.22 BA + 0.27 μM NAA (**Figure 2**). Higher concentrations of BA and NAA resulted in undesirable increased callus production. A subsequent refinement study evaluated BA concentrations (**Table 3**). Although the greatest shoot fresh and dry weights were achieved with 1.78 μM BA + 0.27 NAA, significantly

TABLE 1 | Artemisinin concentration per plant, and kg/ha from six selected clones of *Artemisia annua*.

Genotype	Artemisinin (%)			Plant height (cm)[z]	Plant width (cm)[z]	Stem dry weight (kg)[z]	Leaf dry weight[z]		Artemisinin (kg/ha)[z]
	2012	2013	Average				(kg)	(t/ha)	
C1	2.13	2.19	2.16a	179a[y]	113a	0.69a	0.32ab	3.22	70.6
C10	1.93	2.13	2.03ab	188a	106ab	0.77a	0.28ab	2.81	59.9
B6	1.65	2.21	1.93ab	181a	112ab	0.67a	0.26ab	2.61	57.8
P137	1.93	1.68	1.81bc	192a	111ab	0.81a	0.39a	3.88	65.2
P63	1.81	1.53	1.67c	144b	100bc	0.44b	0.25b	2.46	37.7
B4	1.83	1.37	1.60c	140b	89c	0.34b	0.27ab	2.65	36.3

[z]2012 data. [y]Mean separation Tukey test, α = 0.05. Artemisinin productivity is based on leaf dry weight, 1 plant/m^2, and without considering a commercial extraction loss of 25%. Means within the same column followed by the same letter are not significantly different.

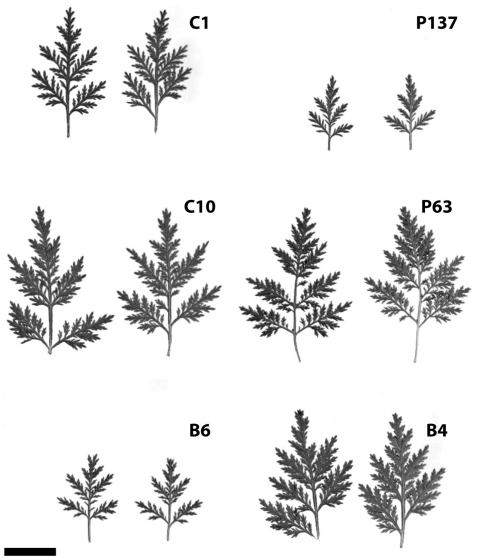

FIGURE 1 | (A–F) Variation in leaf size of six selected clones of *Artemisia annua* grown under field conditions (bar = 2 cm).

higher shoot numbers (1.5 times greater) were obtained using a lower BA concentration (0.89 μM BA). In contrast, the two highest BA levels evaluated were ineffective and produced short, chlorotic and browning shoot clumps. To assess the widespread applicability of the shoot regeneration methods, shoot and callus growth were evaluated for five *A. annua* genotypes (**Table 4**). The results over all genotypes confirmed that high numbers of shoots can be produced using BA in combination with NAA; excessive callus growth occurs with high BA concentrations. Furthermore, different genotypes exhibited variable responses in shoot and callus growth. For example, shoot numbers exhibited a 3.5 fold difference in genotype C10 versus 3M. This indicates that optimization on an individual genotype basis may be warranted.

In Vitro Rooting

Shoots placed on rooting medium containing IBA readily produced roots within 4 weeks (**Table 5**). Percent rooting was significantly higher at the two higher IBA concentrations evaluated with 100% rooting obtained for C10 and 92% for MP11 genotype. While IBA at 9.8 μM produced significantly higher numbers of primary and lateral roots than other concentrations, there was continuing shoot proliferation and callusing on the base of shoots. An intermediate treatment was used to overcome this problem where shoots were placed on basal medium with no plant growth regulators to promote shoot elongation and arrest continued shoot proliferation. The rooting responses of elongated shoots obtained from four different genotypes were assessed using a rooting medium supplemented with 9.8 μM IBA (**Table 6**). Percent rooting with 3M, C10, and B6 genotypes was greater than 98%. Significantly lower rooting at 78% was obtained with MP11. Root number was significantly affected by genotype, ranging from 6 to 17 roots per shoot.

TABLE 2 | Effect of cutting type on rooting of two genotypes of *Artemisia annua*; *n* = 6 replicates of 18 cuttings each.

	B4 clone		C1 clone	
Cutting type	**Rooting (%)[z]**	**Root dry weight (mg)**	**Rooting (mg)**	**Root dry weight (mg)**
Tip	97.2a	4.0ab	74.1a	11.3a
Lateral tip	89.8b	6.0a	88.3a	8.9ab
One node	100.0a	3.2b	87.4a	6.2ab
Two nodes	98.2a	4.7ab	90.5a	3.4b
Average	96.3	4.3	85.1	7.4

[z]*Mean separation Tukey test, α = 0.05. Means within the same column followed by the same letter are not significantly different.*

Micropropagation Protocol

A tissue culture protocol via shoot proliferation was successfully developed for *A. annua*. A scheme depicting culture initiation, shoot induction, shoot multiplication, shoot elongation, rooting, and outplanting into the field is shown in **Figure 3**. Cultures can be initiated from shoot tip or leaf explants of established plants. Unlike systems requiring seedling explants, clonal lines thus can be established from genotypes identified as having high artemisinin leaf concentration and excellent agronomic characteristics.

Field Performance of Tissue Culture-Derived Plants

Field studies evaluated the performance of two clonally propagated genotypes and of plants derived from seed. Plants propagated both by tissue culture and cuttings produced similar artemisinin (**Table 7**). The relative standard deviation (RSD) values varied from 5.86 to 14.7%. In contrast, plants generated from open-pollinated seedlings had an RSD of 33.65% (**Table 7**), indicating that the variance in artemisinin content was higher with the seedling population. Clonal propagation, whether by tissue culture or cuttings, produced greater uniformity than that obtained from seedlings regarding artemisinin concentration.

Plant growth characteristics of field-grown plants propagated using cuttings or tissue culture are shown in **Table 8**. No significant differences were observed in leaf dry weight, shoot dry weight, root dry weight, total plant dry weight, leaf:shoot ratio, or leaf area. This indicates that plant growth characteristics of tissue-cultured plants are similar to that of conventionally propagated cuttings.

Effect of Growing Conditions on Sesquiterpenes

Artemisinin, dihydroartemisinic acid, and artemisinic acid were evaluated from leaves obtained from plants grown under field, greenhouse, or tissue culture conditions. Plants grown under field and greenhouse conditions produced very similar levels of artemisinin (**Table 9**). Clone 3M had average artemisinin concentrations of 1.80 and 1.94% under greenhouse and field conditions, respectively, while the MP11 genotype had

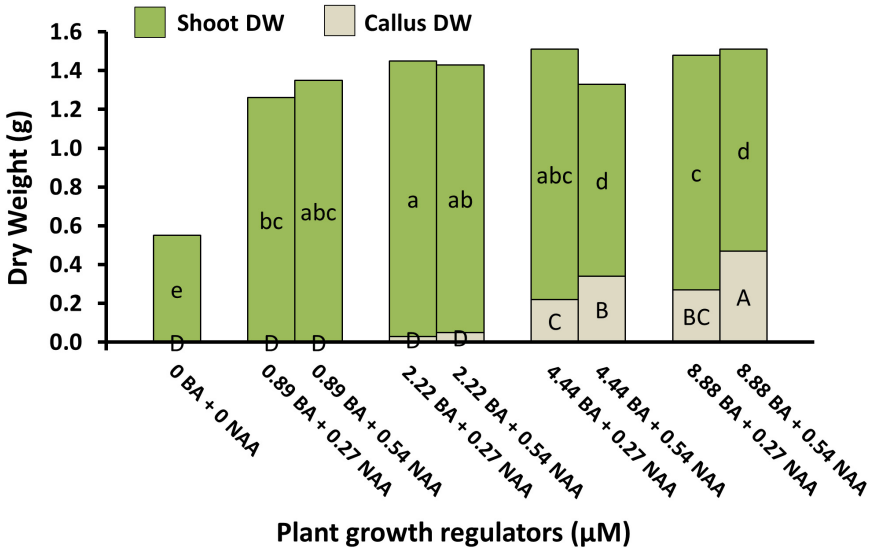

FIGURE 2 | Shoot and callus dry weights of *A. annua* genotype C10 shoot cultures under different plant growth regulator combinations after 6 weeks. Means separated within shoot dry weight (lower) or callus dry weight (upper) by LSD, $p = 0.05$. Treatment means ($n = 24$) with the same letter within a group are not significantly different.

respective concentrations of 1.25 and 1.21% (**Table 9**). The concentrations of dihydroartemisinic acid and artemisinic acid in those plants were also very similar under both greenhouse and field conditions. However, artemisinin concentration in tissue culture plants were 40–97 times less than greenhouse or field grown plants (**Table 9**).

These results confirm that greenhouse-grown plants can be used for selection and biochemical analysis of artemisinin and related compounds, and provide accurate estimations of plant performance in the field. Current studies concur with the effectiveness of using greenhouse grown material for screening artemisinin content as was used by Graham et al. (2010).

DISCUSSION

The present study describes several selections we have identified that produce high levels of artemisinin (up to 2.16%) and which exhibit superior agronomic characteristics including high leaf area and biomass production. When grown as clonal plots, artemisinin yields per hectare were remarkable. Our best genotype, C1, when planted at the density of 1 plant/m^2, had a 2.16% artemisinin content and produced 3.22 t/ha leaf dry weight, for an estimated gross primary productivity of 69.6 kg of artemisinin/ha. In nature, artemisinin content in the leaves and flowers of wild-type *A. annua* is low (0.03–0.8%) (Charles et al., 1990; Ferreira et al., 1995; Alejos-Gonzalez et al., 2011; Liu et al., 2011). Improving artemisinin content through genetic breeding has increased content. Nonetheless, yields are usually 0.5–1.2% artemisinin, yield of dry leaf per hectare varies from 1.5 to 2 t per hectare and reports indicate that a yield of 6–14 kg of artemisinin per hectare from well-managed plantations can be expected (CNAP, 2017).

Growers in Madagascar have used cuttings of selected plants for their commercial crops for their desirable agronomic characteristics. Although this practice is labor-intense it produces more robust plants than the ones generated from seedlings (Ellman and Bartlett, 2010). These authors also mentioned a plant density of 1 plant/m^2 for robust plants and up to 3 plants/m^2 for less robust plants. However, there is no mention of cuttings being used to produce a crop with robust plants that are also higher in artemisinin concentration or for a homogeneous crop regarding artemisinin concentration per plant.

Artemisinin concentration is an extremely variable trait in *A. annua* ranging from 0.5 to 1.07% (Delabays et al., 2001). Although the high-heritability of artemisinin content has been experimentally confirmed by broad and narrow-sense heritability (Ferreira et al., 1995; Delabays et al., 2002), production of F_1 hybrids produced from homozygous inbred plants has been problematic because *A. annua* exhibits self-incompatibility (Peter-Blanc, 1992; Wetzstein et al., 2014) which results in

TABLE 3 | Effects of plant growth regulators on shoot and callus production in *Artemisia annua* cultures after 6 weeks; $n = 24$.

BA (µM)	NAA (µM)	Shoot		Callus		No. shoots[y]
		FW (g)	DW (g)	FW (g)	DW (g)	
0	0	0.69c[z]	0.13c	0b	0b	1.4c
0.89	0.27	8.88b	0.86b	1.83a	0.20a	42.3a
1.78	0.27	12.56a	1.08a	1.30ab	0.13ab	26.9b
2.67	0.27	9.42b	0.92ab	2.45a	0.25a	20.1b
3.56	0.27	9.88b	0.81b	2.45a	0.24a	12.2bc

[z]*Mean separation by LSD, p = 0.05. Means within the same column followed by the same letter are not significantly different.* [y]*n = 9.*

TABLE 4 | Effects of BA in combination with NAA on shoot and callus growth for different genotypes of *Artemisia annua* after 6 weeks.

Treatment (μM)		FW (g)		DW (g)		WC (%)		No. shoots[y]
BA	**NAA**	**Callus**	**Shoot**	**Callus**	**Shoot**	**Callus**	**Shoot**	
0.89	0.27	1.2c[z]	14.4b	0.1c	1.3a	1.1c	13.2b	55.2a
1.78	0.27	2.5b	15.6ab	0.2b	1.3a	2.3b	14.2ab	64.4a
3.56	0.27	3.9a	17.3a	0.3a	1.4a	3.5a	15.9a	54.1a
Genotype								
C10		0.8c	18.5b	0.09c	1.6a	0.7c	16.8b	91.4a
B6		5.0a	16.0c	0.38a	1.4b	4.6a	14.6c	59.2b
MP11		1.9bc	21.9a	0.16bc	1.7a	1.7bc	20.2a	53.8b
3M		2.4b	6.6d	0.23b	0.6c	2.1b	6.0d	26.0c

[z]Mean separation by LSD, p = 0.05. Means within the same column followed by the same letter are not significantly different. [y]n = 24 cultures.

TABLE 5 | Effects of IBA concentration on the rooting of regenerated shoots in two genotypes of *Artemisia annua* after 4 weeks.

IBA (μM)	C10 clone			MP11 clone		
	Rooting (%)	**No. roots**	**No. lateral roots**	**Rooting (%)**	**No. roots**	**No. lateral roots**
0	8.3c[z]	0.1c	0.3b	22.2c	1.2c	1.0b
2.4	66.7b	2.2c	0.9b	70.4b	4.9c	1.3b
4.9	83.3ab	5.8b	2.3b	92.6a	12.3b	3.7b
9.8	100.0a	13.6a	5.1a	92.6a	26.3a	8.6a

[z]Mean separation by LSD, p = 0.05. Means within the same column followed by the same letter are not significantly different.

the inability to produce homozygous lines by inbreeding. The so-called hybrid seed presently available for *A. annua* is produced by crossing two heterozygous and genetically-different parental genotypes, which results in highly variable progeny. The production of inbred lines can potentially be accomplished by producing double haploids (Liu et al., 2016), but this technique must be demonstrated for *A. annua* and would be an extensive effort.

Vegetative propagation and the use of clones are standard methods used in horticultural crop production of floriculture, vegetable and major plantation crops. Cloning produces plants that are genetically identical, maintain desired characteristics, and is a means for the immediate capture of improvements in species that are difficult to breed by conventional means such as *A. annua*.

Methods for the vegetative propagation of clonal lines selected for high artemisinin have been demonstrated in this paper using two strategies: (1) *in vitro* tissue culture and (2) cutting propagation. Further, proof of concept studies verified that clonally-propagated plants provide consistent sesquiterpene production originally found in mother plants, and crop uniformity. Plants were morphologically similar in vegetative characters such as branching, shoot growth patterns, and leaf morphology. Observations in our clonal plots indicated that time-to-flowering was consistent within a genotype (data not presented) which will aid in time-to-harvest decisions. Harvest is often timed for the peak in artemisinin and biomass, which were prior to flowering for both early and late flowering clones (Delabays et al., 2001; Ferreira, 2008) making reproductive uniformity within a field plot an advantage.

Micropropagation or tissue culture affords some distinct advantages as a propagation strategy including the ability to produce millions of contaminant-free elite plants. High propagation rates were achieved in the current study using adventitious shoot formation. The methods were effective for many genotypes, and cultures lines can be initiated from mature greenhouse or field-grown plants. Unlike culture systems that require axenically-germinated seed or young seedling tissues for culture initiation, plants with proven artemisinin content and field performance can be used. Some genotypic differences in culture were observed. Thus, media optimization studies are anticipated to be necessary for different genotypes. Also, tissue culture plants analyzed by HPLC-UV, which had no developed roots, and had only traces or no artemisinin, dihydroartemisinic acid, or artemisinic acid. These results agree with a previous report that rootless *A. annua* plants had negligible amounts of artemisinin when compared to control rooted tissue culture plants (Ferreira and Janick, 1996).

TABLE 6 | Rooting response of different *Artemisia annua* genotypes after 4 weeks on media containing 9.8 μm IBA; *n* = 50.

Genotype	Rooting (%)	No. roots
3M	98a[z]	17.0a
C10	100a	14.5ab
B6	100a	9.6bc
MP11	78b	6.2c

[z]Mean separation by LSD, p = 0.05. Means within the same column followed by the same letter are not significantly different.

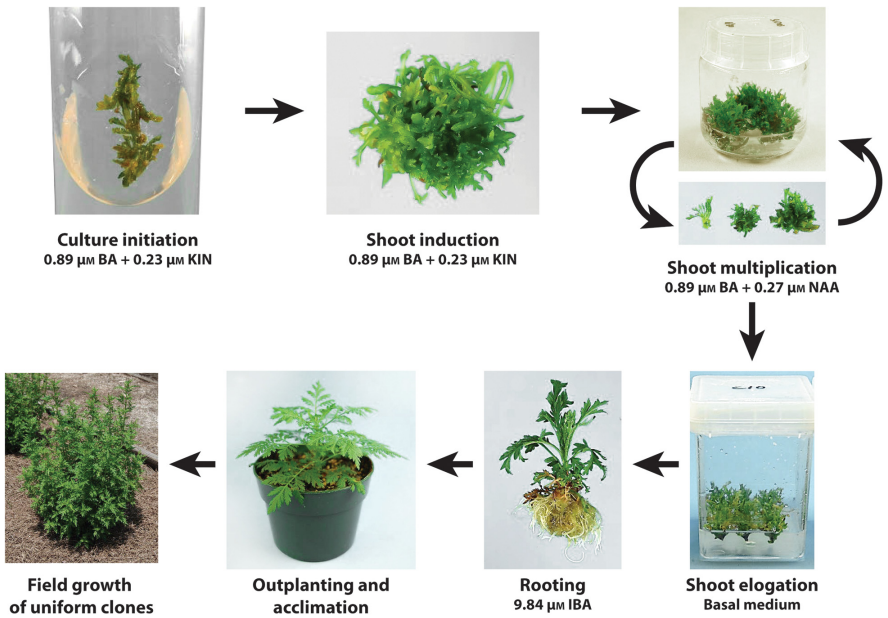

FIGURE 3 | Scheme showing the tissue culture protocol developed for the clonal propagation of *A. annua*. Cultures can be initiated from shoot tip or leaf explants of established plants placed on a shoot induction medium. Shoot multiplication is facilitated on a medium with BA and KIN. Transfer of shoots to a basal medium promotes the elongation of shoots, prevents continued shoot proliferation and enhances rooting of shoots when transferred to a medium with IBA. Following acclimation, plantlets outplanted into the field exhibit uniform growth.

TABLE 7 | Artemisinin concentration (g/100 g DW) of leaves from field-grown plants of two cloned genotypes (3M and MP11) propagated by tissue culture or rooted cuttings.

Plant material	Propagation method	Artemisinin (%) (n = 4)	RSD[z] (%)	Significance (p)
3M clone	Tissue culture	0.78	14.4	0.83^{ns}
	Cutting	0.76	14.7	
MP11 clone	Tissue culture	0.79	10.4	1.00^{ns}
	Cutting	0.78	5.86	
Open pollinated seedlings		0.70	33.65	N/A

Variability (RSD) was compared to plants derived from open-pollinated seed. Plants were placed in the field on 24 June and harvested on 14 September. [z]RSD, relative standard deviation; ns, no significant difference.

Although plant tissue culture has been used to produce natural and pharmaceutical products in a number of systems, the current study confirms that shoot cultures are a poor source for sesquiterpenes. The production of artemisinin by means of cell, tissue, or organ cultures is not viable (Nair et al., 1986; Ferreira and Janick, 1996). The low artemisinin concentrations of *A. annua* leaves developed *in vitro* is a common observation (Covello et al., 2007), and may be a function of the scarcity of glandular trichomes in tissue-cultured shoots (H. Wetzstein, personal communication). Callus grown in tissue culture contains little or no artemisinin (Nair et al., 1986; Ferreira and Janick, 1996). Production of artemisinin in bioreactors has not achieved high artemisinin levels (Kim et al., 2001; Liu et al., 2003, 2006). Although nutrients, growth regulators, oxygen, and culture systems play important roles in optimizing final artemisinin concentration (Weathers et al., 1997; Kim et al., 2001; Mohammad et al., 2014), bioreactors are not a commercially feasible approach to produced artemisinin. An approach using genetically engineered yeast cultures has produced artemisinic acid (Ro et al., 2006), but commercial production of artemisinin using this technology has not materialized. More recently, artemisinin has been produced in engineered moss (Khairul Ikram et al., 2017), but with a very low concentration (0.021%). Thus, we envision the use of *in vitro* culture in *A. annua* as a method for micropropagation.

Propagation by cuttings was also found to be an effective method for propagation of *A. annua.* High rates of rooting were obtained using both tip and nodal cuttings. Plant material could be provided to growers as rooted cuttings or as unrooted cuttings that would be placed in misted field nurseries for rooting before field transplanting. Use of cuttings is widespread for ornamentals production and about 5 billion cuttings are produced per year in tropical countries and air-freighted to temperate growers (Faust et al., 2017). Cuttage operations are simpler and require less infrastructure and expertise than needed for tissue culture. However in this case, special greenhouse facilities would be required for cuttage technology because artemisia is a short-day, monocarpic species which flowers, sets seed, and then dies if plants are not maintained under long days. Mother plants must be maintained in greenhouses supplied with artificial light to remain vegetative.

Generally, vegetative propagation is more costly (per unit propagule) than seed propagation (Hartman et al., 2011). Facilities needed for vegetative propagation include protected

TABLE 8 | Plant growth characteristics of field-grown plants propagated by tissue culture or cuttings.

Propagation method[z]	Dry weight (g)				Leaf:shoot ratio	Leaf area (cm^2)
	Leaf	Shoot	Root	Total plant		
Cuttings	225a[y]	446a	124a	796a	0.52a	12.8a
Tissue culture	198a	415a	102a	714a	0.48a	13.1a

[z]n = 6 plants per propagation method. Planting date 24 June; harvest date 14 September. [y]Mean separation by LSD, p = 0.05. Means within the same column followed by the same letter are not significantly different.

TABLE 9 | The effect of growing conditions on artemisinin (ART), dihydroartemisinic acid (DHAA), and artemisinic acid (AA) content in three genotypes of *Artemisia annua*.

Genotype[z]	Growth conditions	ART (%)	DHAA (%)	AA (%)
3M	Field	1.94 ± 0.23	0.80 ± 0.13	0.10 ± 0.02
	Greenhouse	1.80 ± 0.21	0.68 ± 0.12	0.07 ± 0.01
	Tissue culture	0.02 ± 0.02	0.02 ± 0.01	0.00 ± 0.00
MP11	Field	1.21 ± 0.07	0.53 ± 0.16	0.07 ± 0.01
	Greenhouse	1.25 ± 0.07	0.44 ± 0.04	0.06 ± 0.006
	Tissue culture	0.02 ± 0.06	0.08 ± 0.032	0.01 ± 0.002
C10[y]	Greenhouse	1.23 ± 0.06	1.24 ± 0.12	0.32 ± 0.02
	Tissue culture	0.03 ± 0.01	0.10 ± 0.05	0.01 ± 0.002

[z]n = 4 for each genotype and growing condition. [y]Field material unavailable at the time of analysis.

culture, mist/high humidity for cuttings, and laboratories if tissue culture is employed (autoclaves, aseptic hoods, and growth rooms). However for many crop species, the superiority, consistent quality, and uniformity of clonal plants justifies the higher propagation costs. An economic analysis would have to be made to determine if the increase in yield obtained from high-artemisinin clones would compensate for the increased cost of planting stock. Currently, cultivation of *A. annua* is accomplished by seed. Because seed are so small (10–15,000 per gram), sowing and germination of seed in a nursery, with transplantation to allow seedlings to make additional growth prior to transplanting in the field are commonly practiced, particularly when purchased high-value seed is used (Laughlin et al., 2002). Thus, some of the costs of clonal propagation, i.e., shoot elongation and explant rooting, may compare similarly to current steps in seed production, such as thinning and transplanting. A high-efficiency clonal micropropagation system could be an economically-feasible alternative to current seed propagation practices if regeneration rates are high and enhanced artemisinin production is sufficiently elevated.

Commercial micropropagation is often limited to crops generating high unit prices, including ornamental plants and food crops (Kane et al., 2015). The application of additional *in vitro* systems such as somatic embryogenesis, bioreactors, and temporary immersion systems for plant propagation could provide extremely high regeneration rates, are amenable to scale up, can provide higher quality plant material, and thus can significantly decrease the cost of tissue-culture derived plants (Etienne and Berthouly, 2002; Georgiev et al., 2014). In horticultural crop production, tissue culture is often used to maintain and multiply disease-free mother plants used for cutting propagation. Clones of high-artemisinin lines could be propagated in individual farms or as a separate operation which is common in many clonally-propagated crops. Cultures can be maintained and shipped to locations for rooting and to set up plant blocks from which mother plants are propagated for cuttings.

The goals of these studies were to select superior high-artemisinin-producing genotypes of *A. annua*, and to develop methodology to propagate these superior genotypes. The approach of combining conventional hybridization/selection of superior genotypes with clonal propagation is a means to enhance crop yield and artemisinin production. The clonal propagation of superior high artemisinin-yielding cultivars would provide significant improvements in crop production, particularly since to date even the best seed available produce plants highly variable in artemisinin content and agronomic characteristics (Graham et al., 2010). Proof of concept studies substantiated that both tissue culture-regenerated plants and those produced by cuttings performed better than plants derived from seed in terms of uniformity, yield, and consistently high artemisinin content. Using vegetative propagation to produce plants with homogeneously-high artemisinin can provide a consistent source of improved plant material that could rapidly become available to local farmers, help growers to markedly increase artemisinin yield per cultivated area, and feasibly be adopted in the world's major production areas of Southeast Asia and Africa. Cost-benefit analysis is needed to reveal best management practices employing sustainable and profitable production criteria.

CONCLUSION

The results of these studies indicate that selection can produce plants of *A. annua* with artemisinin levels above 2%. The current study identified four clones with artemisinin levels ranging from 1.8 to 2.2% and possessing improved agronomic characteristics such as high leaf area and shoot biomass production. Artemisinin production from these genotypes produced an estimated gross primary productivity from 58 to 70 kg/ha artemisinin, with a crop density of 1 plant m^{-2}. High artemisinin clones can be propagated vegetatively either by cuttings or micropropagation. Further, tissue culture can be used to propagate and provide clean stock plants to disseminate for cuttings. Further studies are needed to determine if clonal propagation is cost effective. The efficiency would be a function

of artemisinin content, biomass production, and costs to produce plants by cuttings or micropropagation compared to seedling propagation. The adoption of the vegetative propagation of superior genotypes, with the development of marketing channels, will provide a means to meet the growing global demand of artemisinin and its derivatives, improve human health, and lead to rural economic growth in some of the world's poorest regions. Such value-added enterprises, filling a major void in rural health and nutrition, will reduce poverty, diversify rural incomes, and reduce gender inequity. Thus, we envision that the use of clonal propagation through *in vitro* cultures or cuttings of high-artemisinin clones of *A. annua* can become a more accessible and practical method for producing homogeneously-high artemisinin crops that can reduce the price of artemisinin-combination therapy and continue to be provide a means of generating income to Asian and African communities afflicted by poverty and malaria.

AUTHOR CONTRIBUTIONS

HW designed the study, devised tissue culture methods, interpreted the results, and drafted the manuscript. JP assisted in field trials and tissue culture experiments, ran the artemisinin analyses, collected and analyzed data. JF helped with study design and performed sesquiterpene analyses. JF and JJ interpreted results, contributed to the manuscript, and provided germplasm for the selection studies. TM helped design and conducted tissue culture and field studies, analyzed data, and contributed to the manuscript.

FUNDING

This research was supported by the University of Georgia Research Foundation Cultivar Development Program.

ACKNOWLEDGMENTS

Thanks are due to Drs. Pedro M. de Magalhães (CPQBA, Brazil), Xavier Simonet (Mediplant, Switzerland), and Kevin Mak (China, unknown affiliation) for providing plant material. Thanks to Mr. Barry Harter (USDA-ARS) for his invaluable help with the sesquiterpene extractions and HPLC analyses; and to Shonda Davis, Lauren Hill, Victoria Ramirez, and Laurie Leveille (University of Georgia) for assistance in tissue culture and field studies.

REFERENCES

Alejos-Gonzalez, F., Qu, G., Zhou, L.-L., Saravitz, C. H., Shurtleff, J. L., and Xie, D.-Y. (2011). Characterization of development and artemisinin biosynthesis in self-pollinated *Artemisia annua* plants. *Planta* 234, 685–697. doi: 10.1007/s00425-011-1430-z

Bhakuni, R. S., Jain, D. C., Sharma, R. P., and Kumar, S. (2001). Secondary metabolites of *Artemisia annua* and their biological activity. *Curr. Sci.* 80, 35–48.

CNAP (2017). *Artemisia Research Project*. Available at: https://www.york.ac.uk/org/cnap/artemisiaproject/fact_sheets_aa.htm

Charles, D. J., Simon, J. E., Wood, K. V., and Heinstein, P. (1990). Germplasm variation in artemisinin content of *Artemisia annua* using an alternative method of artemisinin analysis from crude plant extracts. *J. Nat. Prod.* 53, 157–160. doi: 10.1021/np50067a021

Covello, P. S., Teoh, K. H., Polichuk, D. R., Reed, D. W., and Nowak, G. (2007). Functional genomics and the biosynthesis of artemisinin. *Phytochemistry* 68, 1864–1971. doi: 10.1016/j.phytochem.2007.02.016

Delabays, N., Darbekkay, C., and Galland, N. (2002). "Variation and heritability of artemisinin content in *Artemisia annua* L," in *Artemisia*, ed. C. W. Wright (Boca Raton, FL: CRC Press), 197–209.

Delabays, N., Simonnet, X., and Gaudin, M. (2001). The genetics of artemisinin content in *Artemisia annua* L. and the breeding of high yielding cultivars. *Curr. Med. Chem.* 8, 1795–1801. doi: 10.2174/0929867013371635

Duke, M. V., Paul, R. N., Elsohly, H. N., Sturtz, G., and Duke, S. O. (1994). Localization of artemisinin and artemisitene in foliar tissues of glanded and glandless biotypes of *Artemisia annua L. Int. J. Plant Sci.* 155, 365–373. doi: 10.1086/297173

Ellman, A., and Bartlett, E. (2010). Cultivation of *Artemisia annua* in Africa and Asia. *Outlooks Pest Manag.* 21, 84–88. doi: 10.1564/21apr08 doi: 10.1564/21apr08

Etienne, H., and Berthouly, M. (2002). Temporary immersion systems in plant micropropagation. *Plant Cell Tissue Organ Cult.* 69, 215–231. doi: 10.1023/A:1015668610465

Faust, J. E., Dole, J. M., and Lopez, R. G. (2017). The floriculture vegetative cutting industry. *Hortic. Rev.* 44, 121–172.

Ferreira, J. F., and Gonzalez, J. M. (2009). Analysis of underivatized artemisinin and related sesquiterpene lactones by high-performance liquid chromatography with ultraviolet detection. *Phytochem. Anal.* 20, 91–97. doi: 10.1002/pca.1101

Ferreira, J. F. S. (2008). Seasonal and post-harvest accumulation of artemisinin, artemisinic acid, and dihydroartemisinic acid in three accessions of *Artemisia annua* cultivated in West Virginia, USA. *Planta Med.* 74, 310–311. doi: 10.1055/s-2008-1075155

Ferreira, J. F. S., and Janick, J. (1995). Floral morphology of *Artemisia annua* with special reference to trichomes. *Int. J. Plant Sci.* 156, 807–815. doi: 10.1086/297304

Ferreira, J. F. S., and Janick, J. (1996). Roots as an enhancing factor for the production of artemisinin in shoot cultures of *Artemisia annua*. *Plant Cell Tissue Organ Cult.* 44, 211–217. doi: 10.1007/BF00048526

Ferreira, J. F. S., and Janick, J. (1997). *Artemisia annua*: botany, horticulture, pharmacology. *Hortic. Rev.* 19, 319–371.

Ferreira, J. F. S., Laughlin, J. C., Delabays, N., and de Magalhães, P. M. (2005). Cultivation and genetics of *Artemisia annau* L. for increased production of the antimalarial artemisinin. *Plant Genet. Resour.* 3, 206–229. doi: 10.1079/PGR200585

Ferreira, J. F., Simon, J. E., and Janick, J. (1995). Relationship of artemisinin content of tissue-cultured, greenhouse-grown, and field-grown plants of *Artemisia annua*. *Planta Med.* 61, 351–355. doi: 10.1055/s-2006-958098

Gamborg, O. L., Miller, R. A., and Ojima, K. (1968). Nutrient requirements of suspension cultures of soybean root cells. *Exp. Cell Res.* 50, 151–158. doi: 10.1016/0014-4827(68)90403-5

Georgiev, G. V., Schumann, A., Pavlov, A., and Bley, T. (2014). Temporary immersion systems in plant biotechnology. *Eng. Life Sci.* 14, 607–621. doi: 10.1002/elsc.201300166

Graham, I. A., Besser, K., Blumer, S., Braniga, C. A., Czechowski, T., Elias, L., et al. (2010). The genetic map of *Artemisia annua* L. identifies loci affecting yield of the antimalarial drug artemisinin. *Science* 327, 328–331. doi: 10.1126/science.1182612

Hartman, H. T., Kester, D. E., Davies, F. T., and Geneve, R. L. (2011). *Plant Propagation Principles and Practices*, 8th Edn. Upper Saddle River, NJ: Prentice Hall.

Kane, M. E., Kauth, P. J., and Stewart, S. L. (2015). "Micropropagation," in *Plant Propagation Concepts and Laboratory Exercises*, eds C. A. Beyl and R. N. Trigiano (Boca Raton, FL: CRC Press), 359–370.

Khairul Ikram, N. K. B., Beyraghdar Kashkooli, A., Peramuna, A. V., van der Krol, A. R., Bouwmeester, H., and Simonsen, H. T. (2017). Stable production of the antimalarial drug artemisinin in the moss *Physcomitrella patens*. *Front. Bioeng. Biotechnol.* 5:47. doi: 10.3389/fbioe.2017.00047

Kim, Y., Wyslouzil, B. E., and Weathers, P. J. (2001). A comparative study of mist and bubble column reactors in the in vitro production of artemisinin. *Plant Cell Rep.* 20, 451–455. doi: 10.1007/s002990100342

Larson, T. R., Branigan, C., Harvey, D., Penfield, T., Bowles, D., and Graham, I. A. (2013). A survey of artemisinic and dihydroartemisinic acid contents in glasshouse and global field-grown populations of the artemisinin-producing plant *Artemisia annua* L. *Ind. Crops Prod.* 45, 1–6. doi: 10.1016/j.indcrop.2012.12.004

Laughlin, J. C., Heazlewood, G. N., and Beattie, B. M. (2002). "Cultivation of *Artemisia annua* L," in *Artemisia*, ed. C. W. Wright (Boca Raton, FL: CRC Press), 159–195.

Liu, B., Wang, H., Du, Z. G., Li, G. F., and Ye, H. C. (2011). Metabolic engineering of artemisinin biosynthesis in *Artemisia annua* L. *Plant Cell Rep.* 30, 689–694. doi: 10.1007/s00299-010-0967-9

Liu, C.-Z., Guo, C., Wang, Y., and Ouyang, F. (2003). Factors influencing artemisinin production from shoot cultures of *Artemisia annua* L. *World J. Microbiol. Biotechnol.* 19, 535–538. doi: 10.1023/A:1025158416832

Liu, C.-Z., Zhao, Y., and Wang, Y. (2006). Artemisinin: current state and perspectives for biotechnological production of an antimalarial drug. *Appl. Microbiol. Biotechnol.* 72, 11–20. doi: 10.1007/s00253-006-0452-0

Liu, Z., Wang, Y., Jiaojiao, H., Mei, M., Frei, U., Trampe, B., and Lübberstedt, T. G. (2016). Maize doubled haploids. *Plant Breed. Rev.* 40, 123–166. doi: 10.1002/9781119279723.ch3

Mohammad, A., Alam, P., Ahmad, M., Ali, A., Ahmad, J., and Abdin, M. Z. (2014). Impact of plant growth regulators (PGRs) on callogenesis and artemisinin content in *Artemisia annua* L. plants. *Indian J. Biotechnol.* 13, 26–33.

Murashige, T., and Skoog, F. (1962). A revised medium for rapid growth and bio assays with tobacco tissue cultures. *Physiol. Plant.* 15, 473–497. doi: 10.1111/j.1399-3054.1962.tb08052.x

Nair, M. S. R., Acton, N., and Klayman, D. L. (1986). Production of artemisinin in tissue cultures of *Artemisia annua*. *J. Nat. Prod.* 49, 504–507. doi: 10.1021/np50045a021

Peter-Blanc, C. (1992). *Dévelopment et Biologie de la Reproduction de l"Artemisia annua*. Lausanne: Travail de diplôme, Univ. de Lausanne.

Ro, D.-K., Paradise, E. M., Ouellet, M., Fisher, K. J., Newman, K. L., Ndungu, J. M., et al. (2006). Production of the antimalarial drug precursor artemisinic acid in engineered yeast. *Nature* 440, 940–943. doi: 10.1038/nature04640

Weathers, P. J., Hemmavanh, D. D., Walcerz, D. B., Cheetham, R. D., and Smith, T. C. (1997). Interactive effects of nitrate and phosphate slats, sucrose, and inoculum culture age on growth and sesquiterpene production in *Artemisia annua* hairy root cultures. *In Vitro Cell. Dev. Biol. Plant* 33, 306–312. doi: 10.1007/s11627-997-0056-0

Wetzstein, H. W., Porter, J. A., Janick, J., and Ferreira, J. F. S. (2014). Flower morphology and floral sequence in *Artemisia annua* (Asteraceae). *Am. J. Bot.* 101, 875–885. doi: 10.3732/ajb.1300329

World Malaria Report (2016). *Summary*. Geneva: World Health Organization.

Conflict of Interest Statement: The authors declare that the research was conducted in the absence of any commercial or financial relationships that could be construed as a potential conflict of interest.

frontiers in Plant Science

ORIGINAL RESEARCH
published: 05 April 2018
doi: 10.3389/fpls.2018.00413

AaEIN3 Mediates the Downregulation of Artemisinin Biosynthesis by Ethylene Signaling Through Promoting Leaf Senescence in *Artemisia annua*

*Yueli Tang, Ling Li, Tingxiang Yan, Xueqing Fu, Pu Shi, Qian Shen, Xiaofen Sun and Kexuan Tang**

Joint International Research Laboratory of Metabolic & Developmental Sciences, Key Laboratory of Urban Agriculture (South) Ministry of Agriculture, Plant Biotechnology Research Center, Fudan-SJTU-Nottingham Plant Biotechnology R&D Center, School of Agriculture and Biology, Shanghai Jiao Tong University, Shanghai, China

Artemisinin is an important drug for malaria treatment, which is exclusively produced in *Artemisia annua*. It's important to dissect the regulatory mechanism of artemisinin biosynthesis by diverse plant hormones and transcription factors. Our study shows ethylene, a plant hormone which accelerates flower and leaf senescence and fruit ripening, suppressed the expression of genes encoding three key enzymes ADS, DBR2, CYP71AV1, and a positive regulator AaORA involved in artemisinin biosynthesis. Then we isolated the gene encoding ETHYLENE-INSENSITIVE3 (EIN3), a key transcription factor in ethylene signaling pathway, by screening the transcriptome and genome database from *Artemisia annua*, named *AaEIN3*. Overexpressing *AaEIN3* suppressed artemisinin biosynthesis, while repressing its expression with RNAi enhanced artemisinin biosynthesis in *Artemisia annua*, indicating AaEIN3 negatively regulates artemisinin biosynthesis. Further study showed the downregulation of artemisinin biosynthesis by ethylene required the mediation of AaEIN3. AaEIN3 could accelerate leaf senescence, and leaf senescence attenuated the expression of *ADS*, *DBR2*, *CYP71AV1*, and *AaORA* that are involved in artemisinin biosynthesis. Collectively, our study demonstrated a negative correlation between ethylene signaling and artemisinin biosynthesis, which is ascribed to AaEIN3-induced senescence process of leaves. Our work provided novel knowledge on the regulatory network of plant hormones for artemisinin metabolic pathway.

Keywords: ethylene, AaEIN3, leaf senescence, downregulation, artemisinin

OPEN ACCESS

Edited by:
Tomasz Czechowski, University of York, United Kingdom

Reviewed by:
Shan Lu, Nanjing University, China
Mehar Hasan Asif, National Botanical Research Institute (CSIR), India

****Correspondence:***
Kexuan Tang
kxtang@sjtu.edu.cn;
kxtang1@163.com

Specialty section:
This article was submitted to Plant Biotechnology, a section of the journal Frontiers in Plant Science

Received: *14 October 2017*
Accepted: *14 March 2018*
Published: *05 April 2018*

Citation:
Tang Y, Li L, Yan T, Fu X, Shi P, Shen Q, Sun X and Tang K (2018) AaEIN3 Mediates the Downregulation of Artemisinin Biosynthesis by Ethylene Signaling Through Promoting Leaf Senescence in Artemisia annua. Front. Plant Sci. 9:413. doi: 10.3389/fpls.2018.00413

INTRODUCTION

Malaria is a malignant infectious disease caused by plasmodium, severely threatening humans' health. Nowadays this disease is still prevalent in many areas of Southeast Asia and Africa. Artemisinin is a well-known remedy for curing malaria, which is isolated from *Artemisia annua* and was found first by Chinese scientists in the 1970s. Artemisinin Combination

Therapy (ACT) has become the first choice for curing malaria recommended by World Health Organization (WHO) (Mutabingwa, 2005; Graham et al., 2010; Weathers et al., 2011). Meanwhile, artemisinin and its derivatives have been found to have anti-schistosomiasis, anti-tumor, and anti-inflammatory activities (Bhattarai et al., 2007; Efferth, 2007; Efferth et al., 2008). Therefore, artemisinin and its derivatives have a good prospect for application as a multi-purpose natural medication. Artemisinin is mainly extracted from leaves of *Artemisia annua*, but its content in wild *Artemisia annua* is low (0.1–0.8% dry weight) (Duke et al., 1994; Kumar et al., 2004). So it's of great significance to elevate artemisinin production in *Artemisia annua* by all kinds of strategies like metabolic engineering, environmental regulation and genetic breeding. Studying and understanding the regulatory mechanisms of artemisinin biosynthesis by diverse plant hormones and transcription factors will conduce to people's practice for improving artemisinin production by the above strategies.

The precursor for artemisinin biosynthesis is farnesyl diphosphate (FDP) containing three isoprenyl 5-carbon (C5) units. FDP is formed by the condensation of three isoprenyl diphosphates (IPPs) through the catalysis of farnesyl diphosphate synthase (FPS). Then FDP is converted into dihydroartemisinic acid (DHAA) by sequential catalysis of amorpha-4,11-diene synthase (ADS), cytochrome P450 monooxygenase (CYP71AV1), artemisinic aldehyde Δ11 (13) reductase (DBR2) and aldehyde dehydrogenase 1 (ALDH1) (Tang et al., 2014). Finally, the conversion of DHAA into artemisinin is an automatic reaction under light, without the need of enzymatic catalysis (Sy and Brown, 2002; Brown and Sy, 2004).

Many transcription factors are found to participate in artemisinin metabolic regulation. The first discovered transcription factor that positively regulates artemisinin biosynthesis in *Artemisia annua* is AaWRKY1, which activates the expression of key enzyme genes in artemisinin biosynthetic pathway (Ma et al., 2009). Afterwards, other transcription factors, such as AaERF1 and AaERF2 (Yu et al., 2012), AaORA (Lu et al., 2013), AaMYC2 (Shen et al., 2016), AabZIP1 (Zhang et al., 2015), were successively discovered to act positive roles in the regulation of artemisinin biosynthetic pathway. Now it has been found that some plant hormones as jasmonate (JA) (Wang et al., 2010; Caretto et al., 2011), abscisic acid (ABA) (Jing et al., 2009) and salicylic acid (SA) (Pu et al., 2009; Aftab et al., 2011) could increase artemisinin production. And the regulatory mechanism of artemisinin biosynthesis by these hormones signaling has been partially revealed. The regulation of artemisinin biosynthesis by these hormones mainly involves the functioning of MYC2, bZIP1, and NAC-like transcription factors, respectively (Zhang et al., 2015; Lv et al., 2016; Shen et al., 2016). Moreover, it was reported that adding ethephon in the medium led to a decrease of artemisinin content in the roots of *Artemisia annua* seedlings (Weathers et al., 2005), but it's still unclear about the mechanism being responsible for the decrease of artemisinin content under ethephon treatment.

Ethylene is a major plant hormone, modulating the process of plant development, secondary metabolism and stress response. For example, ethylene could cause morphological changes in plant seedlings grown in darkness, including the repression of root and hypocotyl's extension, the thickening of hypocotyl's lateral growth, and the exaggerated apical hook curvature (Bleecker et al., 1988; Ecker, 1995). And as a well-known senescence inducer, ethylene could accelerate fruit ripening and the senescence of flower and leaves (Abeles et al., 1988). In the regulatory process by ethylene signaling, ethylene signals are first perceived by and bind with ethylene-receptor proteins: ETR1/2, ERS1/2, and EIN4, leading to the inactivation of receptor-CTR1 complex (Kieber et al., 1993; Hua and Meyerowitz, 1998). Inactive receptor-CTR1 complex cannot phosphorylate EIN2, a component downstream in ethylene signaling pathway, so that EIN2 would not be degraded and gets activated (Alonso et al., 1999; Qiao et al., 2012). Then active EIN2 protein suppresses the accumulation of two F-box proteins EBF1 and EBF2, thus precluding the degradation of EIN3/EIL1 protein via the EBF1/2-mediated 26S ubiquitin-proteasome pathway (Guo and Ecker, 2003; An et al., 2010). So at the presence of ethylene, EIN3/EIL1 protein can be maintained and accumulate stably, which would regulate the expression of ERF transcription factors and thereby activate the expression of ethylene-responsive genes downstream (Guo, 2011). Besides that ethylene's presence could enhance the stability of EIN3/EIL1 protein to increase its accumulation, the transcription level of *EIN3* gene in leaves would increase with leaves aging. EIN3 protein in *Arabidopsis* could directly repress microRNA164 transcription, thus promoting the expression of senescence-associated genes *SAG12* and *NAC2* (also named *ORE1*) and accelerating the process of leaf senescence. Therefore, *EIN3* is a senescence-associated gene, involved in regulating the process of leaf senescence induced by ethylene or aging (Li et al., 2013).

Previous experimental results of our lab showed that *ADS*, *DBR2*, *CYP71AV1*, three key enzyme genes in artemisinin biosynthetic pathway and *AaORA*, a positive regulator in artemisinin biosynthesis, have relatively high expression level in young leaves of *Artemisia annua*. As leaves get matured and senescent, their expression level drops rapidly (Lu et al., 2013). Meanwhile, the content of DHAA, the end-product of enzymatic reactions in artemisinin biosynthetic pathway, is relatively high in young leaves, and its content declines sharply with leaf maturation and aging (Zhang et al., 2012). This indicated that leaf aging and senescence will attenuate artemisinin biosynthesis.

This study mainly focuses on the regulatory effect of ethylene signaling pathway on artemisinin biosynthesis and tries to unravel the possible mechanism behind it. Our results demonstrates that ethylene negatively regulates the expression of *ADS*, *DBR2*, *CYP71AV1*, and *AaORA* that are involved in artemisinin biosynthesis, and that such negative regulation is associated with leaf senescence induced by EIN3, a key component acting in ethylene signaling pathway. Our work revealed a possible mechanism by which ethylene affects

artemisinin biosynthesis and provided more knowledge and clues for researching the regulatory effect of plant hormones on artemisinin metabolic pathway.

MATERIALS AND METHODS

Cloning and Homology Analysis of *AaEIN3*

By analyzing the sequence information in transcriptome database and full genome database of *Artemisia annua* established by our lab (most of sequences in the databases have been annotated), and by sequence alignment with reported EIN3/EIL1s from other plant species, the gene sequence highly homologous to other *EIN3/EIL1*s was selected out from the transcriptome database of *Artemisia annua*, named as *AaEIN3*. Homologous alignments of nucleotide and protein sequences were performed with Protein-Blast Tool at NCBI website and Vector NTI 9.0 software. Phylogenetic analysis of AaEIN3 was done through neighbor-joining (NJ) method with MEGA 5.0 software. Full-length coding region of *AaEIN3* was obtained and amplified with primers AaEIN3-ORF1 (5′-GGATCCATGGGGATGGGGATCTTTGAAG-3′) and AaEIN3-ORF2 (5′-CTGCAGTCAAAGGTACCACATTG AC ATATC-3′).

Plant Hormone Treatment

Artemisia annua plants were grown in soil matrix in a chamber (16 h light/8 h dark) at 25°C for the day/22°C for the night with 65% relative humidity. For analysis of gene expression mode under ethephon (Et) and aminoxyacetic acid (AOA) treatments, 500 μM Et solution, 200 μM AOA solution and sterile water (as the mock) were sprayed evenly over 14-day-old seedlings of *Artemisia annua* separately. Young leaves at the same position from 8 to 10 seedlings were excised and gathered in the microfuge tube as one biological sample after 0, 1, 3, 6, 9, 12, and 24 h of the treatment, respectively. These samples were stored at −80°C for subsequent RNA extraction and qPCR analysis. For analysis of gene expression mode in transgenic plants under Et treatment, 500 μM Et solution was sprayed evenly over *AaEIN3*-ox, WT, and RNAi plant lines. Then the 2nd leaves counted downward from top meristems were sampled after 0 and 6 h of the treatment, and stored at −80°C for subsequent RNA extraction and qPCR analysis.

Gene Expression Analysis by qPCR

The expression levels of all genes of interest in the study were detected by quantitative PCR (qPCR). Total RNA was extracted from plant samples with the Plant RNA Extraction Kit (Tiangen Biotech, Peking, China) according to the kit's instructions. Aliquots of 1 μg total RNA was used for cDNA synthesis in a reverse transcription system (Takara, Tokyo, Japan). The amplification reaction of qPCR was performed in a Roche LightCycler 96 Real-Time PCR Device, using SYBR Green qPCR Master Mix reagents (Tiangen Biotech, Peking, China) according to the manufacturer's instructions. Relative expression levels of genes were normalized to the expression of β-*Actin* from *Artemisia annua*. The specific primers for each gene used in qPCR are listed in Supplementary Table S1. mRNA expression levels of the target genes were measured with $2^{-\Delta C_t}$.

Vector Construction and Transformation of *Artemisia annua*

For *AaEIN3*-overexpression vector construction, the coding region of *AaEIN3* with a BamHI and a PstI restriction site on either end, respectively, was ligated into the pHB+ vector under the control of the CaMV35S promoter to generate pHB-35S:sGFP-AaEIN3:Noster construct, with the sGFP fused to the N-terminal of AaEIN3. For RNA interference (RNAi) vector construction, the primers AaEIN3-RiF (5′-CA CCTGAATCGTGGCGGAACGCTAAA-3′) and AaEIN3-RiR (5′-ACTGAAACCCTGCTGGCATAAA-3′) were designed to amplify a 350 bp-long RNAi fragment with cDNA of *AaEIN3* as the template. By using the gateway cloning system, the RNAi fragment was first ligated into TOPO vector and then cloned into the pHellsGate12 vector via LR reaction (Invitrogen, United States) to generate the final pHellsGate-RNAi construct. The resulting *AaEIN3*-overexpression and RNAi constructs were transduced into *Agrobacterium tumefaciens* strain EHA105, respectively, and then introduced into *Artemisia annua* to generate transgenic *Artemisia annua* plants as previously described (Shen et al., 2012). Independent transgenic lines were grown and selected in hygromycin-containing MS medium for pHB-*AaEIN3* overexpression transformants, and in kanamycin-containing MS medium for pHellsGate-RNAi transformants. *AaEIN3*-overexpression plant lines were confirmed by PCR detection with primers AaEIN3-ORF1 (5′-GGATCCATGGGGATGGGGATCTTTGAAG-3′) and rbc48-A (5′-GCATTGAACTTGACGAACGTTGTCGA-3′). And *AaEIN3*-RNAi lines were confirmed by PCR detection with primers p35S-FP (5′-TTCGTCAACATGGTGGAGCA-3′) and AaEIN3-RiR (5′-ACTGAAACCCTGCTGGCATAAA-3′). These transgenic lines were transferred to soil and kept for further analyses.

HPLC Analysis of Dihydroartemisinic Acid (DHAA) and Artemisinin Contents

HPLC analysis was used to detect the contents of DHAA and artemisinin in leaves of *Artemisia annua*. Samples were prepared as described previously (Lu et al., 2013). *Artemisia annua* leaves were dried in a drying oven at 45–50°C for 48–72 h, and then ground to powder in a mortar. 0.1 g dried leaf powder was added into 1.5 ml methanol and ultrasonically oscillated for 30 min at 25°C/50W. After centrifugation at 10000*g* for 10 min, the clear supernatant was collected and the extraction was repeated once more. The resulting supernatant was filtered through a 0.22-μm membrane. The filtrates were analyzed by a Waters Alliance 2695 HPLC system coupled with a Waters 2420 ELSD detector (Milford, MA, United States). The mobile phase was methanol/H_2O (v:v = 6:4) for artemisinin measurement, and acetonitrile/0.1% acetate

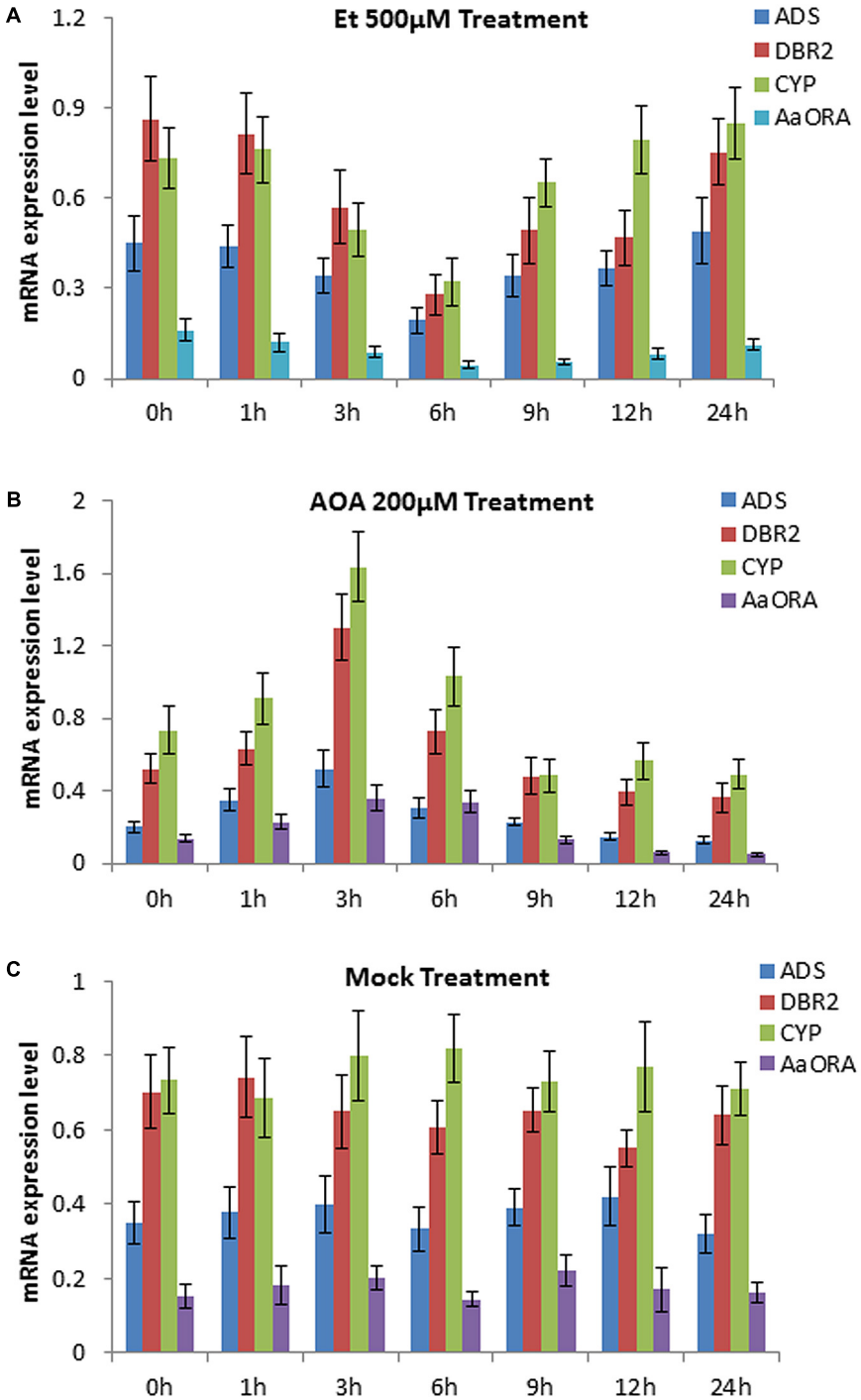

FIGURE 1 | Expression levels of genes involved in artemisinin biosynthesis at different time points after ethephon (Et) and aminoxyacetic acid (AOA) treatments, measured by qPCR. Sterile water was used as the mock treatment. **(A)** Expression levels of *ADS*, *DBR2*, *CYP71AV1* (*CYP*), and *AaORA* after 0, 1, 3, 6, 9, 12, and 24 h of 500 μM Et treatment. **(B)** Expression levels of *ADS*, *DBR2*, *CYP71AV1* (*CYP*), and *AaORA* after 0, 1, 3, 6, 9, 12, and 24 h of 200 μM AOA treatment. **(C)** Expression levels of *ADS*, *DBR2*, *CYP71AV1* (*CYP*), and *AaORA* after 0, 1, 3, 6, 9, 12, and 24 h of sterile water treatment as the mock. Error bars indicate ± SD of three experimental replicates.

(v:v = 6:4) for DHAA measurement. The HPLC conditions were set as described previously (Lu et al., 2013). The standard of artemisinin was purchased from Sigma-Aldrich (Shanghai, China), and the standard of DHAA was purchased from Honsea Sunshine Bio Science & Technology Co., Ltd. (Guangzhou, China).

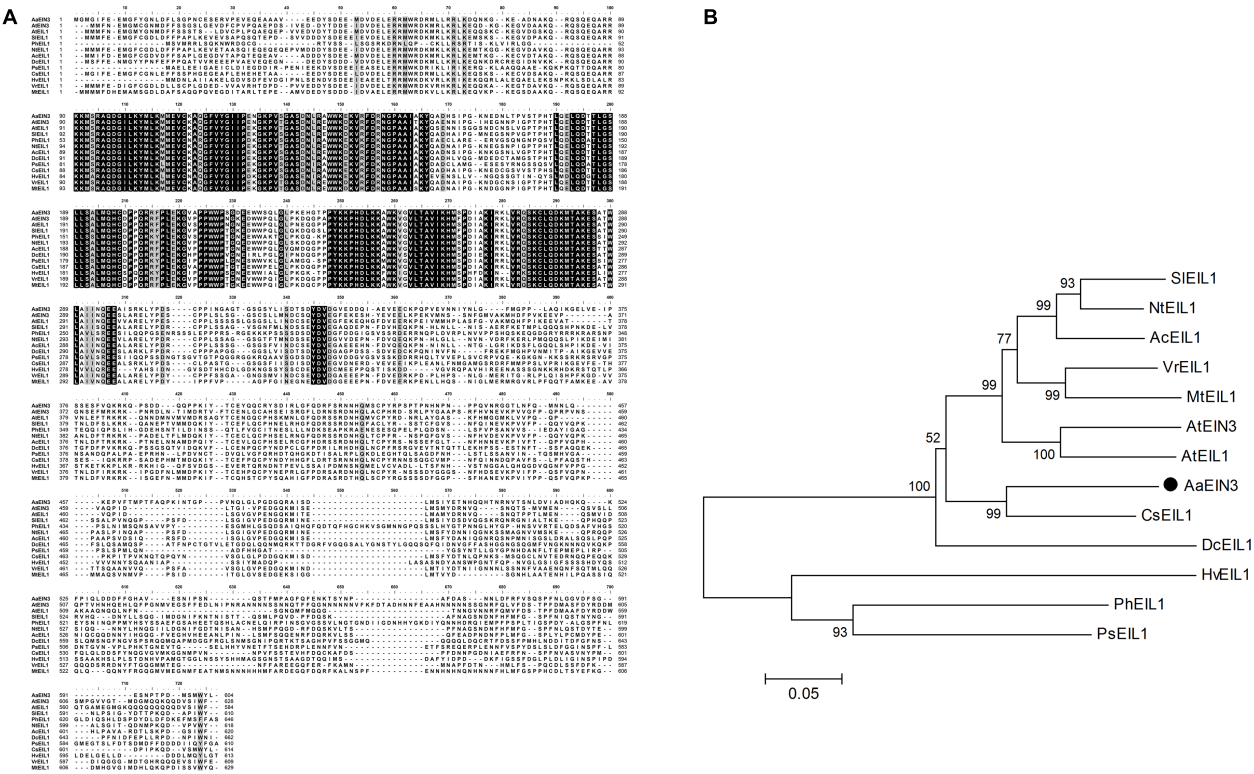

FIGURE 2 | Sequence characterization of AaEIN3. **(A)** Sequence alignment of EIN3/EIL1s. Amino acid sequences were aligned as follows: AaEIN3 (*Artemisia annua*), AtEIN3 (*Arabidopsis thaliana*, Genbank Accession No. AAC49749), AtEIL1 (*Arabidopsis thaliana*, AEC07930), SlEIL1 (*Solanum lycopersicum*, AAK58857), PhEIL1 (*Petunia x hybrid*, AAR08677), NtEIL1 (*Nicotiana tabacum*, AAP03997), AcEIL1 (*Actinidia chinensis*, AID55343), DcEIL1 (*Dianthus caryophyllus*, AAF69017), PsEIL1 (*Paeonia suffruticosa*, AFI61907), CsEIL1 (*Citrus sinensis*, NP_001275851), HvEIL1 (*Hordeum vulgare*, ADO21118), VrEIL1 (*Vigna radiata*, AAL76272), and MtEIL1 (*Medicago truncatula*, ACX54782). The completely identical amino acids were shown with capital letters against black background. Less conserved amino acids were shown with capital letters against dark-gray or relatively light-gray background. Non-conserved amino acids were shown with capital letters against white background. The darker background there is, the higher sequence homology there is. **(B)** Phylogenetic analysis of EIN3/EIL1s from different plant species. AaEIN3 was marked with●.

RESULTS AND DISCUSSION

Ethylene Negatively Regulates the Expression of Genes Involved in Artemisinin Biosynthesis

An earlier report showed that applying 15 mg/L ethephon (Et) in the growing medium of *Artemisia Annua* seedlings would lead to a decrease of artemisinin content in the roots (Weathers et al., 2005). To detect whether ethylene has an impact on the expression of artemisinin biosynthesis-related genes, we sprayed 500 μM Et solution and 200 μM AOA (an inhibitor of endogenous ethylene biosynthesis) respectively, to 14-day old wild type seedlings of *Artemisia annua*. The plants of mock group were treated with sterile water. qPCR was done to detect the expression mode of *ADS*, *DBR2*, *CYP71AV1* (*CYP*), and *AaORA*, four important artemisinin biosynthesis-associated genes at different time points after the treatment. The result showed that Et treatment significantly downregulated the expression level of *ADS*, *DBR2*, *CYP71AV1,* and *AaORA* in leaves, compared to the mock group (**Figures 1A,C**). The expression level of the four genes dropped to the lowest level after 6 h of Et treatment, and gradually rose back to the normal level afterward (**Figure 1A**). Meanwhile, treatment with AOA significantly upregulated the expression level of *ADS*, *DBR2*, *CYP71AV1*, and *AaORA* in leaves, compared to the mock group (**Figures 1B,C**). The expression level of the four genes rose to the peak after 3 h of AOA treatment, and gradually dropped back afterward (**Figure 1B**). This indicated that suppressing endogenous ethylene biosynthesis could enhance the expression of *ADS*, *DBR2*, *CYP71AV1*, and *AaORA*. The above result demonstrated that ethylene negatively regulates the expression of three key enzyme genes *ADS*, *DBR2*, *CYP71AV1*, and a positive regulator gene *AaORA* that are involved in artemisinin biosynthesis.

Isolation and Characterization of EIN3 Sequence in *Artemisia Annua*

ETHYLENE-INSENSITIVE3 (EIN3) is a key transcription factor in ethylene signaling pathway. Ethylene regulates the expression of ethylene-responsive genes downstream via EIN3/EIL1's functioning, thus further affecting diverse physiological

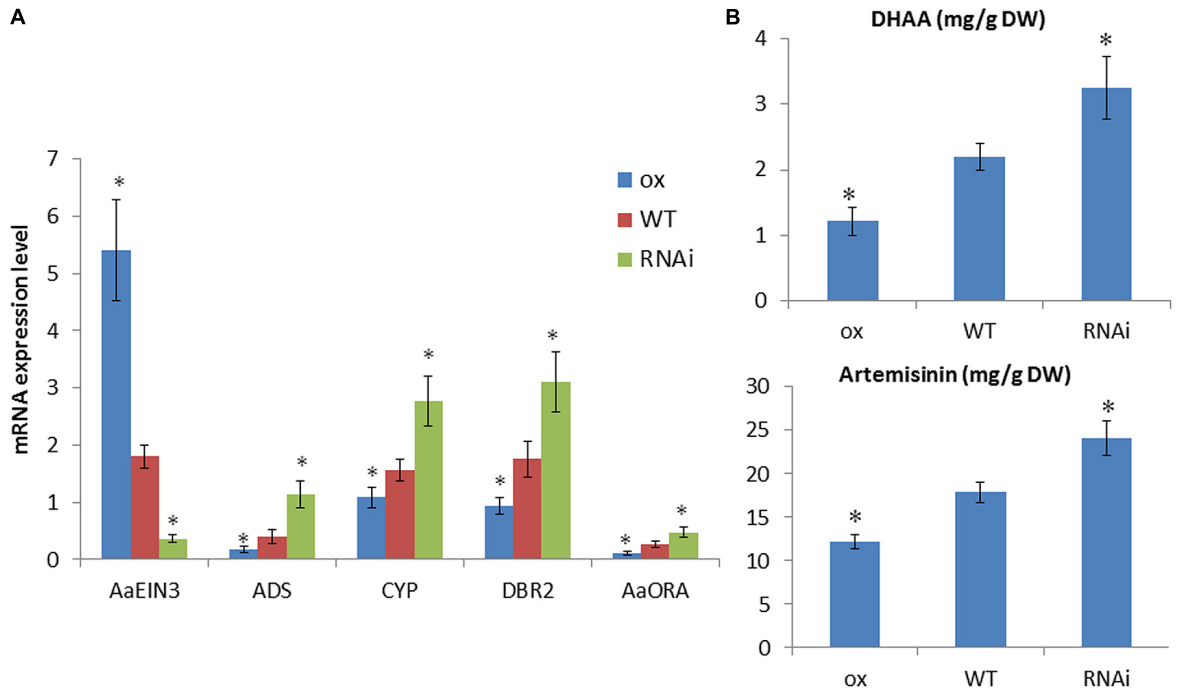

FIGURE 3 | Analyses of **(A)** expression levels of *AaEIN3*, *ADS*, *DBR2*, *CYP71AV1* (*CYP*), and *AaORA* and **(B)** DHAA and artemisinin contents in *AaEIN3*-ox, WT, and RNAi plant lines. Data is the mean value ± SD of biological replicates ($n \geq 5$) from different independent plant lines. Asterisk indicated a significant difference compared to the value of WT (Student's *t*-test, $P < 0.05$).

courses of plants as germination and development, secondary metabolism and stress response. We speculated, the repression of the expression of these artemisinin biosynthesis-associated genes by ethylene may involve the mediation of EIN3/EIL1 protein. Therefore, dissecting the role of EIN3 in ethylene's regulating artemisinin biosynthesis became our major goal in the research.

Through homologous alignments among the sequences from transcriptome database of *Artemisia Annua* and EIN3/EIL1 gene sequences reported in other species, we isolated the gene sequence of *EIN3* from *Artemisia Annua* transcriptome database, which is highly homologous to *EIN3*/*EIL1* sequences from other species, named *AaEIN3*. *AaEIN3* encodes 604 amino acids, with a coding region of 1815 bp. Multiple alignment showed an identity of 56–67% in protein sequence between AaEIN3 and EIN3/EIL1s from other plant species (**Figure 2A**). Phylogenetic analysis showed AaEIN3 is closest in evolutionary relationship to EIL1 from *Citrus sinensis* (CsEIL1) (**Figure 2B**).

AaEIN3 Negatively Regulates Artemisinin Biosynthesis

To detect whether AaEIN3 affects artemisinin biosynthesis, we constructed *AaEIN3*-overexpressing (ox) vector and RNAi vector, respectively, and transformed them into *Artemisia Annua* plants. PCR was done to select out *AaEIN3*-overexpressing (ox) and RNAi transgenic plant lines. These transgenic plants were kept for further analysis. qPCR result showed that the expression level of *AaEIN3* in *AaEIN3*-ox plants was significantly elevated, compared to wild type plants (WT), while the expression level of *ADS*, *DBR2*, and *CYP71AV1*, three key enzyme genes in artemisinin biosynthesis, was significantly lower than that of WT (**Figure 3A**). Meanwhile, the expression level of *AaORA*, a transcription factor positively regulating these key enzyme genes expression, also significantly declined relative to that in WT (**Figure 3A**). This indicated that AaEIN3 overexpression reduced the expression of *ADS*, *DBR2*, *CYP71AV1*, and *AaORA*, which are involved in artemisinin biosynthesis. On the other hand, in RNAi plants, the expression of *AaEIN3* got significantly repressed, compared to that in WT, while the expression level of *ADS*, *DBR2*, *CYP71AV1*, and *AaORA* was significantly higher than that in WT (**Figure 3A**). This indicated that repression of *AaEIN3* expression led to an increase of *ADS*, *DBR2*, *CYP71AV1*, and *AaORA* expression. These results demonstrated AaEIN3 negatively regulates the expression of *ADS*, *DBR2*, *CYP71AV1*, and *AaORA* that are involved in artemisinin biosynthesis.

Then we detected the contents of DHAA and artemisinin in *AaEIN3*-ox, RNAi and WT plants by HPLC. The result showed that in *AaEIN3*-ox plants, both of DHAA and artemisinin contents were significantly lower than that in WT plants; while in RNAi plants, both of DHAA and artemisinin contents were significantly higher than that in WT plants (**Figure 3B**). These above results demonstrated AaEIN3 is a negative regulator in artemisinin biosynthesis.

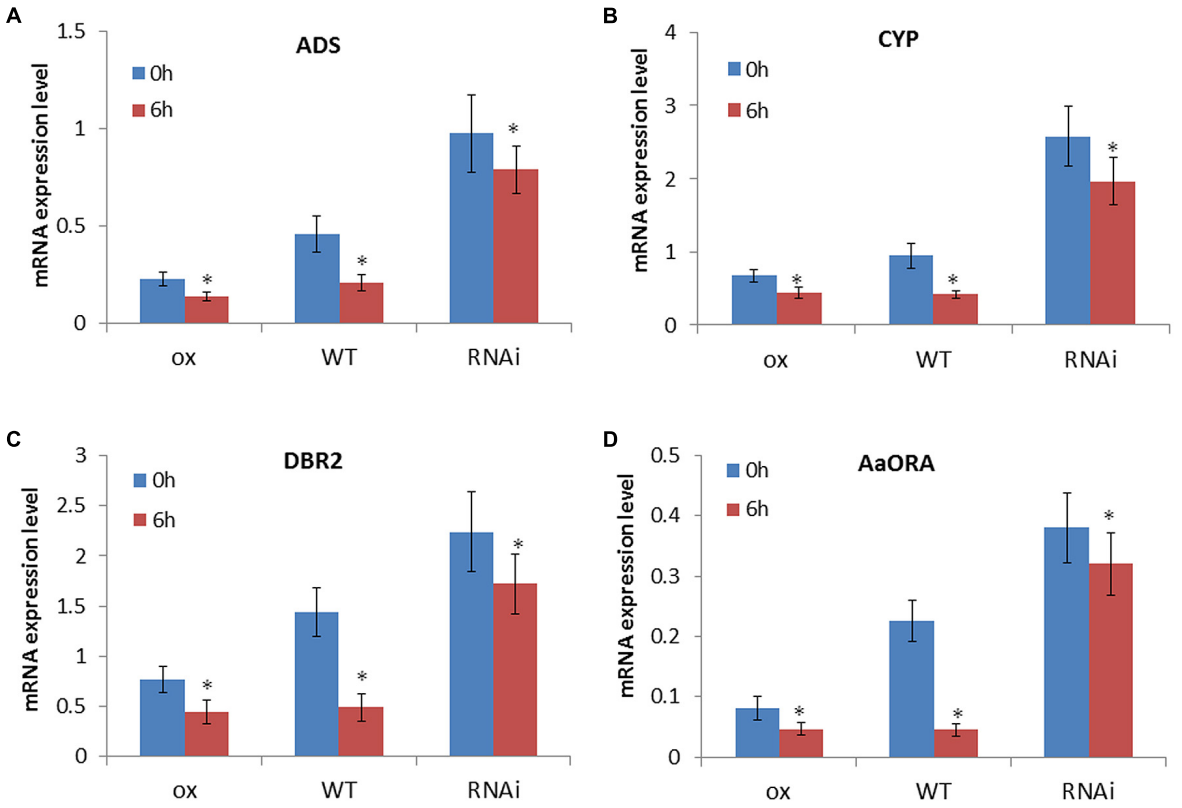

FIGURE 4 | Expression levels of **(A)** *ADS*, **(B)** *CYP71AV1* (*CYP*), **(C)** *DBR2*, and **(D)** *AaORA* in *AaEIN3*-ox, WT, and RNAi plants after 0 and 6 h of 500 μM ethephon (Et) treatment. Data is the mean value ± SD of biological replicates ($n = 5$) from different independent plant lines. Asterisk indicated a significant difference compared to the value at 0 h under Et treatment (Student's *t*-test, $P < 0.05$).

The Downregulation of Artemisinin Biosynthesis by Ethylene Requires the Mediation of AaEIN3

To detect whether the downregulation of artemisinin biosynthesis by ethylene involves the function of AaEIN3, we evenly sprayed *AaEIN3*-ox, WT, and RNAi plants with 500 μM Et solution, and detected the expression mode of *ADS*, *DBR2*, *CYP71AV1*, and *AaORA* in leaves of these plant lines at 0 and 6 h after the treatment. The result is shown in **Figure 4**. Et treatment led to a decline of expression of *ADS*, *DBR2*, *CYP71AV1*, and *AaORA* in all of *AaEIN3*-ox, WT, and RNAi plant lines. But in WT, the downregulation effect of Et on the four genes' expression was the most significant of all. When *AaEIN3* expression got repressed by RNAi, the downregulation effect of Et on the expression of *ADS*, *DBR2*, *CYP71AV1*, and *AaORA* got significantly attenuated relative to that in WT, or rather the responsiveness of the four genes to ethylene signals got attenuated when *AaEIN3* expression was repressed by RNAi. These results indicated that ethylene signals downregulate artemisinin biosynthesis via the mediation of AaEIN3.

What is more, overexpression of *AaEIN3* significantly reduced the expression level of *ADS*, *DBR2*, *CYP71AV1*, and *AaORA*, and Et treatment further attenuated the four genes' expression in *AaEIN3*-ox plants. But in *AaEIN3*-ox plants, the extent of the reduction in the four genes' expression level was not so significant as that in WT after Et treatment (**Figure 4**). We speculate the expression amount of AaEIN3 in *AaEIN3*-ox plants has surpassed the normal need for regulating the genes downstream, and is sufficient to downregulate the expression level of those genes to the full extent. Ethylene could repress the degradation of EIN3 protein to make it accumulate gradually. Under the context of *AaEIN3* overexpression driven by 35S promoter, the further accumulation of EIN3 impelled by exogenous Et strengthened the negative regulation effect of EIN3 on genes expression not so significantly as that in WT. This may explain why the decline in the four genes' expression level in *AaEIN3*-ox plants after Et treatment is much lesser than that in WT plants. This result also suggested a crucial role of AaEIN3 in the regulation of artemisinin biosynthesis by ethylene signaling pathway from the other side.

The Downregulation of Artemisinin Biosynthesis by Ethylene Is Associated With AaEIN3-Induced Leaf Senescence

Previous study of our lab found that the expression level of *ADS*, *DBR2*, *CYP71AV1*, and *AaORA*, and the content of

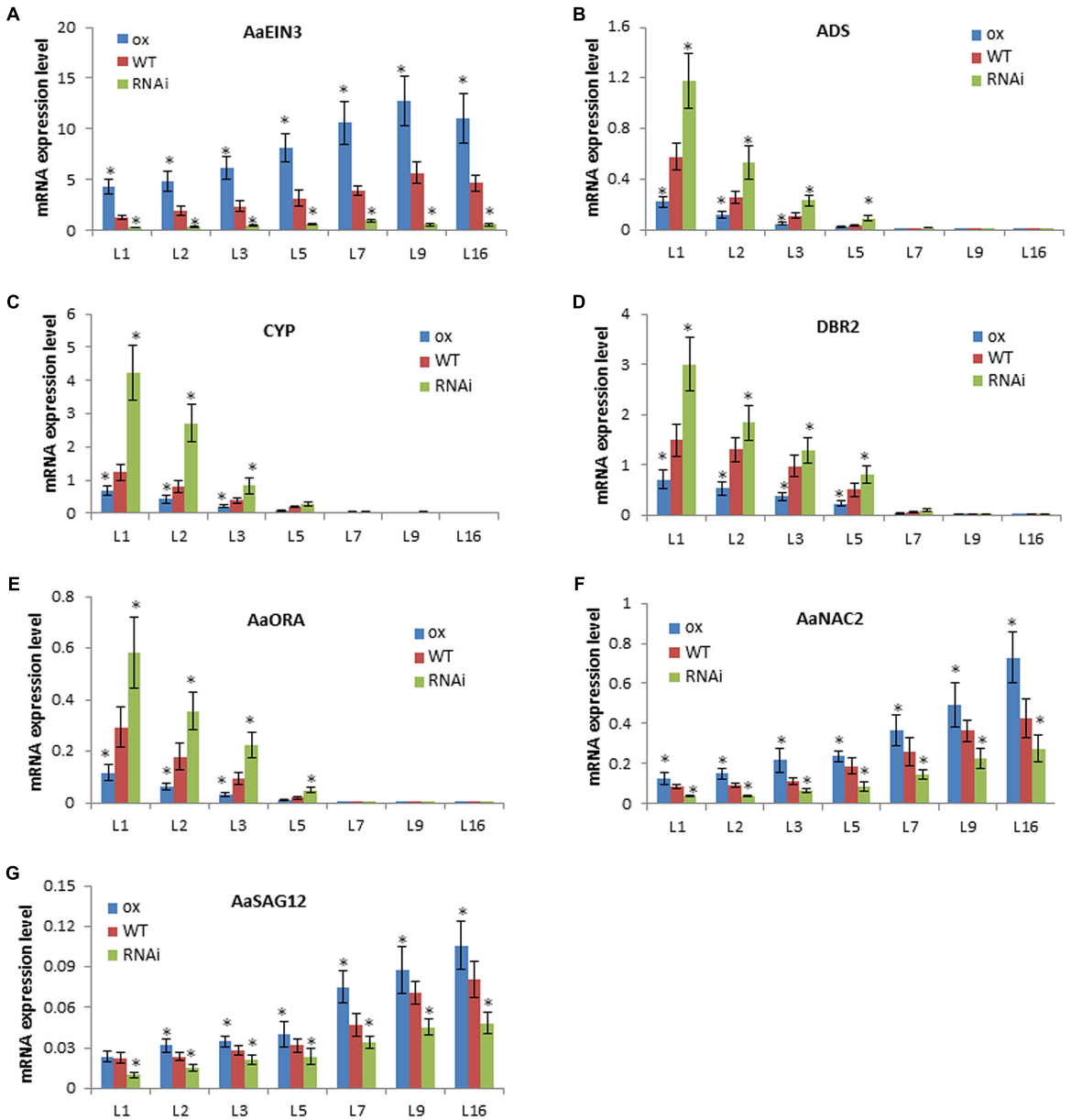

FIGURE 5 | Gene expression levels in leaves at different developmental stages in *AaEIN3*-ox, WT, and RNAi plant lines. **(A–G)** show the expression level of *AaEIN3*, *ADS*, *CYP71AV1* (*CYP*), *DBR2*, *AaORA*, *AaNAC2*, and *AaSAG12*, respectively, in the 1st, 2nd, 3rd, 5th, 7th, 9th, 16th leaf (L1, L2, L3, L5, L7, L9, L16) counted downward from the top meristem in *AaEIN3*-ox, WT, and RNAi plants. The lower located, the more aged and senescent the leaf is. Data is the mean value ± SD of biological replicates ($n = 5$) from different independent plant lines. Asterisk indicated a significant difference compared to the value of WT (Student's *t*-test, $P < 0.05$).

DHAA, the end-product of enzymatic reactions in artemisinin biosynthesis, are relatively higher in younger leaves. As leaves get matured and senescent, the four genes expression level and DHAA content get lower rapidly, that demonstrated that the process of leaf maturation and senescence repressed the expression of these genes participating in artemisinin biosynthesis (Zhang et al., 2012; Lu et al., 2013). Besides, an earlier study reported that EIN3 transcription in leaves of *Arabidopsis* would increase with leaves aging, and that EIN3 protein could directly repress miR164 transcription to increase the expression of senescence-associated genes as *NAC2* (also named *ORE1*) and *SAG12*, thus accelerating leaf senescence (Li et al., 2013). Therefore, *EIN3* is a senescence-associated gene, which can promote the process of ethylene- or age-dependent leaf senescence. Based on the previous findings, we infer that ethylene's negative regulation of artemisinin biosynthesis may correlate with EIN3-induced leaf senescence.

To confirm such inference, qPCR analysis was done to detect the expression mode of genes in leaves at different ages or developmental stages in the same phyllotaxy. On a stem

FIGURE 6 | The phenotype difference of leaves at different developmental stages on the phyllotaxy among *AaEIN3*-ox, WT, and RNAi plants. L1, L2, L3, L5, L7, L9, L16 is the 1st, 2nd, 3rd, 5th, 7th, 9th, 16th leaf counted downward from the top meristem, respectively. The lower the leaf is located, the more aged and senescent it is.

of the plant, the closer to top meristems, the younger the leaf is; the lower located, the more aged and senescent the leaf is. qPCR result showed that *AaEIN3* expression level is lowest in the youngest leaf closest to top meristems (marked as L1 in **Figure 5**), and gets higher as leaf becomes aged and senescent in all of *AaEIN3*-ox, WT, and RNAi plant lines (**Figure 5A**). But the expression mode of *ADS*, *CYP71AV1*, *DBR2*, and *AaORA*, is on the contrary to that of *AaEIN3*: the more aged and senescent the leaf is, the lower their expression level gets (**Figures 5B–E**). This result is consistent with the previous report, indicating the aging and senescence of leaves attenuated the expression of the four genes involved in artemisinin biosynthesis.

Then, to detect whether AaEIN3 expression could accelerate leaves' senescence process, we screened *Artemisia Annua* transcriptome database and its full genome database (the sequence information of both databases has not been published yet), and selected out the cDNA sequences of a senescence-associated gene *NAC2* and a senescence marker gene *SAG12* in *Artemisia Annua*, named *AaNAC2* and *AaSAG12*, respectively. qPCR result showed that the expression level of *AaNAC2* and *AaSAG12* increased with the increase of leaves age (**Figures 5F,G**), as does the expression level of *NAC2* (*ORE1*) and *SAG12* in *Arabidopsis thaliana* reported previously (Li et al., 2013). Through comparing the expression level of *AaNAC2* and *AaSAG12* in the leaves at the same developmental stage (ranking at the same position in the phyllotaxy) among *AaEIN3*-ox, WT, and RNAi plants, we found *AaEIN3* overexpression increased *AaNAC2* and *AaSAG12* expression, while repressing *AaEIN3* expression by RNAi reduced *AaNAC2* and *AaSAG12* expression (**Figures 5F,G**). This indicated *AaEIN3* could promote the expression of leaf senescence-associated genes.

Moreover, we observed the phenotype of leaves in the same phyllotaxy in *AaEIN3*-ox, WT, and RNAi plants. In *AaEIN3*-ox plants, the point at the edge of the 5th leaf counted downward from the top meristems (L5) began to show slight etiolation, and the etiolation phenomenon became more and more visible in the 7th, 9th, and 16th leaves counted downward from the top meristems (L7, L9, L16). Compared to *AaEIN3*-ox plants, L5 in WT plants has not shown etiolation, and the point at the edge of L7 and L9 in WT only exhibited slight trace of etiolation. The etiolation signs got more visible in L16 of WT plants, but the etiolation extent of L16 in WT plants was still lesser than that in *AaEIN3*-ox plants. On the other hand, none of the leaves L1–L16 in RNAi plants exhibited etiolation signs (**Figure 6**). These phenomena indicated *AaEIN3* overexpression accelerated leaf senescence, and repression of *AaEIN3* expression by RNAi delayed leaf senescence, which further demonstrated *AaEIN3* is a senescence-associated gene that can induce leaf senescence in *Artemisia annua*.

Taken together, our study proposed a mechanism by which ethylene negatively regulates artemisinin biosynthesis, shown in **Figure 7**. Ethylene signal promotes the senescence process of leaves in *Artemisia annua* via the mediation of AaEIN3, a key component in ethylene signaling pathway. And leaf senescence attenuates the expression of *ADS*, *DBR2*, *CYP71AV1*, and *AaORA*, thus reducing DHAA biosynthesis and finally leading to the decrease of artemisinin accumulation in *Artemisia annua*.

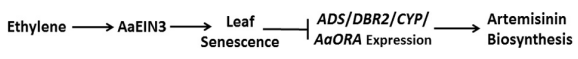

FIGURE 7 | Illustration of the mechanism by which ethylene signaling negatively regulates artemisinin biosynthesis.

Our work discovered the first negative regulator (AaEIN3) for artemisinin biosynthesis and provided more novel knowledge and clues on how plant hormone signals regulate artemisinin metabolic pathway. However, it's still to be explored and studied as for the issues how the process of maturation and senescence of leaves modulates the expression of key genes involved in artemisinin biosynthesis, and what transcription factors or other signaling pathways get involved in this modulation. All of these issues need further research.

AUTHOR CONTRIBUTIONS

YT, LL, and KT conceived and designed the experiments. YT, TY, and PS performed the experiments. YT, XF, and QS analyzed the data. YT, XS, and KT contributed reagents, materials, and analysis tools. YT and KT wrote the manuscript.

FUNDING

This work was funded by the China Postdoctoral Science Foundation (Grant No. 2016M591664).

ACKNOWLEDGMENTS

We are grateful to Pin Liu for her technical help during HPLC analysis.

SUPPLEMENTARY MATERIAL

The Supplementary Material for this article can be found online at: https://www.frontiersin.org/articles/10.3389/fpls.2018.00413/full#supplementary-material

REFERENCES

Abeles, F. B., Dunn, L. J., Morgens, P., Callahan, A., Dinterman, R. E., and Schmidt, J. (1988). Induction of 33-kD and 60-kD peroxidases during ethylene-induced senescence of cucumber cotyledons. *Plant Physiol.* 87, 609–615. doi: 10.1104/pp.87.3.609

Aftab, T., Khan, M. A., Silva, J. T., Idrees, M., Naeem, M., and Moinuddin (2011). Role of salicylic acid in promoting salt stress tolerance and enhanced artemisinin production in *Artemisia annua* L. *J. Plant Growth Regul.* 30, 425–435. doi: 10.1007/s00344-011-9205-0

Alonso, J. M., Hirayama, T., Roman, G., Nourizadeh, S., and Ecker, J. R. (1999). EIN2, a bifunctional transducer of ethylene and stress responses in *Arabidopsis*. *Science* 284, 2148–2152. doi: 10.1126/science.284.5423.2148

An, F., Zhao, Q., Ji, Y., Li, W., Jiang, Z., Yu, X., et al. (2010). Ethylene-induced stabilization of ETHYLENE INSENSITIVE3 and EIN3-LIKE1 is mediated by proteasomal degradation of EIN3 binding F-box 1 and 2 that requires EIN2 in *Arabidopsis*. *Plant Cell* 22, 2384–2401. doi: 10.1105/tpc.110.076588

Bhattarai, A., Ali, A. S., Kachur, S. P., Mårtensson, A., Abbas, A. K., Khatib, R., et al. (2007). Impact of artemisinin-based combination therapy and insecticide-treated nets on malaria burden in Zanzibar. *PLoS Med.* 4:e309. doi: 10.1371/journal.pmed.0040309

Bleecker, A. B., Estelle, M. A., Somerville, C., and Kende, H. (1988). Insensitivity to ethylene conferred by a dominant mutation in *Arabidopsis thaliana*. *Science* 241, 1086–1089. doi: 10.1126/science.241.4869.1086

Brown, G. D., and Sy, L. K. (2004). In vivo transformations of dihydroartemisinic acid in *Artemisia annua* plants. *Tetrahedron* 60, 1139–1159. doi: 10.1016/j.tet.2003.11.070

Caretto, S., Quarta, A., Durante, M., Nisi, R., De Paolis, A., Blando, F., et al. (2011). Methyl jasmonate and miconazole differently affect artemisinin production and gene expression in *Artemisia annua* suspension cultures. *Plant Biol.* 13, 51–58. doi: 10.1111/j.1438-8677.2009.00306.x

Duke, M. V., Paul, R. N., Elsohly, H. N., Sturtz, G., and Duke, S. O. (1994). Localization of artemisinin and artemisitene in foliar tissues of glanded and glandless biotypes of *Artemisia annua* L. *Int. J. Plant Sci.* 155, 365–372. doi: 10.1086/297173

Ecker, J. R. (1995). The ethylene signal transduction pathway in plants. *Science* 268, 667–675. doi: 10.1126/science.7732375

Efferth, T. (2007). Antiplasmodial and antitumor activity of artemisinin from bench to bedside. *Planta Med.* 73, 299–309. doi: 10.1055/s-2007-967138

Efferth, T., Romero, M. R., Wolf, D. G., Stamminger, T., Marin, J. J., and Marschall, M. (2008). The antiviral activities of artemisinin and artesunate. *Clin. Infect. Dis.* 47, 804–811. doi: 10.1086/591195

Graham, I. A., Besser, K., Blumer, S., Branigan, C. A., Czechowski, T., Elias, L., et al. (2010). The genetic map of *Artemisia annua* L. identifies loci affecting yield of the antimalarial drug artemisinin. *Science* 327, 328–331. doi: 10.1126/science.1182612

Guo, H. (2011). Understanding the mode of phytohormones' action in plants. *Sci. China Life Sci.* 54, 1062–1063. doi: 10.1139/G10-059

Guo, H., and Ecker, J. R. (2003). Plant responses to ethylene gas are mediated by SCFEBF1/EBF2-dependent proteolysis of EIN3 transcription factor. *Cell* 115, 667–677. doi: 10.1016/S0092-8674(03)00969-3

Hua, J., and Meyerowitz, E. M. (1998). Ethylene responses are negatively regulated by a receptor gene family in *Arabidopsis thaliana*. *Cell* 94, 261–271. doi: 10.1016/S0092-8674(00)81425-7

Jing, F., Zhang, L., Li, M., Tang, Y., Wang, Y., Wang, Y., et al. (2009). Abscisic acid (ABA) treatment increases artemisinin content in *Artemisia annua* by enhancing the expression of genes in artemisinin biosynthetic pathway. *Biologia* 64, 319–323. doi: 10.2478/s11756-009-0040-8

Kieber, J. J., Rothenberg, M., Roman, G., Feldmann, K. A., and Ecker, J. R. (1993). *CTR1*, a negative regulator of the ethylene response pathway in *Arabidopsis*, encodes a member of the raf family of protein kinases. *Cell* 72, 427–441. doi: 10.1016/0092-8674(93)90119-B

Kumar, S., Gupta, S. K., Singh, P., Bajpai, P., Gupta, M. M., Singh, D., et al. (2004). High yields of artemisinin by multi-harvest of *Artemisia annua* crops. *Ind. Crop Prod.* 19, 77–90. doi: 10.1016/j.indcrop.2003.07.003

Li, Z., Peng, J., Wen, X., and Guo, H. (2013). *ETHYLENE-INSENSITIVE3* is a senescence-associated gene that accelerates age-dependent leaf senescence by directly repressing *miR164* transcription in *Arabidopsis*. *Plant Cell* 25, 3311–3328. doi: 10.1105/tpc.113.113340

Lu, X., Zhang, L., Zhang, F., Jiang, W., Shen, Q., Zhang, L., et al. (2013). AaORA, a trichome-specific AP2/ERF transcription factor of *Artemisia annua*, is a positive regulator in the artemisinin biosynthetic pathway and in disease resistance to *Botrytis cinerea*. *New Phytol.* 198, 1191–1202. doi: 10.1111/nph.12207

Lv, Z., Wang, S., Zhang, F., Chen, L., Hao, X., Pan, Q., et al. (2016). Overexpression of a novel NAC domain-containing transcription factor (AaNAC1) enhances the content of artemisinin and increases tolerance to drought and *Botrytis cinerea* in *Artemisia annua*. *Plant Cell Physiol.* 57, 1961–1971. doi: 10.1093/pcp/pcw118

Ma, D., Pu, G., Lei, C., Ma, L., Wang, H., Guo, Y., et al. (2009). Isolation and characterization of AaWRKY1, an *Artemisia annua* transcription factor that regulates the amorpha-4,11-diene synthase gene, a key gene of artemisinin biosynthesis. *Plant Cell Physiol.* 50, 2146–2161. doi: 10.1093/pcp/pcp149

Mutabingwa, T. K. (2005). Artemisinin-based combination therapies (ACTS): best hope for malaria treatment but inaccessible to the needy! *Acta Trop.* 95, 305–315. doi: 10.1016/j.actatropica.2005.06.009

Pu, G. B., Ma, D. M., Chen, J. L., Ma, L. Q., Wang, H., Li, G. F., et al. (2009). Salicylic acid activates artemisinin biosynthesis in *Artemisia annua* L. *Plant Cell Rep.* 28, 1127–1135. doi: 10.1007/s00299-009-0713-3

Qiao, H., Shen, Z., Huang, S. S., Schmitz, R. J., Urich, M. A., Briggs, S. P., et al. (2012). Processing and subcellular trafficking of ER-tethered EIN2 control response to ethylene gas. *Science* 338, 390–393. doi: 10.1126/science.1225974

Shen, Q., Chen, Y., Wang, T., Wu, S., Lu, X., Zhang, L., et al. (2012). Overexpression of the cytochrome P450 monooxygenase (*cyp71av1*) and cytochrome P450 reductase (*cpr*) genes increased artemisinin content in *Artemisia annua* (Asteraceae). *Genet. Mol. Res.* 11, 3298–3309. doi: 10.4238/2012.September.12.13

Shen, Q., Lu, X., Yan, T., Fu, X., Lv, Z., Zhang, F., et al. (2016). The jasmonate-responsive AaMYC2 transcription factor positively regulates artemisinin biosynthesis in *Artemisia annua*. *New Phytol.* 210, 1269–1281. doi: 10.1111/nph.13874

Sy, L. K., and Brown, G. D. (2002). The mechanism of the spontaneous autoxidation of dihydroartemisinic acid. *Tetrahedron* 58, 897–908. doi: 10.1016/S0040-4020(01)01193-0

Tang, K., Shen, Q., Yan, T., and Fu, X. (2014). Transgenic approach to increase artemisinin content in *Artemisia annua* L. *Plant Cell Rep.* 33, 605–615. doi: 10.1007/s00299-014-1566-y

Wang, H., Ma, C., Li, Z., Ma, L., Wang, H., Ye, H., et al. (2010). Effects of exogenous methyl jasmonate on artemisinin biosynthesis and secondary metabolites in *Artemisia annua* L. *Ind. Crop Prod.* 31, 214–218. doi: 10.1016/j.indcrop.2009.10.008

Weathers, P. J., Arsenault, P. R., Covello, P. S., McMickle, A., Teoh, K. H., and Reed, D. W. (2011). Artemisinin production in *Artemisia annua*: studies in planta and results of a novel delivery method for treating malaria and other neglected diseases. *Phytochem. Rev.* 10, 173–183. doi: 10.1007/s11101-010-9166-0

Weathers, P. J., Bunk, G., and McCoy, M. C. (2005). The effect of phytohormones on growth and artemisinin production in *Artemisia annua* hairy roots. *In Vitro Cell. Dev. Biol.* 41, 47–53. doi: 10.1079/IVP2004604

Yu, Z., Li, J., Yang, C., Hu, W., Wang, L., and Chen, X. (2012). The jasmonate-responsive AP2/ERF transcription factors AaERF1 and AaERF2 positively regulate artemisinin biosynthesis in *Artemisia annua* L. *Mol. Plant* 5, 353–365. doi: 10.1093/mp/ssr087

Zhang, F., Fu, X., Lv, Z., Lu, X., Shen, Q., Zhang, L., et al. (2015). A basic leucine zipper transcription factor, AabZIP1, connects abscisic acid signaling with artemisinin biosynthesis in *Artemisia annua*. *Mol. Plant* 8, 163–175. doi: 10.1016/j.molp.2014.12.004

Zhang, L., Lu, X., Shen, Q., Chen, Y., Wang, T., Zhang, F., et al. (2012). Identification of putative *Artemisia annua* ABCG transporter unigenes related to artemisinin yield following expression analysis in different plant tissues and in response to methyl jasmonate and abscisic acid treatments. *Plant Mol. Biol. Rep.* 4, 838–847. doi: 10.1007/s11105-011-0400-8

Conflict of Interest Statement: The authors declare that the research was conducted in the absence of any commercial or financial relationships that could be construed as a potential conflict of interest.

frontiers in Plant Science

ORIGINAL RESEARCH
published: 18 May 2018
doi: 10.3389/fpls.2018.00641

Detailed Phytochemical Analysis of High- and Low Artemisinin-Producing Chemotypes of *Artemisia annua*

Tomasz Czechowski[1], *Tony R. Larson*[1], *Theresa M. Catania*[1], *David Harvey*[1], *Cenxi Wei*[2], *Michel Essome*[2], *Geoffrey D. Brown*[2]* *and Ian A. Graham*[1]*

[1] Department of Biology, Centre for Novel Agricultural Products, University of York, York, United Kingdom, [2] Department of Chemistry, University of Reading, Reading, United Kingdom

Chemical derivatives of artemisinin, a sesquiterpene lactone produced by *Artemisia annua,* are the active ingredient in the most effective treatment for malaria. Comprehensive phytochemical analysis of two contrasting chemotypes of *A. annua* resulted in the characterization of over 80 natural products by NMR, more than 20 of which are novel and described here for the first time. Analysis of high- and low-artemisinin producing (HAP and LAP) chemotypes of *A. annua* confirmed the latter to have a low level of *DBR2* (artemisinic aldehyde $\Delta^{11(13)}$ reductase) gene expression. Here we show that the LAP chemotype accumulates high levels of artemisinic acid, arteannuin B, *epi*-deoxyarteannuin B and other amorpha-4,11-diene derived sesquiterpenes which are unsaturated at the 11,13-position. By contrast, the HAP chemotype is rich in sesquiterpenes saturated at the 11,13-position (dihydroartemisinic acid, artemisinin and dihydro-*epi*-deoxyarteannunin B), which is consistent with higher expression levels of *DBR2*, and also with the presence of a HAP-chemotype version of CYP71AV1 (amorpha-4,11-diene C-12 oxidase). Our results indicate that the conversion steps from artemisinic acid to arteannuin B, *epi*-deoxyarteannuin B and artemisitene in the LAP chemotype are non-enzymatic and parallel the non-enzymatic conversion of DHAA to artemisinin and dihyro-*epi*-deoxyarteannuin B in the HAP chemotype. Interestingly, artemisinic acid in the LAP chemotype preferentially converts to arteannuin B rather than the endoperoxide bridge containing artemisitene. In contrast, in the HAP chemotype, DHAA preferentially converts to artemisinin. Broader metabolomic and transcriptomic profiling revealed significantly different terpenoid profiles and related terpenoid gene expression in these two morphologically distinct chemotypes.

Keywords: ***Artemisia annua*, chemotype, artemisinin, NMR, sesquiterpenes, glandular trichomes**

OPEN ACCESS

Edited by:
James Lloyd,
Stellenbosch University, South Africa

Reviewed by:
Xiaoya Chen,
Institute of Plant Physiology and Ecology, Shanghai Institutes for Biological Sciences (CAS), China
Patrick Smithers Covello,
Biotechnology Research Institute (NRC-CNRC), Canada

***Correspondence:**
Geoffrey D. Brown
g.d.brown@reading.ac.uk
Ian A. Graham
ian.graham@york.ac.uk

Specialty section:
This article was submitted to Plant Biotechnology, a section of the journal Frontiers in Plant Science

Received: *02 February 2018*
Accepted: *26 April 2018*
Published: *18 May 2018*

Citation:
Czechowski T, Larson TR, Catania TM, Harvey D, Wei C, Essome M, Brown GD and Graham IA (2018) Detailed Phytochemical Analysis of High- and Low Artemisinin-Producing Chemotypes of Artemisia annua. Front. Plant Sci. 9:641. doi: 10.3389/fpls.2018.00641

INTRODUCTION

Chemical derivatives of the sesquiterpene lactone, artemisinin, such as: artesunate, artemether or dihydroartemisinin are one of several active ingredients in artemisinin-combination therapies (ACTs)—the most effective treatment for malaria currently available. Biosynthesis of artemisinin occurs in specialized 10-celled biseriate glandular trichomes present on the leaves, stems

and inflorescences of *Artemisia annua* (Duke and Paul, 1993; Duke et al., 1994; Ferreira and Janick, 1995). Concentrations of artemisinin can range from 0.01 to 1.4% of leaf dry weight (Larson et al., 2013). The biosynthetic pathway from artemisinin precursors has been fully elucidated over the past decade (**Figure 3C**). It starts from the cyclization of farnesyl pyrophosphate (FPP) to amorpha-4,11-diene (A-4,11-D) by amorph-4,11-diene synthase (AMS) (Bouwmeester et al., 1999; Mercke et al., 2000) followed by the three-step oxidation of A-4,11-D by amorpha-4,11-diene C-12 oxidase (CYP71AV1), to artemisinic alcohol (AAOH), artemisinic aldehyde (AAA), and artemisinic acid (AA) (Ro et al., 2006; Teoh et al., 2006). ADH1—NAD-dependent alcohol dehydrogenase with specificity toward artemisinic alcohol plays a role in the formation of artemisinic aldehyde in the artemisinin pathway of *A. annua* (Paddon et al., 2013). The *ADH1* gene has been used to improve yields of artemisinic acid production in yeast (Paddon et al., 2013). Artemisinic aldehyde Δ11(13) reductase (DBR2) catalyzes the formation of dihydroartemisinic aldehyde (DHAAA) from AAA (Zhang et al., 2008). DHAAA is subsequently oxidized in the final enzymatic reaction to dihydroartemisinic acid (DHAA) by aldehyde dehydrogenase ALDH1 (Teoh et al., 2009). Genes encoding all of these biosynthetic enzymes have been shown to be highly expressed in apical and sub-apical cells of *A. annua* glandular trichomes (Olsson et al., 2009; Soetaert et al., 2013). Recent studies have revealed that the conversion of DHAA to artemisinin and dihydro-*epi*-deoxyarteannuin B (DHEDB) proceeds *via* a series of non-enzymatic and spontaneous photochemical reactions, involving the highly reactive tertiary allylic hydroperoxide of dihydroartemisinic acid, DHAAOOH (Wallaart et al., 1999; Sy and Brown, 2002; Brown and Sy, 2004). Similarly, it has previously been proposed that AA is photochemically converted to arteannuin B (ArtB) *via* the tertiary allylic hydroperoxide of artemisinic acid (Brown and Sy, 2007).

Based on the content of artemisinin and its precursors, two contrasting chemotypes of *A. annua* have been described: a low-artemisinin production (LAP) chemotype and a high-artemisinin production (HAP) chemotype (Wallaart et al., 2000). Both chemotypes contain artemisinin, but the HAP chemotype has a relatively high content of DHAA and artemisinin, whereas the LAP chemotype has a high content of AA and ArtB (Lommen et al., 2006; Arsenault et al., 2010; Larson et al., 2013). Recent studies have concluded that a major factor in determining the biochemical phenotype of HAPs and LAPs is the differential expression of *DBR2*—with low expression in LAP chemotypes correlating with a number of insertions/deletions in the *DBR2* promoter sequence (Yang et al., 2015). We have recently shown that the overall pathway to artemisinin biosynthesis is under strict developmental control with early steps in the pathway occurring in young leaves and later steps in mature leaves (Czechowski et al., 2016). In the present study, we have used both metabolomics and transcriptomics to investigate the developmental regulation of sesquiterpene biosynthesis in HAP and LAP chemotypes. Using a combination of NMR and UPLC-/GC-MS techniques we have characterized a number of amorphane and cadinane sesquiterpenes in addition to other terpenes isolated from leaf glandular trichomes. We have also extended the transcript analysis in HAPs and LAPs beyond the genes encoding artemisinin-pathway enzymes. Our findings suggest profound differences in general terpenoid metabolism between HAP and LAP chemotypes that extend well beyond altered *DBR2* expression and artemisinin content.

MATERIALS AND METHODS

Plant Material

Artemis is an F1 hybrid variety of *A. annua* developed by Mediplant (Conthey, Switzerland), produced by crossing C4 and C1 parental material of East Asian origin (Delabays et al., 2001). Artemisinin content has been reported to reach 1.4% of the leaf dry weight when grown in the field, and its metabolite profile is typical for the HAP chemotype (Larson et al., 2013). NCV ("non-commercial variety"), an "open-pollinated" variety of European origin was also provided by Mediplant, and has the lowest reported artemisinin content from any *A. annua* germplasm in addition to a metabolite profile characteristic of the LAP chemotype (Larson et al., 2013). Plants were grown from seeds in glasshouse conditions as previously described (Graham et al., 2010).

Leaf Area Measurements

The leaf area of glasshouse-grown plants was measured by scanning for leaves 14–16 (counting from the apical meristem), followed by calculation of the leaf area using LAMINA software (Bylesjö et al., 2008).

Trichome Density Measurements

Trichome density was quantified on the abaxial surface of the terminal leaflets of leaves 14–16 (counting from the apical meristem). Trichomes were visualized using a Zeiss fluorescent dissecting microscope (fitted with a 470/40 nm excitation filter/ 525/50 nm emission filter). Images were recorded using AxioVision 4.7 software (Carl Zeiss Ltd. Herts., UK). Trichome number was counted manually across a 3×0.5 mm^2 leaflet sample area and the average (mean) trichome density was then calculated for the whole leaf.

NMR Structural Data for Natural Compounds From Artemis and NCV

Leaf and stem material from Artemis (5 Kg) was extracted in $CHCl_3$ (20 L). The organic solvent was removed by rotary evaporation and a portion of the residual dark green aromatic plant extract (*ca* 2.5% w/w) was "dry-loaded" on to a silica column for gradient column chromatography (see Table section Gradient Column Chromatography of the Artemis Variety of *A. annua*).

Gradient Column Chromatography of the Artemis Variety of *A. annua*

Solvent	Fraction
10% EtOAc/hexane	A, B∗, C and D∗
20% EtOAc/hexane	E, F, G, H, I and J
30% EtOAc/hexane	K, L, M, N and O∗
50% EtOAc/hexane	P and Q
EtOAc	R, S, T∗, U and V
Methanol	W, X and Y

Each of the fractions A-Y from gradient column chromatography of Artemis were then further purified by isocratic preparative normal-phase HPLC (*fractions B, D, I, O, and T were also subjected to a second round of isocratic column chromatography prior to prep. HPLC); and individual metabolites were then characterized by NMR, as listed in **Figure 1A** and the Supplemental Table 1 (1D- and 2D-NMR data for all metabolites is also given in the Supplementary List 1). Selected fractions were analyzed by UPLC-APCI-high resolution MS to verify molecular weights and chemical formulae. Confirmed annotations were used to update m/z and retention time reference data, to enable reporting of these compounds from plant extracts by UPLC-MS.

Leaf and stem material from the NCV variety of *A. annua* (780 g) was extracted in $CHCl_3$ (4 L). The organic solvent was then removed by rotary evaporation and the residual dark green aromatic plant extract (16.6 g; *ca* 2% w/w) was dry-loaded onto a silica column for gradient column chromatography (see Table section Gradient Column Chromatography of the NCV Variety of *A. annua*).

Gradient Column Chromatography of the NCV Variety of *A. annua*

Solvent	Fraction
2% EtOAc/hexane	A, B and C
10% EtOAc/hexane	D, E, F and G
20% EtOAc/hexane	G, H and I
40% EtOAc/hexane	J, K and L
EtOAc	M and N
Methanol	N

Each of the fractions A-N from gradient column chromatography of NCV were then further purified by isocratic preparative normal-phase HPLC; individual metabolites were then characterized by NMR, as listed in **Figure 1B** and the Supplemental Table 1 (1D- and 2D-NMR data for all metabolites are also given in the Supplementary List 2). Selected fractions were analyzed by UPLC-APCI-high resolution MS to verify molecular weights and chemical formulae. Confirmed annotations were used to update m/z and retention time reference data, to enable reporting of these compounds from plant extracts by UPLC-MS.

Metabolite Analysis by UPLC-MS and GC-MS

Metabolite analysis by UPLC- and GC-MS were performed as described previously (Czechowski et al., 2016). Fifteen plants from each of five genotype classes were grown from seeds in 4-inch pots under 16 h days for 12 weeks. Metabolite profiles were generated from 50 mg fresh weight (FW) pooled samples of leaves collected at two different developmental stages: 1–5 (counted from the apical meristem), representing the juvenile stage; and leaves 11–13, representing the mature, expanded stage (**Figure 3A**). Fresh leaf samples were stored at −80°C, pending analysis. In addition, dry leaf material was also obtained from 14-week old plants, cut just above the zone of senescing leaves, and dried for 14 days at 40°C. Leaves were stripped from the plants, and leaf material sieved through 5 mm mesh to remove small stems. Trichome-specific metabolites were extracted as described previously (Czechowski et al., 2016) with minor modifications. Briefly, 50 mg of fresh material was extracted by gentle shaking in 500 µl chloroform for 1 h. Supernatant was taken out and remaining plant material was fully dried in a centrifugal evaporator (GeneVac® Ez-2 plus, Genevac Ltd, Ipswich, UK). Weight of the extracted and dried material was taken and used to quantify abundance of the specific compounds per unit of extracted dry weight. Dry leaf material (0.5 g) was ground to a fine powder using a TissueLyser II ball mill fitted with stainless steel grinding jars (Qiagen, Crawley, UK) operated at 25 Hz for 1 min. Ten mg sub-samples of dry leaf material were extracted in 9:1 (v/v) chloroform:ethanol with gentle shaking for 1 h and then analyzed as per fresh material.

For UPLC-MS analysis of sesquiterpenes, a diluted (1:5 (v/v) extract:ethanol) 2 µL aliquot was injected on an Acquity UPLC system (Waters, Elstree, UK) fitted with a Luna 50 × 2 mm 2.5 µm HST column (Phenomenex, Macclesfield, UK). Metabolites were eluted at 0.6 mL/min and 60°C using a linear gradient from 60 to 100% A:B over 2.5 min, where A = 5% (v/v) aqueous MeOH and B = MeOH, with both A and B containing 0.1% (v/v) formic acid. Pseudomolecular $[M+H]^+$ ions were detected using a Thermo Fisher LTQ-Orbitrap (ThermoFisher, Hemel Hempstead, UK) mass spectrometer fitted with an atmospheric pressure chemical ionization source operating in positive ionization mode under the control of Xcalibur 2.1 software. Data was acquired over the m/z range 100–1,000 in FTMS centroid mode with resolution set to 7500 FWHM at m/z 400. Data extraction and analysis was performed using packages and custom scripts in R 3.2.2 (https://www.R-project.org/). XCMS (Smith et al., 2006) incorporating the centWave algorithm (Tautenhahn et al., 2008) was used for untargeted peak extraction. Deisotoping, fragment and adduct removal was performed using CAMERA (Kuhl et al., 2012). Artemisinin was quantified using the standard curve of the response ratio of artemisinin (Sigma, Poole, UK) to internal standard (β-artemether; Hallochem Pharmaceutical, Hong Kong) that was previously added to extracts and standards. Metabolites were

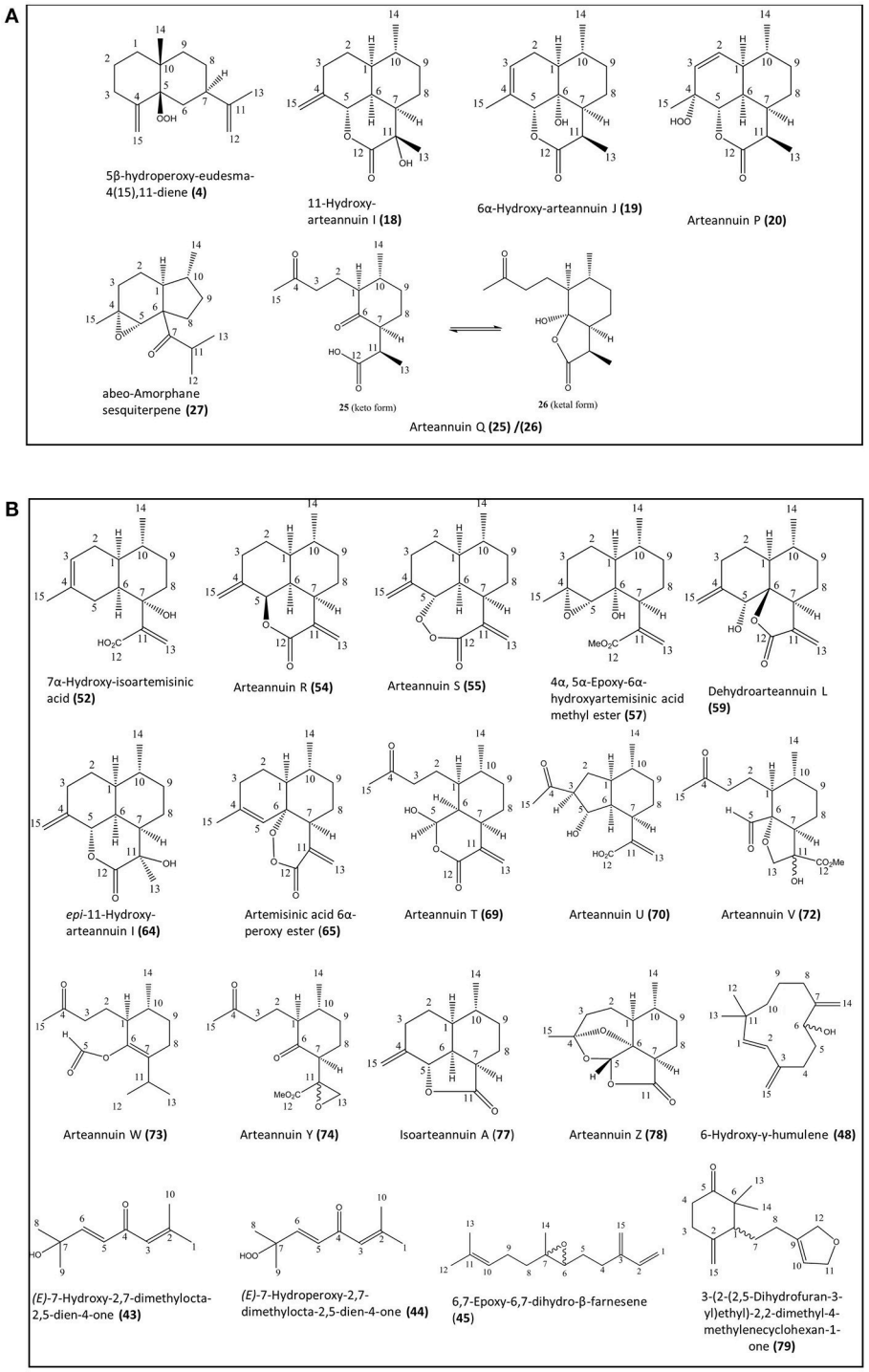

FIGURE 1 | Novel natural compounds characterized from the Artemis **(A)** and NCV **(B)** varieties of *A. annua* by the NMR approach. Numbering of compounds is consistent with Supplementary Lists 1 and 2. Numbering of carbon atoms showed.

identified with reference to authentic standards or NMR-resolved structures and empirical mass formulae calculated using the R package rcdk (Guha, 2007) within 10 ppm error and elemental constraints of: C = 1–100, H = 1–200, O = 0–20, N = 0–1. Peak concentrations were calculated using bracketed response curves, where standard curves were run every ∼30 samples. Metabolite concentrations were expressed as a proportion of the residual dry leaf material following extraction.

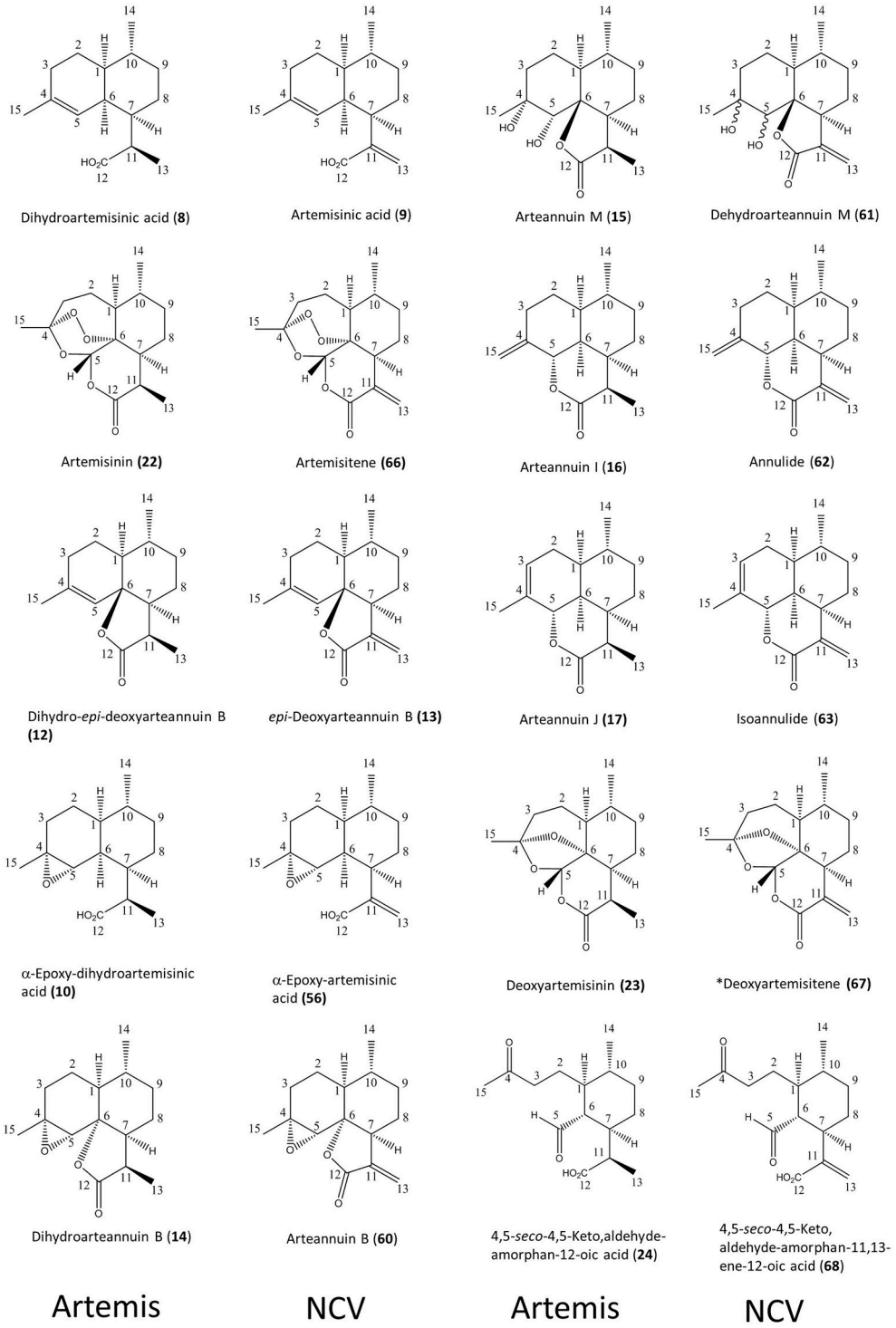

FIGURE 2 | Ten pairs of 11,13-dihdyro/ 11,13-dehydro amorphanolides between Artemis (left-hand side) and NCV (right-hand side) varieties of *A. annua* characterized by the NMR approach. Numbering of compounds is consistent with Supplementary Lists 1, 2. Numbering of carbon atoms showed. Novel compound indicated by asterisk.

For analysis of monoterpenes and volatile sesquiterpenes from fresh leaf samples, an aliquot of chloroform extract (prior to dilution with ethanol for UPLC analysis) was taken for GC-MS analysis using an Agilent 6890 GC interfaced to a Leco Pegasus IV TOF MS (Leco, Stockport, UK). A 1 μL aliquot was injected into a CIS4 injector (Gerstel, Mülheim an der Ruhr, Germany) fitted

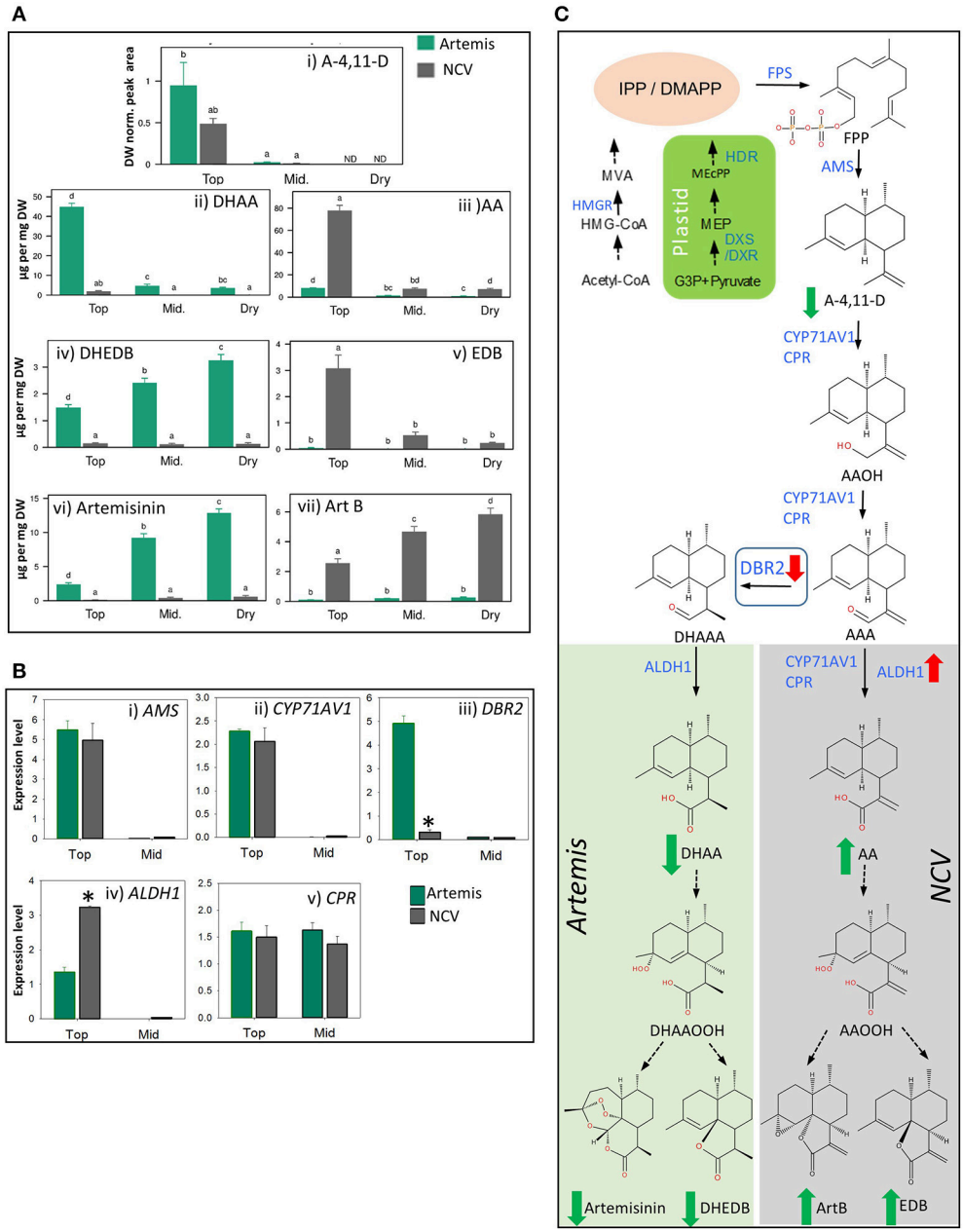

FIGURE 3 | Metabolic and transcriptomic comparison of the artemisinin pathway in the low- vs. high-artemisinin chemotypes of *A. annua.* **(A)** Level of selected sesquiterpenes were quantified by GC-MS **(i)** and UPLC-MS **(ii–vii)** in fresh juvenile leaf 1–5 (Top), fresh mature leaf 11–13 (Mid.) and oven-dried whole plant-stripped leaves (Dry) from 12-weeks old glasshouse-grown Artemis (green bars) and NCV (gray bars) varieties as described in Materials and methods. error bars—SEM ($n = 15$ for Top and Mid. leaf; $n = 6$ for Dry leaf). Letters represent Tukey's range test results after one way ANOVA or REML (see Materials and Methods for details). Groups not sharing letters indicate statistically significant differences. **(B)** Transcript profiling of enzymes involved in the artemisinin biosynthetic pathway, in two types of leaf material as on **(A)** was done as described in Materials and Methods, error bars—SE ($n = 9$). Asterisk indicates *t*-test statically significant difference between Artemis (green bars) and NCV (gray bars) at $p < 0.05$. **(C)** Summary of the metabolite and transcriptional differences between Artemis and NCV for the artemisinin biosynthetic pathway: full arrows—known enzymatic steps, dashed arrows—non-enzymatic conversions, red arrows—transcript changes in juvenile leaves of NCV vs. Artemis, green arrows—metabolite changes of NCV vs. Artemis (all types of leaves). DBR2 position in the pathway highlighted in a square. Metabolite abbreviations: G-3-P, glyceraldehyde-3-phosphate; MEP, 2-C-methylerythritol 4-phosphate; MEcPP, 2-C-methyl-D-erythritol-2,4-cyclopyrophosphate. Cytosolic precursors: HMG-CoA, 3-hydroxy-3-methylglutaryl-CoA; MVA, mevalonate; IPP, isopentenyl pyrophosphate; DMAPP, dimethylallyl pyrophosphate; FPP, farnesyl pyrophosphate; A-4,11-D, amorpha-4,11-diene; AAOH, artemsinic alcohol; AAA, artemsinic aldehyde; AA, artemsinic acid; ArtB, arteannuin B; DHAAA - dihydroartemsinic aldehyde; DHAA, dihydroartemsinic acid; DHAAOOH, dihydroartemsinic acid tertiary hydroperoxide; DHEDB, dihydro-*epi*-deoxyarteanniun B; AAOOH, artemsinic acid tertiary hydroperoxide; EDB, *epi*-deoxyarteannuin B. Enzyme abbreviations: HMGR-, 3-hydroxy-3-methylglutaryl coenzyme A reductase; HDR-, 4-hydroxy-3-methylbut-2-enyl diphosphate reductase; DXR, 1-deoxy-D-xylulose-5-phosphate reductoisomerase; DXS-, 1-deoxy-D-xylulose-5-phosphate synthase; FPS, farnesyl diphosphate synthase. AMS, amorpha-4,11-diene synthase; CYP71AV1, amorpha-4,11-diene C-12 oxidase; CPR, cytochrome P450 reductase; DBR2, artemisinic aldehyde Δ 11 (13) reductase; ALDH1, aldehyde dehydrogenase.

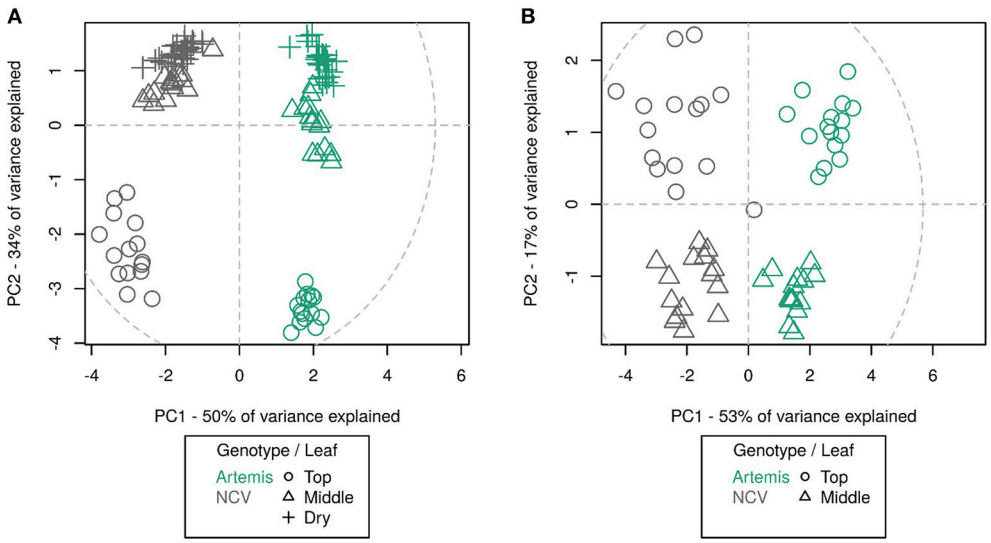

FIGURE 4 | Principal component analysis of UPLC-MS **(A)** and GC-MS **(B)** data from different leaf types from Artemis and NCV varieties. Principal component analysis of 75 UPLC-MS identified peaks **(A)** and 202 GC-MS identified metabolites **(B)**. Leaf types, corresponding with **Figure 3** are represented by symbols: circles—leaf 1–5, triangles—leaf 11–13, crosshairs—oven-dried leaf. Two chemotypes represented by colors green—Artemis and gray—NCV. PCA was performed on log-scaled data and mean-centered data; dotted ellipse = Hotelling's 95% confidence interval.

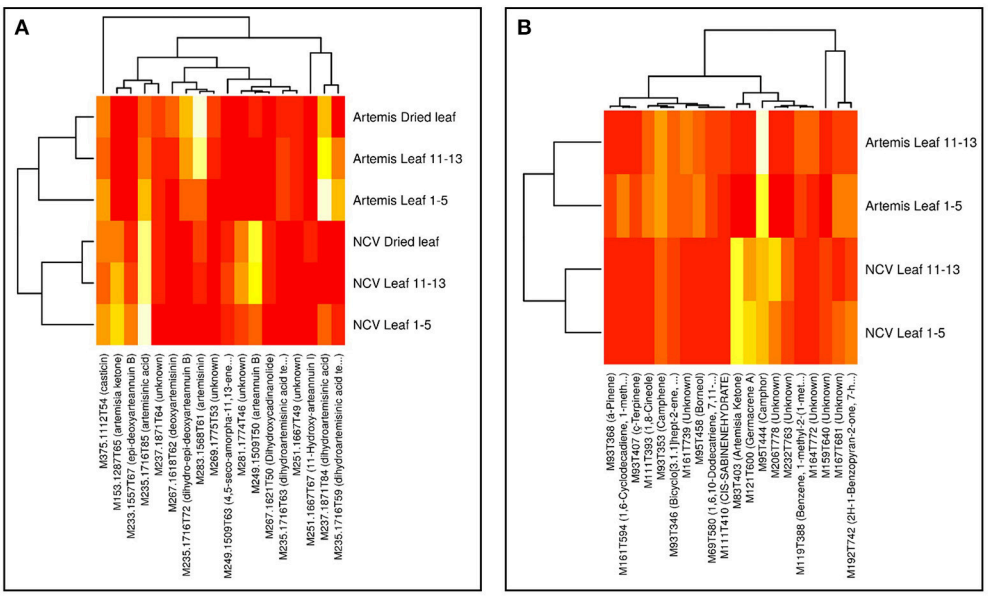

FIGURE 5 | Heatmaps of influential metabolites from UPLC- and GC-MS PCA analyses. Top-n [UPLC-MS = 18 **(A)**; GC-MS = 20 **(B)**] metabolites were chosen for visualization based on loadings plots (Supplementary Figure 1) from the PC1 dimensions in the PCA analyses (Supplementary Figure 1). Mean data were log-scaled and then row-scaled for color intensity plotting (lighter = more abundant). Hierarchical clustering was performed with average linkage, with Euclidean distances for genotypes and 1-absolute values of correlations as distances for metabolites. Metabolite names are abbreviated where necessary for clarity and are given in full in Supplementary Tables 2, 3.

with a 2 mm ID glass liner containing deactivated glass wool at 10°C. The injector was ramped from 10 to 300°C at 12°C/s then held at 300°C for 5 min. The carrier gas was He at a constant flow of 1 mL/min and the injection split ratio was 1:10. Peaks were eluted using a Restek Rxi-5Sil MS column, 30 m × 0.25 mm ID × 0.25 µm film thickness (Thames Restek, Saunderton, UK). The following temperature gradient was used: isothermal 40°C 2 min; ramp at 20°C/min to 320°C then hold for 1 min; total run time ∼20 min. The transfer line was maintained at 250°C and the MS used to collect−70 eV EI scans over the m/z range 20–450

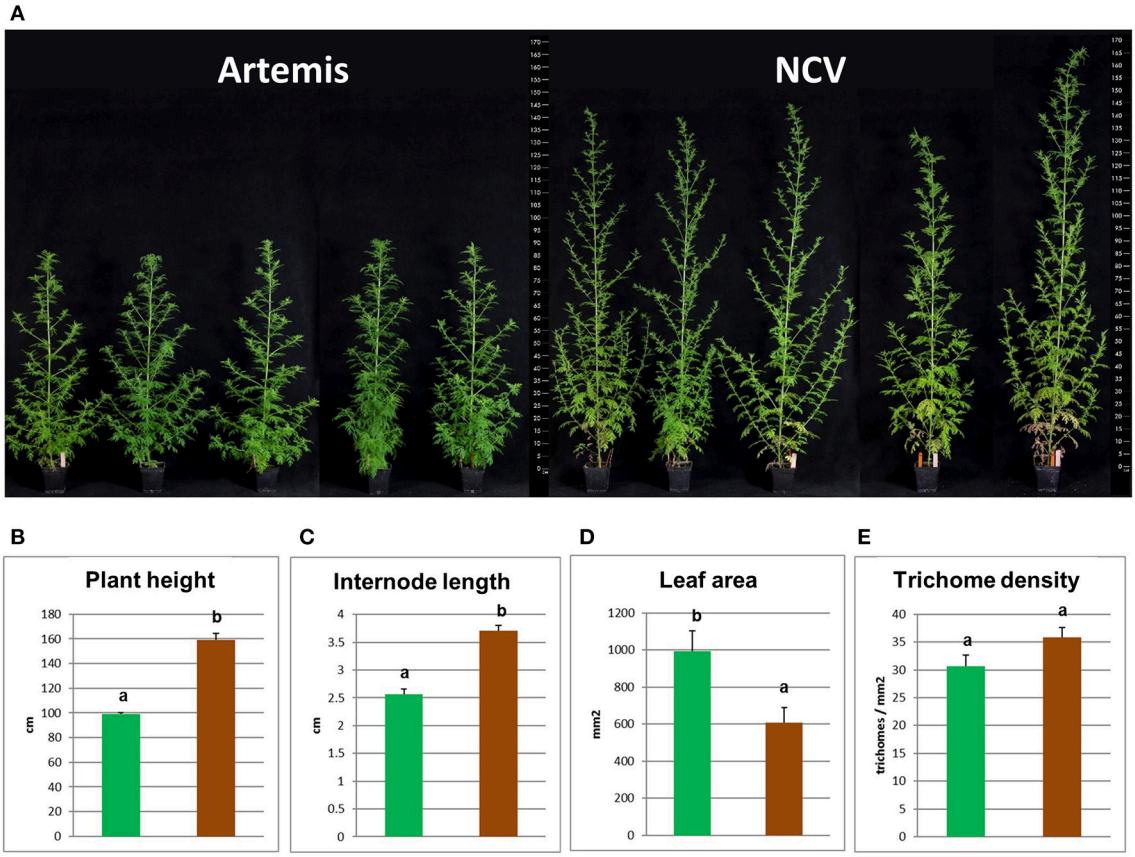

FIGURE 6 | Morphological characterization of low- and high-artemisinin natural chemotypes of *A. annua*. **(A)** Photographs show four representative 12-week old plants from each two chemotypes of *A. annua*, ruler scaled in cm showed on both sides; Plant height **(B)**, internode length **(C)**, leaf area **(D)**, and glandular secretory trichome density **(E)** recorded for 12-week old plants. Green bars represent Artemis (HAP-chemotype) and brown bars represent NCV (LAP-chemotype). Error bars—SEM ($n = 15$), letters represent one-way ANOVA Tukey's range test results; Groups not sharing letters indicate statistically significant differences.

at a scan rate of 20 spectra/s. Acquisition was controlled by ChromaTof 4.5 software (Leco). ChromaTof was used to identify peaks and deconvolute spectra from each run, assuming a peak width of 3 s and a minimum *s/n* of 10. Peak areas were reported as deconvoluted total ion traces (DTIC). Further analyses including annotation against authentic standards, between-sample peak alignment, grouping, consensus DTIC reporting, and missing value imputation were performed using custom scripts in R.

R was used for all statistical data analysis using the stats base package, nlme (http://CRAN.R-project.org/package=nlme) and pcaMethods (Stacklies et al., 2007).

RNA Isolation, cDNA Synthesis, and Quantitative RT-PCR

Leaf tissue from juvenile and mature-stage leaves sampled as described above was ground to a fine powder using Qiagen Retsch MM300 TissueLyser (Qiagen, Hilden, Germany) and total RNA extracted using the RNAeasy kit (Qiagen, Hilden, Germany). RNA was quantified using NanoDrop-1000 (NanoDrop products, Wilmington, USA) and integrity was checked on 2200 Tape Station Instrument (Agilent, Santa Clara, CA, USA). Only samples scoring RIN number ≥7.0 were taken for further analysis. Removal of genomic DNA was performed by treating with TURBO DNA-free™ (Life Technologies Ltd, Paisley, UK) following manufacturer's instructions. 5 ug of total RNA, pooled from 4 individual plants, representing 3 biological replicates, was reversely transcribed using SuperScript II kit (Life Technologies Ltd, Paisley, UK) and Oligo(dT)12-18 Primer (Life Technologies Ltd, Paisley, UK) according to manufacturer's instructions. PCR using primers (AMS_Ex4 for 5′-GGCTGTCTCTGCACCTCCTC-3′, AMS_Ex5 for 5′- CAG CCATCAATAACGGCCTTG-3′) designed spanning intron 4 of the *AMS* gene (GenBank: AF327527). Only samples that resulted in amplification of the 251 bp fragment from cDNA and not the 363 bp fragment from genomic DNA were taken for further qPCR analysis.

Expression levels of amorpha-4,11-diene synthase (AMS), amorpha-4,11-diene C-12 oxidase (CYP71AV1), cytochrome P450 reductase (CPR), artemisinic aldehyde Δ 11 (13) reductase (DBR2) and aldehyde dehydrogenase (ALDH1), relative to ubiquitin (UBI) were determined by qPCR. Reactions were run in 3 technical replicates. Gene-specific primers used were: AMS for

5′- GGGAGATCAGTTTCTCATCTATGAA- 3′; AMS_Rev 5′- CTTTTAGTAGTTGCCGCACTTCTT-3′; 5′ALDH1 for 5′- GAT GTGTGTGGCAGGGTCTC-3′; ALDH1_Rev 5- ACGAGTGGC GAGATCAAAAG-3′; CYP71AV1 for 5′- TCAACTGGAAAC TCCCCAvcATG-3′; CYP71AV1_Rev 5′- CGGTCATGTCGA TCTGGTCA-3′; CPR_For 5′- GCTCGGAACAGCCATCTTATT CTT-3′, CPR_Rev 5′- GAAGCCTTCTGAGTCATCTTGTGT-3′, DBR2 for 5′- GAACGGACGAATATGGTGGG-3′; DBR2_Rev 5′- GCAGTATGAATTTGCAGCGGT-3′, UBI for 5′-TGATTG GCGTCGTCTTCGA-3′ and UBI_Rev 5′-CCCATCCTCCAT TTCTAGCTCAT-3′. Reactions conditions and qPCR analysis were performed as above, 1 ul of 1/20 first strand cDNA dilution was used instead of genomic DNA. Background subtraction, average PCR efficiency for each amplicon and N0 values were calculated using LinRegPCR ver. 2012 software (Ruijter et al., 2009). Expression levels for each sample and gene of interest (GOI) were represented as N0 GOI/N0 UBI.

RESULTS

NMR Spectroscopic Analysis Uncovers Novel Metabolites in Both HAP and LAP Chemotypes

The natural products found in *A. annua* have previously been grouped into eight broad categories, including: (i) monoterpenes; (ii) sesquiterpenes; (iii) diterpenes, (iv) sterols and triterpenes; (v) aliphatic hydrocarbons, alcohols, aldehydes and acids; (vi) aromatic alcohols, ketones and acids; (vii) phenylpropanoids; and (viii) flavonoids (Brown, 2010). In the present work we have used the Artemis variety of *A. annua* as a representative of the HAP chemotype and NCV as a representative of the LAP chemotype (Larson et al., 2013). Our initial investigations using NMR analysis of leaf extracts of Artemis resulted in the isolation of 41 metabolites (6 of which were novel) representing all eight classes of natural products (**Figure 1A**, Supplementary List 1). The structures of all compounds were determined by 1D- and 2D- NMR spectroscopy (detailed NMR data in Supplementary Section). Novel compounds which have not been isolated before as natural products include four new 11,13-dihydroamorphanes: 5β-hydroperoxy-eudesma-4(15),11-diene **(4),** 11-hydroxy-arteannuin I **(18),** 6α-hydroxy-arteannuin J **(19)**, arteannuin P **(20)**, the ketal form of arteannuin Q **(26)** and abeo-amorphane sesquiterpene **(27)**. Artemisinin **(22)** was the most abundant metabolite in this analysis (**Figure 2**, Supplementary List 1, and Supplemental Table 1); but the Artemis extract also contained two other sesquiterpenes: dihydroartemisinic acid (DHAA, **8**), and dihydro-*epi*-deoxyarteannuin B (DHEDB, **12**) in substantial amounts (**Figure 2**, Supplementary List 1 and Supplemental Table 1). In addition, a further nine known 11,13-dihydroamorphanoic acid derivatives (α-epoxy-dihydroartemisinic acid **(10)**; 4α,5α-epoxy-6α-hydroxyamorphan-12-oic acid **(11)**; dihydroarteannuin B **(14)**; arteannuin M **(15)**; arteannuins H, I and J (**21, 16,** and **17**); deoxyartemisinin **(23)**; and a 4,5-*seco*-4,5-diketo-amorphan-12-oic acid **(24)** (see **Figure 1A**, Supplementary List 1 and Supplemental Table 1) were also isolated as minor components from the Artemis leaf extracts (**Figure 2**, Supplementary List 1 and Supplemental Table 1).

Phytochemical investigation of the NCV variety by NMR yielded 57 metabolites, 20 of which were novel (**Figure 1B** and Supplementary List 2), representing 7 of the 8 categories above. Novel metabolites from the NCV variety are depicted in **Figure 1B** and include: *(E)*-7-hydroxy-2,7-dimethylocta-2,5-dien-4-one (**43**), (*E*)-7-hydroperoxy-2,7-dimethylocta-2,5-dien-4-one (**44**), 6,7-epoxy-6,7-dihydro-β-farnesene (**45**), 6-hydroxy-γ-humulene (**48**), 7α-hydroxy-artemisinic acid (**52**), arteannuin R (**54**), arteannuin S (**55**), 4α, 5α-epoxy-6α-hydroxyartemisinic acid methyl ester (**57**), dehydroarteannuin L (**59**), *epi*-11-hydroxy-arteannuin I (**64**), artemisinic acid, 6α-peroxy ester (**65**), deoxyartemistene (**67**), arteannuin T (**69**), arteannuin U (**70**), arteannuin V (**72**), arteannuin W (**73**), arteannuin Y (**74**), isoarteannuin A (**77**), arteannuin Z (**78**), and 3-(2-(2,5-dihydrofuran-3-yl)ethyl)-2,2-dimethyl-4-methylenecyclohexan-1-one (**79**).

As might have been expected, the most striking difference between the NCV and *Artemis* varieties was the almost complete absence of artemisinin, dihydroartemisinic acid (DHAA, (**8**)) and dihydro-epi-deoxyarteannuin B (DHEDB, (**12**)) in the former (Supplemental Table 1). The NCV variety did, however, have relatively high levels of three 11-13-unsaturated amorphanes, which were found only as minor components in the *Artemis* variety, namely: artemisinic acid (AA, **9**), arteannuin B (ArtB, **60**) and *epi*-deoxyarteannuin B (EDB, **13**) (**Figure 2** and Supplemental Table 1). All the other amorphane sesquiterpenes isolated and characterized from the NCV variety by NMR shared this same trait: i.e., possession of an 11,13-unsaturated methylene group (**Figures 1B**, **2** and Supplemental Table 1), and there is an almost complete absence of 11,13-dihydro-amorphanes from NCV, that contrasts with the abundance of these compounds in the *Artemis* variety (Supplementary List 2 and Supplemental Table 1). It is interesting to note that there are ten examples where 11,13-dihdyro/ 11,13-dehydro amorphanolides seem to occur as "pairs" between *Artemis* and NCV as depicted in **Figure 2**. These include: DHAA **(8)**/AA **(9)**; artemisinin **(22)**/artemisitene **(66)**; dihydro-*epi*-deoxyarteannuin B **(12)**/*epi*-deoxyarteannuin B **(13)**; α-epoxy-dihydroartemisinic acid **(10)**/α-epoxy-artemisinic acid **(56)**; dihydroarteannuin B **(14)**/arteannuin B **(60);** arteannuin M **(15)**/dehydroarteannuin M **(61)**; arteannuin I **(16)**/annulide **(62)**; arteannuin J **(17)**/isoannulide **(63)**; deoxyartemsinin **(23)**/deoxyartemsitene **(67)**; and 4,5-*seco*-4,5-diketo-amorphan-12-oic acid **(24)** and its 11,13-dehydro-analog **(68)**. It is also noteworthy that 9 of the 20 novel amorphane and *seco*-amorphane sesquiterpenes isolated and characterized from the NCV variety by NMR, possess an 11, 13-unsaturated methylene group (**Figures 1B**, **2** and Supplementary List 2).

All the above results are consistent with a higher DBR2 activity in the HAP chemotype compared to the LAP chemotype (Yang et al., 2015). The relative abundances for 8 of these 10 "pairs" are also well matched between the *Artemis* and NCV varieties, suggesting a "shared" further metabolism for DHAA in *Artemis* and AA in NCV. The first exception is arteannuin B (ArtB **60**), which is abundant in NCV, whilst its analog, dihydroarteannuin

B (**14**), is relatively low in *Artemis* (Supplemental Table 1). The second is artemisitene, the 11,13-dehydro analoge of artemisinin (Acton and Klayman, 1985; Woerdenbag et al., 1994; **Figure 1**; Supplemental Table 1) which is a minor compound in NCV, while its "partner" artemisinin is the most abundant metabolite in *Artemis* (Supplemental Table 1). These observations suggest that while there are many parallels in the pathways that further transform DHAA (**8**) and AA (**9**) in the HAP and LAP chemotypes there are also some significant differences.

Metabolomic and Gene Expression Studies Reveal Multiple Differences Between HAP and LAP Chemotypes

Using a leaf maturation time-series, we recently demonstrated that artemisinin levels increase gradually from juvenile to mature leaves and remain stable during the post-harvest drying process in Artemis HAP chemotype plants (Czechowski et al., 2016). Using a similar time-series (which included fresh leaf 1–5 (juvenile), and 11–13 (mature) (counting from the apical meristem); plus oven-dried whole plant-stripped leaves (dry) from 12-week-old glasshouse-grown plants), we have now performed UPLC- and GC-MS based metabolite profiling of extracts from both HAP (Artemis*)* and LAP (NCV) chemotypes. We found that the pathway entry–point metabolite, amorpha-4,11-diene (A-4,11-D), is only detectable in juvenile leaves, and at approximately 2-fold higher concentration in Artemis as compared to NCV (**Figure 3Ai**; Supplemental Table 3). A much greater difference was seen for the enzymatically-produced artemisinin precursor, dihydroartemisinic acid (DHAA), which was present at a 24-fold higher concentration in juvenile Artemis leaves compared to NCV (**Figure 3Aii**), Supplemental Table 2). Artemisinic acid (AA) on the other hand accumulated in NCV leaves at a 10-fold higher concentration than in Artemis (**Figure 3Aiii**), Supplemental Table 1). Interestingly the levels of AA in the young leaves of NCV variety are approximately twice the levels of DHAA in young leaves of Artemis (**Figures 3Aii,iii**), Supplemental Table 2). The levels of both DHAA and AA dropped sharply beyond the juvenile leaf stage in Artemis and NCV, respectively (**Figures 3Aii,iii**), Supplemental Table 2). These changes in metabolite levels occur during leaf maturation are mirrored by changes in steady state mRNA levels of genes encoding the enzymes involved in their biosynthesis including: amorpha-4,11-diene synthase (AMS), amorpha-4,11-diene C-12 oxidase (CYP71AV1), artemisinic aldehyde $\Delta^{11,(13)}$ reductase (DBR2) and aldehyde dehydrogenase (ALDH1) which are expressed at levels two to three orders of magnitude higher in juvenile than in mature leaves (**Figures 3Bi–iv**).

Previous work has suggested that *in vivo* conversions beyond DHAA (**8**) (Czechowski et al., 2016) and *in vitro* conversions beyond AA (**9**) (Brown and Sy, 2007) are non-enzymatic. Consistent with this, we have found that mature leaves of NCV contain high levels of *epi*-deoxyarteannuin B (EDB, **13**) and arteannuin B (ArtB, **60**) (**Figures 3Av,vii**), Supplemental Table 2), while Artemis accumulates dihydro-*epi*-deoxyarteannuin B (DHEDB, **12**) and artemisinin (**22**) (**Figures 3Aiv,vi**) Supplemental Table 2) at 20–30-fold higher levels than NCV. Both artemisinin (**22**) and arteannuin B (**60**) continue to accumulate in the post-harvest drying process in Artemis and NCV respectively (**Figures 3Avi,vii**). Post-harvest accumulation of artemisinin has been reported before (Ferreira and Luthria, 2010) and it might be related to light-dependent conversion of DHAA. However slightly different batch specific environmental effects during drying might explain the difference between the artemisinin accumulation pattern shown in **Figure 3Avi**) and that which was previously reported for the Artemis variety (Czechowski et al., 2016). Interestingly, the developmental pattern of DHEDB (**12**) accumulation in Artemis leaves is different to its 11,13-dehydro analog, EDB (**13**) in NCV leaves. DHEDB (**12**) follows the same accumulation pattern as for artemisinin (**22**) in Artemis (**Figures 3Aiv,vi**); whereas EDB (**13**) is found predominantly in juvenile leaves of the NCV variety (**Figure 3Av**). We have found that production of the artemisinin 11,13-dehydro analog, artemisitene (**66**) in NCV parallels the accumulation of artemisinin (**22**) in Artemis (Supplemental Table 2), albeit at very much reduced levels. The levels of deoxyartemisinin (**23**), another product of non-enzymatic conversion of DHAA through the DHAA allylic hydroperoxide, increase during dry leaf storage, accumulating to 0.1% leaf dry weight (Supplemental Table 2), which is consistent with previous findings (Czechowski et al., 2016). This process is paralleled by accumulation of deoxyartemisitene (**67**) (the 11,13-dehydro analog of deoxyartemisinin) in the NCV variety (Supplemental Table 2).

RT-qPCR analysis confirmed the expression level for *DBR2* to be significantly repressed (8-fold lower) in the juvenile leaves of NCV compared to Artemis, which is consistent with previous findings (Yang et al., 2015). Interestingly, *DBR2* transcript abundance had decreased to the same levels in mature leaves of both chemotypes (**Figure 3Biii**), highlighting the importance of developmental timing in regulating flux and partitioning of sesquiterpene metabolites. More surprisingly, *ALDH1* expression is increased in juvenile leaves (2.4-fold) and further increased in mature leaves (40-fold) of NCV (**Figure 3Biv**) compared to Artemis. Thus it would appear that in addition to *DBR2* being down-regulated in the NCV (LAP) chemotype, *ALDH1* is up-regulated at the transcriptional level. This could also account for the increase in flux into artemisinic acid and the arteannuin B branch of sesquiterpene metabolism. The major differences in metabolite levels and gene expression between Artemis and NCV varieties for the artemisinin biosynthetic pathway are summarized in **Figure 3C**.

NMR analysis revealed that metabolite differences between Artemis and NCV are not restricted to artemisinin-related sesquiterpenes. Monoterpenes also vary between the two chemotypes, with for example camphor being most abundant in Artemis while artemisia ketone level is much more abundant in NCV (Supplemental Table 1). Unfortunately, NMR-analysis could only provide approximate information about the relative abundance of the metabolites, therefore metabolite content of both chemotypes was also studied by GC- and UPLC-MS (Supplemental Tables 2, 3). We were able to detect 75 unique compounds in three leaf types by UPLC-MS of which annotations were assigned to 30 compounds based on NMR-verified

standards as described in the Materials and Methods. The majority of the known compounds were sesquiterpenes and flavonoids. GC-MS detected 202 unique compounds in juvenile and mature leaves, of which 33 had assigned annotations. The majority of known GC-MS-detected compounds were mono- and sesquiterpenes. Using principal component analysis, it can be seen that the overall metabolite profile of NCV appears strikingly different to that of Artemis; as much as the difference between the profiles between juvenile leaves and mature- and/or dry leaves. In fact, UPLC- and GC-MS PCA plots show four distinct clusters (**Figures 4A** and **B**). Developmental differences are most apparent in juvenile leaf tissue, which show the highest abundance of most of the terpenes described below (**Figure 4**, Supplemental Tables 2 and 3). Our findings that the metabolite profiles in Artemis and NCV young leaf tissues are considerably different to mature and dry leaves in both varieties are consistent with our previous findings (Czechowski et al., 2016).

There are a number of compounds specifically produced by NCV, mostly in low quantities (Supplemental Tables 2 and 3) which have known medicinal use including, for example, isofraxidin **(39),** which is five-fold more abundant in the juvenile leaves of NCV as compared to Artemis (Supplemental Table 2). Isofraxidin is a coumarin with anti-inflammatory (Niu et al., 2012) and anti-tumor activities (Yamazaki and Tokiwa, 2010). Artemisia ketone **(42)**, an irregular monoterpene found in the essential oil from various *A. annua* varieties displaying antifungal activities (Santomauro et al., 2016) is the most abundant volatile in the juvenile and mature leaves of NCV, but virtually absent in Artemis (Supplemental Table 3). The juvenile and mature leaves of Artemis accumulate velleral, a sesquiterpene dialdehyde which has proposed antibacterial activities (Anke and Sterner, 1991), which is virtually absent in the NCV variety (Supplemental Table 3). GC-MS analysis further revealed that several major montoerpenes are also more abundant in juvenile and mature leaves of Artemis, including camphor (3.7-fold higher), camphene (3.4-fold higher), borneol, (16-fold higher), α-pinene (4.6-fold higher) and 1,8-cineole (8-fold higher) (Supplemental Table 3). Some minor monoterpenes detected in the Artemis variety, such as: α-myrcene, α –terpinene, chrysanthenone and α-copaene, are virtually absent in young and mature NCV leaves (Supplemental Table 3). A few striking differences were noted for the level of artemisinin-unrelated abundant sesquiterpenes, such as sabinene and *cis*-sabinene hydrate, which are 7.5- and 38-fold (respectively) more abundant in Artemis young leaves than in NCV (Supplemental Table 3). Germacrene A is a sesquiterpene common across the Asteraceae family for which it has been demonstrated that its downstream metabolism parallels artemisinic acid biosynthetic pathway (Nguyen et al., 2010). Germacrene A levels are 32- and 17-fold higher in NCV young and mature leaves (respectively) making it the most abundant volatile in mature and the second most abundant in young leaves of the NCV variety.

Visualization of the loadings from the multivariate analyses were used to identify the most influential compounds discriminating chemotypes. PC1 loading plots identified 18 compounds from UPLC- and 20 from GC-MS analysis (Supplementary Figure 1), which were used to create the heatmaps presented in **Figure 5**. The vast majority of the most influential compounds distinguishing between two chemotypes from UPLC-MS analysis were the amorphane sesquiterpenes (**Figure 5A**). The mono- and sesquiterpenes mentioned above (together with some unknown compounds) were the most influential GC-MS-detectable metabolites distinguishing between two chemotypes (**Figure 5B**).

Morphological Difference Between Two Chemotypes of *A. annua*

In addition to having very distinct phytochemical compositions the F1 *Artemis* HAP chemotype and the open pollinated NCV LAP chemotype varieties also have very distinct morphological features (**Figure 6**). Most strikingly, NCV is much taller with longer internodes but produces smaller leaves than *Artemis*. The density of glandular secretory trichomes, the site of artemisinin synthesis, is similar for both varieties (**Figure 6E**), which is consistent with the main difference in artemisinin production being due to an alteration in metabolism rather than trichome density. *A. annua* varieties typically require short day length for flowering (Wetzstein et al., 2014), but we observed that NCV, unlike *Artemis,* can also flower under long days. However, the two chemotypes do cross-pollinate and produce viable progeny.

DISCUSSION

This manuscript presents the first detailed phytochemical comparison of high- (HAP) and low-artemisinin producing (LAP) chemotypes chemotypes of *A. annua*.

Twenty six of the 85 metabolites that have been characterized by NMR from the HAP and LAP varieties of *A. annua* in this study are novel as natural products (all are mono- and sesquiterpenes). And of these, 19 are amorphane sesquiterpenes, which is the most diverse and the most abundant sub-class (Supplemental Table 1, Supplementary Lists 1 and 2). The majority of these amorphane sesquiterpenes are highly oxygenated with structures that would be consistent with further oxidative metabolism of DHAA (11,13-saturated, **8**) in the HAP variety and AA (11,13-unsaturated, **9**) in the LAP variety (**Figures 1** and **2**, Supplemental Table 1, Supplementary Lists 1 and 2).

UPLC- and GC-MS analysis of leaf developmental series also revealed amorphanes either saturated or unsaturated at the 11,13-position in the HAP and LAP chemotypes, respectively (**Figure 3**, Supplemental Table 2). This observation is consistent with the expression of the *DBR*2 gene, which encodes the enzyme responsible for reducing the 11,13-double bond of artemisinic aldehyde (the precursor for 11,13-dihydroamorphane/cadinane sesquiterpenes), being strongly down-regulated in juvenile leaves of NCV (**Figure 3Biii**). These findings are in complete agreement with the recent report on reduced levels of *DBR2* in LAP compared with HAP chemotypes (Yang et al., 2015). In addition to altered expression of *DBR2*, we also found that expression of *aldehyde dehydrogenase* (*ALDH1*), which converts artemsinic and dihydroartemsinic aldehydes to their respective acids (Teoh et al., 2009), is significantly elevated in juvenile and mature leaves

of NCV compared to Artemis. This may lead to an increased flux from A-4,11-D to AA (8) in NCV when compared with flux from A-4,11-D to DHAA (9) in Artemis which is reflected by a significantly higher concentration of AA found in juvenile leaves of NCV when compared to the concentration of DHAA in young Artemis leaves (**Figures 3Aii,iii**). The elevated flux from A-4,11-D to AA (8) might also explain lower levels of A-4,11-D found in juvenile leaves of NCV when compared with Artemis (**Figure 3Ai**) as the expression of *amorpha-4,11-diene synthase (AMS)* is at very similar level in both varieties (**Figure 3Bi**). We have also observed that the NCV (LAP) variety expresses a sequence variant of amorpha-4,11-diene C-12 oxidase (*CYP71AV1*) with a 7 amino acid N-extension (Supplementary Figure 2). This LAP-chemotype associated sequence variant upon transient expression in *Nicotiana benthamiana*, in combination with the other artemisinin pathway genes resulted in a qualitatively different product profile ("chemotype"); that is a shift in the ratio between the unsaturated and saturated (dihydro) branch of the pathway (Ting et al., 2013). That result strongly suggests the two distinct isoforms of CYP71AV1 are associated with HAP- and LAP-branches of the artemisinin pathway in *Artemisia annua* (**Figure 3C**). A number of previous reports have described the existence of LAP- and HAP-chemotypes of *A. annua* arising from distinct geographical locations (Lommen et al., 2006; Arsenault et al., 2010; Larson et al., 2013). It would be interesting to establish if sequence variant forms of *CYP71AV1* and differential expression of *DBR2* are generally found between these other LAP- and HAP-chemotypes.

Recent attempts to constitutively overexpress *DBR2* in transgenic *A. annua* resulted in doubling of the artemisinin concentration, which was also accompanied by a significant increase in DHAA and AA production (Yuan et al., 2015). Improvements in artemisinin concentration obtained in these experiments by Yuan et al. were significantly better than those achieved by constitutive co-expression of *CYP71AV1* and *CPR* (Shen et al., 2012), where the LAP-sequence variant of *CYP71AV1* was overexpressed in transgenic *A. annua*. Our results suggest the glandular trichome-targeted overexpression of *DBR2* specifically in the HAP-type of *CYP71AV1* might be the more efficient route to improving artemisinin production in transgenic *A. annua.*

Although arteannuin B (ArtB) was almost entirely absent from young leaf tissue of the NCV variety, as leaves matured it accumulated to become the most abundant natural product (**Figure 3Avii**). This observation seemed to parallel both the accumulation of artemisinin in the mature tissues of Artemis that has been noted above (**Figure 3vi**), as well as the recently described accumulation of arteannuin X in the mature leaves of the *cyp71av1-1* mutant of *A. annua* (Czechowski et al., 2016). The accumulation of both artemisinin and arteannuin X are considered to be the result of non-enzymatic processes, in which the 4,5-double bond of a precursor sesquiterpene undergoes spontaneous autoxidation with molecular oxygen to produce a tertiary allylic hydroperoxide. The metabolic fate of this hydroperoxide is critically dependent on the identity of the precursor—and in particular on the functionality contained elsewhere in the molecule. Thus, in the case of Artemis, the precursor is DHAA which presents a 12-carboxylic acid group (as well as saturation at the 11,13-position); whilst for the *cyp71av1-1* mutant it is amorpha-4,11-diene (A-4,11-D), which presents a 11,13-double bond (Czechowski et al., 2016). Both *in vivo* and *in vitro* experiments indicate that this difference in functionality is the basis of why DHAA-OOH (the tertiary allylic hydroperoxide from DHAA) is converted to artemisinin, whereas A-4,11-D-OOH is converted to arteannuin X (Czechowski et al., 2016).

We therefore hypothesized that the conversion of artemisinic acid (AA) to artemisitene (ArtB) in NCV may also be a non-enzymatic process, paralleling the conversion of DHAA into artemisinin in Artemis (Supplementary Figures 3A and B) and of amorpha-4,11-diene to arteannuin X in the *cyp71av1-1* mutant (Czechowski et al., 2016). The tertiary allylic hydroperoxide from artemisinic acid (AA-OOH) differs from the two foregoing examples in that it incorporates both a 12-carboxylic acid group and unsaturation at the 11,13-position. In support of this hypothesis, when a sample of AA-OOH (produced by photosensitized oxygenation of AA; and purified by HPLC) was left unattended for several weeks, it was indeed found to have been converted predominantly to ArtB (albeit at a rate that was significantly slower than for the conversion of DHAA-OOH to artemisinin). This unexpected transformation is mostly simply explained by attack of the 12-carboxylic acid group at the allylic position of the hydroperoxide, as is shown in Supplementary Figure 3A. Further studies will be required to explain why it should be that this (apparently) rather subtle modification to the 12-CO_2H group (i.e., the introduction of 11,13-unsaturation in AA-OOH) has resulted in such a radically different pathway, as compared with DHAA-OOH.

The second most abundant product of AA-OOH conversion is *epi*-deoxyarteannuin B (EDB), which accumulates predominantly in young leaves of NCV. The EDB accumulation pattern is therefore different to DHEDB (the 11,13-saturated anaolog), where the latter's concentration rises from top to mature and dry leaves in Artemis, broadly following the accumulation pattern of artemisinin. We have proposed that the spontaneous conversions of AA into EDB and DHAA into DHEDB progress via very similar molecular mechanisms (Supplementary Figures 3C and D). Interestingly we have observed very little EDB arising from the spontaneous conversions of AA-OOH described above, which was predominantly converted to ArtB. It is known that a hydrophobic (lipophilic) environment promotes conversions of DHAA-OOH into artemisinin whereas an aqueous, acidic medium promotes DHAA-OOH conversions to DHEDB (Brown and Sy, 2004). This may also explain the very minor conversion of AA-OOH into EDB which was carried out in a hydrophobic environment (deuterated chloroform), and which promoted AA-OOH conversions to ArtB. This highlights the parallels between artemisinin and arteannuin B biogenesis shown in Supplementary Figures 3A and B. It also suggests that *in vivo* conversions of AA-OOH to EDB requires an aqueous intracellular environment, which might be expected to be present in young leaf trichomes, but less so in mature leaf trichomes where the sub-apical hydrophobic cavities are predominant (Ferreira and Janick, 1995), or upon cell dehydration (in dried leaf material).

Differences between the LAP and HAP chemotypes extended well beyond artemisinin-related sequiterpenes to other classes

of terpenes (**Figures 4** and **5**, Supplemental Tables 1–3). This divergence at the level of metabolism is not that surprising given that these chemotypes also exhibit significant differences in their morphology (**Figure 6**). Artemis is an F1 hybrid derived from HAP parents of East Asian origin (Delabays et al., 2001) while NCV is an open-pollinated variety of European origin (personal communication with Dr. Michael Schwerdtfeger, curator of Botanical Garden at the University of Göttingen, Germany). This is consistent with the general trend for the *A. annua* varieties of European and North American origin which mostly represent the LAP chemotype and the majority of East-Asian origin varieties which represent the HAP chemotype (Wallaart et al., 2000), Details of the genetic divergence of these varieties remains a topic for further investigation that could reveal further insight into the sesquiterpene flux into different end products.

CONCLUSION

This first comparative phytochemical analysis of high- (HAP) and LAP chemotypes of *A. annua* has resulted in the characterization of over 85 natural products by NMR, 26 of which have not previously been described in *A. annua*. We have also shown that the vast majority of *amorphane* sesquiterpenes are unsaturated at the 11,13-position in the LAP-chemotype as opposed to the majority of them being saturated at the 11,13-position in the HAP-chemotype. This is explained by existence of two sequence variants of *CYP71AV1* in the two investigated chemotypes and differential expression of the key branching enzyme in the artemisinin pathway, namely artemisinic aldehyde Δ 11 (13) reductase *(DBR2)*. By highlighting the main points of difference between HAP and LAP chemotypes our findings will help inform strategies for the future improvement of artemisinin production in either *A. annua* or heterologous hosts.

AUTHOR CONTRIBUTIONS

TC planned and performed the experiments, analyzed the data, and wrote the manuscript. TL planned the UPLC-MS and GC-MS experiments, analyzed data and reviewed the manuscript. TMC planned and performed morphological plant analysis. DH performed UPLC-MS and GC-MS experiments. CW planned and performed extraction, purifications and NMR experiments and analyzed data. ME performed extraction, purifications and NMR experiments. GDB planned and performed NMR experiments, analyzed data, wrote and reviewed the manuscript. IAG planned and supervised the experiments and wrote the manuscript.

FUNDING

We acknowledge financial support for this project from The Bill and Melinda Gates Foundation as well as from The Garfield Weston Foundation. This work was also supported by the Biotechnology and Biological Sciences Research Council Grant BB/G008744/1 (to GDB), The Biosynthesis of Artemisinin.

ACKNOWLEDGMENTS

We would like to thank: Dr Caroline Calvert for project management; C. Abbot and A. Fenwick for horticulture assistance; X. Simonnet and Médiplant for access to the Artemis and NCV varieties. IAG thanks The Bill and Melinda Gates Foundation and the Garfield Weston Foundation for their support. GDB would like to thank the BBSRC for financial support and the Chemical Analysis Facility (CAF) at the University of Reading for the provision of the 700 MHz NMR spectrometer used in these studies.

SUPPLEMENTARY MATERIAL

The Supplementary Material for this article can be found online at: https://www.frontiersin.org/articles/10.3389/fpls.2018.00641/full#supplementary-material

REFERENCES

Acton, N., and Klayman, D. L. (1985). Artemisitene, a new sesquiterpene lactone endoperoxide from *Artemisia* annua. *Planta Med.* 51, 441–442.

Anke, H., and Sterner, O. (1991). Comparison of the antimicrobial and cytotoxic activities of twenty unsaturated sesquiterpene dialdehydes from plants and mushrooms. *Planta Med.* 57, 344–346. doi: 10.1055/s-2006-960114

Arsenault, P. R., Vail, D., Wobbe, K. K., Erickson, K., and Weathers, P. J. (2010). Reproductive development modulates gene expression and metabolite levels with possible feedback inhibition of artemisinin in *Artemisia annua*. *Plant Physiol.* 154, 958–968. doi: 10.1104/pp.110.162552

Bouwmeester, H. J., Wallaart, T. E., Janssen, M. H., van Loo, B., Jansen, B. J., Posthumus, M. A., et al. (1999). Amorpha-4,11-diene synthase catalyses the first probable step in artemisinin biosynthesis. *Phytochemistry* 52, 843–854. doi: 10.1016/S0031-9422(99)00206-X

Brown, G. D. (2010). The biosynthesis of artemisinin (Qinghaosu) and the phytochemistry of *Artemisia annua* L. (Qinghao). *Molecules* 15, 7603–7698. doi: 10.3390/molecules15117603

Brown, G. D., and Sy, L.-K. (2004). *In vivo* transformations of dihydroartemisinic acid in *Artemisia annua* plants. *Tetrahedron* 60, 1139–1159. doi: 10.1016/j.tet.2003.11.070

Brown, G. D., and Sy, L.-K. (2007). *In vivo* transformations of artemisinic acid in *Artemisia annua* plants. *Tetrahedron* 63, 9548–9566. doi: 10.1016/j.tet.2007.06.062

Bylesjö, M., Segura, V., Soolanayakanahally, R. Y., Rae, A. M., Trygg, J., Gustafsson, P., et al. (2008). LAMINA: a tool for rapid quantification of leaf size and shape parameters. *BMC Plant Biol.* 8:82. doi: 10.1186/1471-2229-8-82

Czechowski, T., Larson, T. R., Catania, T. M., Harvey, D., Brown, G. D., and Graham, I. A. (2016). *Artemisia annua* mutant impaired in artemisinin synthesis demonstrates importance of nonenzymatic conversion in terpenoid metabolism. *Proc. Natl. Acad. Sci. U.S.A.* 113, 15150–15155. doi: 10.1073/pnas.1611567113

Delabays, N., Simonnet, X., and Gaudin, M. (2001). The genetics of artemisinin content in *Artemisia annua* L. and the breeding of high yielding cultivars. *Curr. Med. Chem.* 8, 1795–1801. doi: 10.2174/0929867013371635

Duke, M. V., Paul, R. N., Elsohly, H. N., Sturtz, G., and Duke, S. O. (1994). Localization of artemisinin and artemisitene in foliar tissues of glanded and

glandless biotypes of *Artemisia-Annua* L. *Int. J. Plant Sci.* 155, 365–372. doi: 10.1086/297173

Duke, S. O., and Paul, R. N. (1993). Development and fine structure of the glandular trichomes of *Artemisia annua* L. *Int. J. Plant Sci.* 154, 107–118. doi: 10.1086/297096

Ferreira, J. F., and Luthria, D. L. (2010). Drying affects artemisinin, dihydroartemisinic acid, artemisinic acid, and the antioxidant capacity of *Artemisia annua* L. leaves. *J. Agric. Food Chem.* 58, 1691–1698. doi: 10.1021/jf903222j

Ferreira, J. F. S., and Janick, J. (1995). Floral morphology of artemisia-annua with special reference to trichomes. *Int. J. Plant Sci.* 156, 807–815. doi: 10.1086/297304

Graham, I. A., Besser, K., Blumer, S., Branigan, C. A., Czechowski, T., Elias, L., et al. (2010). The genetic map of *Artemisia annua* L. identifies loci affecting yield of the antimalarial drug artemisinin. *Science* 327, 328–331. doi: 10.1126/science.1182612

Guha, R. (2007). Chemical informatics functionality in R. *J. Stat. Softw.* 18:16. doi: 10.18637/jss.v018.i05

Kuhl, C., Tautenhahn, R., Böttcher, C., Larson, T. R., and Neumann, S. (2012). CAMERA: an integrated strategy for compound spectra extraction and annotation of liquid chromatography/mass spectrometry data sets. *Anal. Chem.* 84, 283–289. doi: 10.1021/ac202450g

Larson, T. R., Branigan, C., Harvey, D., Penfield, T., Bowles, D., and Graham, I. A. (2013). A survey of artemisinic and dihydroartemisinic acid contents in glasshouse and global field-grown populations of the artemisinin-producing plant *Artemisia annua* L. *Ind. Crops Prod.* 45, 1–6. doi: 10.1016/j.indcrop.2012.12.004

Lommen, W. J., Schenk, E., Bouwmeester, H. J., and Verstappen, F. W. (2006). Trichome dynamics and artemisinin accumulation during development and senescence of *Artemisia annua* leaves. *Planta Med.* 72, 336–345. doi: 10.1055/s-2005-916202

Mercke, P., Bengtsson, M., Bouwmeester, H. J., Posthumus, M. A., and Brodelius, P. E. (2000). Molecular cloning, expression, and characterization of amorpha-4,11-diene synthase, a key enzyme of artemisinin biosynthesis in *Artemisia annua* L. *Arch. Biochem. Biophys.* 381, 173–180. doi: 10.1006/abbi.2000.1962

Nguyen, D. T., Göpfert, J. C., Ikezawa, N., Macnevin, G., Kathiresan, M., Conrad, J., et al. (2010). Biochemical conservation and evolution of germacrene A oxidase in asteraceae. *J. Biol. Chem.* 285, 16588–16598. doi: 10.1074/jbc.M110.111757

Niu, X., Xing, W., Li, W., Fan, T., Hu, H., and Li, Y. (2012). Isofraxidin exhibited anti-inflammatory effects *in vivo* and inhibited TNF-alpha production in LPS-induced mouse peritoneal macrophages *in vitro* via the MAPK pathway. *Int. Immunopharmacol.* 14, 164–171. doi: 10.1016/j.intimp.2012.06.022

Olsson, M. E., Olofsson, L. M., Lindahl, A. L., Lundgren, A., Brodelius, M., and Brodelius, P. E. (2009). Localization of enzymes of artemisinin biosynthesis to the apical cells of glandular secretory trichomes of *Artemisia annua* L. *Phytochemistry* 70, 1123–1128. doi: 10.1016/j.phytochem.2009.07.009

Paddon, C. J., Westfall, P. J., Pitera, D. J., Benjamin, K., Fisher, K., McPhee, D., et al. (2013). High-level semi-synthetic production of the potent antimalarial artemisinin. *Nature* 496, 528–532. doi: 10.1038/nature12051

Ro, D. K., Paradise, E. M., Ouellet, M., Fisher, K. J., Newman, K. L., Ndungu, J. M., et al. (2006). Production of the antimalarial drug precursor artemisinic acid in engineered yeast. *Nature* 440, 940–943. doi: 10.1038/nature04640

Ruijter, J. M., Ramakers, C., Hoogaars, W. M., Karlen, Y., Bakker, O., van den Hoff, M. J., et al. (2009). Amplification efficiency: linking baseline and bias in the analysis of quantitative PCR data. Nucleic Acids Res. 37:e45. doi: 10.1093/nar/gkp045

Santomauro, F., Donato, R., Sacco, C., Pini, G., Flamini, G., and Bilia, A. R. (2016). Vapour and liquid-phase *Artemisia annua* essential oil activities against several clinical strains of candida. *Planta Med.* 82, 1016–1020. doi: 10.1055/s-0042-108740

Shen, Q., Chen, Y. F., Wang, T., Wu, S. Y., Lu, X., Zhang, L., et al. (2012). Overexpression of the cytochrome P450 monooxygenase (cyp71av1) and cytochrome P450 reductase (cpr) genes increased artemisinin content in *Artemisia annua* (Asteraceae). *Genet. Mol. Res.* 11, 3298–3309. doi: 10.4238/2012.September.12.13

Smith, C. A., Want, E. J., O'Maille, G., Abagyan, R., and Siuzdak, G. (2006). XCMS: processing mass spectrometry data for metabolite profiling using nonlinear peak alignment, matching, and identification. *Anal. Chem.* 78, 779–787. doi: 10.1021/ac051437y

Soetaert, S. S., Van Neste, C. M., Vandewoestyne, M. L., Head, S. R., Goossens, A., Van Nieuwerburgh, F. C., et al. (2013). Differential transcriptome analysis of glandular and filamentous trichomes in *Artemisia annua*. *BMC Plant Biol.* 13:220. doi: 10.1186/1471-2229-13-220

Stacklies, W., Redestig, H., Scholz, M., Walther, D., and Selbig, J. (2007). pcaMethods–a bioconductor package providing PCA methods for incomplete data. *Bioinformatics* 23, 1164–1167. doi: 10.1093/bioinformatics/btm069

Sy, L. K., and Brown, G. D. (2002). The role of the 12-carboxyllic acid group in the spontaneous autoxidation of dihydroartemisinic acid. *Tetrahedron* 58, 909–923. doi: 10.1016/S0040-4020(01)01192-9

Tautenhahn, R., Böttcher, C., and Neumann, S. (2008). Highly sensitive feature detection for high resolution LC/MS. *BMC Bioinformatics* 9:504. doi: 10.1186/1471-2105-9-504

Teoh, K. H., Polichuk, D. R., Reed, D. W., and Covello, P. S. (2009). Molecular cloning of an aldehyde dehydrogenase implicated in artemisinin biosynthesis in *Artemisia annua* botany 87, 635–642. doi: 10.1139/b09-032

Teoh, K. H., Polichuk, D. R., Reed, D. W., Nowak, G., and Covello, P. S. (2006). *Artemisia annua* L. (Asteraceae) trichome-specific cDNAs reveal CYP71AV1, a cytochrome P450 with a key role in the biosynthesis of the antimalarial sesquiterpene lactone artemisinin. *FEBS Lett.* 580, 1411–1416. doi: 10.1016/j.febslet.2006.01.065

Ting, H. M., Wang, B., Rydén, A. M., Woittiez, L., van Herpen, T., Verstappen, F. W., et al. (2013). The metabolite chemotype of Nicotiana benthamiana transiently expressing artemisinin biosynthetic pathway genes is a function of CYP71AV1 type and relative gene dosage. *New Phytol.* 199, 352–366. doi: 10.1111/nph.12274

Wallaart, T. E., Pras, N., Beekman, A. C., and Quax, W. J. (2000). Seasonal variation of artemisinin and its biosynthetic precursors in plants of *Artemisia annua* of different geographical origin: proof for the existence of chemotypes. *Planta Med.* 66, 57–62. doi: 10.1055/s-2000-11115

Wallaart, T. E., Pras, N., and Quax, W. J. (1999). Isolation and identification of dihydroartemisinic acid hydroperoxide from *Artemisia annua*: a novel biosynthetic precursor of artemisinin. *J. Nat. Prod.* 62, 1160–1162. doi: 10.1021/np9900122

Wetzstein, H. Y., Porter, J. A., Janick, J., and Ferreira, J. F. (2014). Flower morphology and floral sequence in *Artemisia annua* (Asteraceae)1. *Am. J. Bot.* 101, 875–885. doi: 10.3732/ajb.1300329

Woerdenbag, H. J., Pras, N., Chan, N. G., Bang, B. T., Bos, R., Vanuden, W., et al. (1994). Artemisinin, related sesquiterpenes, and essential oil in artemisia-annua during a vegetation period in vietnam. *Planta Med.* 60, 272–275. doi: 10.1055/s-2006-959474

Yamazaki, T., and Tokiwa, T. (2010). Isofraxidin, a coumarin component from Acanthopanax senticosus, inhibits matrix metalloproteinase-7 expression and cell invasion of human hepatoma cells. *Biol. Pharm. Bull.* 33, 1716–1722. doi: 10.1248/bpb.33.1716

Yang, K., Monafared, R. S., Wang, H., Lundgren, A., and Brodelius, P. E. (2015). The activity of the artemisinic aldehyde Delta11(13) reductase promoter is important for artemisinin yield in different chemotypes of *Artemisia annua* L. *Plant Mol. Biol.* 88, 325–340. doi: 10.1007/s11103-015-0284-3

Yuan, Y., Liu, W. H., Zhang, Q. Z., Xiang, L. E., Liu, X. Q., Chen, M., et al. (2015). Overexpression of artemisinic aldehyde Delta 11 (13) reductase gene-enhanced artemisinin and its relative metabolite biosynthesis in transgenic *Artemisia annua* L. *Biotechnol. Appl. Biochem.* 62, 17–23. doi: 10.1002/bab.1234

Zhang, Y., Teoh, K. H., Reed, D. W., Maes, L., Goossens, A., Olson, D. J., et al. (2008). The molecular cloning of artemisinic aldehyde Delta11(13) reductase and its role in glandular trichome-dependent biosynthesis of artemisinin in *Artemisia annua*. *J. Biol. Chem.* 283, 21501–21508. doi: 10.1074/jbc.M803090200

Conflict of Interest Statement: The authors declare that the research was conducted in the absence of any commercial or financial relationships that could be construed as a potential conflict of interest.

frontiers in Plant Science

ORIGINAL RESEARCH
published: 29 May 2018
doi: 10.3389/fpls.2018.00547

Silencing *amorpha-4,11-diene synthase* Genes in *Artemisia annua* Leads to FPP Accumulation

*Theresa M. Catania, Caroline A. Branigan, Natalia Stawniak, Jennifer Hodson, David Harvey, Tony R. Larson, Tomasz Czechowski and Ian A. Graham**

Centre for Novel Agricultural Products, Department of Biology, University of York, York, United Kingdom

OPEN ACCESS

Edited by:
Henrik Toft Simonsen, Technical University of Denmark, Denmark

Reviewed by:
Wolfgang Eisenreich, Technische Universität München, Germany
Jiang Xu, China Academy of Chinese Medical Sciences, China

****Correspondence:***
Ian A. Graham
ian.graham@york.ac.uk

Specialty section:
This article was submitted to Plant Biotechnology, a section of the journal Frontiers in Plant Science

Received: *02 February 2018*
Accepted: *09 April 2018*
Published: *29 May 2018*

Citation:
Catania TM, Branigan CA, Stawniak N, Hodson J, Harvey D, Larson TR, Czechowski T and Graham IA (2018) Silencing amorpha-4,11-diene synthase Genes in Artemisia annua Leads to FPP Accumulation. Front. Plant Sci. 9:547. doi: 10.3389/fpls.2018.00547

Artemisia annua is established as an efficient crop for the production of the anti-malarial compound artemisinin, a sesquiterpene lactone synthesized and stored in Glandular Secretory Trichomes (GSTs) located on the leaves and inflorescences. *Amorpha-4,11-diene* synthase (AMS) catalyzes the conversion of farnesyl pyrophosphate (FPP) to amorpha-4,11-diene and diphosphate, which is the first committed step in the synthesis of artemisinin. FPP is the precursor for sesquiterpene and sterol biosynthesis in the plant. This work aimed to investigate the effect of blocking the synthesis of artemisinin in the GSTs of a high artemisinin yielding line, Artemis, by down regulating *AMS*. We determined that there are up to 12 *AMS* gene copies in Artemis, all expressed in GSTs. We used sequence homology to design an RNAi construct under the control of a GST specific promoter that was predicted to be effective against all 12 of these genes. Stable transformation of Artemis with this construct resulted in over 95% reduction in the content of artemisinin and related products, and a significant increase in the FPP pool. The Artemis *AMS* silenced lines showed no morphological alterations, and metabolomic and gene expression analysis did not detect any changes in the levels of other major sesquiterpene compounds or sesquiterpene synthase genes in leaf material. FPP also acts as a precursor for squalene and sterol biosynthesis but levels of these compounds were also not altered in the *AMS* silenced lines. Four unknown oxygenated sesquiterpenes were produced in these lines, but at extremely low levels compared to Artemis non-transformed controls (NTC). This study finds that engineering *A. annua* GSTs in an Artemis background results in endogenous terpenes related to artemisinin being depleted with the precursor FPP actually accumulating rather than being utilized by other endogenous enzymes. The challenge now is to establish if this precursor pool can act as substrate for production of alternative sesquiterpenes in *A. annua.*

Keywords: *Artemisia annua*, artemisinin, sesquiterpene, glandular trichome, amorpha-4,11-diene synthase, farnesyl pyrophosphate

INTRODUCTION

Artemisia annua (A. annua) is a herbaceous plant from the Asteraceae family native to Asia, known to synthesize the leading antimalarial compound artemisinin a sesquiterpene lactone, within its glandular secretory trichomes (GSTs) (Duke et al., 1994; Olsson et al., 2009). The GSTs of *A. annua* are biseriate glandular trichomes made up of 10 cells topped with a secretory sac. The secretory sac is bounded by a cuticle proximal to the three apical pairs of cells. This arrangement allows phytotoxic compounds such as artemisinin to be sequestered away from the plant, preventing autotoxicity (Duke and Paul, 1993; Duke et al., 1994; Ferreira and Janick, 1995). The distribution of *A. annua* GSTs across leaves, stems, and inflorescences, combined with the relative ease of artemisinin extraction using organic solvents, has made feasible the commercial scale growth and processing of whole plants for production of the compound as an active pharmaceutical ingredient in Artemisinin Combination Therapies (ACTs). The efficiency of the *A. annua* production system, which can yield artemisinin at greater than 1% lead dry weight and 41.3 Kg per Ha (Ferreira et al., 2005) has meant that it persists as the most efficient and economically feasible platform for production of artemisinin today. With *A. annua* as the sole source of artemisinin, demands for the drug have influenced farmers on whether to grow the crop or not, leading to large market price fluctuations (highs of $1,100 in 2005 to less than $250 per kilogram in 2007 and again in 2015 (Van Noorden, 2010; Peplow, 2016). A desire to both stabilize and reduce costs in the supply chain has driven research into yield improvement through modern marker assisted plant breeding and genetic engineering methods and through engineering artemisinin (or precursor) synthesis in heterologous hosts (Ferreira et al., 2005; Han et al., 2006; Graham et al., 2010; Zhang et al., 2011; Paddon and Keasling, 2014; Tang et al., 2014; Pulice et al., 2016).

The commercial importance of artemisinin synthesis has stimulated ongoing research into the biosynthetic pathways and metabolic capabilities of *A. annua* GSTs. Transcriptomic analysis of GSTs from *A. annua* has identified multiple genes including cytochrome P450s and terpene synthases, which have been subsequently characterized in detail and their trichome-specific expression patterns confirmed (Olsson et al., 2009; Wang et al., 2009; Graham et al., 2010; Olofsson et al., 2011, 2012; Soetaert et al., 2013). Metabolomic analysis in *A. annua* has identified almost 600 secondary and/or specialized metabolites, whose production can be linked to the expression of the identified synthases (Brown, 2010). This suggests that the GSTs of *A. annua* are highly evolved terpenoid-producing factories, with the potential for producing and storing a diverse range of compounds.

The biosynthesis of terpenoids including artemisinin in *A. annua* starts with the biosynthetic precursors, isopentenyl diphosphate (IPP) and its isomer dimethylallyl diphosphate (DMAPP), which are in turn products of the methyl erythritol phosphate (MEP) and mevalonate (MVA) pathways (Croteau et al., 2000; Weathers et al., 2006; Wu et al., 2006). IPP and DMAPP precursors for the synthesis of farnesyl pyrophosphate (FPP), which is in turn the immediate precursor of both sterols and sesquiterpenes including artemisinin (**Figure 1**). Currently 5 sesquiterpene synthases have been cloned from *A. annua*, *amorpha-4,11-diene synthase* (*AMS*), the first step in artemisinin synthesis (Bouwmeester and Wallaart, 1999); *caryophyllene synthase* (*CPS*) (Cai et al., 2002); *germacrene A synthase* (*GAS*) (Bertea et al., 2006); *δ-epicederol synthase* (*ECS*) (Mercke et al., 1999) and *beta farnesene synthase* (*FS*) (Picaud et al., 2005). The expression of these synthases is shown to be predominantly in GSTs and young leaf tissue (Graham et al., 2010; Olofsson et al., 2011) Other sesquiterpenes such as guaianes, longipinanes, and eudesmanes have also been isolated suggesting the expression of other sesquiterpene synthases (Brown, 2010; Olofsson et al., 2011). These synthases all compete for the precursor FPP, and engineering of the pathway from this point by overexpression of *AMS* (Ma et al., 2009, 2015; Han et al., 2016) or silencing of CPS, BFS, GAS, and ECS (Chen et al., 2011; Lv et al., 2016) has been a strategy for increasing artemisinin production. FPP is also utilized by *squalene synthase* (*SQS*) in the first committed step to sterol synthesis. Silencing of this synthase is shown to remove the sink on FPP from squalene and sterol production resulting in increased artemisinin yield (Yang et al., 2008; Zhang et al., 2009). In these studies flux is altered in the artemisinin pathway leading to increased artemisinin yields when compared to wild type, Ma et al. (2015) and Lv et al. (2016) also show that by manipulating the pathway other endogenous terpenes were also affected.

Czechowski et al. (2016) showed a mutation disrupting the amorpha-4,11-diene C-12 oxidase (CYP71AV1) in the high artemisinin yielding cultivar Artemis, produced a novel sesquiterpene epoxide derivative at levels similar to artemisinin (arteannuin X; 0.3–0.5% of leaf dry weight). This discovery demonstrates the possibility of engineering *A. annua* GSTs to produce alternative, potentially useful, sesquiterpenes at commercially viable levels. GSTs are targeted for engineering based on their ability to synthesize and store specialized metabolites (Huchelmann et al., 2017). Efforts to engineer GSTs reported in the literature include examples in tobacco, and tomato. Tissier et al. (2012) engineered tobacco GSTs to successfully produce casbene and taxadiene, although production was at levels lower than that for endogenous diterpenoids. The engineering of tomato trichomes has also been carried out by expressing sesquiterpene synthases from wild relatives to confer pest resistance (Bleeker et al., 2012; Yu and Pichersky, 2014). Kortbeek et al. (2016) have also used the GSTs of tomato as a platform for engineering sesquiterpenoid production by the overexpression of an avian FPS (farnesyl diphosphate synthase), to increase FPP availability for sesquiterpene production. Engineering of *A. annua* trichomes has been mainly centered on enhancing artemisinin production by constitutively expressing upstream enzymes, artemisinin biosynthetic genes and transcription factors (Tang et al., 2014; Xie et al., 2016; Ikram and Simonsen, 2017). More complex pathway regulation has also been attempted—a patent by Tang et al. (2011) describes a method for using the trichome specific *cyp71av1* promoter to drive both the expression of an *ADS (amorpha-4,11- diene synthase /AMS)* silencing construct and the patchouli alcohol biosynthesis enzyme, to allow the production of patchouli alcohol in *A. annua*.

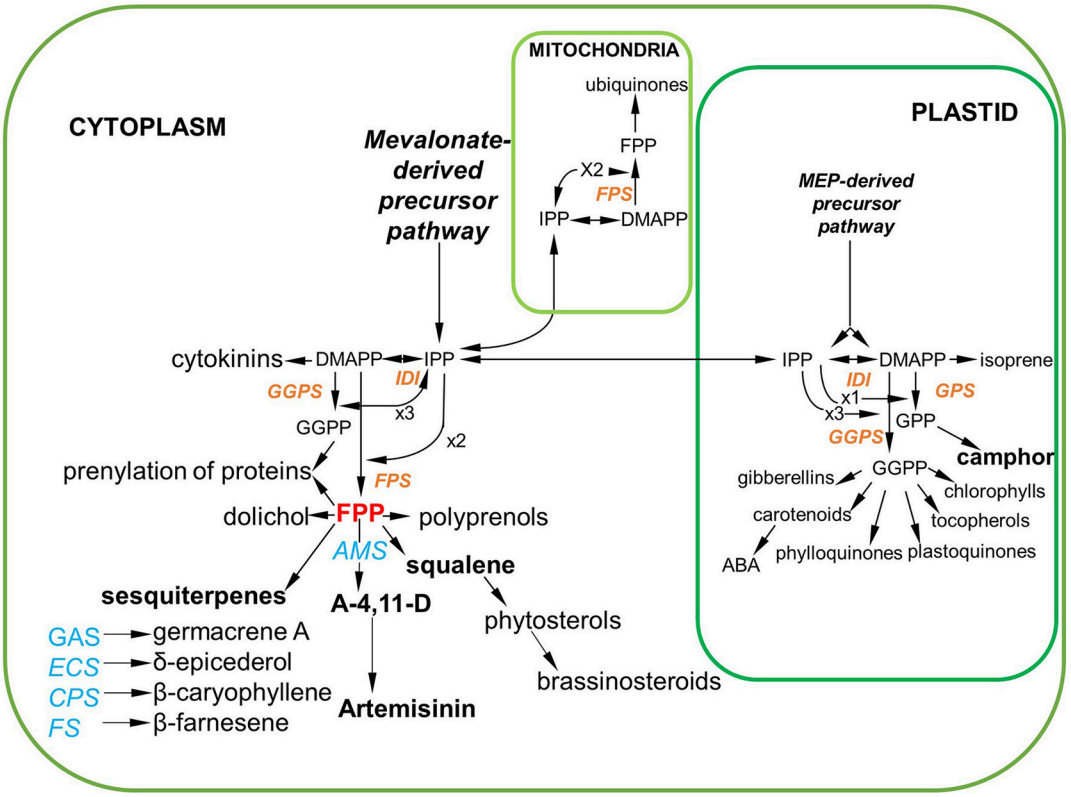

FIGURE 1 | Summary of sesquiterpene production in *Artemisia annua* via the mevalonate (MVA) pathway in the cytosol FPP is highlighted as the key precursor not only for artemisinin synthesis but also for Squalene and other sequiterpenes. The plastidial methyl erythritol phosphate (MEP) pathway that leads to monoterpene production is also included. enzymes in red have been cloned from *A. annua* and the sesquiterpene synthases and squalene synthases also cloned from *A. annua* are in blue (DMAPP, dimethylallyl diphosphate; GGPP, geranyl geranyl diphosphate; GPP, geranyl pyrophosphate; GGPS, geranylgeranyl pyrophosphate synthase; IPP, isopentenyl diphosphate; IDI, isopentyl diphosphate isomerase; ABA, abscisic acid; *FPS, farnesyl diphosphate synthase*; FPP, farnesyl pyrophosphate; *AMS, amorpha-4,11-diene synthase; SQS, squalene synthase; GAS, germacrene A synthase; ECS, δ-epicederol synthase; CPS, caryophyllene synthase; FS, beta farnesene synthase).*

The objective of the current work was to silence AMS in the GSTs of Artemis a high artemisinin yielding cultivar. Silencing of AMS in this background allowed us to investigate how carbon flux through FPP is affected, in contrast to previous studies performed in low-ART yielding systems where alternative products accumulate (Ma et al., 2015; Lv et al., 2016). We demonstrate that removing artemisinin and related compounds elevates the FPP pool with only minor increases in alternative endogenous metabolites. We conclude that such manipulations, done in a carefully selected genetic background, have the potential to provide a clean chemical background for pathway engineering, without detrimental effects on plant growth and development.

METHODS

Plant Material

The *A. annua* cultivar Artemis, an F1 hybrid from Mediplant (Conthey, Switzerland) (described in Graham et al., 2010) was used to generate stably transformed material.

AMS Gene Copy Determination by qPCR

DNA extraction was carried out on 30–50 mg of fresh leaf material harvested from plants growing in the glasshouse and prepared following the methods as described in Graham et al. (2010) and Czechowski et al. (2016).

Three technical replications of a 10 µl reaction containing 1 ng of leaf genomic DNA from single plants, 200 nM gene-specific primers in 1x Power SYBER Green PCR Master Mix (Life Technologies Ltd.), were run on a ViiA7 Real-Time PCR system (Life Technologies Ltd.) The gene specific primers were as follows:

*AMS*_3′endF: TCTACTCGTTTATCCTATGAGTATATGACT ACC
*AMS*_3′endR: GGCTATGCACGAAGGATTGGT
*AMS*_5′endF: TTACCGAAATACAACGGGCAC
*AMS*_5′endR: TTGGCAACCTTTTCCAAAGG

Amplification conditions and data normalization were as described in Czechowski et al. (2016).

RNA Isolation and cDNA Synthesis

Fresh young leaf material (leaves 1–5) (30–50 mg) from 12-week-old glasshouse grown cuttings was harvested and flash frozen in

liquid nitrogen for RNA extraction. The extraction was carried out using the Qiagen RNAeasy kit following the manufacturer's plant protocol including the on column Qiagen DNase treatment. Extracted RNA was quantified spectrophotometrically using the NanoDrop-8000 (NanoDrop products). cDNA was synthesized from 3 μg of the extracted RNA using Invitrogen superscript II reverse transcriptase kit (Thermo Fischer Scientific) using the oligo (dT) primer following the manufacturers protocol.

Construction of hpRNA Vector Targeting the AMS Gene

Two sections of the *AMS* gene (AF138959) from bases 96–192 and 1485–1615 were selected and joined to create a 227 bp sequence which was checked for its specificity to the *AMS* target relative to other sesquiterpene synthases from *A. annua* (Mercke et al., 1999; Cai et al., 2002; Picaud et al., 2005; Bertea et al., 2006; Supplemental Figure 1). This sequence was then placed in a forward and reverse direction either side of the Chalcone synthase A intron (petunia hybrida) to create a hairpin construct (Watson et al., 2005), this was driven by the trichome specific promoter *cypav171* (Wang et al., 2011). The full construct was synthesized by GENEART Thermo life technologies. The 3.8 kb construct was cloned into the pRSC2 binary vector and transformed into stratagene solopack gold competent cells. The resulting colonies were tested by PCR using Promega Gotaq and primers designed for the pRSC2 vector.

AP1435 pRSC2_activ	TAACATCCAACGTCGCTTTCAG
AP1436 pRSC2_RB_in	GCCAATATATCCTGTCAAACAC

Positive colonies were confirmed by sequencing and the binary vector was then transferred into *Agrobacterium tumefaciens* (LBA4404) by electroporation and 100 μl glycerol stocks set up for subsequent transformations. Forty eight hours prior to transformation the agrobacterium pre-cultures were set up from glycerol stocks in Luria-Bertani broth (LB) including antibiotic selection (50 mg/L rifampicin, spectomycin and streptomycin). After 24 h, a 50 ml main culture was set up and allowed to grow overnight to an optical density (OD) of between 0.3 and 0.8. At this stage the cultures were spun down and resuspended in co-cultivation media (Murashige and Skoog medium (MS) with 3% sucrose and 100 uM acetosyringone) to an OD of 0.2. The culture was then left to shake at 28 °C for 2 h.

Artemisia annua Transformation

Artemis seed were surface sterilized for 1 h using chlorine vapor [3% HCL in water + one presept tablet (Advanced sterilization products)] in a sealed box. Seeds were sown into sterile glass jars on MS basal media containing 3% sucrose, 1x MS vitamins and 0.8% plant agar. After sowing the jars were closed and sealed with parafilm and transferred to a growth room 16 h daylength at 29°C to germinate and grow for 2.5 weeks.

The first true leaves of 2.5-week-old seedlings were excised and immersed in petri dishes into either an agrobacterium suspension, or for non-transformed controls (NTC), co-cultivation media without agrobacterium, and placed on a rotary platform. After 15 min, the explants were blotted on sterile filter paper and transferred to labeled co-cultivation plates (MS with 3% sucrose and 100 *u*M acetosyringone +0.8% plant agar) the plates were wrapped in foil and stored in the growth room at 25°C. After 48 h the explants were transferred to selection plates (MS medium with 3% sucrose, 0.5 mg/L 6-benzylaminopurine (BAP) and 0.05 mg/L α-naphthalene acetic acid (NAA), 0.8% agar, 500 mg/L carbenicillin and 15 mg/L kanamycin. NTC explants were plated out without kanamycin selection. Explants were transferred to fresh plates after a week and thereafter every 2 weeks. Shoots were excised from the plates as they emerged and placed onto shooting medium in jars (MS medium with 3% sucrose, 0.5 mg/L BAP, and 0.05 mg/L NAA, 0.8% plant agar, 500 mg/L carbenicillin, 15 mg/L kanamycin), and transferred on every 3 weeks. NTC shoots were placed into shooting medium containing no antibiotic. Once the shoots were well-established they were transferred to rooting medium (1/2 MS medium, 1% sucrose, 0.6% plant agar, 500 mg/L carb, 15 mg/L kanamycin, (NTCs with no antibiotics). Once roots had begun to appear, the shoots were transferred to F2+S compost in P40s and kept in green propagator trays with lids on to maintain humidity. Once well rooted the plants were hardened off and transferred to 4-inch pots in F2 compost and grown in glasshouse facilities at the University of York under long day conditions maintained with supplemental lighting and temperature between 22 and 25°C. Putatively transformed lines were confirmed by PCR for the presence of the NPTII gene using the Phire plant direct PCR kit (Thermo Fisher Scientific). Transformed plants alongside NTCs were propagated via cuttings and grown in triplicate for 12 weeks to provide material for DNA and RNA extractions and for metabolite profiling by UPLC-MS and GC-MS.

Quantitative RT-PCR

Expression levels of *amorpha-4,11-diene synthase* (AMS), squalene synthase (SQS), germacrene A synthase (GAS); δ-epicederol synthase (ECS); beta farnesene synthase (BFS); and caryophyllene synthase (CPS) relative to ubiquitin (UBI; Genbank accession: GQ901904) were determined by quantitative RT-PCR. Expression levels of each gene were determined for cDNA from NTC and transformed young leaf material prepared as described above (section AMS Gene Copy Determination by qPCR). Gene-specific primers used were:

*AMS*_For	5′- GGGAGATCAGTTTCTCATCTATGAA- 3′
*AMS*_Rev	5′- CTTTTAGTAGTTGCCGCACTTCTT-3′
*CPS*_For	5′-CAACGATGTAGAAGGCTTGCTTGA-3′
*CPS*_Rev	5′-GTAGATAGTGTTGGGTTGGTGTGA-3′
*ECS*_For	5′-GCAACAAGCCTACGAATCACTCAA-3′
*ECS*_Rev	5′-CGTGAAAAATTAAGGACCCTCATAG-3′
*GAS*_For	5′-CTCGTTACTCCTTGGCAAGAATCAT-3′
*GAS*_Rev	5′-GCTCCATAGCACTAATATCCCACTT-3′
*SQS*_For	5′-GACCAGTTCCACCATGTTTCTACT-3′
*SQS*_Rev	5′-GCTTTGACAACCCTATTCCAACAAG-3′
*FS*_For	5′-GCAAAAGAGTTGGTTCGCAATTAC-3′
*FS*_Rev	5′-GTACCCCTCTTTTAGCCATCTGG-3′
*UBI*_For	5′-TGATTGGCGTCGTCTTCGA-3′
*UBI*_Rev	5′-CCCATCCTCCATTTCTAGCTCAT-3′

Amplification conditions and data analysis were as described in Graham et al. (2010) and Czechowski et al. (2016).

Metabolite Analysis by UPLC-MS and GC-MS

Three replicate cuttings from the NTC and each transformed line were grown in 4-inch pots under 16-h days for 12 wk. Metabolite profiles were generated from 50 mg fresh weight pooled samples of leaves at young (first emerging leaf to leaf 6) or mature (the tips of leaves 11–13) developmental stages the fresh leaf samples collected were stored at −80°C. Dry leaf material was obtained from 18-week-old plants, cut just above the zone of senescing leaves, and dried for 14 d at 40°C. Leaves were stripped from the plants, and leaf material was sieved through 5-mm mesh to remove small stems. Trichome-specific metabolites (Supplemental Figure 2) were extracted and analyzed as previously described (Graham et al., 2010; Czechowski et al., 2016).

Architecture and Leaf Traits and Trichome Density

Height, leaf area and trichome density were also measured on the NTC and transformed lines as described in Graham et al. (2010).

FPP Quantification

FPP quantification was carried out on isolated GSTs and young leaf material using pooled leaf tips (meristem to leaf 6) collected from the apical meristem and each axillary branch counting down to the axillary branch at leaf position 20. Glandular trichomes were isolated as described in Graham et al. (2010). The young leaf material was ground under liquid nitrogen and 1 gram weighed out for extraction. Both the isolated trichomes and the ground leaf were extracted in methanol:water (7:3, v/v), including a total of 0.3 μg farnesyl S-thiolodiphosphate (FSPP; Echelon Biosciences) added as an internal standard. Extracts were processed according to Nagel et al. (2014). Briefly, each extract was passed through a Chromabond HX RA column (150 mg packing), which had first been conditioned with 5 ml methanol and 5 ml of water, and compounds eluted under gravity with 3 ml of 1 M ammonium formate in methanol. The eluate was evaporated under a stream of nitrogen to dryness, dissolved in 250 μL of water:methanol (1:1.v/v), and a 2 μL aliquot injected on a Waters Acquity I-Class UPLC system interfaced to a Thermo Orbitrap Fusion Tribrid mass spectrometer under Xcalibur 4.0 control. Compounds were eluted on a Waters Acquity C18 BEH column (2.1 mm × 100 mm, 1.7 μm) at 50°C using the following binary gradient program: solvent A = 20 mM ammonium bicarbonate + 0.1% triethylamine; solvent B = 4:1 acetonitrile:water + 0.1% triethylamine; flowrate 0.4 ml/min; 0–100% B linear gradient over 4 min. Post-column, compounds were ionized using a heated electrospray source (vaporizer = 358°C; N_2 flows for sheath/aux/sweep = 45/13/1 arbitrary units; source = 2.5 kV; ion transfer tube = −30 V and 342°C; tube lens = −40 V). Data was acquired in full scan mode with the following settings: orbitrap resolution = 15 k, 100–500 m/z range, max ion time 100 ms, 1 microscan, AGC target = 200,000, S-Lens RF Level = 60. FPP eluted at ∼2.4 min and the internal standard (FSPP) at ∼2.5 min. The deprotonated pseudomolecular ions ($[M\text{-}H]^-$) of 381.1227 and 397.0998 for FPP and FSPP, respectively, were used for quantification (±5 ppm window) against a 0.1–100 μM linear FPP/FSPP response ratio calibration curve ($R^2 = 0.99$), using Xcalibur 4.0 software (Thermo). For less complex trichome-only samples, a Thermo LTQ Orbitrap Classic instrument was used in ion trap mode.

Sterol Quantification

A 200 mg sample of pooled leaf material from the NTC and AMS silenced lines was ground and extracted by sonication in dichloromethane as described by Zhang et al. (2009). Extracts were centrifuged, the upper phase collected and a 1 uL aliquot analyzed by GC-MS as described in Czechowski et al. (2016), except that the final GC oven temperature and hold time were increased to 350°C and 8 min, respectively, to ensure elution of sterols and squalene. ChomaTof 4.0 software (Leco) was used for spectral processing, to produce deconvoluted spectra for identification against the NIST 2014 database and authentic standards. ChromaTof-selected unique masses were used to generate and integrate peak areas under selected ion traces for quantification against authentic sterol and squalene standards.

Data Analysis

Peak lists for UPLC-MS and GC-MS data were obtained and processed using bespoke R scripts as described in Czechowski et al. (2016). Data from GC-MS and UPLC-MS for the young mature and dried leaf were analyzed by ANOVAs using GENSTAT software (VSN international) with the Bonferroni *post-hoc* test ($p \leq 0.05$) to compare between NTC and transformed lines.

RESULTS

Silencing the First Committed Step in Artemisinin Production Results in Accumulation of the Sesquiterpene Precursor FPP in Glandular Secretory Trichomes of *A. annua*

The *Amorpha-4,11-diene synthase* (*AMS*) enzyme responsible for catalyzing the first committed step in artemisinin production is encoded by a small gene family averaging 12 copies in the Artemis F1 hybrid variety (**Figure 2**). We built a hairpin-based gene silencing construct that included regions showing the least amount of sequence variation to maximize the sequence homology and thus silencing effect across all the members of the gene family (Supplemental Figure 1 of *AMS* ORF consensus sequence). The trichome specific promoter of the *cyp7av1* gene (Wang et al., 2011) was used to drive expression of the *AMS* gene silencing construct in-planta. *Agrobacterium tumefaciens* based transformation was used to generate three independent transgenic lines expressing the *cyp71av1::AMS*_RNAi construct in Artemis. Phenotypically the *AMS* silenced lines showed no significant differences when compared to NTCs in terms of height, branch number and leaf total dry weight (Supplemental

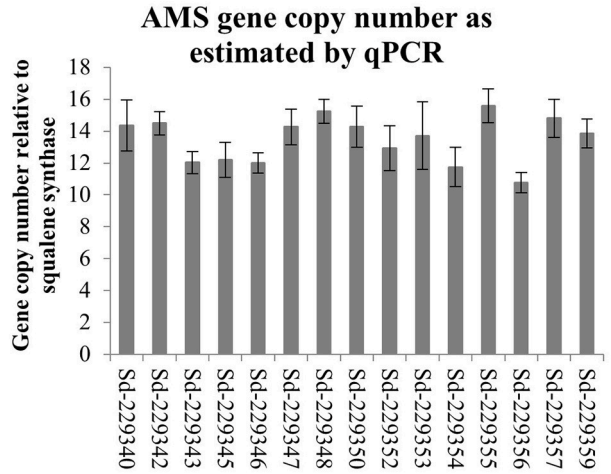

FIGURE 2 | *AMS* gene copy number in 15 individual lines of the *A. annua* cultivar Artemis estimated by qPCR. Error bars represent standard error ($n = 4$). Sd prefixed numbers represent individual Artemis plants.

Figure 3). Presence of the transgene was determined by PCR using primers designed to detect the *NPTII* selectable marker gene (**Figure 3A**). Q-RT-PCR revealed that there is a major reduction in steady state levels of *AMS* mRNA in all of the *AMS* silenced lines carrying the gene silencing construct (**Figure 3B**). This was mirrored by a dramatic decrease in artemisinin concentration in young, mature and dry leaves of the *AMS* silenced lines compared to the NTCs (**Figure 3C**). Amorpha 4-11-diene levels were found to be higher in young leaf tissue when compared to the mature and dry leaf material in both the NTC and AMS silenced lines with two of the lines showing a significant increase compared to the NTC control (**Figure 4A**). There was a significant reduction in all other intermediates downstream of amorpha 4-11-diene in the *AMS* silenced lines compared to NTC (**Figure 4**).

Quantification of farnesyl diphosphate (FPP) in methanolic extracts from ground young leaf tips revealed a significant increase in *AMS* silenced lines compared to the NTCs (**Figure 5A**). This increase was also confirmed in isolated trichomes (**Figure 5B**).

The Consequence of FPP Increases on Known Sesquiterpene Synthase and Squalene Synthase Gene Expression

The effect of silencing *AMS* on the expression of the other known sesquiterpene synthases and squalene synthase (detailed in **Figure 1**) was investigated by carrying out qRT-PCR on young leaf material (**Figure 6**). In the NTC the expression levels of *SQS*, *GAS*, *ECS*, *CPS,* and *FS* was found to be ∼3- times lower than *AMS*. In the *AMS*_silenced lines *SQS* and *GAS* become the most highly expressed synthases although in comparison to the NTC they were not significantly increased. Comparison of expression of *SQS, GAS, ECS, CPS,* and *FS* between the NTC and *AMS*_silenced lines showed they are all lower in the latter except for *GAS* expression in the *AMS* silenced line, *AMS*_ RNAi_1 and

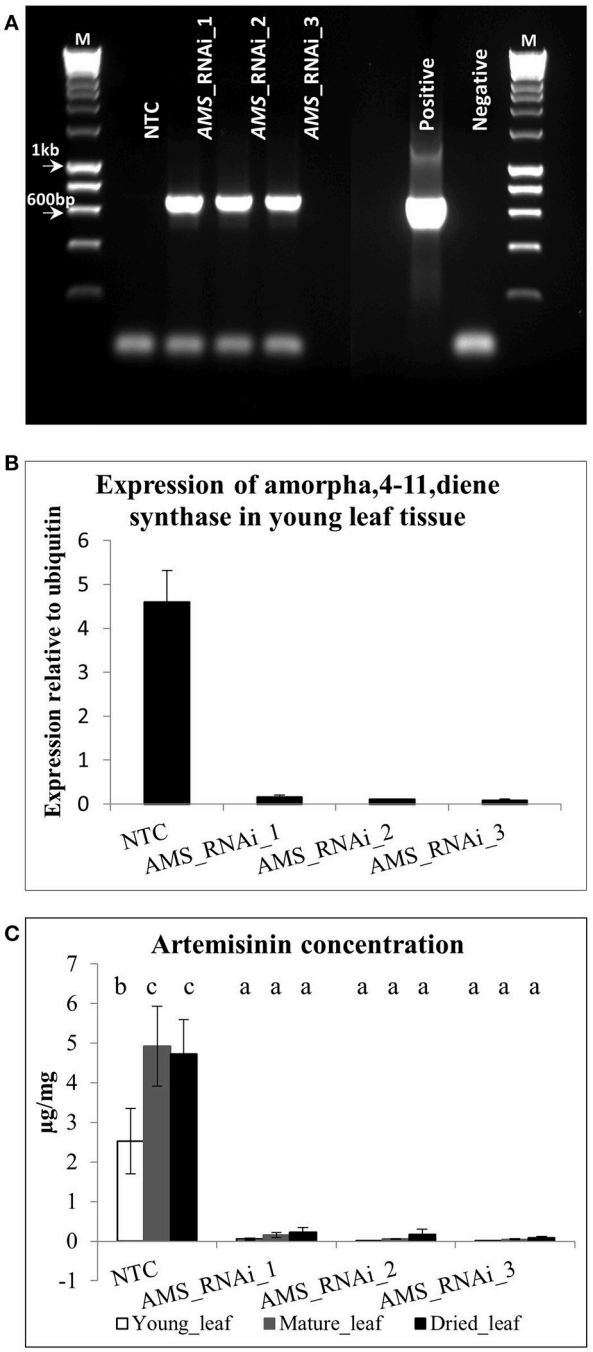

FIGURE 3 | (A) PCR results for *NPTII* primers M − 1 kb hyperladder™ (Bioline), **(B)** Q-RT-PCR of AMS gene expression and **(C)** Artemisinin concentration (µg/mg extracted dry weight) in young and mature leaves and dried pooled leaf material for the NTC and *AMS* silenced lines. Error bars ±SD (NTC—$n = 6$, *AMS*_RNAi lines—$n = 3$). Letters represent Bonferroni test results after ANOVA, groups not sharing letters indicate statistically significant differences ($p \leq 0.05$).

ECS expression in the *AMS* silenced *AMS*_RNAi_3. However, these slight differences in gene expression between NTC and the *AMS* silenced lines were not found to be significant.

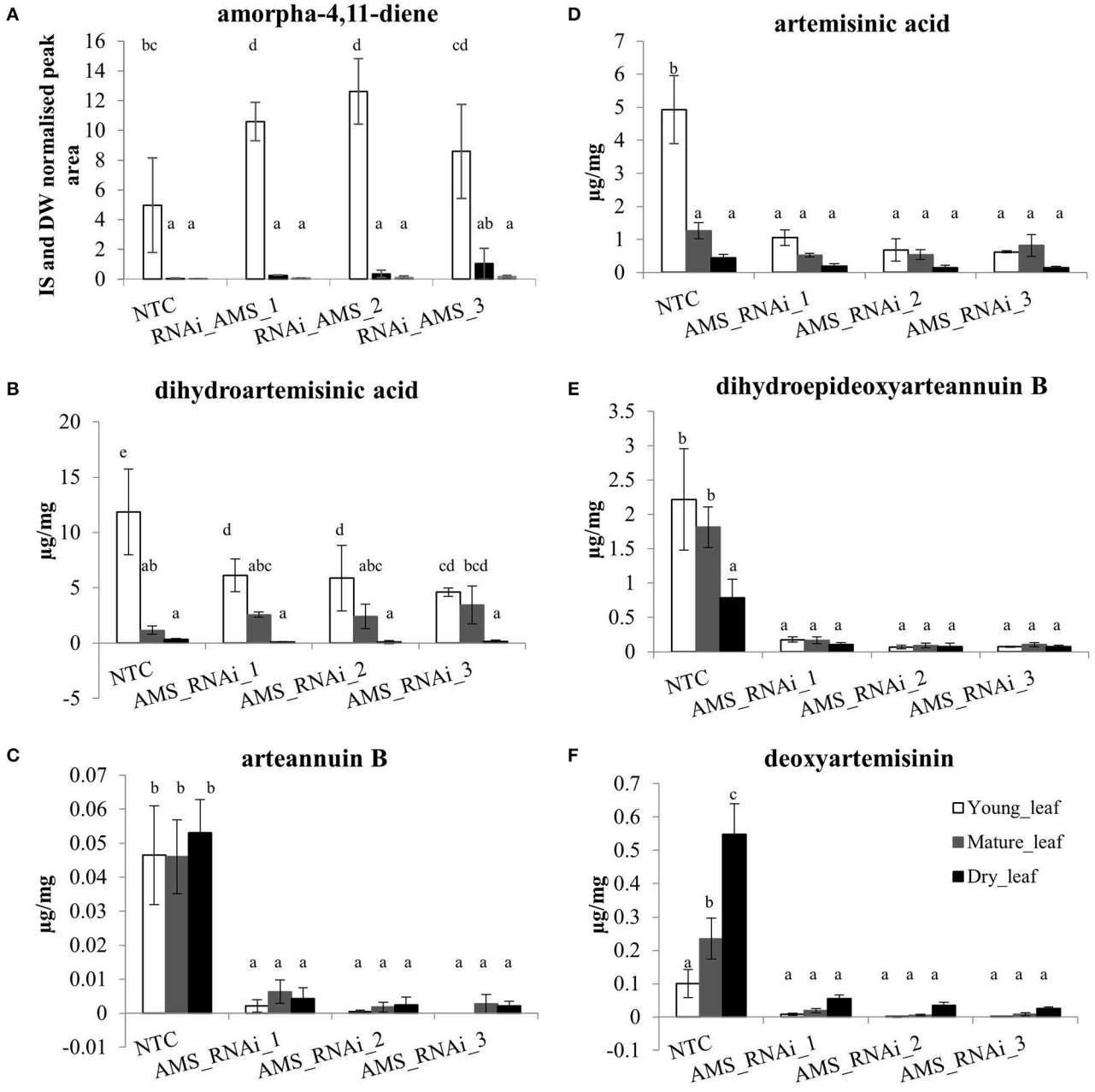

FIGURE 4 | The concentration (µg/mg extracted dry weight) of known artemisinin pathway compounds in young leaves, mature leaves and dried pooled leaf material for NTC and *AMS*_RNAi lines. **(A)** amorpha-4,11-diene, **(B)** artemisinic acid, **(C)** dihydroartemisinic acid, **(D)** dihydroepideoxyarteannuin B, **(E)** arteannuin B, **(F)** deoxyartemisinin. Error bars ±SD (NTC—$n = 6$, *AMS*_RNAi lines—$n = 3$). Letters represent Bonferroni test results after ANOVA, groups not sharing letters indicate statistically significant differences ($p \leq 0.05$).

The Downstream Effect of Increased FPP Levels on Sterol and Sesquiterpene Synthesis in Artemis as Quantified by GC-MS and UPLC

In *A. annua* FPP is a precursor for not only artemisinin and other sequiterpenes but also squalene and sterols and these could all therefore be additional sinks for FPP that does not flux into the artemisinin pathway via *AMS* (**Figure 1**). To determine if the silencing of *AMS* led to a redirection of FPP flux, squalene and sterol levels were quantified from dried leaf material by GC-MS. Squalene, stigmasterol, β-sitosterol and campesterol were identified in both the NTC and transformed lines (**Figure 7**). Stigmasterol and β-sitosterol were present at higher levels in comparison to squalene and campesterol but overall no significant

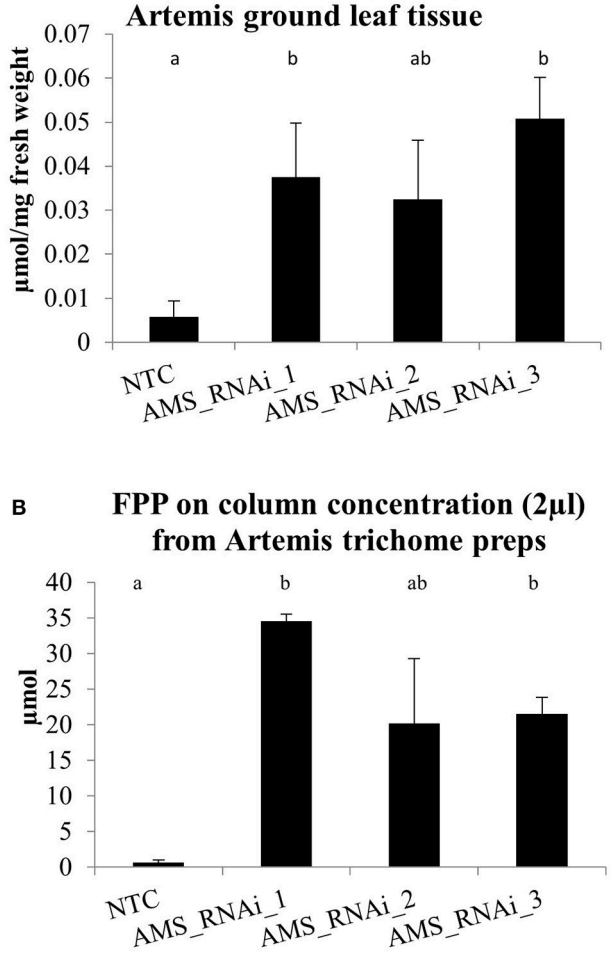

FIGURE 5 | (A) FPP concentrations in µmol/g for ground young leaf material for the Artemis NTC and Artemis *AMS* silenced lines (concentrations were measured on Thermo Orbitrap Fusion Tribrid mass spectrometer). Error bars ±SD (NTC—$n = 6$, *AMS*_RNAi lines—$n = 3$). **(B)** On column FPP concentrations in µmol measured from isolated trichome extracts for Artemis NTC and Artemis *AMS* silenced lines (concentrations were measured on a Thermo LTQ Orbitrap Classic instrument, used in ion trap mode). Error bars ±SD (NTC—$n = 6$, *AMS*_RNAi lines—$n = 3$). Letters represent Bonferroni test results after ANOVA, groups not sharing letters indicate statistically significant differences ($p \leq 0.05$).

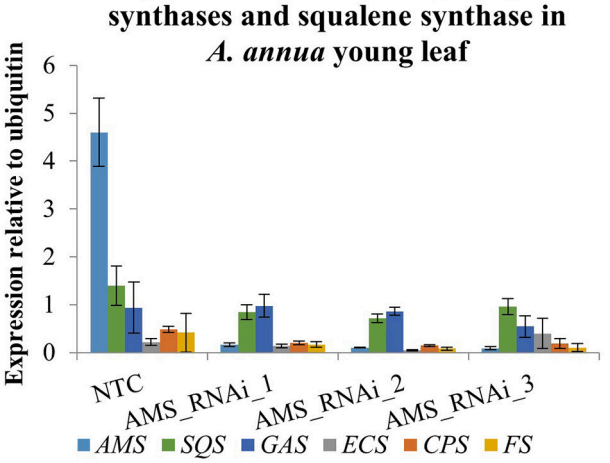

FIGURE 6 | Expression of functionally characterized sesquiterpene synthase (*AMS*, *GAS*, *ECS*, *CPS*, and *FS*) and *SQUALENE SYNTHASE* (*SQS*) genes in young leaf tissue from NTC and *AMS* silenced lines. Error bars ±SD (NTC—$n = 6$, *AMS*_RNAi lines—$n = 3$).

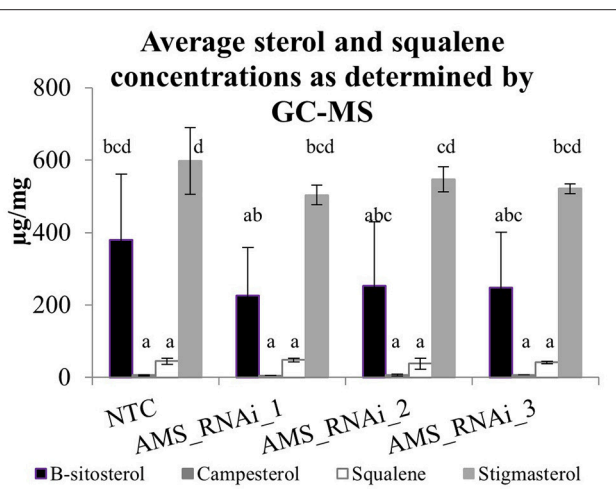

FIGURE 7 | Average peak area from GC-MS for squalene and sterol compounds identified from dried pooled leaf material for NTC and *AMS* silenced lines. Error bars ±SD (NTC—$n = 6$, *AMS*_RNAi lines—$n = 3$). Letters represent Bonferroni test results after ANOVA, groups not sharing letters indicate statistically significant differences ($p \leq 0.05$).

differences were found between the NTC and the *AMS* silenced lines.

To determine if *AMS* silencing led to an increase in sesquiterpenes other than artemisinin, GC- and UPLC-MS analysis was carried out on fresh, young, and mature leaf material, and pooled dried leaf material. From the GC-MS analysis of NTC and transformed lines, 105 compounds were identified, 30 of which were sesquiterpenes. Comparisons between the leaf material sampled (young/mature/dried) revealed the level of sesquiterpenes to be higher in the young leaf samples in comparison to the mature and dried leaf material (Supplemental Table 1). Further statistical analysis to investigate differences between the 3 *AMS* silenced lines and the NTC found that for 17 of the sesquiterpene compounds levels were significantly higher in the NTC. Significant increases in the *AMS* silenced lines were found for only 6 sesquiterpene compounds (Supplemental Table 1). In young leaf material these were: beta-farnescene and germacrene; in mature leaf there were increases in 2 unknown compounds with putative $C_{15}H_{24}$ formulae, and in dried leaf material germacrene D and ledene oxide were significantly higher (**Figure 8**). For the other 7 sesquiterpene compounds no differences were observed.

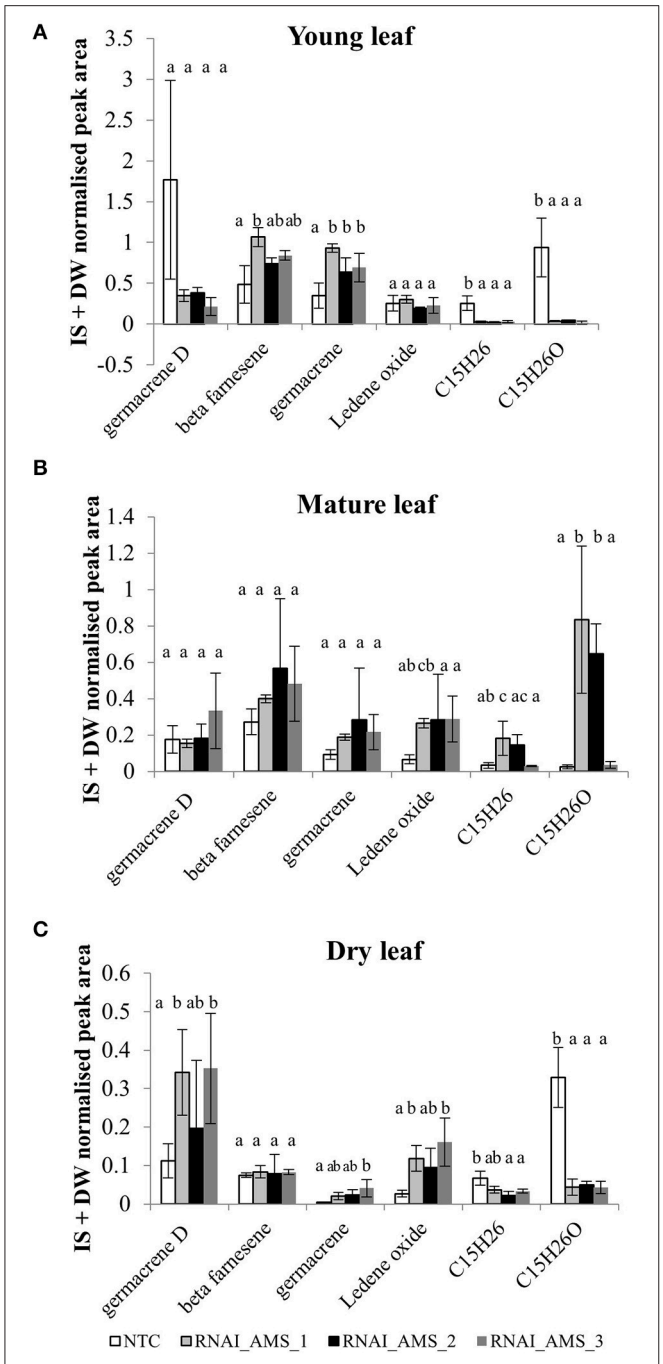

FIGURE 8 | Internal standard (IS) and dry weight normalized peak area averages for sesquiterpene levels in **(A)** young leaf, **(B)** mature leaf, and **(C)** -pooled dried leaf material in NTC and *AMS* silenced lines. Error bars ±SD (NTC—$n = 6$, *AMS*_RNAi—$n = 3$). Letters represent Bonferroni test results after ANOVA, groups not sharing letters indicate statistically significant differences ($p \leq 0.05$).

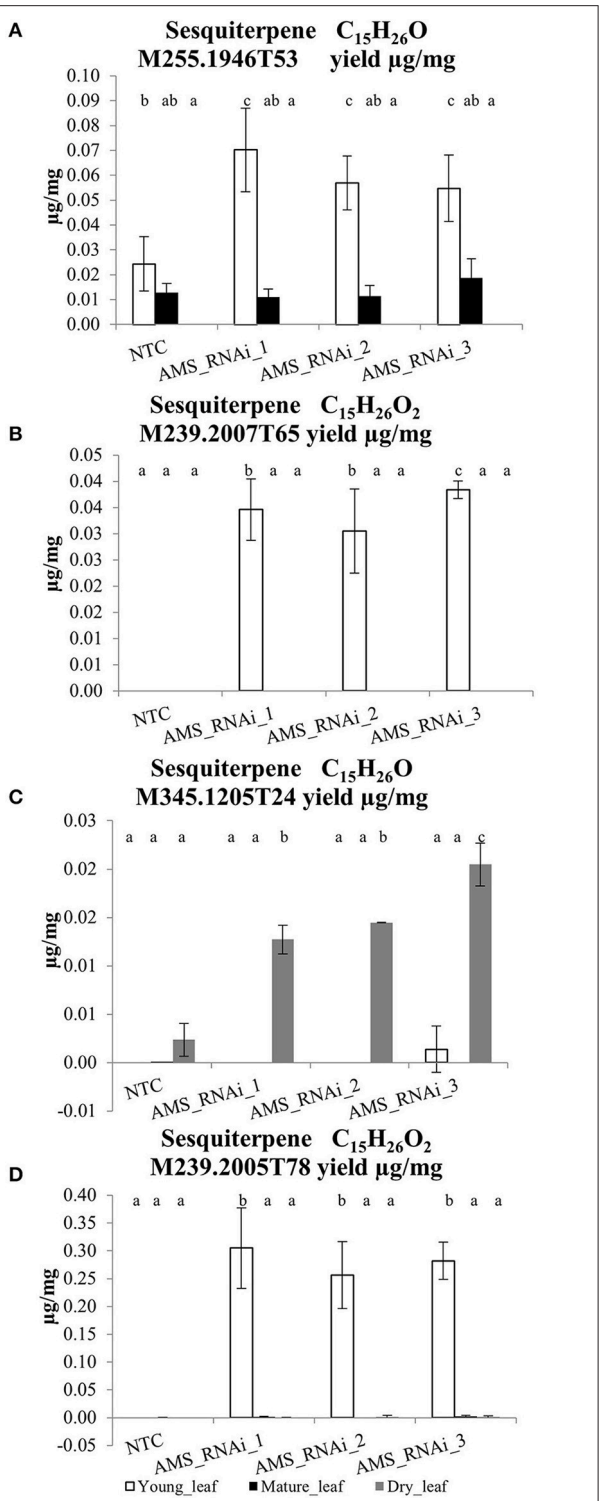

FIGURE 9 | The concentration (µg/mg extracted dry weight) of putative novel sesquiterpene compounds in young and mature leaves and dried pooled leaf material for the *AMS* silenced lines and NTCs. **(A)** sesquiterpene M255.1946T53, **(B)** sesquiterpene M345.1205T24, **(C)** —M239.2007T65, and **(D)** —sesquiterpene M239.2005T78 Error bars ±SD (NTC—$n = 6$, *AMS*_RNAi lines—$n = 3$). Letters represent Bonferroni test results after ANOVA, groups not sharing letters indicate statistically significant differences ($p \leq 0.05$).

As well as artemisinin and its associated compounds derived from the artemisinin pathway, the UPLC-MS analysis also identified four putative novel oxygenated sesquiterpene ($C_{15}H_{24}O$) compounds in the *AMS* silenced lines. These

compounds were identified as being significantly increased although the levels at which they were present was very low, ranging from 0.03- to 0.4 μg/mg DW which is 100–10 times (respectively) lower than artemisinin levels (**Figure 9**). Putative sesquiterpenes: M255.1946T53 M239.2007T65 and M239.2005T78 were all found to be significantly increased in young leaf tissue in the transformed lines in comparison to the NTC. M345.1205T24 was found to be significantly increased in only the dried leaf tissue of the *AMS* silenced lines in comparison to the NTC.

DISCUSSION

Silencing AMS Leads to Accumulation of the Sesquiterpene Precursor FPP in *A. annua* GSTs

In *A. anuua* the first committed step in the artemisinin pathway converting FPP to amorpha-4,11-diene is *AMS*. It was hypothesized that by blocking this step FPP would either accumulate or be channeled into the production of known or novel sesquiterpenes. Previous work had shown that *AMS* was not only highly expressed in the Artemis cultivar, but that recovered *AMS* gene sequences were polymorphic (Graham et al., 2010). This indicated that multiple copies of the gene could exist which we confirmed by qPCR (**Figure 2**). The high copy numbers for *AMS* present in the *A. annua cv.* Artemis could be linked to its high artemisinin yield, and its success as an elite hybrid for commercial production of artemisinin (Delabays et al., 2001). To effectively silence all the *AMS* copies two separate sections of the sequence were selected and joined to create an *AMS* specific sequence, this was driven by the *cyp71av1* trichome specific promoter (Wang et al., 2011). Stably transformed lines expressing the construct were achieved, with *AMS* expression reduced to less than 4% of the NTC. Artemisinin content was reduced by 95% alongside a reduction in all artemisinin-related compounds downstream of the *AMS*-catalyzed step.

One exception was amorpha-4,11-diene where levels were found to be significantly higher in young leaf tissue of the *AMS* silenced lines compared to the NTC (**Figure 4A**). No such increase was present in mature or dry leaves. The levels of amorpha-4,11-diene in *A. annua* are reported to be low as a consequence of artemisinin biosynthesis (Bouwmeester and Wallaart, 1999). Detection of this early step precursor in young leaves of NTC is consistent with previous findings (Czechowski et al., 2016) which suggest the pathway to artemisinin only becomes active as leaves mature. The increase in the *AMS* silenced lines is unexpected and the reason not obvious—but could relate to the metabolic sink being somehow further compromised as a result of the decreased *AMS*.

To establish the impact of silencing *AMS* on FPP levels we adapted a protocol from Nagel et al. (2014) that allowed us to quantify this important precursor for the first time in *A. annua*. We found that silencing of *AMS* led to a significant accumulation of FPP in young leaf tissue and this increase was also confirmed as being trichome specific by carrying out the same extraction on young leaf isolated GSTs (**Figures 5A,B**).

The Downstream Effect of Increased FPP Levels on Sterol and Sesquiterpene Synthesis in Artemis as Quantified by UPLC-MS and GC-MS

Increasing FPP by knocking down *AMS* had no effect on the expression of any of the other known sesquiterpene synthases genes or squalene synthase known to be expressed in either the GSTs or young leaf tissue (**Figure 6**). UPLC-MS and GC-MS analysis of leaf material was carried out to determine if the FPP accumulating in the AMS silenced lines was being redirected into sterol or sesquiterpene production. GC-MS analysis found no significant differences in squalene and sterol levels between the NTC and the *AMS* silenced lines (**Figure 7**) despite this pathway being considered the main competitor for FPP after artemisinin (Zhang et al., 2009). The GC-MS analysis also revealed very few changes in volatiles in the *AMS* silenced lines (Supplemental Table 1). Where significant differences were observed the magnitude, changes were very low (**Figure 8**). These results differ to the findings of Ma et al. (2015) who silenced *AMS* in a low artemisinin background (artemisinin yields of 0.025 μg/mg). Alongside reporting a decrease in artemisinin, they also found a significant increase in the levels of caryophyllene and copaene in their *AMS* silenced plants. The increase in these sesquiterpene compounds could be linked to the low artemisinin cultivar used for transformation having other active endogenous sesquiterpene synthases. In Artemis a high yielding cultivar the endogenous synthases would appear not to be as active in their ability to utilize the FPP made available away from artemisinin being silenced.

Although no differences were seen in known sesquiterpene levels in the AMS silenced lines, putative novel sesquiterpene compounds were detected and characterized by UPLC-MS. Significant differences were seen between Artemis NTCs and the *AMS* silenced lines for 4 putative sesquiterpene compounds although the concentrations were around 30 times lower than artemisinin. The compounds were also mainly identified in young leaf tissue suggesting that these compounds are not end products but rather are further converted as the leaf matures. Compound M345.1205T24 was an exception to the other 3 as it was found in dried leaf only. The very low concentrations of these novel compounds in available plant material ruled out structural determination attempts by NMR.

The lack of diversion of the accumulated FPP to other sesquiterpenes or sterols in the *AMS* silenced lines is somewhat surprising. One possible explanation for this is that the Artemis hybrid has been selected for high yield artemisinin and the flux of FPP may already be optimized to flow toward artemisinin production.

Trichomes With Elevated FPP as a Potential Production Platform for High Value Sesquiterpenes

A. annua is already established as a very efficient crop plant for artemisinin production, with the potential to produce this high value chemical at a relatively low cost of less than $250 per kilogram. Disruption of *cyp71av1*, leading to novel arteannuin

X accumulation demonstrated the plasticity of GST metabolism in *A. annua*, suggesting their potential as factories for new compound production (Czechowski et al., 2016). The GSTs provide an optimal environment for the synthesis of many natural products based on the availability of precursors, co-enzymes, mRNA and protein processing. In *A. annua* the problem of toxicity of some of these compounds is overcome as the GSTs can sequester them in the extracellular cavities of the trichome secretory cells. This coupled with the location of the GSTs on the surface of leaves is advantageous as the compounds are both contained and readily extractable.

By silencing *AMS* in a high artemisinin yielding *A. annua* cultivar we have significantly decreased the amount of artemisinin and related compounds produced in the GSTs. As a further result of the silencing we also show that the precursor FPP is accumulated in the GSTs and not catalyzed by endogenous synthases. The lack of production of novel compounds at significant amounts suggests that the elevated pool of GST localized FPP is either not available to or not utilized by other sesquiterpene, squalene synthase enzymes. Consequently, the *AMS* silenced lines may represent a platform for production of other high value compounds that require FPP as a precursor and for which genes encoding biosynthetic enzymes are known.

AUTHOR CONTRIBUTIONS

TC, TMC, and IG designed the experiments; TC, TMC, CB, NS, JH, and DH performed the experiments; TMC, TC, CB, DH, and TL analyzed the data; TMC, TC, TL, and IAG wrote the manuscript; and all authors revised and approved the manuscript.

FUNDING

We acknowledge financial support for this project from The Bill and Melinda Gates Foundation as well as from The Garfield Weston Foundation.

ACKNOWLEDGMENTS

We thank the University of York horticulture team for horticultural assistance; C. Calvert, W. Lawley, for project management; D. Rathbone and S. Heywood for preliminary experimental involvement. We thank X. Simonnet and Médiplant for access to the Artemis pedigree. Mass spectrometry analysis was in part supported by instrumentation within the York Centre of Excellence in Mass Spectrometry (CoEMS). The CoEMS was created thanks to a major capital investment through Science City York, supported by Yorkshire Forward with funds from the Northern Way Initiative, and subsequent support from EPSRC (EP/K039660/1; EP/M02 8127/1).

SUPPLEMENTARY MATERIAL

The Supplementary Material for this article can be found online at: https://www.frontiersin.org/articles/10.3389/fpls.2018.00547/full#supplementary-material

REFERENCES

Bertea, C. M., Voster, A., Verstappen, F. W., Maffei, M., Beekwilder, J., and Bouwmeester, H. J. (2006). Isoprenoid biosynthesis in *Artemisia annua*: cloning and heterologous expression of a germacrene a synthase from a glandular trichome cDNA library. *Arch. Biochem. Biophys.* 448, 3–12. doi: 10.1016/j.abb.2006.02.026

Bleeker, P. M., Mirabella, R., Diergaarde, P. J., VanDoorn, A., Tissier, A., Kant, M. R., et al. (2012). Improved herbivore resistance in cultivated tomato with the sesquiterpene biosynthetic pathway from a wild relative. *Proc. Natl. Acad. Sci. U.S.A.* 109, 20124–20129. doi: 10.1073/pnas.12087 56109

Bouwmeester, H. J., and Wallaart, T. E. (1999). Amorpha-4, 11-diene synthase catalyses the first probable step in artemisinin biosynthesis. *Phytochemistry* 52, 843–854. doi: 10.1016/S0031-9422(99)00206-X

Brown, G. D. (2010). The biosynthesis of artemisinin (Qinghaosu) and the phytochemistry of *Artemisia annua* L. (Qinghao). *Molecules* 15, 7603–7698. doi: 10.3390/molecules15117603

Cai, Y., Jia, J.-W., Crock, J., Lin, Z.-X., Chen, X.-Y., and Croteau, R. (2002). A cDNA clone for beta-caryophyllene synthase from *Artemisia annua*. *Phytochemistry* 61, 523–529. doi: 10.1016/S0031-9422(02)00265-0

Chen, J. L., Fang, H. M., Ji, Y. P., Pu, G., Bin, Guo, Y. W., et al. (2011). Artemisinin biosynthesis enhancement in transgenic *Artemisia annua* plants by downregulation of the β-Caryophyllene synthase gene. *Planta Med.* 77, 1759–1765. doi: 10.1055/s-0030-1271038

Croteau, R., Kutchan, T. M., and Lewis, N. G. (2000). Secondary metabolites. *Biochem. Mol. Biol. Plants* 7, 1250–1318. doi: 10.1016/j.phytochem.2011.10.011

Czechowski, T., Larson, T. R., Catania, T. M., Harvey, D., Brown, G. D., and Graham, I. A. (2016). *Artemisia annua* mutant impaired in artemisinin synthesis demonstrates importance of nonenzymatic conversion in terpenoid metabolism. *Proc. Natl. Acad. Sci. U.S.A.* 113, 15150–15155. doi: 10.1073/pnas.1611567113

Delabays, N., Simonnet, X., and Gaudin, M. (2001). The genetics of artemisinin content in *Artemisia annua* L. and the breeding of high yielding cultivars. *Curr. Med. Chem.* 8, 1795–1801. doi: 10.2174/0929867013371635

Duke, M. V., Paul, R. N., Elsohly, H. N., Sturtz, G., and Duke, S. O. (1994). Localization of artemisinin and artemisitene in foliar tissues of glanded and glandless biotypes of *Artemisia annua* L. *Int. J. Plant Sci.* 155, 365–372. doi: 10.1086/297173

Duke, S. O., and Paul, R. N. (1993). Development and fine structure of the glandular trichomes of *Artemisia annua* L. *Int. J. Plant Sci.* 154, 107–118. doi: 10.1086/297096

Ferreira, J. F. S., and Janick, J. (1995). Floral morphology of *Artemisia annua* with special reference to trichomes. *Int. J. Plant Sci.* 156, 807–815. doi: 10.1086/297304

Ferreira, J. F. S., Laughlin, J. C., Delabays, N., and de Magalhães, P. M. (2005). Cultivation and genetics of *Artemisia annua* L. for increased production of the antimalarial artemisinin. *Plant Genet. Resour. Charact. Util.* 3, 206–229. doi: 10.1079/PGR200585

Graham, I. A., Besser, K., Blumer, S., Branigan, C. A., Czechowski, T., Elias, et al. (2010). The genetic map of *Artemisia annua* L. identifies loci affecting yield of the antimalarial Drug Artemisinin. *Science.* 327, 328–331. doi: 10.1126/science.1182612

Han, J. L., Liu, B. Y., Ye, H. C., Wang, H., Li, Z. Q., and Li, G. F. (2006). Effects of overexpression of the endogenous farnesyl diphosphate synthase on the artemisinin content in *Artemisia annua* L. *J. Integr. Plant Biol.* 48, 482–487. doi: 10.1111/j.1744-7909.2006.00208.x

Han, J., Wang, H., Kanagarajan, S., Hao, M., Lundgren, A., and Brodelius, P. E. (2016). Promoting artemisinin biosynthesis in *Artemisia annua* plants by substrate channeling. *Mol. Plant.* 9, 946–948. doi: 10.1016/j.molp.2016.03.004

Huchelmann, A., Boutry, M., and Hachez, C. (2017). Plant glandular trichomes: natural cell factories of high biotechnological interest. *Plant Physiol.* 175, 6–22. doi: 10.1104/pp.17.00727

Ikram, N. K. B. K., and Simonsen, H. T. (2017). A review of biotechnological artemisinin production in plants. *Front. Plant Sci.* 8:1966. doi: 10.3389/fpls.2017.01966

Kortbeek, R. W., Xu, J., Ramirez, A., Spyropoulou, E., Diergaarde, P., Otten-Bruggeman, M., et al. (2016). Engineering of tomato glandular trichomes for the production of specialized metabolites. *Methods Enzymol.* 576, 305–331. doi: 10.1016/bs.mie.2016.02.014

Lv, Z., Zhang, F., Pan, Q., Fu, X., Jiang, W., Shen, Q., et al. (2016). Branch pathway blocking in *Artemisia annua* is a useful method for obtaining high yield artemisinin. *Plant Cell Physiol.* 57, 588–602. doi: 10.1093/pcp/pcw014

Ma, C., Wang, H., Lu, X., Wang, H., Xu, G., and Liu, B. (2009). Terpenoid metabolic profiling analysis of transgenic *Artemisia annua* L. by comprehensive two-dimensional gas chromatography time-of-flight mass spectrometry. *Metabolomics* 5, 497–506. doi: 10.1007/s11306-009-0170- 6

Ma, D. M., Wang, Z., Wang, L., Alejos-Gonzales, F., Sun, M. A., and Xie, D. Y. (2015). A Genome-wide scenario of terpene pathways in self-pollinated *Artemisia annua*. *Mol. Plant* 8, 1580–1598. doi: 10.1016/j.molp.2015.07.004

Mercke, P., Crock, J., Croteau, R., and Brodelius, P. E. (1999). Cloning, expression, and characterization of epi-cedrol synthase, a sesquiterpene cyclase from *Artemisia annua* L. *Arch. Biochem. Biophys.* 369, 213–222. doi: 10.1006/abbi.1999.1358

Nagel, R., Berasategui, A., Paetz, C., Gershenzon, J., and Schmidt, A. (2014). Overexpression of an isoprenyl diphosphate synthase in spruce leads to unexpected terpene diversion products that function in plant defense. *Plant Physiol.* 164, 555–569. doi: 10.1104/pp.113.228940

Olofsson, L., Engström, A., Lundgren, A., and Brodelius, P. E. (2011). Relative expression of genes of terpene metabolism in different tissues of *Artemisia annua* L. *BMC Plant Biol.* 11:45. doi: 10.1186/1471-2229-11-45

Olofsson, L., Lundgren, A., and Brodelius, P. E. (2012). Trichome isolation with and without fixation using laser microdissection and pressure catapulting followed by RNA amplification: expression of genes of terpene metabolism in apical and sub-apical trichome cells of *Artemisia annua* L. *Plant Sci.* 183, 9–13. doi: 10.1016/j.plantsci.2011.10.019

Olsson, M. E., Olofsson, L. M., Lindahl, A. L., Lundgren, A., Brodelius, M., and Brodelius, P. E. (2009). Localization of enzymes of artemisinin biosynthesis to the apical cells of glandular secretory trichomes of *Artemisia annua* L. *Phytochemistry* 70, 1123–1128. doi: 10.1016/j.phytochem.2009.07.009

Paddon, C. J., and Keasling, J. D. (2014). Semi-synthetic artemisinin: a model for the use of synthetic biology in pharmaceutical development. *Nat. Rev. Microbiol.* 12, 355–367. doi: 10.1038/nrmicro3240

Peplow, M. (2016). Synthetic biology's first malaria drug meets market resistance. *Nature* 530, 389–390. doi: 10.1038/530390a

Picaud, S., Brodelius, M., and Brodelius, P. E. (2005). Expression, purification and characterization of recombinant (E)-beta-farnesene synthase from *Artemisia annua*. *Phytochemistry* 66, 961–967. doi: 10.1016/j.phytochem.2005.03.027

Pulice, G., Pelaz, S., and Matías-Hernández, L. (2016). Molecular farming in *Artemisia annua*, a promising approach to improve anti-malarial drug production. *Front. Plant Sci.* 7:329. doi: 10.3389/fpls.2016.00329

Soetaert, S. S., Van Neste, C. M., Vandewoestyne, M. L., Head, S. R., Goossens, A., Van Nieuwerburgh, F. C., et al. (2013). Differential transcriptome analysis of glandular and filamentous trichomes in *Artemisia annua*. *BMC Plant Biol.* 13:220. doi: 10.1186/1471-2229-13-220

Tang, K., Shen, Q., Yan, T., and Fu, X. (2014). Transgenic approach to increase artemisinin content in *Artemisia annua* L. *Plant Cell Rep.* 33, 605–615. doi: 10.1007/s00299-014-1566-y

Tang, K. X., Wang, Y. Y., Tang, Y. L., and Chen, D. (2011). Method of utilizing the pts gene and RNA interference of the ads gene to increase patchouli alcohol content in *Artemisia annua* l. U.S. Patent No 0300546A1.

Tissier, A., Sallaud, C., and Rontein, D. (2012). "Tobacco trichomes as a platform for terpenoid biosynthesis engineering," in *Isoprenoid Synthesis in Plants and Microorganisms*, eds T. Bach and M. Rohmer (New York, NY: Springer), 271–283.

Van Noorden, R. (2010). Demand for malaria drug soars. *Nature* 466, 672–673 doi: 10.1038/466672a

Wang, W., Wang, Y., Zhang, Q., Qi, Y., and Guo, D. (2009). Global characterization of *Artemisia annua* glandular trichome transcriptome using 454 pyrosequencing. *BMC Genomics* 10:465. doi: 10.1186/1471-2164-10-465

Wang, Y., Yang, K., Jing, F., Li, M., Deng, T., Huang, R., et al. (2011). Cloning and characterization of trichome-specific promoter of cpr71av1 gene involved in artemisinin biosynthesis in *Artemisia annua* L. *Mol. Biol.* 45, 751–758. doi: 10.1134/S0026893311040145

Watson, J. M., Fusaro, A. F., Wang, M., and Waterhouse, P. M. (2005). RNA silencing platforms in plants. *FEBS Lett.* 579, 5821–6009. doi: 10.1016/j.febslet.2005.08.014

Weathers, P. J., Elkholy, S., and Wobbe, K. K. (2006). Artemisinin: the biosynthetic pathway and its regulation in *Artemisia annua*, a terpenoid-rich species. *Vitr. Cell. Dev. Biol. Plant* 42, 309–317. doi: 10.1079/IVP2006782

Wu, S., Schalk, M., Clark, A., Miles, R. B., Coates, R., and Chappell, J. (2006). Redirection of cytosolic or plastidic isoprenoid precursors elevates terpene production in plants. *Nat. Biotechnol.* 24, 1441–1447. doi: 10.1038/nbt1251

Xie, D. Y., Ma, D. M., Judd, R., and Jones, A. L. (2016). Artemisinin biosynthesis in *Artemisia annua* and metabolic engineering: questions, challenges, and perspectives. *Phytochem. Rev.* 15, 1093–1114. doi: 10.1007/s11101-016-9480-2

Yang, R. Y., Feng, L. L., Yang, X. Q., Yin, L. L., Xu, X. L., and Zeng, Q. P. (2008). Quantitative transcript profiling reveals down-regulation of a sterol pathway relevant gene and overexpression of artemisinin biogenetic genes in transgenic *Artemisia annua* plants. *Planta Med.* 74, 1510–1516. doi: 10.1055/s-2008-1081333

Yu, G., and Pichersky, E. (2014). Heterologous expression of methylketone synthase1 and methylketone synthase2 leads to production of methylketones and myristic acid in transgenic plants. *Plant Physiol.* 164, 612–622. doi: 10.1104/pp.113.228502

Zhang, L., Jing, F., Li, F., Li, M., Wang, Y., Wang, G., et al. (2009). Development of transgenic *Artemisia annua* (Chinese wormwood) plants with an enhanced content of artemisinin, an effective anti-malarial drug, by hairpin-RNA-mediated gene silencing. *Biotechnol. Appl. Biochem.* 52, 199–207. doi: 10.1042/BA20080068

Zhang, Y., Nowak, G., Reed, D. W., and Covello, P. S. (2011). The production of artemisinin precursors in tobacco. *Plant Biotechnol. J.* 9, 445–454. doi: 10.1111/j.1467-7652.2010.00556.x

Conflict of Interest Statement: The authors declare that the research was conducted in the absence of any commercial or financial relationships that could be construed as a potential conflict of interest.

frontiers in Plant Science

ORIGINAL RESEARCH
published: 19 June 2018
doi: 10.3389/fpls.2018.00828

Overexpression of *Artemisia annua* Cinnamyl Alcohol Dehydrogenase Increases Lignin and Coumarin and Reduces Artemisinin and Other Sesquiterpenes

Dongming Ma[1,2†], Chong Xu[1†], Fatima Alejos-Gonzalez[2], Hong Wang[3], Jinfen Yang[1], Rika Judd[2] and De-Yu Xie[2]*

[1] Research Center of Chinese Herbal Resource Science and Engineering, Guangzhou University of Chinese Medicine, Guangzhou, China, [2] Department of Plant & Microbial Biology, North Carolina State University, Raleigh, NC, United States, [3] Graduate University of Chinese Academy of Sciences, Beijing, China

OPEN ACCESS

Edited by:
Tomasz Czechowski, University of York, United Kingdom

Reviewed by:
Patrick Smithers Covello, Biotechnology Research Institute (NRC-CNRC), Canada
Yongzhen Pang, Institute of Botany (CAS), China

***Correspondence:**
De-Yu Xie
dxie@ncsu.edu

† These authors have contributed equally to this work.

Specialty section:
This article was submitted to Plant Biotechnology, a section of the journal Frontiers in Plant Science

Received: *23 January 2018*
Accepted: *28 May 2018*
Published: *19 June 2018*

Citation:
Ma D, Xu C, Alejos-Gonzalez F, Wang H, Yang J, Judd R and Xie D-Y (2018) Overexpression of Artemisia annua Cinnamyl Alcohol Dehydrogenase Increases Lignin and Coumarin and Reduces Artemisinin and Other Sesquiterpenes. Front. Plant Sci. 9:828. doi: 10.3389/fpls.2018.00828

Artemisia annua is the only medicinal crop that produces artemisinin for malarial treatment. Herein, we describe the cloning of a cinnamyl alcohol dehydrogenase (AaCAD) from an inbred self-pollinating (SP) *A. annua* cultivar and its effects on lignin and artemisinin production. A recombinant AaCAD was purified via heterogeneous expression. Enzyme assays showed that the recombinant AaCAD converted p-coumaryl, coniferyl, and sinapyl aldehydes to their corresponding alcohols, which are key intermediates involved in the biosynthesis of lignin. Km, Vmax, and Vmax/Km values were calculated for all three substrates. To characterize its function *in planta*, *AaCAD* was overexpressed in SP plants. Quantification using acetyl bromide (AcBr) showed significantly higher lignin contents in transgenics compared with wild-type (WT) plants. Moreover, GC-MS-based profiling revealed a significant increase in coumarin contents in transgenic plants. By contrast, HPLC-MS analysis showed significantly reduced artemisinin contents in transgenics compared with WT plants. Furthermore, GC-MS analysis revealed a decrease in the contents of arteannuin B and six other sesquiterpenes in transgenic plants. Confocal microscopy analysis showed the cytosolic localization of AaCAD. These data demonstrate that AaCAD plays a dual pathway function in the cytosol, in which it positively enhances lignin formation but negatively controls artemisinin formation. Based on these data, crosstalk between these two pathways mediated by AaCAD catalysis is discussed to understand the metabolic control of artemisinin biosynthesis in plants for high production.

Keywords: ***Artemisia annua*, artemisinin, arteannuin B, cinnamyl alcohol dehydrogenases, coumarin, lignin, sesquiterpenes**

INTRODUCTION

Artemisinin-based combination therapy (ACT) is the first-line treatment for malaria (WHO, 2006, 2013; Maude et al., 2009). *Artemisia annua* L. (sweet wormwood), an effective antimalarial plant, is the only natural resource to produce artemisinin, an endoperoxide sesquiterpene lactone. Due to the global demand for ACT, understanding artemisinin biosynthesis in this medicinal

plant is critical for metabolic engineering purposes for high production of this sesquiterpene. To date, numerous studies have molecularly and biochemically characterized the main steps of the artemisinin biosynthetic pathway, starting with amorpha-4,11-diene (amorphadiene) localized in the cytosol of glandular trichomes (**Figure 1**) (Bouwmeester et al., 1999; Teoh et al., 2006; Covello et al., 2007; Zhang et al., 2008; Czechowski et al., 2016). A recent review summarized enzyme assay, synthetic biology, and multiple transgenic studies that solidly demonstrate the first step catalyzed by amorpha-4, 11-diene synthase (ADS) s (Xie et al., 2016). The second step is catalyzed by a cytochrome P450 mono-oxygenase (CYP71AV1) coupled with a cytochrome P450 reductase 1 (CPR1). These two enzymes were originally demonstrated to convert amorpha-4, 11-diene to artemisinic alcohol and then to artemisinic aldehyde (Ro et al., 2006;Teoh et al., 2006). Recently, a new gene encoding an *A. annua* alcohol dehydrogenase 1 (AaADH1) was cloned from glandular trichomes of *A. annua* and demonstrated to catalyze the conversion of artemisinic alcohol to artemisinic aldehyde (Paddon et al., 2013). This discovery has greatly enhanced our understanding of the second step. A double-bond reductase (DBR) and an aldehyde dehydrogenase (ALDH) subsequently convert artemisinic aldehyde to dihydroartemisinic aldehyde and then dihydroartemisinic acid (DHAA) (Xie et al., 2016). The spontaneous oxidation of DHAA finally produces artemisinin. In addition, arteannuin B is derived from artemisinic aldehyde (**Figure 1**). Recently, a *cyp71av1* mutant of *A. annua* was generated to provide fundamental genetic evidence demonstrating the essential role of CYP71AV1 in controlling the artemisinin biosynthetic pathway *in planta* (Czechowski et al., 2016). This mutant further provided solid evidence to demonstrate the formation of artemisinin through spontaneous oxidation. In addition to research conducted in plants, fundamental successes in synthetic biology have further demonstrated the steps catalyzed by ADS, CYP71AV1, CPR1, and AaADH1 (Ro et al., 2006; Paddon et al., 2013; Turconi et al., 2014). Although these previous achievements have demonstrated fundamental promising methods to improve the artemisinin supply, global production from current sweet wormwood crops still lacks stability and is unable to meet the increase in medicinal demands (Paddon et al., 2013; Ma et al., 2017a). Therefore, continuous research efforts are urgently necessary to elucidate the regulatory mechanisms of artemisinin biosynthesis to improve the global yield.

Cinnamyl alcohol dehydrogenase (CAD) is categorized in a group of short-chain oxidoreductases in the family of nicotinamide adenine dinucleotide phosphate (reduced form)-dependent enzymes. It has been appropriately characterized to catalyze the conversion of phenylpropenyl aldehydes to alcohols in the late steps of lignin biosynthesis (**Figure 1**) (Sarni et al., 1984; Somers et al., 1995; Baucher et al., 1999; Chabannes et al., 2001). A large number of studies have succeeded in manipulating *CAD* expression in potent biotechnological efforts to reduce lignin in trees and crops for different economic applications (Baucher et al., 1999; MacKay et al., 1999; Chabannes et al., 2001; Fu et al., 2011; d'Yvoire et al., 2013; Trabucco et al., 2013; Anderson et al., 2015; Ozparpucu et al., 2017). The main

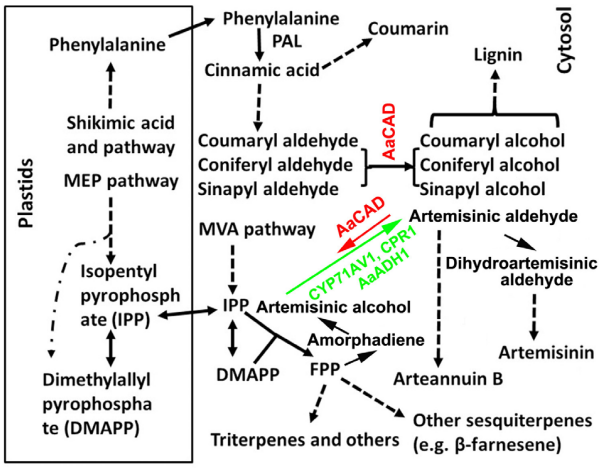

FIGURE 1 | A simplified scheme showing the cellular compartmentation associated with the biosynthesis of lignin, coumarin, artemisinin, and other metabolites. Pathway abbreviations: MEP, 2-C-methyl-D-erythritol 4-phosphate and MVA, mevalonate pathway; enzyme abbreviations; ADS, amorphadiene synthase; AaADH1, *Artemisia annua* alcohol dehydrogenase; AaCAD, *Artemisia annua* cinnamyl alcohol dehydrogenase; CPR1, cytochrome P450 reductase 1; CYP71AV1, cytochrome P450 mono-oxygenase; and PAL, phenylalanine ammonia-lyase. Dashed arrows and lines denote multiple steps. Solid arrows denote one step. The short arrow for AaCAD in the artemisinin pathway denotes a partial reverse. The long arrow for CYP71AV1 and CPR1 denotes the main direction toward artemisinin.

successes associated with using *CAD* downregulation include improved digestibility of forage crops, reduction of lignin in trees for pulping and biofuel, and different renewable plants for biofuel feedstock (Lapierre et al., 2000; Fu et al., 2011; Wang Y.H. et al., 2015; Ozparpucu et al., 2017; Ponniah et al., 2017). For example, downregulation of *CAD* in alfalfa has been shown to lead to a decrease in lignin and improved digestibility of this forage crop (Baucher et al., 1999). Suppression of *CAD* in rice has demonstrated the potential to facilitate cellulose production for biofuel feedstock (Ponniah et al., 2017). A downregulation of *CAD* has also been reported to improve saccharification in switchgrass for biofuel conversion (Fu et al., 2011).

In our previous study, we reported the cloning of a *CAD* homolog from glandular trichomes of an heterozygous (cross-pollination) *A. annua* cultivar and *in vitro* enzyme assays to show that it used cinnamyl aldehyde, coniferyl aldehyde, sinapyl aldehyde, and artemisinic aldehyde as substrates (Li et al., 2012). To date, whether this CAD can affect lignin and other metabolic pathways in *A. annua* remains to be investigated. Herein, we report the cloning of a new *CAD* homolog from a novel self-pollinating (SP) *A. annua* and characterize its enzyme kinetics and overexpression in plants. Phytochemical analysis, GC-MS-based metabolic profiling, and LC-MS analysis were conducted to characterize phenylpropanoid and terpenoid metabolism in transgenic plants. The resulting data showed that not only was this new AaCAD involved in lignin biosynthesis, but it was also associated with coumarin formation.

By contrast, artemisinin and other sesquiterpenes contents were significantly decreased in transgenic plants. These data show that AaCAD can play a dual function by establishing a crosstalk between two distinct cytosolic pathways, the phenylpropanoid and sesquiterpene pathways. Although overexpression of *AaCAD* leads to a reduction of artemisinin contents, this research is very instructional for future metabolic engineering designs to improve artemisinin production in *A. annua*.

MATERIALS AND METHODS

Plant Materials and Growth Conditions

The progeny of a self-pollinating (SP) *A. annua* variety were grown in the phytotron for seeds as described previously (Alejos-Gonzalez et al., 2011). The photoperiod and temperature in the phytotron was 16/8 h (light/dark) and 25/22°C (day and night). Seedlings of the F3 progeny were used for gene cloning, genetic transformation, and metabolite analysis.

Cloning of *AaCAD* cDNA

DNA-free total RNA was isolated from 2-month-old seedlings of SP *A. annua* using the RNeasy Plant Mini Kit (Qiagen, United States) as described previously (Ma et al., 2015). The first-strand cDNA was synthesized with 1.0 μg of total RNA and Powerscript reverse transcriptase (Clontech). The resulting cDNA was used as template to clone *AaCAD*. A pair of primers consisting of CAD-F (5′- ATG GGA AGC ATG AAA GAA GAA AG-3′) and CAD-R (5′-ATT TGT TGT TTC CTC TTC CAA A-3′) was designed for RT-PCR, which was carried out to obtain the open reading frame (ORF) fragment of *AaCAD*. The PCR product was further sequenced to analyze its nucleotides. The resulting ORF was deduced to determine the amino acid sequence, which was aligned with a reported CAD sequence obtained from GenBank. The sequence alignment was completed using an online Cluster Omega program[1].

Heterogeneous Expression of Recombinant AaCAD

The ORF of *AaCAD* containing its stop codon TAA was cloned into the pENTR/D-TOPO vector (Gateway, Invitrogen) to obtain a recombinant pENTR-AaCAD plasmid. The LR Clonase II enzyme mix (Invitrogen) was used to digest the pENTR-AaCAD plasmid and the destination vector pDEST17 (6xHis tag). As a result, the *AaCAD* ORF was cloned into pDEST17 to obtain a new pDEST17-AaCAD plasmid for protein expression. All cloning steps followed the manufacturer's protocol. The pDEST17-AaCAD plasmid was further introduced into competent *E. coli* strain BL21 cells to induce recombinant protein.

For protein induction, a single colony was selected and then cultured in 200 ml liquid LB medium supplied with 50 mg/L ampicillin at 37°C in 500-ml E-flasks. When the OD value of the suspension culture was approximately 0.6 at 600 nm, 0.1% L-arabinose and 0.1 mM IPTG were added the flask. The suspension culture was continuously incubated for an additional 20 h at 16°C. As described in our recent report (Ma et al., 2017a), the recombinant AaCAD was purified using Ni-NTA Superflow Columns (Qiagen, 1.5 ml) according to the manufacturer's protocol. The resulting purified recombinant AaCAD was loaded onto PD-10 columns (Amersham Pharmacia Biotech, now GE Healthcare Life Sciences, http://www.gelifesciences.com) to remove salts. Sodium dodecyl sulfate polyacrylamide gel electrophoresis (SDS-PAGE) was performed to examine the purification of the recombinant AaCAD. The resulting desalted protein was used for the enzyme assay immediately or stored in a −20°C freezer for late use as described below.

Enzyme Assay and Kinetics Analysis

Three lignin substrates, coniferyl aldehyde, p-coumaryl aldehyde, and sinapyl aldehyde (Sigma-Aldrich), were used to examine the catalytic activity of the recombinant AaCAD. Three substrates were dissolved in methanol. Enzymatic reactions were carried out in a 200-μl volume composed of 0.1 mM substrate, 50 mM Tris–HCl (pH 7.5), 0.5 mM NADPH, 2.0 mM dithiothreitol, and 1.3 μg purified recombinant AaCAD. All reactions were initiated by addition of AaCAD to the reaction mixture at 30°C. After 30 min, all reactions were stopped by addition of 15 μl of glacial acetic acid, followed by centrifugation at 10,000 × *g* for 10 min. The resulting supernatant was pipetted into a 200-μl glass insert, which was further placed into a 2-ml glass vial for high-performance liquid chromatograph (HPLC) analysis. All experiments were repeated three times, each with three replicates.

HPLC analysis was performed on a Waters 2695 instrument. Metabolites were separated on an Agilent ZORBAX Eclipse XDB-C18 column (4.6 × 150 mm, 5 μm). Two HPLC grade solvents, methanol (solvent A) and water (solvent B), were used as the mobile phase. A gradient solvent program, which was composed of A:B from 5:95 to 95:5 from 0 to 40 min, was developed to elute the metabolites. The flow rate was 1.0 ml/min, and the injection volume was 20 μl. The wavelengths for detection of the metabolites were 260 nm and 340 nm.

To characterize the kinetics of the recombinant AaCAD, eight concentrations (6, 8, 10, 12, 14, 20, and 30 μM) of each substrate were tested. Except for the different concentrations of the substrates used, other components in the reaction mixture were the same as described above. All reactions were performed in 200 μl in 96-well microplates. Measurements of enzymatic products were performed using an Epoch Microplate reader (BioTek instruments Inc., United States). All reactions were initiated by the addition of enzyme and then maintained at 30°C for 10 min. All tubes were placed on a microplate for 40 min of declination recorded at 340 nm, which is classically used to quantify aldehyde and NADPH because they have maximum absorbance values at this wavelength (Goffner et al., 1992; Ma, 2010; Saathoff et al., 2011; Rong et al., 2016). This method uses extinction coefficients (14.7×10^{-3} to 19.45×10^{-3} M^{-1} cm^{-1}) for both aldehyde and NADPH to calculate the relative contribution of each to the 340-nm signal (Hawkins and Boudet, 1994; Saathoff et al., 2011), which allows the elimination of potential spectrophotometric interference. We used this method to record absorbance values at one-min

[1]http://www.ebi.ac.uk/Tools/msa/clustalo/

intervals for each tube (reaction). Each reaction was continuously recorded 40 times to obtain 40 values. The resulting data were analyzed using GraphPad Prism 6 software to determine the Km, Vmax, and Kcat values. All experiments were performed three times, each with three replicates.

Development of Binary Vector, Genetic Transformation of *A. annua*, and Genotyping

The *AaCAD* ORF, including its stop codon, was cloned into the pENTR/D-TOPO vector (Gateway, Invitrogen) to obtain a new recombinant pENTR-AaCAD plasmid, which was introduced into competent *E. coli* DH5α cells. The destination vector used for the development of binary vectors was PMDC-84 (Xi et al., 2016). The pENTR-AaCAD and PMDC-84 plasmids were digested and interchanged using the LR Clonase II enzyme mixture (Invitrogen) following the manufacturer's protocol. This cloning step resulted in a binary vector, namely, PMDC-84-AaCAD, in its T-DNA cassette of which *AaCAD* was cloned at the immediate downstream of a 2× 35S promoter, and a hygromycin gene was used for selection (**Figure 3A**). This binary vector was introduced into competent *A. tumefaciens* strain LBA4404 cells, from which one positive colony was selected for genetic transformation of *A. annua*, as described previously (Ma et al., 2015). Multiple transgenic shoots were generated on the hygromycin selection medium and rooted to obtain plantlets. More than 10 plantlets were planted in pot soil and placed in the phytotron for continuous growth to flower and then seed production. In addition, transgenic plants for other genes reported previously (Ma et al., 2015) were used as vector controls in this study. We further used a Leica MZ FLIII fluorescence stereomicroscope to examine trichomes including glandular and other shaped trichomes on the surfaces of leaves and stems of transgenic vs. wild-type plants.

Genomic DNA was extracted from leaf tissues of transformed plants using the DNeasy Plant Mini Kit (Qiagen, United States). A total of 50 ng of genomic DNA was used as template for PCR using a pair of primers consisting of a forward primer (5′-TCT AGA ACT AGT TAA TTA AGA AT-3′) designed based on the 35S promoter and a reverse primer (5′-ATT TGT TGT TTC CTC TTC CAA A-3′) designed based on *AaCAD*. The thermal program for PCR was composed of 94°C for 5 min, followed by 35 cycles at 94°C for 1 min, annealing for 1 min at 5°C, and extension of 1 min at 72°C, and a final extension at 72°C for 5 min. All PCR experiments were performed with three biological replicates, each repeated at least three times.

Subcellular Localization Analysis

Subcellular localization of AaCAD was carried out as described in our recent reports (Ma et al., 2017a,b). In brief, a gateway technique was used to insert the *AaCAD* ORF without its stop codon into the pENTR/D-TOPO vector (Gateway, Invitrogen, United States) following the manufacturer's protocol. This cloning generated a new recombinant plasmid, namely, pENTR/D-TOPO-CAD. The destination vector used was pSITEII-N1-enhanced green fluorescent protein (EGFP) (with the EGFP epitopic tag in the C-terminus). Then, *AaCAD* in the pENTR/D-TOPO-CAD vector was cloned into pSITEII-N1 by LR reactions following the manufacturer's protocol. This cloning step generated a new pSITEII-N1-CAD/EGFP plasmid, in which *AaCAD* (without its stop codon) was directly ligated at the 5′-end of *EGFP*. The new plasmid was then introduced into *Agrobacterium tumefaciens* strain GV3101. A positive colony was selected and then activated for leaf agroinfiltration of *N. benthamiana* to transiently analyze protein expression. After 30 h of infection, leaf tissues were examined using a confocal microscope (Carl Zeiss). GFP fluorescence was excited at 488 nm and observed between 495 and 550 nm according to a method reported previously (Wang G.F. et al., 2015). All analyses were performed with three groups of biological replicates, each with at least three replicates.

Reverse Transcription-Polymerase Chain Reaction and Western Blot Analysis

Total RNA was isolated from the young leaves of transgenic candidates and WT plants using an RNeasy Plant Mini Kit (Qiagen, CA, United States). Samples were then treated with DNase to obtain DNA-free RNA. The first-strand cDNA was synthesized using 1.0 μg of DNA-free RNA and Powerscript reverse transcriptase (RT, Clontech, United States). One microliter of cDNA was used as template for PCR using Taq polymerase (Promega, United States). The steps of these three types of experiments followed the manufacturers' protocols, respectively. Reverse transcription-polymerase chain reaction (RT-PCR) was carried out for *AaCAD* transgenic and WT plants. The housekeeping gene β-actin was used as a reference control. The gene-specific primer pair for PCR was 5-ATGGGAAGCATGAAAGAAGAAAG-3 (forward primer) and 5′-ATTTGTTGTTTCCTCTTCCAAA-3′ (reverse primer). The thermal program was as described above for genotyping. RT-PCR experiments were performed with three groups of biological replicates, each with three replicates.

A polypeptide consisting of MGSMKEERKITGWAC selected from the AaCAD amino acid sequence was used for antibody development. This peptide was synthesized and then used to develop a polyclonal antibody in rabbit at Genscript Company (NJ 08854, United States) for western blot analysis. Western blot was performed as described in our recent reports (Ma et al., 2017a,b). In brief, total proteins were extracted from leaves of transgenic vs. wild-type plants and separated by SDS-PAGE. Separated proteins were transferred to a nitrocellulose membrane and then probed with anti-AaCAD antibody. An anti-rabbit IgG HPR conjugate was used as a second antibody (Promega). An enhanced chemiluminescence system (Thermo Scientific, IL, United States) was used to detect the hybridization signal for immunoblot analysis. Western blot analysis was repeated three times.

Lignin Measurement

The lignin content was measured using the acetyl bromide (AcBr) method (Fukushima and Kerley, 2011; Moreira-Vilar et al., 2014). Small revisions were developed to obtain the protein-free cell wall

fraction. All dried stems and branches of each plant were ground into powder and filtered using a sieve (120 μm). One gram of fine powder was suspended in 20 ml sodium phosphate buffer (0.1 M, pH 7.2) in a 50-ml capped polyethylene tube at 37°C for 30 min, followed by centrifugation at 4000 rpm for 10 min. The remaining pellet was suspended in 10 ml 70% ethanol, placed in an 80°C water bath for 5 min, and then centrifuged for 10 min to remove the supernatant. This step was repeated five times. The remaining pellet in the tube was suspended in 10 ml acetone at room temperature for 5 min and centrifuged for 5 min to remove the supernatant. These treatments obtained protein-free cell wall fraction. The pellet was completely dried in a 37°C oven until there was no weight change. Five milligrams of the dry residue sample was dissolved in 2.5 ml of acetyl bromide:acetic acid (1:3, v/v) solution in a glass tube. This treatment was maintained 24 h at room temperature. The mixture was completely transferred to a 10-ml volumetric flask, followed by addition of 0.35 ml of 0.5 M hydroxylamine hydrochloride. Glacial acetic acid was added to the volumetric flask to 10 ml. The flask was gently shaken in the upside-down direction to thoroughly mix the sample. The absorbance of the resulting mixture was recorded at 280 nm using an ultra-visible spectrometer. An extinction coefficient of 23.077 g^{-1} l cm^{-1} was used to calculate the AcBr concentration. The resulting data were used to calculate the contents of lignin extracted from the samples. Three biological replicates were analyzed for each plant. Each biological replicate was repeated three times.

Extraction of Non-polar Metabolites and Gas Chromatograph-Mass Spectrometry Analysis

A protocol was developed to extract and profile nonpolar metabolites from tissues of *A. annua* (Ma et al., 2015). In brief, hexane was used to extract nonpolar metabolites from the leaves of 8–12 nodes of two-month-old plants grown in the phytotron (**Figure 3B**), and gas chromatograph-mass spectrometry (GC-MS) was performed using a gas chromatograph 6890 coupled with 5975C MSD (Agilent Technologies, United States). A RTX-5 capillary column (30 m × 0.25 mm × 0.25 μm) was used to separate the metabolites. Splitless mode was used in the inlet. The injection temperature was set at 250°C. The temperature was initially set at 60°C, then ramped to 260°C at a constant rate of 10°C/min, and held at 260°C for 25 min. Pure helium was used as the carrier gas, with a flow rate of 1 ml/min. A positive electron impact ion source (70 eV) was used to ionize compounds, and mass fragments were scanned in the range from 40 to 800 (m/z), with 4 min of solvent delay. Three biological replicates were analyzed for each genotypic plant. Each biological replicate was repeated three times.

High-Performance Liquid Chromatography-Mass Spectrometry Analysis of Artemisinin

Leaf samples used for nonpolar metabolite analysis were also used for artemisinin measurements. Extraction of artemisinin and high-performance liquid chromatography-mass spectrometry (HPLC-MS) analysis were performed using a 2010 eV LC/UV/ESI/MS instrument (Shimadzu) following our protocols reported previously (Alejos-Gonzalez et al., 2011, 2013). Three biological replicates were analyzed for each genotypic plant, with each biological replicate repeated three times.

Statistical Analyses

Experimental data were analyzed by one-way ANOVA. Subsequent multiple comparisons were performed using Duncan's multiple range test. All statistical analyses were performed using IBM SPSS Statistics Professional Edition, and the statistical significance was set at $P < 0.01$.

RESULTS

Kinetics of Recombinant AaCAD for Three Lignin Substrates

According to a *CAD* homolog sequence (ACB54931) that was cloned from a cross-pollinating cultivar (Li et al., 2012) and curated in the GenBank at NCBI database, we used RT-PCR to clone an *AaCAD* open reading frame (ORF) (GenBank accession ID#: MH017050) from the leaf tissues of self-pollinating (SP) *A. annua*. The full-length ORF is composed of 1086 base pairs of nucleotides that are deduced to encode 362 amino acids. An alignment between the deduced amino acid sequence and the homologous ACB54931 sequence only revealed three different amino acids, showing the high identity of the sequence and predicted structure (Supplementary Figures S2, S3).

The ORF was cloned into pDEST17 (6xHis tag) to induce the recombinant AaCAD. The purified recombinant enzyme was further obtained using Ni-NTA Superflow Columns (Supplementary Figure S1). Three substrates, coniferyl aldehyde, sinapyl aldehyde, and p-coumaryl aldehyde, were used to evaluate the enzymatic activity. After the recombinant AaCAD was incubated with the three substrates, HPLC analysis showed that the recombinant enzyme efficiently converted the three substrates to their corresponding alcohol products, coniferyl alcohol, sinapyl alcohol, and p-coumaryl alcohol, respectively (**Figures 2A–C**). These results demonstrated the biochemical involvement of AaCAD in the lignin biosynthetic pathway (**Figure 1**).

Kinetic analysis was carried out to characterize Km, Vmax, Kcat, and Kcat/Km values for the three substrates. Given that coniferyl alcohol, sinapyl alcohol, and p-coumaryl alcohol produced from AaCAD catalysis have maximum absorbance values at 340 nm, the use of a microplate reader is a highly efficient way to measure their concentrations in the same reaction time frame. The resulting data showed that the Km value of sinapyl aldehyde was lower than those of coniferyl aldehyde and p-coumaryl aldehyde, which had similar values (**Figure 2D**). This result supports a catalytic preference for sinapyl aldehyde. The Vmax values for the three substrates were similar. The Kcat/Km value for sinapyl aldehyde was higher than those of coniferyl

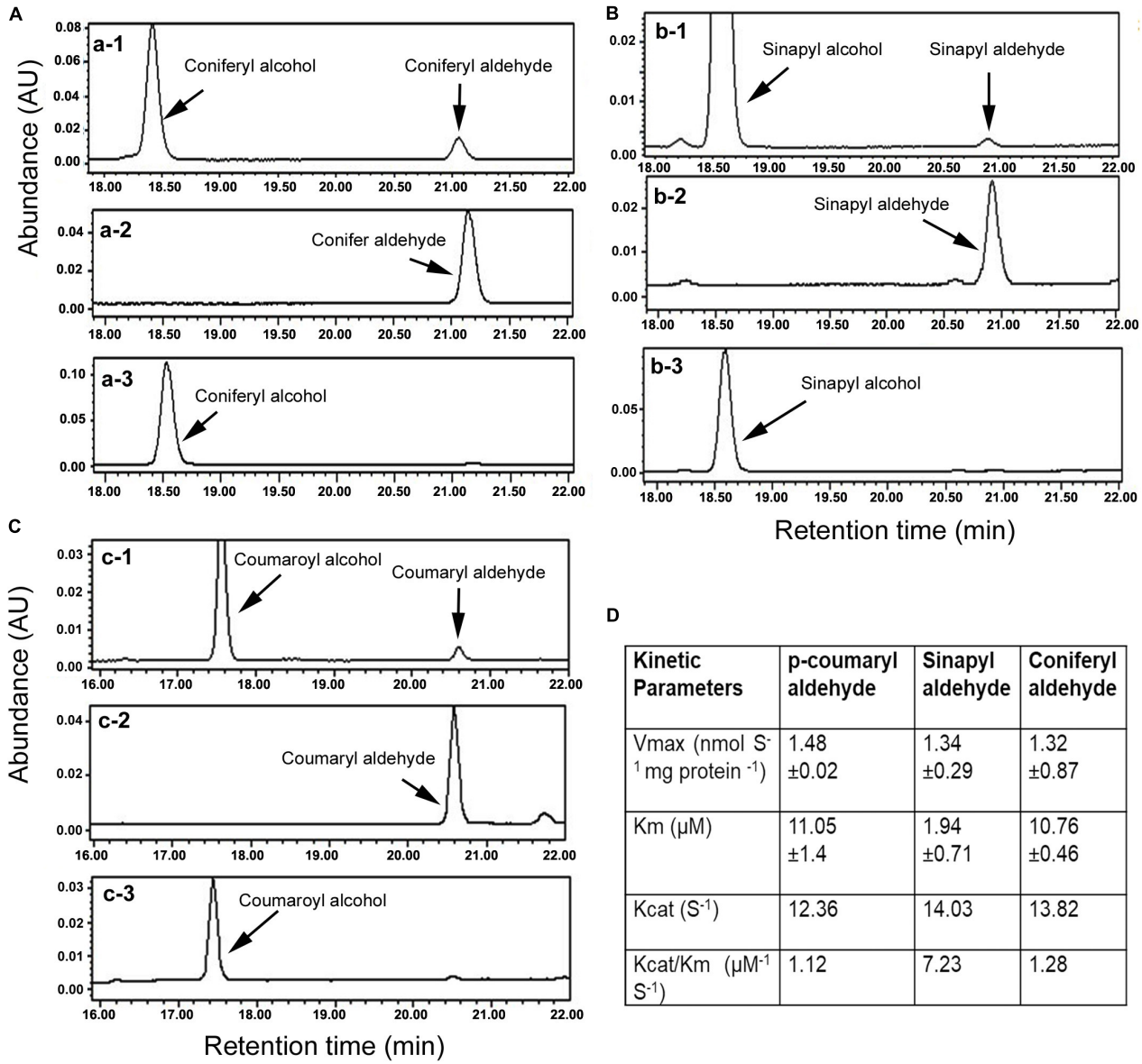

D

Kinetic Parameters	p-coumaryl aldehyde	Sinapyl aldehyde	Coniferyl aldehyde
Vmax (nmol S^{-1} mg protein $^{-1}$)	1.48 ±0.02	1.34 ±0.29	1.32 ±0.87
Km (μM)	11.05 ±1.4	1.94 ±0.71	10.76 ±0.46
Kcat (S^{-1})	12.36	14.03	13.82
Kcat/Km (μM^{-1} S^{-1})	1.12	7.23	1.28

FIGURE 2 | Characterization of enzymatic activity with HPLC analysis and kinetic features. **(A)** HPLC profiles show conversion of coniferyl aldehyde to coniferyl alcohol, a-1: reaction product and substrate, a-2: coniferyl aldehyde standard, and a-3: coniferyl alcohol standard. **(B)** Profiles of HPLC show conversion of sinapyl aldehyde to sinapyl alcohol, b-1: reaction product and substrate, b-2: sinapyl aldehyde standard, and b-3: sinapyl alcohol standard. **(C)** Profiles of HPLC show conversion of p-coumaryl aldehyde to p-coumaryl alcohol, c-1: reaction product and substrate, c-2: p-coumaryl aldehyde standard, and c-3: p-coumaryl alcohol standard. **(D)** Km, Vmax, Kcat, and Vcat/Km values were calculated for three substrates. All experiments in **A–C** were repeated at least three times. All experiments in **D** were carried out with three replicates to calculate the values.

aldehyde and p-coumaryl aldehyde, which had similar values (**Figure 2D**).

Overexpression of *AaCAD* in SP *A. annua*

The ORF of *AaCAD* was cloned into the PMDC-84 vector, and its expression was driven by a 2 × 35S promoter (**Figure 3A**). This construct was introduced into SP *A. annua* via *A. tumefaciens*-mediated transformation of leaf explants. Numerous hygromycin-resistant shoots were regenerated from infected explants and further rooted to obtain multiple transgenic plantlets. More than 10 plantlets were planted in soil contained in pots and grown in the phytotron as reported previously (Ma et al., 2017a). As shown in the photograph of line OE3 and a wild-type plant in **Figure 3B**, the transgenic candidates grew similarly. In addition, vector control transgenic plants such as *ADS* transgenic plants (Ma et al., 2015) were used as a vector control, and no difference in plant growth was observed between *ADS* and AaCAD transgenic plants.

Based on the 35S promoter and *AaCAD* sequences, primers were designed for PCR-based genotyping. The resulting PCR

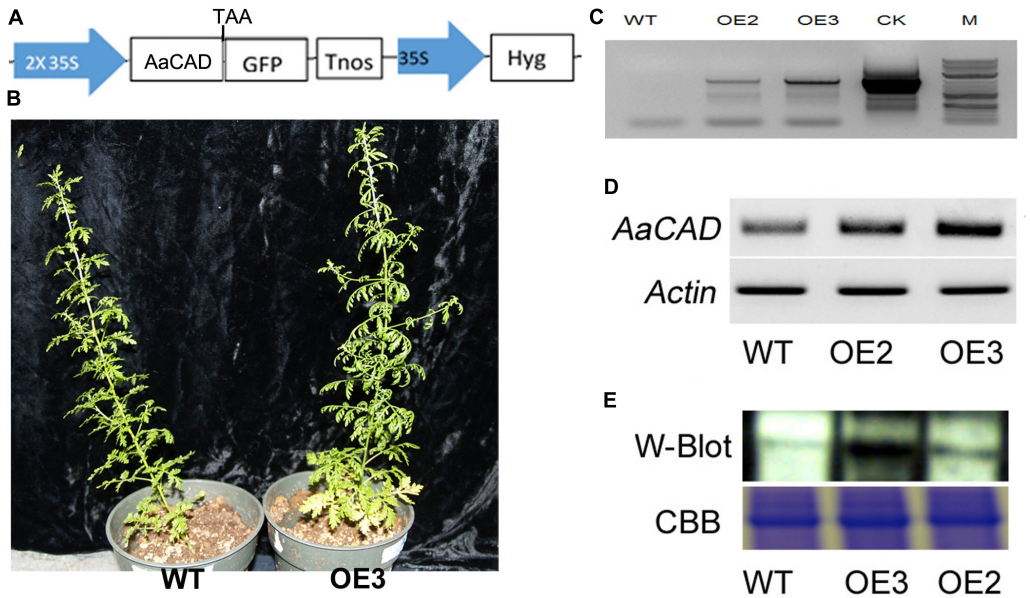

FIGURE 3 | A simplified map of the T-DNA cassette and integration of the transgene in transgenic plants. **(A)** A T-DNA cassette constructed in a binary vector showing the use of the 2 × 35S promoter for overexpression of *AaCAD* in *A. annua*. **(B)** Images show phenotypes of an OE3 transgenic line vs. one wild-type control plant. **(C)** PCR gel images show the genomic DNA fragment amplified from two transgenic lines using a pair of primers consisting of a forward 35S promoter primer and a reverse CAD primer. **(D)** Gel images show the increased expression of *AaCAD* in transgenic plants. **(E)** Gel images show the increased AaCAD protein in transgenic lines. Abbreviations in T-DNA: AaCAD, *Artemisia annua* cinnamyl alcohol dehydrogenase; GFP, green florescent protein; Hyg, hygromycin; Tnos, Nos terminator. Plant name abbreviation: OE2 and OE3, two transgenic lines; WT, wild-type control. PCR and RT-PCR experiments were performed with three biological replicates, each with at least three replicates. Western blotting was repeated three times.

data, as shown for transgenic examples OE2 and OE3 in **Figure 3C**, demonstrated the integration of the 35S and *AaCAD* transgenes into the genome of transgenic candidates. These two candidate lines were further selected for RT-PCR and western blot analysis. RT-PCR using gene-specific primers showed higher expression levels of *AaCAD* in these two transgenic plants compared with the wild-type control (**Figure 3D**). Western blot analysis demonstrated an increased protein level of AaCAD in the two transgenic plants (**Figure 3E**). These data demonstrate that the two candidates are transgenic plants.

To characterize the subcellular localization of AaCAD, confocal microscopy analysis was performed. The stop codon TAA was removed from the *AaCAD* ORF. The resulting TAA-eliminated sequence was fused to the N-end of an EGFP for protein localization. As reported previously for testing transgene functions in SP *A. annua* (Ma et al., 2017a,b), transient expression of AaCAD-EGFP was carried out in *Nicotiana benthamiana*. Both green and red channels were used to localize the proteins. The resulting data from two-channel observations showed that epidermal cells exhibited strong green fluorescence in the cytosol (**Figure 4**), indicating that AaCAD catalyzes reactions in the cytosol.

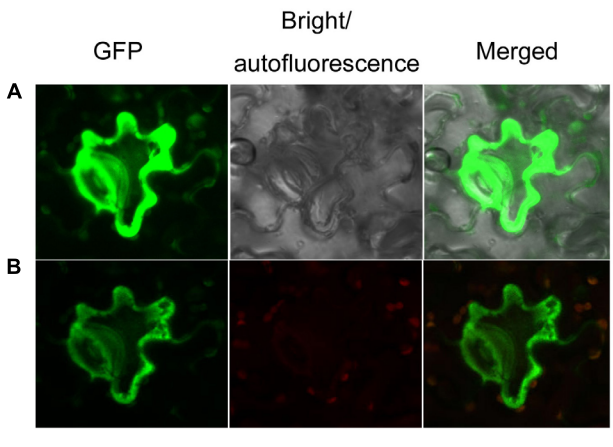

FIGURE 4 | Subcellular localization of AaCAD-EGFP. **(A)** The green fluorescence signal of GFP in cells is shown in images photographed using green and bright channels. **(B)** The green fluorescence signal of GFP in cells is shown in images photographed using green and red channels. Green, green fluorescence of GFP; red, autofluorescence of chloroplasts; merged, green fluorescence of GFP and red autofluorescence of chloroplasts. This experiment was repeated three times, each with at least three biological replicates.

Lignin and Coumarin Contents Are Increased in Transgenic Plants

Lignin and other phenylpropanoid metabolites were analyzed in the transgenic and wild-type plants. Given that T0 transgenic plants were regenerated at different time points, in this study, we mainly focused on OE2 and OE3, which were regenerated at the same time and grew in a synchronous manner. The main

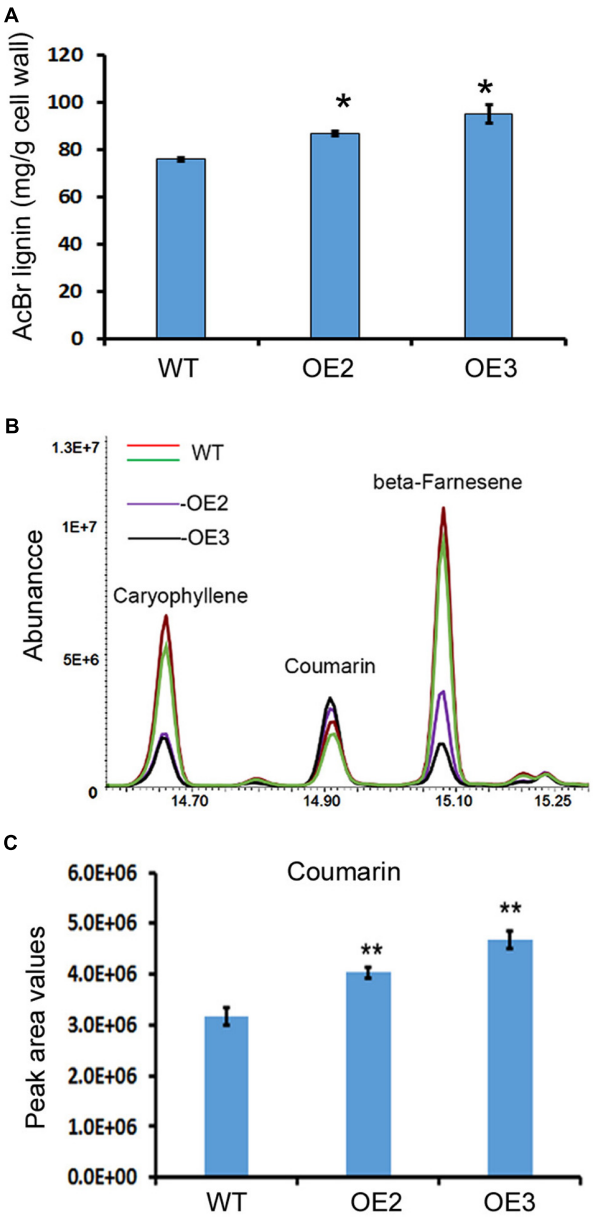

FIGURE 5 | Overexpression of *AaCAD* increases the lignin and coumarin contents in transgenic plants. **(A)** AcBr analysis-based calculation showing the lignin content in leaves of two transgenic lines and wild-type plants. **(B)** Overlay of total ion chromatographs showing increases in coumarin abundance in leaves of the two transgenic lines. **(C)** Peak area values show significant increases in coumarin in leaves of the two transgenic lines. OE2 and OE3, two transgenic lines overexpressing the *AaCAD* transgene; WT, wild-type. * in **(A)** and ** in **(C)** denotes significant differences between transgenic lines and wild-type plants ($N = 3$, $p < 0.01$). All analyses were conducted with three biological replicates, each repeated three times.

stem and all branches of OE2 and OE3 were harvested for lignin analysis after the seeds were collected. Acetyl bromide (AcBr) analysis was completed to measure the lignin contents. The resulting data showed that lignin was significantly increased in the stems and branches of these two transgenic lines (**Figure 5A**).

Coumarin (2H-chromen-2-one) was annotated by GC-MS analysis. The resulting data showed a significant increase in coumarin content in the leaves of these two lines compared with the leaves of the wild-type plants (**Figures 5B,C**), demonstrating that AaCAD is associated with coumarin formation in plants.

Artemisinin, Arteannuin B, and Other Sesquiterpenes Are Decreased in Transgenic Plants

Artemisinin, arteannuin B, and other sesquiterpenes were profiled in the leaves of *AaCAD* transgenic vs. wild-type plants. As reported previously (Ma et al., 2015), artemisinin was measured using HPLC-MS. The resulting data showed that the contents of artemisinin were reduced significantly in two transgenic lines compared with wild-type plants (**Figure 6A**). In addition, arteannuin B and other sesquiterpenes were analyzed using GC-MS as reported previously (Ma et al., 2015). The resulting total ion chromatographs showed that the abundance of many non-polar metabolites was reduced in the two transgenic lines compared with wild-type plants (**Figure 6B**). Peak deconvolution allowed annotation of arteannuin B and other sesquiterpenes (**Figure 6B**). Peak values were recorded for arteannuin B and six other main sesquiterpenes. The resulting data showed that the peak values of arteannuin B and six sesquiterpenes were significantly reduced in the transgenic plants compared with wild-type controls (**Figures 6C,D**). These data indicate that the biosynthetic activity of sesquiterpenes is reduced in *AaCAD* transgenic plants. To determine whether the reduction of these metabolites was associated with the density of glandular trichomes, leaves and stems of transgenic vs. wild-type plants were examined using a Leica MZ FLIII fluorescence stereomicroscope and photographed (Supplementary Figures S4, S5). The resulting data showed that although many transparent or semi-transparent trichomes were observed in both abaxial and adaxial surfaces, most of them are T-shaped trichomes (Supplementary Figure S5) or other sharp stick trichomes. The density of glandular trichomes was low and similar on those leaves between transgenic and wild-type plants (Supplementary Figure S4).

DISCUSSION

The present study shows that understanding the function of AaCAD, a short chain oxidoreductase in *A. annua*, is fundamental for the metabolic engineering of this medicinal crop to achieve high production levels of artemisinin. Numerous studies have reported that CAD is a key enzyme in the biosynthesis of lignin and plays an essential role in plant development associated with plant biomass (Mitchell et al., 1994; Feuillet et al., 1995; Halpin et al., 1998; Bagniewska-Zadworna et al., 2014; Pan et al., 2014; Choi et al., 2016). Downregulation of *CAD* expression or its knockout causes a reduction of lignin, which leads to severe plant dwarfism and a decreased biomass (Sirisha et al., 2012; Anderson et al., 2015; Ozparpucu et al., 2017; Ponniah et al., 2017) as well as decreased plant resistance to pathogens (Bagniewska-Zadworna et al., 2014;

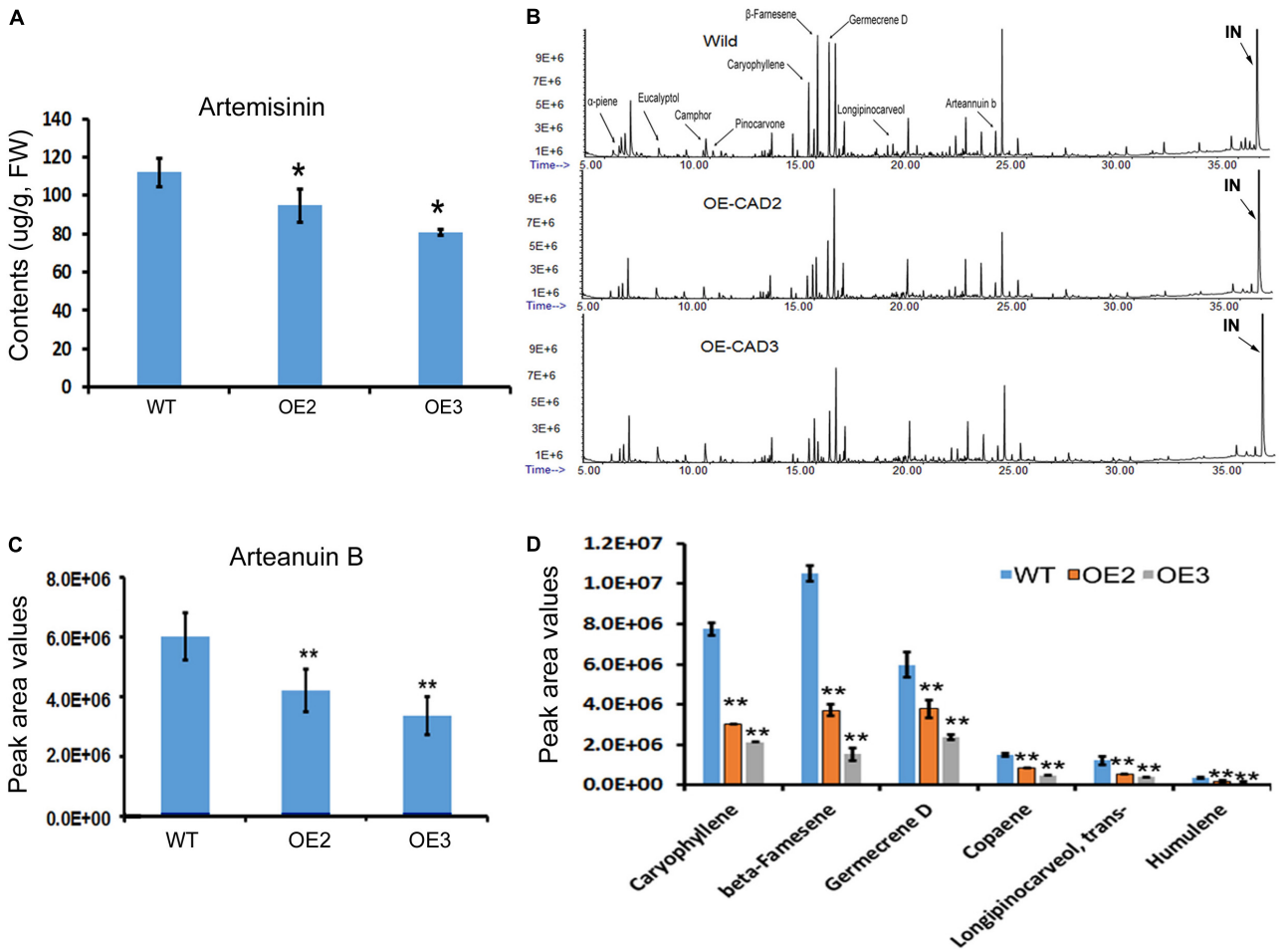

FIGURE 6 | Effects of *AaCAD* overexpression on levels of artemisinin, arteannuin B, and other sesquiterpenes in leaves of transgenic plants. **(A)** LC-MS analysis measurements show decreases in artemisinin contents. **(B)** Overlay of total ion chromatographs shows the abundance reduction of numerous non-polar metabolites, among which arteannuin B and sesquiterpenes are labeled as follows: "IN", internal metabolite as a control. **(C)** Peak area values show the significant reduction of arteannuin B. **(D)** Peak area values show the reduction of five sesquiterpenes. * in **(A)** and ** in **(C)** and **(D)** denote a significant difference in the transgenic lines compared with WT plants. ($N = 3$, $p < 0.01$). All experiments were carried out with three biological replicates, each with three replicates.

Preisner et al., 2014; Rong et al., 2016). However, whether an increase in total lignin via *CAD* overexpression can affect the biosynthesis of terpenoids, such as artemisinin biosynthesis in *A. annua*, remains uninvestigated. We recently reported the cloning of a *CAD* homolog from a cross-pollinating heterozygous cultivar and its biochemical analysis. Our previous *in vitro* enzyme assays showed that the recombinant CAD used coumaryl, coniferyl, and sinapyl aldehydes as substrates in the presence of NADPH (Li et al., 2012). Our previous enzyme assays also showed that this CAD could use artemisinic aldehyde, a sesquiterpenoid metabolite, as a substrate to produce to artemisinic alcohol. Although the Km value of CAD for artemisinic aldehyde is higher than those of coumaryl, coniferyl, and sinapyl aldehydes, the activity using this sesquiterpenoid substrate indicates its catalytic promiscuity. Accordingly, we hypothesize that CAD not only essentially involves lignin formation, but it can also control artemisinin accumulation in *A. annua*. However, a functional analysis of CAD *in planta* has not been performed, given that the cross-pollinating cultivar used to clone *CAD* is a heterozygous species that causes progeny segregation. The heterozygous cultivar is not appropriate material to generate transgenic plants to understand this gene function *in planta*. Herein, we re-cloned a new homolog from our novel inbred SP *A. annua* (F3 progeny) and designated it *AaCAD* to further characterize its functions *in vitro* and *in vivo*. Our enzyme assay showed that this new recombinant AaCAD efficiently converted coumaryl, coniferyl, and sinapyl aldehydes to their corresponding alcohols (Supplementary Figure S2). As expected, the overexpression of *AaCAD* significantly increased the lignin content in SP *A. annua* plants (**Figure 5A**), demonstrating its involvement in lignin biosynthesis. In addition, overexpression increased the content of coumarin (**Figures 5B–C**), indicating its additional function in the phenylpropanoid pathway. Given that amino acid sequence analysis showed that this AaCAD and the previous one from a cross pollinating cultivar had only three amino acid

differences (Supplementary Figure S2) and structural modeling showed the same structure conformation (Supplementary Figure S3), two homologs were anticipated to have similar enzymatic activity to convert artemisinic aldehyde to alcohol. As anticipated, the overexpression of this new *AaCAD* led to significant decreases in the contents of artemisinin, arteannuin B, and other sesquiterpenes in leaves (**Figures 6A,C**). Although these results were not a goal of our metabolic engineering strategy, they supported the findings of our previous *in vitro* enzyme assay showing that recombinant CAD from a cross-pollinating *A. annua* cultivar converted artemisinic aldehyde to artemisinic alcohol (Li et al., 2012), a late step in the reverse direction of the artemisinin pathway (**Figure 1**). To understand whether this reaction could occur in the cytosol of transgenic plant cells, we used GFP fusion to characterize the subcellular localization. Our confocal microscopy analysis revealed the cytosolic localization of AaCAD (**Figure 4**). These data further revealed that the cytosolic localization of AaCAD could reverse the step toward the formation of artemisinin catalyzed by CYP71AV1, CPR1, and AaADH1 and thus catalytically reduce the efficacy of three enzymes in the cytosol. These data indicate that overexpression of *AaCAD* negatively controls the formation of artemisinin in *A. annua*.

Glandular trichomes are the localization of the artemisinin biosynthesis (Duke et al., 1994; Xiao et al., 2016). A field study reported that application of salicylic acid or chitosan oligosaccharidea (out of different stress treatments) could significantly decrease 4–9 glandular trichomes per square of millimeter only on upper leaves from mature plants grown in the field (Kjaer et al., 2012). In the same study, three plants selected from the field were propagated via cutting and the resulting clones were grown in the greenhouse. Kjaer et al. (2012) observed that application of nine stress treatments did not affect the density of glandular trichomes on upper leaves but two stress conditions could significantly reduce about two trichomes per square of millimeter on lower leaves of clones. These results indicate that the density of glandular trichomes can be affected by external stress conditions. In our study, although whether *CAD* can alter glandular and other trichome development remains unknown, we examine glandular trichomes on leaves from 8–12 nodes and those nodes. We did not observe significant density difference of glandular trichomes between wild-type and transgenic plants. It was interesting that certain visual alterations in T-shaped trichomes were observed under microscope (Supplementary Figure S4). Given that glandular trichomes are the tissue of the artemisinin biosynthesis, our herein observation indicates a valuable interest in future studies to thoroughly examine glandular trichomes on all leaves and their effects on artemisinin contents in *CAD* transgenic progeny.

The increase in lignin and the reduction of artemisinin and other sesquiterpenes reveal an interesting crosstalk between two completely distinct pathways via AaCAD catalysis in transgenic plants. Lignin biosynthesis is mainly specialized in vascular tissues in all land plants (Weng and Chapple, 2010; Espineira et al., 2011). By contrast, artemisinin biosynthesis is mainly observed in *A. annua* and potentially other *Artemisia* species. Furthermore, this unique pathway is considered to be limited to a type of specialized glandular trichomes on leaves and flowers (Covello et al., 2007), although its cellular specialization remains controversial (Xie et al., 2016). This type of crosstalk in transgenic plants is most likely associated with two pathway intermediates and co-localization in the cytosol, despite their metabolic distinction (**Figure 1**). In the present transgenic plants, the *AaCAD* transgene was driven by two 35S promoters (**Figure 3A**), leading to constitutive overexpression of the transgene in the tissues, including trichomes. Our previous *in vitro* assay also showed that the recombinant AaCAD catalyzed the conversion of artemisinic aldehyde to alcohol (Li et al., 2012) (**Figure 1**). Accordingly, it is likely that overexpression of AaCAD (**Figure 3E**) enhances the catalytic conversion of artemisinin aldehyde to alcohol in the presence of NADPH in trichomes. In addition to our observations, CAD or CAD-like enzymes have been reported to be involved in the formation of monoterpenoid indole alkaloids in *Rauvolfia serpentine* (Geissler et al., 2016). Moreover, additional biochemical studies have shown that CAD is characterized by a high promiscuity level of different substrates (Chao et al., 2014; Geissler et al., 2016). Based on our and other reports, one hypothesis is that CAD-mediated crosstalk can occur in other metabolic pathways. As more studies are performed, it is anticipated that this type of enzyme-based crosstalk will be observed in different plants. In summary, the observed AaCAD-mediated crosstalk leading to reduced artemisinin contents is instructional for the engineering of *A. annua* for high production.

In conclusion, a new *AaCAD* was cloned from and overexpressed in inbred SP *A. annua*. The enzyme is localized in the cytosol. Overexpression of *AaCAD* in *A. annua* increased lignin and coumarin contents, but it decreased artemisinin, arteannuin B, and other sesquiterpene contents. These data revealed an AaCAD-mediated metabolic crosstalk between the phenylpropanoid (lignin and coumarin) and the sesquiterpene (artemisinin) pathways in the cytosol.

AUTHOR CONTRIBUTIONS

DM and D-YX conceived and designed the research. DM, CX, FA-G, JY, HW, RJ, and D-YX performed the experiments and analyzed the data. DM and D-YX wrote the manuscript. D-YX supervised the entire project. All authors read and approved the manuscript.

FUNDING

This research was supported by the North Carolina Biotechnology Center (grant #: 550031 and reference #: 2009-MRG-1117) and the National Natural Science Foundation of China (81303163).

SUPPLEMENTARY MATERIAL

The Supplementary Material for this article can be found online at: https://www.frontiersin.org/articles/10.3389/fpls.2018.00828/full#supplementary-material

REFERENCES

Alejos-Gonzalez, F., Perkins, K., Winston, M. I., and Xie, D.-Y. (2013). Efficient somatic embryogenesis and organogenesis of self-pollination *Artemisia annua* progeny and artemisinin formation in regenerated plants. *Am. J. Plant Sci.* 4, 2206–2217. doi: 10.4236/ajps.2013.411274

Alejos-Gonzalez, F., Qu, G. S., Zhou, L. L., Saravitz, C. H., Shurtleff, J. L., and Xie, D. Y. (2011). Characterization of development and artemisinin biosynthesis in self-pollinated *Artemisia annua* plants. *Planta* 234, 685–697. doi: 10.1007/s00425-011-1430-z

Anderson, N. A., Tobimatsu, Y., Ciesielski, P. N., Ximenes, E., Ralph, J., Donohoe, B. S., et al. (2015). Manipulation of guaiacyl and syringyl monomer biosynthesis in an Arabidopsis cinnamyl alcohol dehydrogenase mutant results in atypical lignin biosynthesis and modified cell wall structure. *Plant Cell* 27, 2195–2209. doi: 10.1105/tpc.15.00373

Bagniewska-Zadworna, A., Barakat, A., Lakomy, P., Smolinski, D. J., and Zadworny, M. (2014). Lignin and lignans in plant defence: insight from expression profiling of cinnamyl alcohol dehydrogenase genes during development and following fungal infection in *Populus*. *Plant Sci.* 229, 111–121. doi: 10.1016/j.plantsci.2014.08.015

Baucher, M., Bernardvailhe, M. A., Chabbert, B., Besle, J. M., Opsomer, C., Vanmontagu, M., et al. (1999). Down-regulation of cinnamyl alcohol dehydrogenase in transgenic alfalfa (*Medicago sativa* L.) and the effect on lignin composition and digestibility. *Plant Mol. Biol.* 39, 437–447. doi: 10.1023/A:1006182925584

Bouwmeester, H. J., Wallaart, T. E., Janssen, M. H., Van Loo, B., Jansen, B. J., Posthumus, M. A., et al. (1999). Amorpha-4,11-diene synthase catalyses the first probable step in artemisinin biosynthesis. *Phytochemistry* 52, 843–854. doi: 10.1016/S0031-9422(99)00206-X

Chabannes, M., Barakate, A., Lapierre, C., Marita, J. M., Ralph, J., Pean, M., et al. (2001). Strong decrease in lignin content without significant alteration of plant development is induced by simultaneous down-regulation of cinnamoyl CoA reductase (CCR) and cinnamyl alcohol dehydrogenase (CAD) in tobacco plants. *Plant J.* 28, 257–270. doi: 10.1046/j.1365-313X.2001.01140.x

Chao, N., Liu, S. X., Liu, B. M., Li, N., Jiang, X. N., and Gai, Y. (2014). Molecular cloning and functional analysis of nine cinnamyl alcohol dehydrogenase family members in *Populus tomentosa*. *Planta* 240, 1097–1112. doi: 10.1007/s00425-014-2128-9

Choi, B., Chung, J. Y., Bae, H. J., Bae, I., Park, S., and Bae, H. (2016). Functional characterization of cinnamyl alcohol dehydrogenase during developmental stages and under various stress conditions in Kenaf (*Hibiscus cannabinus* L.). *Bioresources* 11, 105–125.

Covello, P. S., Teoh, K. H., Polichuk, D. R., Reed, D. W., and Nowak, G. (2007). Functional genomics and the biosynthesis of artemisinin. *Phytochemistry* 68, 1864–1871. doi: 10.1016/j.phytochem.2007.02.016

Czechowski, T., Larson, T. R., Catania, T. M., Harvey, D., Brown, G. D., and Graham, I. A. (2016). *Artemisia annua* mutant impaired in artemisinin synthesis demonstrates importance of nonenzymatic conversion in terpenoid metabolism. *Proc. Natl. Acad. Sci. U.S.A.* 113, 15150–15155. doi: 10.1073/pnas.1611567113

Duke, M. V., Paul, R. N., Elsohly, H. N., Sturtz, G., and Duke, S. O. (1994). Localization of artemisinin and artemisitene in foliar tissues of glanded and glandless biotypes of *Artemisia annua* L. *Int. J. Plant Sci.* 155, 365–372. doi: 10.1086/297173

d'Yvoire, M. B., Bouchabke-Coussa, O., Voorend, W., Antelme, S., Cezard, L., Legee, F., et al. (2013). Disrupting the cinnamyl alcohol dehydrogenase 1 gene (BdCAD1) leads to altered lignification and improved saccharification in *Brachypodium distachyon*. *Plant J.* 73, 496–508. doi: 10.1111/tpj.12053

Espineira, J. M., Uzal, E. N., Ros, L. V. G., Carrion, J. S., Merino, F., Barcelo, A. R., et al. (2011). Distribution of lignin monomers and the evolution of lignification among lower plants. *Plant Biol.* 13, 59–68. doi: 10.1111/j.1438-8677.2010.00345.x

Feuillet, C., Lauvergeat, V., Deswarte, C., Pilate, G., Boudet, A., and Grima-Pettenati, J. (1995). Tissue- and cell-specific expression of a cinnamyl alcohol dehydrogenase promoter in transgenic poplar plants. *Plant Mol. Biol.* 27, 651–667. doi: 10.1007/BF00020220

Fu, C. X., Xiao, X. R., Xi, Y. J., Ge, Y. X., Chen, F., Bouton, J., et al. (2011). Downregulation of cinnamyl alcohol dehydrogenase (CAD) leads to improved saccharification efficiency in switchgrass. *BioEnergy Res.* 4, 153–164. doi: 10.1007/s12155-010-9109-z

Fukushima, R. S., and Kerley, M. S. (2011). Use of lignin extracted from different plant sources as standards in the spectrophotometric acetyl bromide lignin method. *J. Agric. Food Chem.* 59, 3505–3509. doi: 10.1021/jf104826n

Geissler, M., Burghard, M., Volk, J., Staniek, A., and Warzecha, H. (2016). A novel cinnamyl alcohol dehydrogenase (CAD)-like reductase contributes to the structural diversity of monoterpenoid indole alkaloids in Rauvolfia. *Planta* 243, 813–824. doi: 10.1007/s00425-015-2446-6

Goffner, D., Joffroy, I., Grima-Pettenati, J., Halpin, C., Knight, M. E., Schuch, W., et al. (1992). Purification and characterization of isoforms of cinnamyl alcohol dehydrogenase from Eucalyptus xylem. *Planta* 188, 48–53. doi: 10.1007/BF00198938

Halpin, C., Holt, K., Chojecki, J., Oliver, D., Chabbert, B., Monties, B., et al. (1998). Brown-midrib maize (bm1) - a mutation affecting the cinnamyl alcohol dehydrogenase gene. *Plant J.* 14, 545–553. doi: 10.1046/j.1365-313X.1998.00153.x

Hawkins, S. W., and Boudet, A. M. (1994). Purification and characterization of cinnamyl alcohol dehydrogenase isoforms from the periderm of *Eucalyptus gunnii* Hook. *Plant Physiol.* 104, 75–84. doi: 10.1104/pp.104.1.75

Kjaer, A., Grevsen, K., and Jensen, M. (2012). Effect of external stress on density and size of glandular trichomes in full-grown *Artemisia annua*, the source of anti-malarial artemisinin. *AoB Plants* 2012:ls018. doi: 10.1093/aobpla/pls018

Lapierre, C., Pollet, B., Mackay, J. J., and Sederoff, R. R. (2000). Lignin structure in a mutant pine deficient in cinnamyl alcohol dehydrogenase. *J. Agric. Food Chem.* 48, 2326–2331. doi: 10.1021/jf991398p

Li, X., Ma, D. M., Chen, J. L., Pu, G. B., Ji, Y. P., Lei, C. Y., et al. (2012). Biochemical characterization and identification of a cinnamyl alcohol dehydrogenase from *Artemisia annua*. *Plant Sci.* 193, 85–95. doi: 10.1016/j.plantsci.2012.05.011

Ma, D., Li, G., Alejos-Gonzalez, F., Zhu, Y., Xue, Z., Wang, A., et al. (2017a). Overexpression of a type-I isopentenyl pyrophosphate isomerase of *Artemisia annua* in the cytosol leads to high arteannuin B production and artemisinin increase. *Plant J.* 91, 466–479. doi: 10.1111/tpj.13583

Ma, D., Li, G., Zhu, Y., and Xie, D. Y. (2017b). Overexpression and suppression of *Artemisia annua* 4-hydroxy-3-methylbut-2-enyl diphosphate reductase 1 gene (AaHDR1) differentially regulate artemisinin and terpenoid biosynthesis. *Front. Plant Sci.* 8:77. doi: 10.3389/fpls.2017.00077

Ma, D.-M., Wang, Z., Wang, L., Alejos-Gonzales, F., Sun, M.-A., and Xie, D.-Y. (2015). A genome-wide scenario of terpene pathways in self-pollinated *Artemisia annua*. *Mol. Plant* 8, 1580–1598. doi: 10.1016/j.molp.2015.07.004

Ma, Q. H. (2010). Functional analysis of a cinnamyl alcohol dehydrogenase involved in lignin biosynthesis in wheat. *J. Exp. Bot.* 61, 2735–2744. doi: 10.1093/jxb/erq107

MacKay, J., Presnell, T., Jameel, H., Taneda, H., Omalley, D., and Sederoff, R. (1999). Modified lignin and delignification with a CAD-deficient loblolly pine. *Holzforschung* 53, 403–410. doi: 10.1515/HF.1999.067

Maude, R. J., Pontavornpinyo, W., Saralamba, S., Aguas, R., Shunmay, Y., Dondorp, A. M., et al. (2009). The last man standing is the most resistant: eliminating artemisinin-resistant malaria in Cambodia. *Malaria J.* 8, 1–7. doi: 10.1186/1475-2875-8-31

Mitchell, H. J., Hall, J. L., and Barber, M. S. (1994). Elicitor-induced cinnamyl alcohol dehydrogenase activity in lignifying wheat (*Triticum aestivum* L.) leaves. *Plant Physiol.* 104, 551–556. doi: 10.1104/pp.104.2.551

Moreira-Vilar, F. C., Siqueira-Soares, R. D. C., Finger-Teixeira, A., Oliveira, D. M. D., Ferro, A. P., Da Rocha, G. J., et al. (2014). The acetyl bromide method is faster, simpler and presents best recovery of lignin in different herbaceous tissues than Klason and Thioglycolic Acid Methods. *PLoS One* 9:e110000. doi: 10.1371/journal.pone.0110000

Ozparpucu, M., Ruggeberg, M., Gierlinger, N., Cesarino, I., Vanholme, R., Boerjan, W., et al. (2017). Unravelling the impact of lignin on cell wall mechanics: a comprehensive study on young poplar trees downregulated for cinnamyl alcohol dehydrogenase (CAD). *Plant J.* 91, 480–490. doi: 10.1111/tpj.13584

Paddon, C. J., Westfall, P. J., Pitera, D. J., Benjamin, K., Fisher, K., Mcphee, D., et al. (2013). High-level semi-synthetic production of the potent antimalarial artemisinin. *Nature* 496, 528–532. doi: 10.1038/nature12051

Pan, H. Y., Zhou, R., Louie, G. V., Muhlemann, J. K., Bomati, E. K., Bowman, M. E., et al. (2014). Structural studies of cinnamoyl-CoA reductase and

cinnamyl-alcohol dehydrogenase, key enzymes of monolignol biosynthesis. *Plant Cell* 26, 3709–3727. doi: 10.1105/tpc.114.127399

Ponniah, S. K., Shang, Z. H., Akbudak, M. A., Srivastava, V., and Manoharan, M. (2017). Down-regulation of hydroxycinnamoyl CoA: shikimate hydroxycinnamoyl transferase, cinnamoyl CoA reductase, and cinnamyl alcohol dehydrogenase leads to lignin reduction in rice (*Oryza sativa* L. ssp japonica cv. Nipponbare). *Plant Biotechnol. Rep.* 11, 17–27. doi: 10.1007/s11816-017-0426-y

Preisner, M., Kulma, A., Zebrowski, J., Dyminska, L., Hanuza, J., Arendt, M., et al. (2014). Manipulating cinnamyl alcohol dehydrogenase (CAD) expression in flax affects fibre composition and properties. *BMC Plant Biol.* 14:50. doi: 10.1186/1471-2229-14-50

Ro, D.-K., Paradise, E. M., Ouellet, M., Fisher, K. J., Newman, K. L., Ndungu, J. M., et al. (2006). Production of the antimalarial drug precursor artemisinic acid in engineered yeast. *Nature* 440, 940–943. doi: 10.1038/nature04640

Rong, W., Luo, M. Y., Shan, T. L., Wei, X. N., Du, L. P., Xu, H. J., et al. (2016). A wheat cinnamyl alcohol dehydrogenase TaCAD12 contributes to host resistance to the sharp eyespot disease. *Front. Plant Sci.* 7:1723. doi: 10.3389/fpls.2016.01723

Saathoff, A. J., Sarath, G., Chow, E. K., Dien, B. S., and Tobias, C. M. (2011). Downregulation of cinnamyl-alcohol dehydrogenase in switchgrass by RNA silencing results in enhanced glucose release after cellulase treatment. *PLoS One* 6:e16416. doi: 10.1371/journal.pone.0016416

Sarni, R., Grand, C., and Boudet, A. M. (1984). Purification and properties of cinnamoyl-CoA reductase and cinnamyl alcohol dehydrogenase from poplar stems (*Populus* X *euramericana*). *Eur. J. Biochem.* 139, 259–265. doi: 10.1111/j.1432-1033.1984.tb08002.x

Sirisha, V. L., Prashant, S., Kumar, D. R., Pramod, S., Jalaja, N., Kumari, P. H., et al. (2012). Cloning, characterization and impact of up- and down-regulating subabul cinnamyl alcohol dehydrogenase (CAD) gene on plant growth and lignin profiles in transgenic tobacco. *Plant Growth Regul.* 66, 239–253. doi: 10.1007/s10725-011-9647-1

Somers, D. A., Nourse, J. P., Manners, J. M., Abrahams, S., and Watson, J. M. (1995). A gene encoding a cinnamyl alcohol dehydrogenase homolog in *Arabidopsis thaliana*. *Plant Physiol.* 108, 1309–1310. doi: 10.1104/pp.108.3.1309

Teoh, K. H., Polichuk, D. R., Reed, D. W., Nowak, G., and Covello, P. S. (2006). *Artemisia annua* L. (Asteraceae) trichome-specific cDNAs reveal CYP71AV1, a cytochrome P450 with a key role in the biosynthesis of the antimalarial sesquiterpene lactone artemisinin. *FEBS Lett.* 580, 1411–1416. doi: 10.1016/j.febslet.2006.01.065

Trabucco, G. M., Matos, D. A., Lee, S. J., Saathoff, A. J., Priest, H. D., Mockler, T. C., et al. (2013). Functional characterization of cinnamyl alcohol dehydrogenase and caffeic acid O-methyltransferase in *Brachypodium distachyon*. *BMC Biotechnol.* 13:61. doi: 10.1186/1472-6750-13-61

Turconi, J., Griolet, F., Guevel, R., Oddon, G., Villa, R., Geatti, A., et al. (2014). Semisynthetic artemisinin, the chemical path to industrial production. *Org. Process Res. Dev.* 18, 417–422. doi: 10.1021/op4003196

Wang, G. F., He, Y., Strauch, R., Olukolu, B. A., Nielsen, D., Li, X., et al. (2015). Maize homologs of hydroxycinnamoyltransferase, a key enzyme in lignin biosynthesis, bind the nucleotide binding leucine-rich repeat Rp1 proteins to modulate the defense response. *Plant Physiol.* 169, 2230–2243. doi: 10.1104/pp.15.00703

Wang, Y. H., Jia, Q. B., Zhang, L., Zhang, Z., and Zhang, H. G. (2015). Allelic wariation in cinnamyl alcohol dehydrogenase (LoCAD) associated with wood properties of *Larix olgensis*. *Forests* 6, 1649–1665. doi: 10.3390/f6051649

Weng, J. K., and Chapple, C. (2010). The origin and evolution of lignin biosynthesis. *New Phytol.* 187, 273–285. doi: 10.1111/j.1469-8137.2010.03327.x

WHO (2006). *Meeting on the Production of Artemisinin and Artemisinin-Based Combination Therapies 6-7 June 2005*. Arusha: United Republic Tanzania.

WHO (2013). *Changes in Malaria Incidence and Mortality WHO Global Malaria Programme-World Malaria Report 2013*. Geneva: World Health Organization.

Xi, J., Rossi, L., Lin, X., and Xie, D.-Y. (2016). Overexpression of a synthetic insect–plant geranyl pyrophosphate synthase gene in *Camelina sativa* alters plant growth and terpene biosynthesis. *Planta* 244, 215–230. doi: 10.1007/s00425-016-2504-8

Xiao, L., Tan, H. X., and Zhang, L. (2016). *Artemisia annua* glandular secretory trichomes: the biofactory of antimalarial agent artemisinin. *Sci. Bull.* 61, 26–36. doi: 10.1007/s11434-015-0980-z

Xie, D.-Y., Ma, D.-M., Judd, R., and Jones, A. L. (2016). Artemisinin biosynthesis in *Artemisia annua* and metabolic engineering: questions, challenges, and perspectives. *Phytochem. Rev.* 15, 1093–1114. doi: 10.1007/s11101-016-9480-2

Zhang, Y., Teoh, K. H., Reed, D. W., Maes, L., Goossens, A., Olson, D. J., et al. (2008). The molecular cloning of artemisinic aldehyde Delta11(13) reductase and its role in glandular trichome-dependent biosynthesis of artemisinin in *Artemisia annua*. *J. Biol. Chem.* 283, 21501–21508. doi: 10.1074/jbc.M803090200

Conflict of Interest Statement: The authors declare that the research was conducted in the absence of any commercial or financial relationships that could be construed as a potential conflict of interest.

frontiers in Plant Science

ORIGINAL RESEARCH
published: 02 August 2018
doi: 10.3389/fpls.2018.00952

Molecular Characterization of the *1-Deoxy-D-Xylulose 5-Phosphate Synthase* Gene Family in *Artemisia annua*

Fangyuan Zhang[1†], Wanhong Liu[2†], Jing Xia[1], Junlan Zeng[1], Lien Xiang[1], Shunqin Zhu[1], Qiumin Zheng[1], He Xie[3], Chunxian Yang[1], Min Chen[4] and Zhihua Liao[1]*

[1] Key Laboratory of Eco-Environments in Three Gorges Reservoir Region (Ministry of Education), Chongqing Key Laboratory of Plant Ecology and Resources Research in Three Gorges Reservoir Region, SWU-TAAHC Medicinal Plant Joint R&D Centre, School of Life Sciences, Southwest University, Chongqing, China, [2] School of Chemistry and Chemical Engineering, Chongqing University of Science and Technology, Chongqing, China, [3] Tobacco Breeding and Biotechnology Research Center, Yunnan Academy of Tobacco Agricultural Sciences, Key Laboratory of Tobacco Biotechnological Breeding, National Tobacco Genetic Engineering Research Center, Kunming, China, [4] SWU-TAAHC Medicinal Plant Joint R&D Centre, College of Pharmaceutical Sciences, Southwest University, Chongqing, China

OPEN ACCESS

Edited by:
Henrik T. Simonsen, Technical University of Denmark, Denmark

Reviewed by:
Ian A. Graham, University of York, United Kingdom
Mehar H. Asif, National Botanical Research Institute (CSIR), India

***Correspondence:**
Zhihua Liao
zhliao@swu.edu.cn;
zhihualiao@163.com

† These authors have contributed equally to this work.

Specialty section:
This article was submitted to Plant Biotechnology, a section of the journal Frontiers in Plant Science

Received: *15 January 2018*
Accepted: *13 June 2018*
Published: *02 August 2018*

Citation:
Zhang F, Liu W, Xia J, Zeng J, Xiang L, Zhu S, Zheng Q, Xie H, Yang C, Chen M and Liao Z (2018) Molecular Characterization of the 1-Deoxy-D-Xylulose 5-Phosphate Synthase Gene Family in Artemisia annua. Front. Plant Sci. 9:952. doi: 10.3389/fpls.2018.00952

Artemisia annua produces artemisinin, an effective antimalarial drug. In recent decades, the later steps of artemisinin biosynthesis have been thoroughly investigated; however, little is known about the early steps of artemisinin biosynthesis. Comparative transcriptomics of glandular and filamentous trichomes and $^{13}CO_2$ radioisotope study have shown that the 2-C-methyl-D-erythritol-4-phosphate (MEP) pathway, rather than the mevalonate pathway, plays an important role in artemisinin biosynthesis. In this study, we have cloned three *1-deoxy-D-xylulose 5-phosphate synthase* (*DXS*) genes from *A. annua* (*AaDXS1*, *AaDXS2*, and *AaDXS3*); the DXS enzyme catalyzes the first and rate-limiting enzyme of the MEP pathway. We analyzed the expression of these three genes in different tissues in response to multiple treatments. Phylogenetic analysis revealed that each of the three *DXS* genes belonged to a distinct clade. Subcellular localization analysis indicated that all three AaDXS proteins are targeted to chloroplasts, which is consistent with the presence of plastid transit peptides in their N-terminal regions. Expression analyses revealed that the expression pattern of *AaDXS2* in specific tissues and in response to different treatments, including methyl jasmonate, light, and low temperature, was similar to that of artemisinin biosynthesis genes. To further investigate the tissue-specific expression pattern of *AaDXS2*, the promoter of *AaDXS2* was cloned upstream of the β-*glucuronidase* gene and was introduced in arabidopsis. Histochemical staining assays demonstrated that *AaDXS2* was mainly expressed in the trichomes of Arabidopsis leaves. Together, these results suggest that *AaDXS2* might be the only member of the DXS family in *A. annua* that is involved in artemisinin biosynthesis.

Keywords: *Artemisia annua*, artemisinin, 1-deoxy-D-xylulose 5-phosphate synthase, gene expression, MEP pathway

INTRODUCTION

Terpenoids, also known as isoprenoids, play several important roles in several plant processes. Despite their diverse structures and functions, all terpenoids are derived from the common five-carbon (C_5) building blocks, isopentenyl diphosphate (IPP) and its isomer dimethylallyl diphosphate (DMAPP). In plants, the C_5 building blocks are biosynthesized *via* two-independent pathways: cytosolic mevalonate (MVA) pathway that is found in most eukaryotes and 2-C-methyl-D-erythritol-4-phosphate (MEP) pathway that is found in the chloroplasts of photosynthetic eukaryotes and in eubacteria (Querol et al., 2002). Both these pathways are thought to be largely independent. The MVA pathway is primarily responsible for the biosynthesis of sesquiterpenes and triterpenes, whereas the MEP pathway produces precursors for the biosynthesis of major photosynthetic pigments, hormones, and monoterpenes and diterpenes (Dudareva et al., 2005). However, crosstalk between the MVA and MEP pathways occurs during the biosynthesis of some sesquiterpenes, such as artemisinin (Schramek et al., 2009).

The first reaction of the MEP pathway is the condensation of pyruvate with glyceraldehyde-3-phosphate to produce 1-deoxy-D-xylulose 5-phosphate (DXS), which is catalyzed by DXS (Querol et al., 2002). Subsequently, MEP is converted into a 5:1 mixture of IPP and DMAPP via six enzymatic reactions (Rodriguez-Concepcion and Boronat, 2002). Various studies suggest that DXS is a rate-limiting enzyme in the biosynthesis of terpenoids. The expression of *DXS* increases in plant tissues that require high levels of isoprenoids, as exemplified by maize (*Zea mays*; Cordoba et al., 2011), tomato (*Solanum lycopersicum*; Paetzold et al., 2010), glandular trichomes of peppermint (*Mentha piperita*; Lange et al., 1998), and young seedlings of arapdiopsis (*Arabidopsis thaliana*; Estévez et al., 2001). Overexpression or suppression of *DXS* alters the levels of specific isoprenoids in arapdiopsis (Estévez et al., 2001), tomato (Enfissi et al., 2005), and potato (*Solanum tuberosum*; Morris et al., 2006). Thus, DXS is an important target for the manipulation of isoprenoid biosynthesis.

Although most of the enzymes in the MEP pathway are encoded by single copy genes, the DXS enzymes are usually encoded by a small gene family (Rodriguez-Concepcion and Boronat, 2002; Cordoba et al., 2009), which is divided into three distinct phylogenetic clades (Carretero-Paulet et al., 2013). The expression of genes in the different clades varies with development, tissue type, and environmental conditions. The DXS proteins in clade 1, such as DXS1 in arabidopsis (*Cloroplastos alterados 1*, *CLA1*), primarily perform housekeeping functions (Estévez et al., 2000). In contrast, the expression of *DXS* genes in clade 2 is associated with isoprenoid accumulation. For instance, the expression of *MtDXS2* in barrelclover (*Medicago truncatula*) and *ZmDXS2* in maize is correlated with the production of certain apocarotenoids during mycorrhization (Walter et al., 2002; Cordoba et al., 2011). The suppression of these *MtDXS2* results in reduced apocarotenoid accumulation, whereas the accumulation of *MtDXS1* does not affect apocarotenoid production (Walter et al., 2002). Similarly, the expression of *SlDXS2* in tomato exhibits a positive correlation with colonization by mycorrhizal fungi and the accumulation of apocarotenoids (Paetzold et al., 2010). Furthermore, the suppression of *SlDXS2* in tomato leads to a decrease in the accumulation of the monoterpene, β-phellandrene, and an increase in the levels of two sesquiterpenes in leaf trichomes (Paetzold et al., 2010). Likewise, *OsDXS3* in rice (*Oryza sativa*) has been suggested to be involved in defense responses and secondary metabolism (Okada et al., 2007). Together, these findings suggest that the DXS proteins in clade 2 are dedicated to secondary metabolism.

Artemisinin is a sesquiterpene endoperoxide that has been isolated from sweet wormwood (*Artemisia annua*) and extensively used in the treatment of malaria. Artemisinin has received tremendous interest in recent years because of its potential to treat cancer, diabetes, and tuberculosis (Zheng et al., 2017). Remarkable advances have been made in understanding the artemisinin biosynthetic pathway in recent decades. The first committed step in artemisinin biosynthesis is the cyclization of farnesyl diphosphate (FPP) to amorpha-4, 11-diene by amorpha-4, 11-diene synthase (ADS). Through three additional consecutive enzymatic reactions, amorpha-4, 11-diene is converted into dihydroartemisinic acid (DHAA), which is subsequently converted into artemisinin in an enzyme-independent reaction. Additionally, all four artemisinin biosynthesis genes (*ADS*, *CYP71AV1*, *DBR2*, and *ALDH1*) are specifically expressed in glandular secretory trichomes (GSTs), which are 10-cell structures located primarily on the surface of leaves and flower buds in *A. annua* (Chen et al., 2017).

While substantial progress has been made in understanding the later steps of artemisinin biosynthesis, little is known about the MVA and MEP pathways that supply the precursors for artemisinin biosynthesis. It has long been assumed that terpenoid/isoprenoid precursors provided by the MVA pathway are predominantly responsible for artemisinin biosynthesis; however, more recent studies suggest that the MEP pathway also supplies precursors for artemisinin biosynthesis. Either mevinolin (MVA pathway-specific inhibitor) or fosmidomycin (MEP pathway-specific inhibitor) decreases the artemisinin production in treated plants of *A. annua* (Towler and Weathers, 2007). Furthermore, the $^{13}CO_2$ study demonstrates that the MEP pathway provides the central isoprenoid unit for the biosynthesis of FPP, which is the substrate for ADS (Schramek et al., 2009). Thus, both pathways are involved in artemisinin biosynthesis; however, genes that encode the enzymes of the MEP and MVA pathways, and the functions of these genes, remain elusive.

Given that the MEP pathway supplies precursors for artemisinin biosynthesis, and the DXS is the rate-limiting enzyme in the MEP pathway, a deeper understanding of the individual *DXS* gene family members will further help in understanding artemisinin biosynthesis and provide new target(s) for manipulating this metabolic pathway. Previously, Graham et al. (2010) have reported two *DXS* genes in *A. annua* with differential expression patterns, based on transcriptome sequencing. In the present work, we performed a detailed analysis of *AaDXS* gene family. Three *AaDXS* genes were cloned, each of which represented a distinct phylogenetic clade. Additionally, comprehensive expression analyses showed that the expression

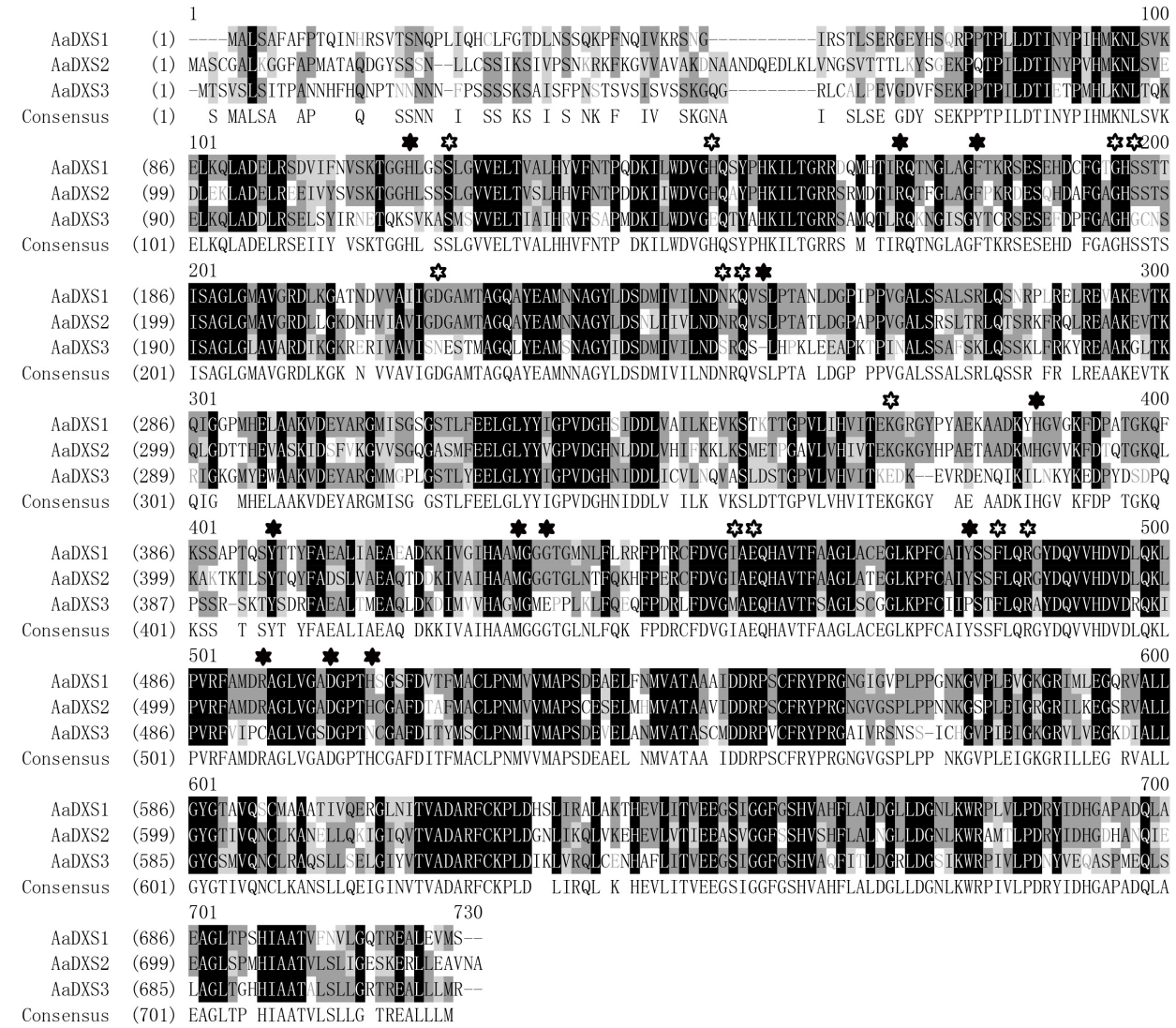

FIGURE 1 | Amino acid sequence alignment of DXS proteins of *Artemisia annua* and *Arabidopsis thaliana*. Solid star indicates the functional residues involved in GAP-binding and hollow star indicates the functional residues involved in TPP-binding.

pattern of *AaDXS2* was highly similar to that of artemisinin biosynthesis genes, suggesting that *AaDXS2* is the primary member of the *AaDXS* gene family that is involved in artemisinin biosynthesis.

MATERIALS AND METHODS

Plant Materials and Treatments

Seeds of *A. annua* were collected from the botanical garden of Southwest University, Chongqing, China and stored at 4°C. Seedlings were grown in the greenhouse at 25 ± 1°C under 16 h light/8 h dark photoperiod. For light induction analysis of *DXS* genes, one-month-old seedlings were grown in the dark for 24 h and then shifted to light (Cordoba et al., 2011). Gene expression was examined in the leaves collected at different time points, ranging from 5 min to 12 h; leaves collected at 0 min were used as a control. In order to determine the expression pattern of *DXS* genes during development, the apical bud and the top seven leaves (leaf 1–8, except leaf 3) on the main stem of two-month-old plants were subjected to quantitative real-time polymerase chain reaction (qPCR) analysis (Lu et al., 2013; Czechowski et al., 2016). To analyze the expression of *DXS* genes in response to methyl jasmonate (MeJA), leaves of 2-month-old plants were treated with 300 μM MeJA and harvested at the indicated time points; leaves harvested from plants treated with 0.8% alcohol were used as a control. To study the effect of cold temperature on *DXS* gene expression, *A. annua* seedlings were transferred to the illumination incubator at 4°C (Liu et al., 2017). Subsequently, leaves collected at the indicated time points were subjected to qPCR analysis; leaves harvested at 0 h were used as a control. For analyzing tissue-specific expression profiles of *DXS* genes,

five-month-old plants were transferred to 8 h light/16 h dark photoperiod to promote flowering. Flowers, leaves, stems, and roots of *A. annua* plants were collected and used for analyzing tissue expression profiles of *DXS* genes. All treatments performed in this study were replicated three times.

Cloning of *DXS* Genes and Sequence Analysis

Total RNA was isolated from plant materials using RNAsimple Kit (No. DP419; Tiangen Biotech, Beijing, China) according to the manufacturer's protocol. Promega M-MLV Kit (Promega, United States) and SMART rapid amplification of cDNA ends (RACE) cDNA Amplification Kit (Clontech, United States) were used for cloning the 3′- and 5′-end of *DXS* cDNAs, respectively. The first-strand 3′- and 5′-RACE-Ready cDNAs were prepared and used as templates for 3′- and 5′-RACE, respectively, according to the manufacturer's protocol. For sequence analysis, *DXS* amino acid sequences of *A. thaliana* were used as queries to search for *AaDXS* nucleotide sequences in the expressed sequence tag (EST) database of *A. annua* (taxid: 35608) using tBLASTn program. Touchdown PCR was carried out to clone the 3′- and 5′-ends of *AaDXS* genes. Each PCR product was cloned into the pMD-18T vector (Takara, Japan) and sequenced. Subsequently, full-length cDNAs of *AaDXS* genes were amplified by PCR using gene-specific primers (**Supplementary Table S1**). Multiple sequence alignments of *DXS* proteins were performed using Vector-NTI Advance 11.5 software package (Invitrogen, Carlsbad, CA, United States). Phylogenetic tree of *DXS* proteins was constructed with MEGA version 3.0 (Kumar et al., 2004) using the neighbor-joining method with a bootstrap of 1,000 replicates (Saitou and Nei, 1987).

Subcellular Localization

The putative plastid transit peptides of DXS isoforms were predicted using TargetP (Emanuelsson et al., 2000). Fragments of *AaDXS* genes encoding transit peptides were amplified by PCR using KOD plus (TOYOBO, Japan). Subsequently, all fragments harboring *Sac*I and *Sal*I restriction sites were inserted into the multiple cloning site of pCAMBIA1300-green fluorescent protein (GFP) in-frame with the coding sequence of the GFP gene. Approximately, 20 μg of each plasmid was introduced into mesophyll protoplasts of tobacco (*Nicotiana tabacum*) using polyethylene glycol-mediated transformation (Yoo et al., 2007). GFP fluorescence and chlorophyll autofluorescence were observed using ZEISS LSM700 laser confocal microscope (ZEISS, Germany) at excitation wavelengths of 488 and 555 nm, respectively.

qPCR Analysis

To investigate the expression of *AaDXS* genes in different tissues as well as under various conditions, qPCR was performed using iQ5 Multicolor Real-Time PCR Detection System (Bio-Rad, United States). The total RNA (2 μg) of *A. annua* was used for first-strand cDNA synthesis using GoScript™ Reverse Transcription System (Promega, United States). The qPCR reaction mixtures were prepared with Go*Taq* qPCR Master Mix (Promega, United States), according to the manufacturer's protocol. PCR amplifications were performed using the following conditions: denaturation at 95°C for 30 s, followed by 40 cycles at denaturation at 95°C for 5 s and annealing and extension at 60°C for 30 s, and a final extension at 72°C for 20 s. Melting curve was used to determine the specificity of amplifications. The *ACTIN* gene was used as reference for normalization of qPCR CT values. Gene-specific primers used for qPCRs were designed using Primer Premier 6 (**Supplementary Table S1**). The $2^{-\Delta\Delta CT}$ method was used to calculate the relative fold-change in gene expression (Livak and Schmittgen, 2001).

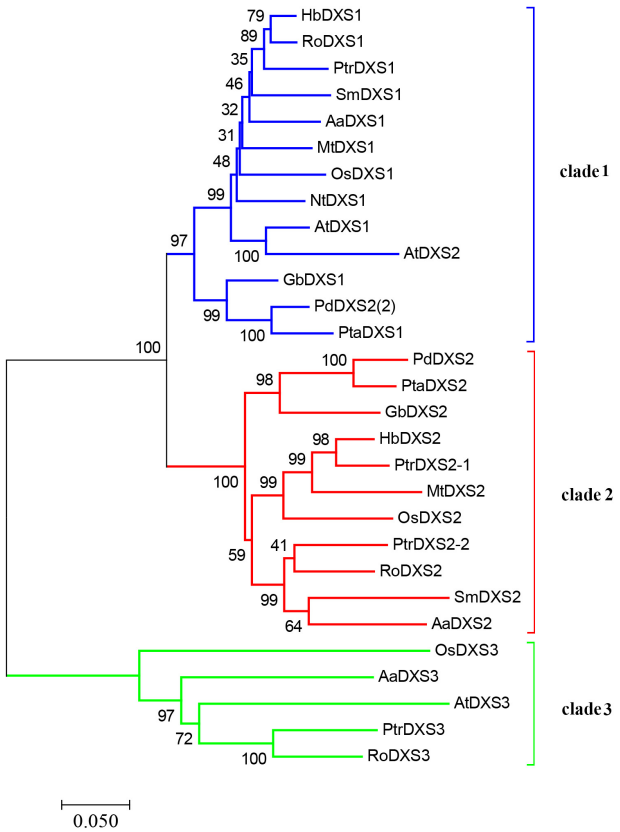

FIGURE 2 | Phylogenetic tree of plant DXS proteins. The tree was constructed with the neighbor-joining method using MEGA program 3.0 with 1,000 bootstrap values. The TAIR or Genebank accession numbers of DXS amino acid sequences used for phylogenetic analysis are as follows: *Arabidopsis thaliana* (DXS1 = *At*4g15560, DXS2 = *At*3g21500, and DXS3 = *At*5G11380); *Ginkgo biloba* (DXS1 = AAS89341.1 and DXS2 = AAR95699.1); *Hevea brasiliensis* (DXS1 = AAS94123.1 and DXS2 = ABF18929.1); *Medicago truncatula* (DXS1 = CAD22530.1 and i = CAN89181.1); *Nicotiana tabacum* (CBA12009.1); *Oryza sativa* (DXS1 = NP_001055524, DXS2 = NP_001059086, and DXS3 = BAA83576); *Pinus densiflora* (DXS1 = ACC54557.1 and DXS2 = ACC54554.1); *Pinus taeda* (DXS1 = ACJ67021.1 and DXS2 = ACJ67020.1); *Populus trichocarpa* (DXS1 = XP_002312717.1, DXS2-1 = XP_002303416.1, DXS2-2 = XP_002331678.1, and DXS3 = XP_002308644.1); *Ricinus communis* (DXS1 = XP_002516843.1, DXS2 = XP_002533688.1, and DXS3 = XP_002514364.1); and *Salvia miltiorrhiza* (DXS1 = ACF21004.1, DXS2 = ACQ66107.1).

Promoter Cloning and β-Glucuronidas (GUS) Histochemical Staining

Genomic DNA of *A. annua* was isolated using the CTAB method. A genome walking method, that is, fusion primer and nested integrated PCR (Wang et al., 2011) was carried out to amplify the promoter of *AaDXS2* (*pAaDXS2*). Primers used to amplify *pAaDXS2* are listed in **Supplementary Table S1**. The TSSP software was used to determine the transcription start site of *AaDXS2* (Solovyev and Shahmuradov, 2003). The *cis*-elements in *pAaDXS2* were analyzed using PlantCARE website[1] and PLACE website[2].

To investigate the expression pattern of *AaDXS2* in plants, the *pAaDXS2* was cloned into pCAMBIA1391.Z to drive the expression of *GUS* gene. The *pAaDXS2::GUS* construct was introduced into *Agrobacterium tumefaciens* strain GV3101 and transformed into *A. thaliana* by the floral dip method (Zhang et al., 2006). Mature leaves and flowers of 45-day-old arabidopsis seedlings as well as siliques from 2-month-old transgenic *A. thaliana* were used for *GUS* histochemical staining as described previously (Jefferson et al., 1987). *GUS* stained tissues were observed under Olympus SZX16 microscope, and pictures were taken using Olympus DP73 digital camera.

RESULTS

The *A. annua* Genome Harbors Three *DXS* Genes

To investigate the *DXS* genes in *A. annua*, tBLASTn program[3] was used. Amino acid sequences of AtDXS proteins (*At*4G15560, *At*3G21500, and *At*5G11380) were used as queries against the EST database of *A. annua* (taxid: 35608). Three *AaDXS* partial coding sequences (contig16978, contig19217, and contig6280) were obtained. Subsequently, primers for RACE PCRs were designed based on the longest EST sequence. The resulting full-length cDNAs of three *AaDXS* genes were named as *AaDXS1*, *AaDXS2*, and *AaDXS3*.

The full-length *AaDXS1* cDNA was 2,529 bp in length and contained 126 bp 5′ untranslated region (5′UTR), 2,142 bp open reading frame (ORF), and 261 bp 3′UTR (**Supplementary Figure S1**). The *AaDXS2* cDNA consisted of 52-bp 5′UTR, 2,187 bp ORF, and 214 bp 3′UTR (**Supplementary Figure S2**). The *AaDXS3* cDNA was the longest among the three *AaDXS* cDNAs (2,761 bp) and comprised 248 bp 5′UTR and 374 bp 3′UTR (**Supplementary Figure S3**). All three AaDXSs showed features similar to those of known DXS from other plant species, including the presence of an N-terminal targeting sequence, a conserved thiamine diphosphate binding site, and pyridine binding DRAG domain (**Figure 1**).

A phylogenetic tree was constructed using neighbor-joining method to reveal the evolutionary relationship among the DXS proteins of thirteen plant species, including *A. annua* (**Figure 2**). Phylogenetic analysis showed three clusters of DXS proteins. AaDXS1 grouped in clade 1, which contained well-characterized DXS1 proteins of arabidopsis and *M. truncatula*. AaDXS2 grouped in clade 2 with the well-characterized DXS2 proteins of *M. truncatula* and *Salvia miltiorrhiza*. Partial members within clade 2 play important roles in plant secondary metabolism, especially isoprenoid biosynthesis (Floss et al., 2008; Kai et al., 2012). Compared with clades 1 and 2, clade 3 contained five DXS proteins from *A. annua*, *A. thaliana*, and *O. sativa*. The biological functions of DXS proteins in clade 3 are unclear; however, the DXS proteins in clade 3 are contained at lower expression levels than those in clades 1 and 2 in maize (Cordoba et al., 2011). Studies in arabidopsis and tomato have shown that the DXS proteins in different clades are involved in different biological processes (Paetzold et al., 2010; Carretero-Paulet et al., 2013). Overall, phylogenetic analysis showed that the three *AaDXS* proteins clustered into three distinct clades, suggesting that these three proteins are involved in different biological processes.

AaDXS Proteins Localize to the Chloroplast

In silico analysis with TargetP 1.1 showed that all three AaDXS proteins carried a plastid transit peptide. To further validate the *in silico* results, nucleotide sequences encoding the putative transit peptides were amplified by PCR and cloned into pCAMBIA1300-GFP vector. These constructs containing the putative transit peptides fused with GFP were then transformed into tobacco mesophyll protoplasts. The GFP signal resulting from the transformation of each vector localized together with the autofluorescence signal of chloroplasts (**Figure 3**). These results demonstrated

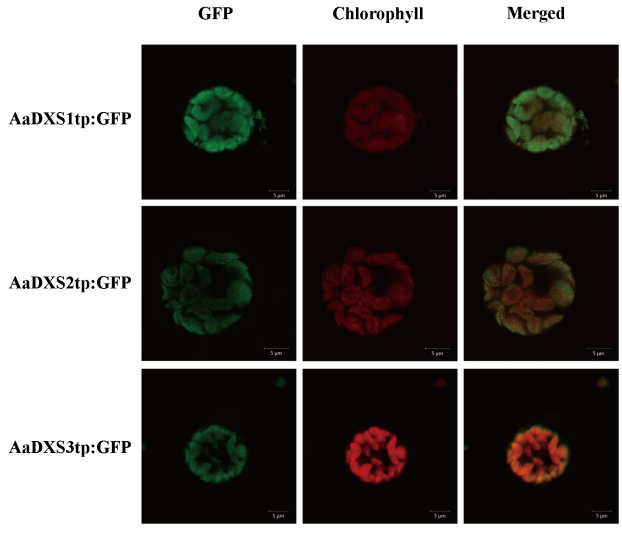

FIGURE 3 | Images of tobacoo mesophyll protoplasts expressing the transit peptides of the *AaDXS* genes fused to the green fluorescent protein (GFP). GFP fluorescence and chlorophyll autofluorescence was detected using confocal microscope.

[1]http://bioinformatics.psb.ugent.be/webtools/plantcare/html/

[2]http://www.dna.affrc.go.jp/PLACE/

[3]https://blast.ncbi.nlm.nih.gov/Blast.cgi

that all three *Aa*DXS proteins localized to the chloroplast; this is consistent with the plastid localization of the MEP pathway.

AaDXS2 and Artemisinin Biosynthesis Genes Show Similar Tissue-Specific Expression

The expression profiles of *AaDXS* genes were analyzed in different tissues, including flowers, leaves, stems, and roots. Many studies have shown that the artemisinin biosynthesis genes have the highest expression levels in flower buds, followed by leaves, and finally, the roots (Zhang et al., 2015). As shown in **Figure 4**, expression levels of *AaDXS1* and *AaDXS3* were significantly lower in flowers than in other tissues of *A. annua*. However, the expression level of *AaDXS2* in flowers was 3-fold higher than that in leaves and 10-fold higher than that in stems and roots (**Figure 4**). Additionally, the expression of *AaDXSs* was also detected in leaves at different positions on the stem, where the density of glandular trichomes and expression of artemisinin biosynthetic genes show significant difference (Lu et al., 2013). Furthermore, the level of artemisinin precursor, DHAA, progressively declines during leaf maturation (Czechowski et al., 2016). Results of qPCR analysis showed that the expression of *AaDXS2* was high in apical buds, whereas they declined sharply during leaf development (**Figure 5B**). The expression pattern of *AaDXS2* was highly similar to that of the *ADS* gene, which encodes the first enzyme involved in artemisinin biosynthesis (**Figure 5D**). By contrast, the expression of *AaDXS1* was relatively constant in leaves at different positions (**Figure 5A**), and the expression of *AaDXS3* was higher in leaf 8 than in other leaves (**Figure 5C**). Overall, the tissue-specific expression profiles of *AaDXS* genes showed that *AaDXS2* was the only gene whose expression pattern was similar to that of the artemisinin biosynthesis genes, which further indicated that *AaDXS2* was probably highly expressed in glandular trichomes, where artemisinin is biosynthesized.

AaDXS2 and Artemisinin Biosynthesis Genes Exhibit Similar Expression Patterns Under Multiple Treatments

Many elicitors and environmental factors, such as MeJA, low temperature, and light, regulate artemisinin biosynthesis (Hao et al., 2017; Liu et al., 2017). The expression of artemisinin biosynthesis genes increases in response to MeJA, cold, and light. To determine which of the three *AaDXS* genes was more important for artemisinin biosynthesis, we analyzed the expression of all three *AaDXS* genes under MeJA, cold, and light treatment. As shown in **Figure 6**, the expression of *AaDXS1* and *AaDXS3* was mildly induced by MeJA treatment at 3 and 9 h (**Figures 6A,C**), whereas that of *AaDXS2* was strongly induced from 1 to 12 h (**Figure 6B**). Under cold treatment, the expression of *AaDXS1* and *AaDXS3* decreased through the time course (**Figures 7A,C**). Although the expression of *AaDXS2* was downregulated at 1 and 3 h under cold stress, its expression was significantly upregulated at 6 and 12 h compared with the control (**Figure 7B**). Additionally, the expression of all three *AaDXS* genes in cold-treated plants was lower than that in the control from 1 to 3 h.

To investigate the effect of light on the expression of *AaDXS* genes, *A. annua* seedlings were placed in a dark room for 24 h and then transferred to the illumination incubator. Leaves were harvested for qPCR analysis at different time points, ranging from 5 min to 12 h. Results of qPCR analysis showed that the expression of *AaDXS1* was slightly induced after 1 h of light exposure (**Figure 8A**); however, no significant differences were detected in the expression of *AaDXS3* throughout the experiment (**Figure 8C**). In contrast, the expression of *AaDXS2* rapidly reached a peak at 5 min and then gradually declined, returning to the control level (**Figure 8B**). Furthermore, expression patterns of *ADS* and *CYP71AV1* under light treatment were similar to that of *AaDXS2* (**Figures 8D,E**).

Overall, the expression analysis of *AaDSX* genes under MeJA, cold, and light treatment demonstrated that among the three *AaDXS* genes, the expression pattern of only *AaDXS2* was similar

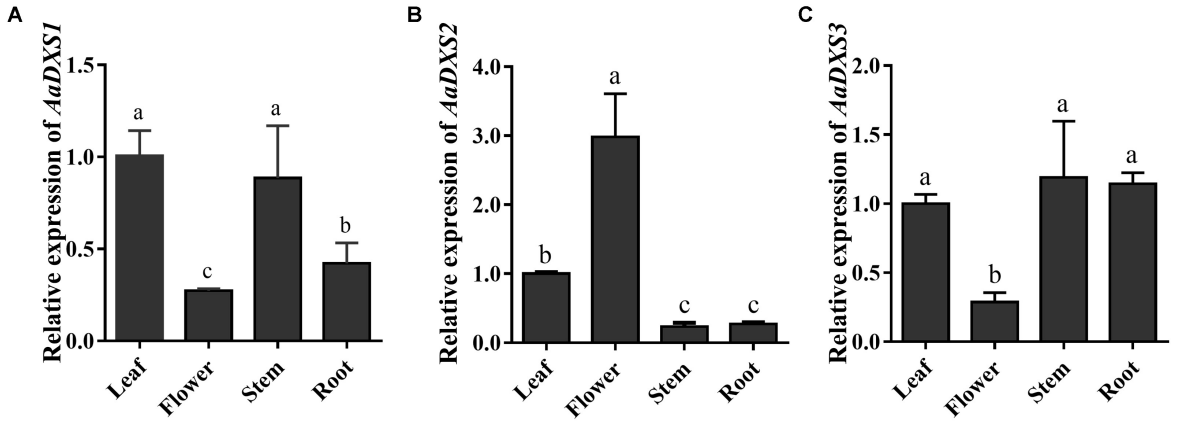

FIGURE 4 | Relative expression levels of *AaDXS1–3* in leaves, flowers, stems, and roots. **(A)** *AaDXS1*; **(B)** *AaDXS2*; and **(C)** *AaDXS3*. Different letters above the bars represent statistically significant differences ($p < 0.05$) detected by Duncan's multiple test. Data represent mean ± SD of three replicates.

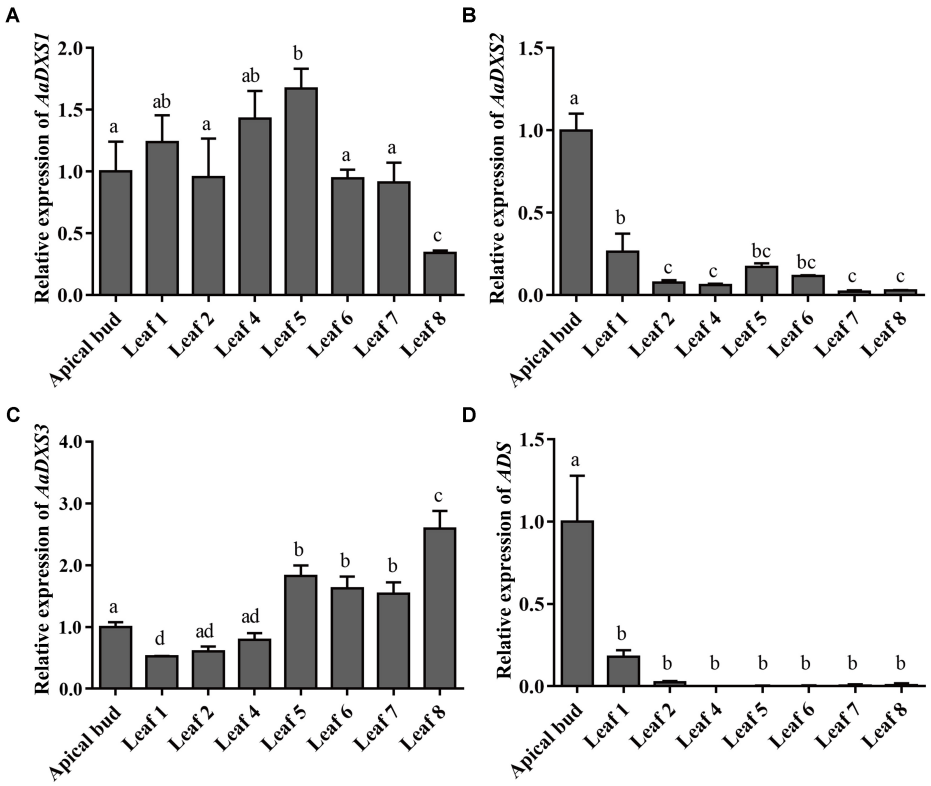

FIGURE 5 | Relative expression levels of *AaDXS1–3* and artemisinin biosynthesis gene, *AaADS,* in the apical bud and in leaves at different positions on the stem. **(A)** *AaDXS1*; **(B)** *AaDXS2*; **(C)** *AaDXS3*; and **(D)** *AaADS*. Different letters above the bars represent statistically significant differences ($p < 0.05$) detected by Duncan's multiple test. Data represent mean ± SD of three biological replicates.

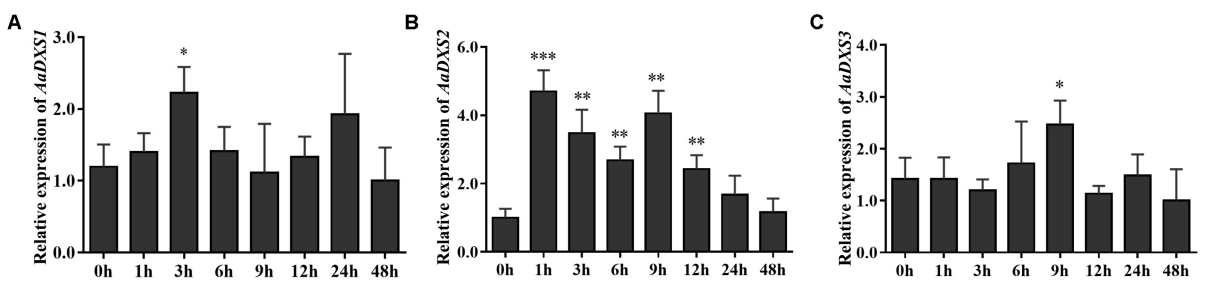

FIGURE 6 | Relative expression levels of *AaDXS1–3* in leaves treated with methyl jasmonate (MeJA). **(A)** *AaDXS1*; **(B)** *AaDXS2*; and **(C)** *AaDXS3*. Statistically significant differences are indicated using asterisks (Student's *t*-test, $*p < 0.1$; $**p < 0.05$; and $***p < 0.01$). Data represent mean ± SD of three biological replicates.

to that of the artemisinin biosynthesis genes. These data suggest that *AaDXS2* is more important than *AaDXS1* and *AaDXS3* in artemisinin biosynthesis.

Analysis of AaDXS2 Promoter Activity in Transgenic *A. thaliana*

Results of qPCR analysis showed that the expression of *AaDXS2* in different tissues and under different conditions was similar to that of the artemisinin biosynthesis genes. Subsequently, we cloned the 1,494-bp promoter of *AaDXS2* (*pAaDXS2*; **Supplementary Figure S4**). Sequence analysis of *pAaDXS2* using PLACE and PlantCARE revealed the presence of several light-responsive elements, such as Box I and GATA-motifs; MeJA-responsive elements, such as CGTCA- and TGACG-motifs; and stress-responsive elements, such as Box-W1 that responds to fungal elicitors, HSE involved in high temperature stress, and TC-rich repeats associated with plant defense and stress. To investigate the cellular compartmentalization of *AaDXS2*, we cloned *pAaDXS2* upstream of the *GUS* reporter gene and transformed the *pAaDXS2::GUS* construct in *A. thaliana*. Different organs of 45-day-old transgenic arabidopsis plants, including mature leaves, flowers, and siliques, were used for

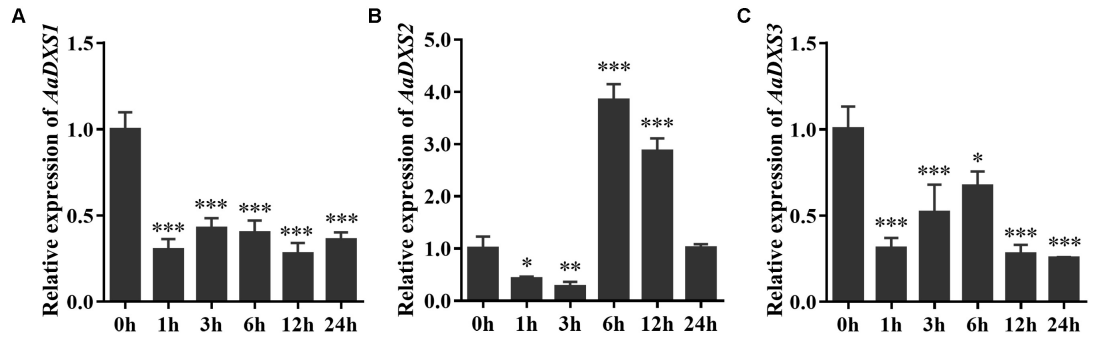

FIGURE 7 | Relative expression levels of *AaDXS1–3* under low temperature (4°C). **(A)** *AaDXS1*; **(B)** *AaDXS2*; and **(C)** *AaDXS3*. Statistically significant differences are indicated using asterisks (Student's *t*-test, $*p < 0.1$; $**p < 0.05$; and $***p < 0.01$). Data represent mean ± SD of three biological replicates.

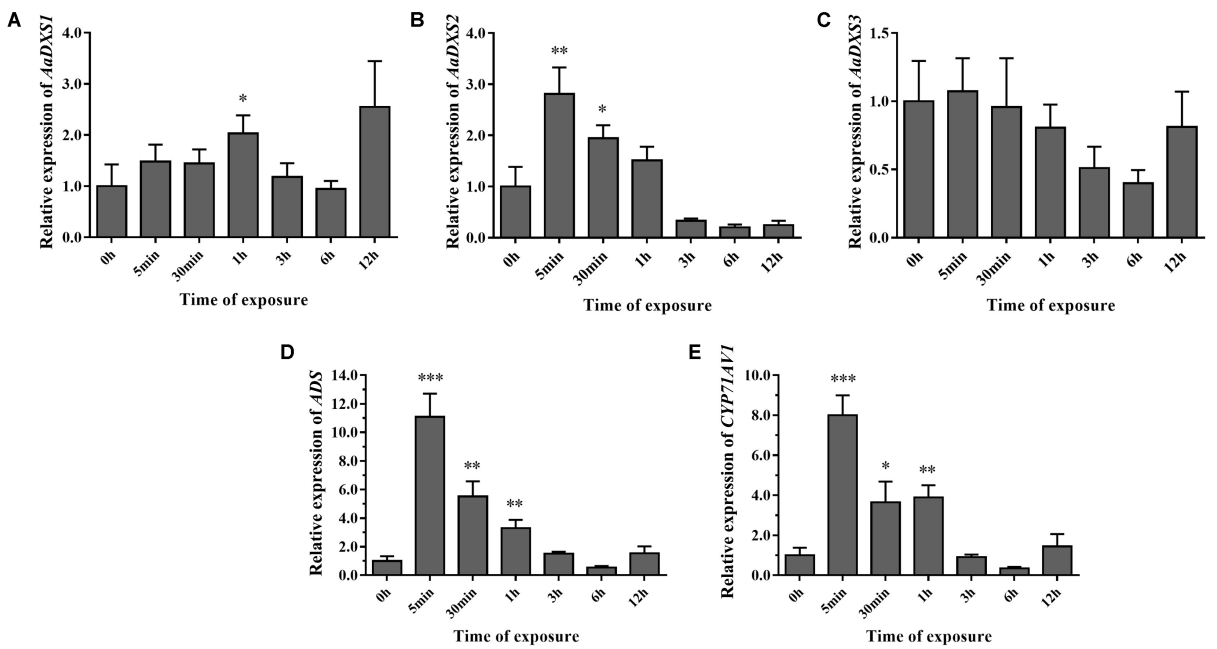

FIGURE 8 | Relative expression levels of *AaDXS1–3* and artemisinin biosynthesis genes (*AaADS*, *AaCYP71AV1*) in leaves exposed to light after 24 h dark treatment. **(A)** *AaDXS1*; **(B)** *AaDXS2*; **(C)** *AaDXS3*; **(D)** *AaADS*; and **(E)** *AaCYP71AV1*. Statistically significant differences are indicated using asterisks (Student's *t*-test, $*p < 0.1$; $**p < 0.05$; and $***p < 0.01$). Data represent mean ± SD of three biological replicates.

GUS histochemical staining. GUS staining was observed in the stigma, stamen, and pedicel but not in petals and young carpel (**Figures 9A–C**). More importantly, strong GUS staining was observed in the trichomes of mature leaves (**Figure 9B**).

DISCUSSION

The MEP pathway provides structural molecules for the synthesis of numerous key metabolites, such as terpenoids, phytohormones, chlorophyll, and carotene. Understanding this biosynthetic route is important for modulating the production of key isoprenoids. Although most of the enzymes in the MEP pathway are encoded by single-copy genes (Rodriguez-Concepcion and Boronat, 2002; Cordoba et al., 2009), the first key enzyme, DXS, is encoded by a small gene family composed of 2–4 genes in plants, such as arabidopsis (Carretero-Paulet et al., 2013), alfalfa (*Medicago sativa*; Walter et al., 2002), and maize (Cordoba et al., 2011). Souret et al. (2002) reported a *DXS* gene, named *DXSPS*, in *A. annua*; the nucleotide sequence of *AaDXSPS* was 98.7% similar to that of *AaDXS1* cloned in this study (**Supplementary Figure S5**). Thus, we propose that *DXPS* and *AaDXS1* represent the same gene. However, transcript levels of *AaDXS1* only showed a slight increase under light treatment, whereas those of *DXPS* significantly increased in root cultures grown under continuous light compared with those grown in the dark (Souret et al., 2002). This discrepancy might be due to the different plant material used in these experiments; Souret et al. (2002) performed expression analysis in *A. annua* root cultures,

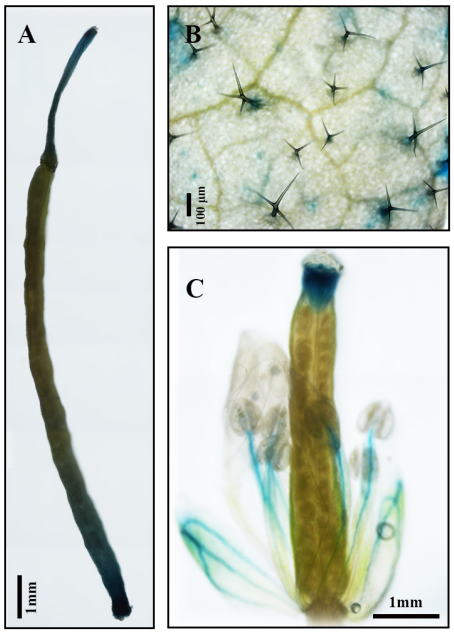

FIGURE 9 | *GUS* histochemical staining of various tissues of *pAaDXS2::GUS* transgenic Arabidopsis plants. The *GUS* reporter gene was driven by the promoter of *AaDXS2* (*pAaDXS2*) and transformed into Arabidopsis. Staining of transgenic **(A)** silique, **(B)** mature leaf, and **(C)** flower is shown.

whereas we used leaves in this study. Previously, 454 sequencing of EST libraries in *A. annua* have revealed two DXS contigs (EZ216572 and EZ167196; Graham et al., 2010). Aligning these two contigs with the *AaDXS* genes cloned in this study showed that EZ216572 and EZ167196 represent partial coding sequences of *AaDXS1* and *AaDXS2*, respectively. Moreover, transcriptome data showed that the expression of EZ167196 was significantly higher in the GSTs of flower buds and young leaves than in those of mature leaves and young leaf meristem. In contrast, EZ216572 showed higher expression levels in the GSTs of young leaves and in cotyledons. These data are consistent with the expression analysis results of this study, showing that *AaDXS2* was mainly expressed in young leaves and flower buds.

Several studies suggest that different genes in the *DXS* family are responsible for the biosynthesis of different isoprenoids (Enfissi et al., 2005; Paetzold et al., 2010; Cordoba et al., 2011). Henceforth, it is important to investigate the roles of different DXS isoforms in the biosynthesis of specific metabolites. Although enzymes involved in artemisinin biosynthesis have been determined, little is known about the enzymes involved in the MEP pathway. In the present study, we cloned three *AaDXS* genes, each of which encoded plastid-localized proteins. Expression analysis of *AaDXS* genes indicated that the expression pattern of *AaDXS2* was similar to that of the artemisinin biosynthesis genes. The analysis of *AaDXS2* promoter in transgenic arabidopsis demonstrated that *AaDXS2* was mainly expressed in trichomes.

Amino acid sequence alignment revealed that the three *AaDXS* proteins shared 42.3% identity. Moreover, low conservation in the TPP and GAP binding sites of *AaDXS3* suggested that *AaDXS3* diverged from *AaDXS1* and *AaDXS2*. The relatively low similarity in DXS protein sequences implies the functional divergence of DXS family members that have been shown previously (Cordoba et al., 2011). Phylogenetic analysis showed that *AaDXS1* clustered with *AtDXS1* and soybean (*Glycine max*) DXS1 in clade 1; it has been shown that the function of *AtDXS1* and *GmDXS1* is related to chloroplast development and chlorophyll synthesis (Mandel et al., 1996; Zhang et al., 2009). Most of the DXS enzymes involved in the biosynthesis of secondary metabolites in plants belonged to clade 2. For example, *MtDXS2*, which plays an important role in apocarotenoid biosynthesis, groups in clade 2 (Floss et al., 2008). The expression of *DXS2* in hairy roots of red sage (*Salvia miltiorrhiza*) is positively correlated with the accumulation of tanshinones (Kai et al., 2012). Although the biological functions of DXS proteins in clades 1 and 2 in plants are relatively clear, those of DXS proteins in clade 3 are still unclear. The expression of *ZmDXS3* is lower than that of the other DXS isogenes in maize, by which we predicted that *ZmDXS3* might be involved in the biosynthesis of derivatives from the MEP pathway at a lower level, such as plant hormones (Cordoba et al., 2009).

Because artemisinin biosynthesis genes are specifically expressed in glandular trichomes, transcripts of artemisinin biosynthesis genes are accumulated to the highest levels in flowers followed by young leaves, as these tissues have more glandular trichomes than the other plant tissues (Lu et al., 2013). In this study, we showed that the expression of both *AaDXS1* and *AaDXS3* was lower in flowers than in other tissues, whereas that of *AaDXS2* was the highest in flowers. Additionally, the expression level of *AaDXS2* in leaves at different positions on the stem was similar to that of the artemisinin biosynthesis genes. This differential expression of *AaDXS2* is consistent with the density of glandular trichomes, which is the highest in the apical bud and decreases in leaves with an increasing developmental age (Lu et al., 2013). Results showed that *AaDXS2* was mainly expressed in the glandular trichomes of leaves, which was consistent with the *GUS* staining patterns observed in transgenic *A. thaliana* (**Figure 9B**). In addition to trichomes of mature leaves, *GUS* staining of transgenic arabidopsis showed that *AaDXS2* was also expressed in the stigma, stamen, and silique. This result was similar to the expression analysis of *AtDXS2* in arabidopsis in which transcripts were detected at highest levels in siliques and inflorescences (Carretero-Paulet et al., 2013). We hypothesized that this might be due to DXS, which is a rate-limiting enzyme in MEP pathway, and which is responsible for biosynthesis of many isoprenoids. *SlDXS2* plays an important role in isoprenoid biosynthesis and trichome development in tomato. The suppression of *SlDXS2 via* RNAi in tomato results in a decrease in the level of the monoterpene, β-phellandrene, and an increase in trichome density (Paetzold et al., 2010). *AaDXS2* might be responsible for the biosynthesis of other isoprenoids excepted to artemisinin. Notably, among the three *DXS* genes of *A. annua*, only *AaDXS2* showed tissue-specific expression patterns that were similar to those of artemisinin biosynthesis genes, suggesting that *AaDXS2* might play a more important role in biosynthesis of artemisinin.

Generally, the *DXS* genes belonging to clade 1 exhibit constitutive expression in plants. For example, *PaDXS1* is ubiquitously expressed in various tissues and is not induced by elicitors (Phillips et al., 2007). Nevertheless, many *DXS* genes in clade 2 exhibit higher expression in response to various elicitors, such as MeJA and light (Cordoba et al., 2011; Kai et al., 2012). Previous studies have shown that MeJA is a powerful elicitor of artemisinin biosynthesis genes; its application induces the expression of artemisinin biosynthesis genes, resulting in a greater accumulation of artemisinin in MeJA-treated plants (Wang et al., 2010; Caretto et al., 2011; Xiang et al., 2015). The strong induction of *AaDXS2* expression following MeJA treatment observed in this study is consistent with the expression of artemisinin biosynthesis genes under MeJA treatment shown previously (Gong et al., 2006; Phillips et al., 2007). Cold stress is effective in enhancing artemisinin biosynthesis via two-independent pathways: converting DHAA into artemisinin (Wallaart et al., 2000) and promoting endogenous MeJA biosyntheis (Liu et al., 2017). Among the three *AaDXS* genes, the expression of *AaDXS1* and *AaDXS3* was inhibited under cold stress, whereas that of *AaDXS2* was significantly increased.

In *A. thaliana*, the MEP pathway genes, except HDR, are upregulated by light, suggesting that light is an important regulator of the MEP pathway in plants (Hsieh and Goodman, 2005). Overexpression of *At*CRY1, a blue light receptor, in *A. annua* promotes artemisinin accumulation, leading to the conclusion that light is a vital factor in regulating artemisinin biosynthesis (Hong et al., 2009). This conclusion is corroborated by a recent study (Hao et al., 2017). The expression of artemisinin biosynthesis genes (*ADS*, *CYP71AV1*, *DBR2*, and *ALDH1*) is upregulated under light. Furthermore, JA-induced artemisinin biosynthesis is dependent on light. Consistent with the study of Hao et al. (2017), we showed that the expression of *ADS* and *CYP71AV1* increased under light. More importantly, only *AaDXS2* was induced rapidly and dramatically after light exposure; this expression pattern of *AaDXS2* was similar to that of the artemisinin biosynthesis genes. Similarly in maize, the expression pattern of *ZmDXS1* and *ZmDXS2* were increased in plants exposed to light treatment (Cordoba et al., 2011). Additionally, the expression pattern of *AaDXS2* was similar with *ADS* and *CYP71AV1* in *A. annua*, indicating that *Aa*DXS2 is involved in the light-mediated regulation of artemisinin biosynthesis.

CONCLUSION

In conclusion, this study reports a detailed analysis of the expression profiles of three *DXS* genes in different tissues of *A. annua*. Additionally, we have shown that elicitors, such as MeJA, and various environmental factors modulate the expression of *AaDXS* genes. The expression of *AaDXS2* was very similar to that of the artemisinin biosynthesis genes, suggesting that *Aa*DXS2 might be the only DXS isoform involved in the biosynthesis of artemisinin. This work extends the analyses of *DXS* genes in other plants and provides a new potential target for the modulation of artemisinin production.

AUTHOR CONTRIBUTIONS

FZ and ZL conceived and designed the study. FZ, WL, and JX performed the RNA isolation, qRT-PCR analysis, and plant transformation. JZ, HX, and LX performed the subcellular localization and GUS staining. SZ, QZ, and CY managed *Artemisia annua* and Arabidopsis. MC analyzed the data. ZL prepared the manuscript. All authors have read and approved the manuscript.

FUNDING

This work was financially supported by the NSFC project (31770335 and 31300333), Fundamental Research Funds for the Central Universities (XDJK2016C114), China Postdoctoral Science Foundation (2015M582497), Foundation of YNTC (2016YN22), the National Undergraduate Training Programs for Innovation and Entrepreneurship of China (201710635075), the Scientific and Technological Research Program of Chongqing Municipal Education Commission (KJ1501321), Chongqing Science and Technology Commission (cstc2016shmszx80101), and the open fund of Chongqing Key Laboratory of Industrial Fermentation Microorganism (LIFM201714).

SUPPLEMENTARY MATERIAL

The Supplementary Material for this article can be found online at: https://www.frontiersin.org/articles/10.3389/fpls.2018.00952/full#supplementary-material

FIGURE S1 | The cDNA sequence of *AaDXS1*.

FIGURE S2 | The cDNA sequence of *AaDXS2*.

FIGURE S3 | The cDNA sequence of *AaDXS3*.

FIGURE S4 | The putative *cis*-elements on the promoter of *AaDXS2*.

FIGURE S5 | Amino acidsequence alignment of *AaDXS1* and *DXPS* (AF182286.2).

TABLE S1 | The primers used in this study.

REFERENCES

Caretto, S., Quarta, A., Durante, M., Nisi, R., De Paolis, A., Blando, F., et al. (2011). Methyl jasmonate and miconazole differently affect arteminisin production and gene expression in *Artemisia annua* suspension cultures. *Plant Biol.* 13, 51–58. doi: 10.1111/j.1438-8677.2009.00306.x

Carretero-Paulet, L., Cairo, A., Talavera, D., Saura, A., Imperial, S., Rodriguez-Concepcion, M., et al. (2013). Functional and evolutionary analysis of DXL1, a non-essential gene encoding a 1-deoxy-D-xylulose 5-phosphate synthase like

protein in *Arabidopsis thaliana*. *Gene* 524, 40–53. doi: 10.1016/j.gene.2012.10.071

Chen, M., Yan, T., Shen, Q., Lu, X., Pan, Q., Huang, Y., et al. (2017). GLANDULAR TRICHOME-SPECIFIC WRKY 1 promotes artemisinin biosynthesis in *Artemisia annua*. *New Phytol.* 214, 304–316. doi: 10.1111/nph.14373

Cordoba, E., Porta, H., Arroyo, A., Roman, C. S., Medina, L., Rodriguez-Concepcion, M., et al. (2011). Functional characterization of the three genes encoding 1-deoxy-D-xylulose 5-phosphate synthase in maize. *J. Exp. Bot.* 62, 2023–2038. doi: 10.1093/jxb/erq393

Cordoba, E., Salmi, M., and Leon, P. (2009). Unravelling the regulatory mechanisms that modulate the MEP pathway in higher plants. *J. Exp. Bot.* 60, 2933–2943. doi: 10.1093/jxb/erp190

Czechowski, T., Larson, T. R., Catania, T. M., Harvey, D., Brown, G. D., and Graham, I. A. (2016). *Artemisia annua* mutant impaired in artemisinin synthesis demonstrates importance of nonenzymatic conversion in terpenoid metabolism. *Proc. Natl. Acad. Sci. U.S.A.* 113, 15150–15155. doi: 10.1073/pnas.1611567113

Dudareva, N., Andersson, S., Orlova, I., Gatto, N., Reichelt, M., Rhodes, D., et al. (2005). The nonmevalonate pathway supports both monoterpene and sesquiterpene formation in snapdragon flowers. *Proc. Natl. Acad. Sci. U.S.A.* 102, 933–938. doi: 10.1073/pnas.0407360102

Emanuelsson, O., Nielsen, H., Brunak, S., and Von Heijne, G. (2000). Predicting subcellular localization of proteins based on their N-terminal amino acid sequence. *J. Mol. Biol.* 300, 1005–1016. doi: 10.1006/jmbi.2000.3903

Enfissi, E., Fraser, P. D., Lois, L. M., Boronat, A., Schuch, W., and Bramley, P. M. (2005). Metabolic engineering of the mevalonate and non-mevalonate isopentenyl diphosphate-forming pathways for the production of health-promoting isoprenoids in tomato. *Plant Biotechnol. J.* 3, 17–27. doi: 10.1111/j.1467-7652.2004.00091.x

Estévez, J. M., Cantero, A., Reindl, A., Reichler, S., and León, P. (2001). 1-Deoxy-D-xylulose-5-phosphate synthase, a limiting enzyme for plastidic isoprenoid biosynthesis in plants. *J. Biol. Chem.* 276, 22901–22909. doi: 10.1074/jbc.M100854200

Estévez, J. M., Cantero, A., Romero, C., Kawaide, H., Jiménez, L. F., Kuzuyama, T., et al. (2000). Analysis of the expression of *CLA1*, a gene that encodes the 1-deoxyxylulose 5-phosphate synthase of the 2-C-methyl-D-erythritol-4-phosphate pathway in Arabidopsis. *Plant Physiol.* 124, 95–104. doi: 10.1104/pp.124.1.95

Floss, D. S., Hause, B., Lange, P. R., Kuster, H., Strack, D., and Walter, M. H. (2008). Knock-down of the MEP pathway isogene 1-deoxy-D-xylulose 5-phosphate synthase 2 inhibits formation of arbuscular mycorrhiza-induced apocarotenoids, and abolishes normal expression of mycorrhiza-specific plant marker genes. *Plant J.* 56, 86–100. doi: 10.1111/j.1365-313X.2008.03575.x

Gong, Y. F., Liao, Z. H., Guo, B. H., Sun, X. F., and Tang, K. X. (2006). Molecular cloning and expression profile analysis of *Ginkgo biloba* DXS gene encoding 1-deoxy-D-xylulose 5-phosphate synthase, the first committed enzyme of the 2-C-methyl-D-erythritol 4-phosphate pathway. *Planta Med.* 72, 329–335. doi: 10.1055/s-2005-916234

Graham, I. A., Besser, K., Blumer, S., Branigan, C. A., Czechowski, T., Elias, L., et al. (2010). The genetic map of *Artemisia annua* L. identifies loci affecting yield of the antimalarial drug artemisinin. *Science* 327, 328–331. doi: 10.1126/science.1182612

Hao, X., Zhong, Y., Fu, X., Lv, Z., Shen, Q., Yan, T., et al. (2017). Transcriptome analysis of genes associated with the artemisinin biosynthesis by jasmonic acid treatment under the light in *Artemisia annua*. *Front. Plant Sci.* 8, 971. doi: 10.3389/fpls.2017.00971

Hong, G.-J., Hu, W.-L., Li, J.-X., Chen, X.-Y., and Wang, L.-J. (2009). Increased accumulation of artemisinin and anthocyanins in *Artemisia annua* expressing the arabidopsis blue light receptor CRY1. *Plant Mol. Biol. Rep.* 27, 334–341. doi: 10.1007/s11105-008-0088-6

Hsieh, M.-H., and Goodman, H. M. (2005). The Arabidopsis IspH homolog is involved in the plastid nonmevalonate pathway of isoprenoid biosynthesis. *Plant Physiol.* 138, 641–653. doi: 10.1104/pp.104.058735

Jefferson, R. A., Kavanagh, T. A., and Bevan, M. W. (1987). GUS fusions: beta-glucuronidase as a sensitive and versatile gene fusion marker in higher plants. *EMBO J.* 6, 3901–3907.

Kai, G., Liao, P., Xu, H., Wang, J., Zhou, C., Zhou, W., et al. (2012). Molecular mechanism of elicitor-induced tanshinone accumulation in *Salvia miltiorrhiza* hairy root cultures. *Acta Physiol. Plant.* 34, 1421–1433. doi: 10.1007/s11738-012-0940-z

Kumar, S., Tamura, K., and Nei, M. (2004). MEGA3: integrated software for molecular evolutionary genetics analysis and sequence alignment. *Brief. Bioinform.* 5, 150–163. doi: 10.1093/bib/5.2.150

Lange, B. M., Wildung, M. R., McCaskill, D., and Croteau, R. (1998). A family of transketolases that directs isoprenoid biosynthesis via a mevalonate-independent pathway. *Proc. Natl. Acad. Sci. U.S.A.* 95, 2100–2104. doi: 10.1073/pnas.95.5.2100

Liu, W., Wang, H., Chen, Y., Zhu, S., Chen, M., Lan, X., et al. (2017). Cold stress improves the production of artemisinin depending on the increase in endogenous jasmonate. *Biotechnol. Appl. Biochem.* 64, 305–314. doi: 10.1002/bab.1493

Livak, K. J., and Schmittgen, T. D. (2001). Analysis of relative gene expression data using real-time quantitative PCR and the 2(-Delta Delta C(T)) Method. *Methods* 25, 402–408. doi: 10.1006/meth.2001.1262

Lu, X., Zhang, L., Zhang, F., Jiang, W., Shen, Q., Zhang, L., et al. (2013). AaORA, a trichome-specific AP2/ERF transcription factor of *Artemisia annua*, is a positive regulator in the artemisinin biosynthetic pathway and in disease resistance to Botrytis cinerea. *New Phytol.* 198, 1191–1202. doi: 10.1111/nph.12207

Mandel, M. A., Feldmann, K. A., Herrera-Estrella, L., Rocha-Sosa, M., and Leon, P. (1996). CLA1, a novel gene required for chloroplast development, is highly conserved in evolution. *Plant J.* 9, 649–658. doi: 10.1046/j.1365-313X.1996.9050649.x

Morris, W. L., Ducreux, L. J. M., Hedden, P., Millam, S., and Taylor, M. A. (2006). Overexpression of a bacterial 1-deoxy-D-xylulose 5-phosphate synthase gene in potato tubers perturbs the isoprenoid metabolic network: implications for the control of the tuber life cycle. *J. Exp. Bot.* 57, 3007–3018. doi: 10.1093/jxb/erl061

Okada, A., Shimizu, T., Okada, K., Kuzuyama, T., Koga, J., Shibuya, N., et al. (2007). Elicitor induced activation of the methylerythritol phosphate pathway toward phytoalexins biosynthesis in rice. *Plant Mol. Biol.* 65, 177–187. doi: 10.1007/s11103-007-9207-2

Paetzold, H., Garms, S., Bartram, S., Wieczorek, J., Uros-Gracia, E. M., Rodriguez-Concepcion, M., et al. (2010). The isogene 1-Deoxy-D-Xylulose 5-phosphate synthase 2 controls isoprenoid profiles, precursor pathway allocation, and density of tomato trichomes. *Mol. Plant* 3, 904–916. doi: 10.1093/mp/ssq032

Phillips, M. A., Walter, M. H., Ralph, S. G., Dabrowska, P., Luck, K., Uros, E. M., et al. (2007). Functional identification and differential expression of 1-deoxy-D-xylulose 5-phosphate synthase in induced terpenoid resin formation of Norway spruce (*Picea abies*). *Plant Mol. Biol.* 65, 243–257. doi: 10.1007/s11103-007-9212-5

Querol, J., Grosdemange-Billiard, C., Rohmer, M., Boronat, A., and Imperial, S. (2002). Enzymatic synthesis of 1-deoxysugar-phosphates using E-coli 1-deoxy-D-xylulose 5-phosphate synthase. *Tetrahedron Lett.* 43, 8265–8268. doi: 10.1016/S0040-4039(02)02018-X

Rodriguez-Concepcion, M., and Boronat, A. (2002). Elucidation of the methylerythritol phosphate pathway for isoprenoid biosynthesis in bacteria and plastids. A metabolic milestone achieved through genomics. *Plant Physiol.* 130, 1079–1089. doi: 10.1104/pp.007138

Saitou, N., and Nei, M. (1987). The neighbor-joining method: a new method for reconstructing phylogenetic trees. *Mol. Biol. Evol.* 4, 406–425.

Schramek, N., Wang, H., Romisch-Margl, W., Keil, B., Radykewicz, T., Winzenhorlein, B., et al. (2009). Artemisinin biosynthesis in growing plants of *Artemisia annua*. A $^{13}CO2$ study. *Phytochemistry* 71, 179–187. doi: 10.1016/j.phytochem.2009.10.015

Solovyev, V. V., and Shahmuradov, I. A. (2003). PromH: promoters identification using orthologous genomic sequences. *Nucleic Acids Res.* 31, 3540–3545. doi: 10.1093/nar/gkg525

Souret, F. F., Weathers, P. J., and Wobbe, K. K. (2002). The mevalonate-independent pathway is expressed in transformed roots of *Artemisia annua* and regulated by light and culture age. *In Vitro Cell. Dev. Biol. Plant* 38, 581–588. doi: 10.1079/IVP2002343

Towler, M. J., and Weathers, P. J. (2007). Evidence of artemisinin production from IPP stemming from both the mevalonate and the nonmevalonate pathways. *Plant Cell Rep.* 26, 2129–2136. doi: 10.1007/s00299-007-0420-x

Wallaart, T. E., Pras, N., Beekman, A. C., and Quax, W. J. (2000). Seasonal variation of artemisinin and its biosynthetic precursors in plants of *Artemisia annua* of different geographical origin: proof for the existence of chemotypes. *Planta Med.* 66, 57–62. doi: 10.1055/s-2000-11115

Walter, M. H., Hans, J., and Strack, D. (2002). Two distantly related genes encoding 1-deoxy-d-xylulose 5-phosphate synthases: differential regulation in shoots and apocarotenoid-accumulating mycorrhizal roots. *Plant J.* 31, 243–254. doi: 10.1046/j.1365-313X.2002.01352.x

Wang, H., Ma, C., Li, Z., Ma, L., Wang, H., Ye, H., et al. (2010). Effects of exogenous methyl jasmonate on artemisinin biosynthesis and secondary metabolites in *Artemisia annua* L. *Ind. Crops Prod.* 31, 214–218. doi: 10.1016/j.indcrop.2009.10.008

Wang, Z., Ye, S., Li, J., Zheng, B., Bao, M., and Ning, G. (2011). Fusion primer and nested integrated PCR (FPNI-PCR): a new high-efficiency strategy for rapid chromosome walking or flanking sequence cloning. *BMC Biotechnol.* 11:109. doi: 10.1186/1472-6750-11-109

Xiang, L., Zhu, S., Zhao, T., Zhang, M., Liu, W., Chen, M., et al. (2015). Enhancement of artemisinin content and relative expression of genes of artemisinin biosynthesis in *Artemisia annua* by exogenous MeJA treatment. *Plant Growth Regul.* 75, 435–441. doi: 10.1007/s10725-014-0004-z

Yoo, S. D., Cho, Y. H., and Sheen, J. (2007). Arabidopsis mesophyll protoplasts: a versatile cell system for transient gene expression analysis. *Nat. Protoc.* 2, 1565–1572. doi: 10.1038/nprot.2007.199

Zhang, F., Fu, X., Lv, Z., Lu, X., Shen, Q., Zhang, L., et al. (2015). A basic leucine zipper transcription factor, AabZIP1, connects abscisic acid signaling with artemisinin biosynthesis in *Artemisia annua*. *Mol. Plant* 8, 163–175. doi: 10.1016/j.molp.2014.12.004

Zhang, M., Li, K., Zhang, C. H., Gai, J. Y., and Yu, D. Y. (2009). Identification and characterization of class 1 DXS gene encoding 1-deoxy-d-xylulose-5-phosphate synthase, the first committed enzyme of the MEP pathway from soybean. *Mol. Biol. Rep.* 36, 879–887. doi: 10.1007/s11033-008-9258-8

Zhang, X., Henriques, R., Lin, S.-S., Niu, Q.-W., and Chua, N.-H. (2006). Agrobacterium-mediated transformation of *Arabidopsis thaliana* using the floral dip method. *Nat. Protoc.* 1, 641–646. doi: 10.1038/nprot.2006.97

Zheng, H., Colvin, C. J., Johnson, B. K., Kirchhoff, P. D., Wilson, M., Jorgensen-Muga, K., et al. (2017). Inhibitors of *Mycobacterium tuberculosis* DosRST signaling and persistence. *Nat. Chem. Biol.* 13, 218–225. doi: 10.1038/nchembio.2259

Conflict of Interest Statement: The authors declare that the research was conducted in the absence of any commercial or financial relationships that could be construed as a potential conflict of interest.

frontiers in Plant Science

ORIGINAL RESEARCH
published: 13 August 2018
doi: 10.3389/fpls.2018.01096

Seasonal and Differential Sesquiterpene Accumulation in *Artemisia annua* Suggest Selection Based on Both Artemisinin and Dihydroartemisinic Acid may Increase Artemisinin *in planta*

Jorge F. S. Ferreira[1], Vagner A. Benedito[2], Devinder Sandhu[1], José A. Marchese[3] and Shuoqian Liu[4]*

[1] US Salinity Laboratory, Riverside, CA, United States, [2] Division of Plant and Soil Sciences, West Virginia University, Morgantown, WV, United States, [3] Biochemistry and Plant Molecular Physiology Laboratory, Agronomy Department, Federal University of Technology–Paraná, Pato Branco, Brazil, [4] Department of Tea Science, College of Horticulture and Hardening, Hunan Agricultural University, Changsha, China

OPEN ACCESS

Edited by:
Ian A. Graham,
University of York, United Kingdom

Reviewed by:
Kexuan Tang,
Shanghai Jiao Tong University, China
Tony Larson,
University of York, United Kingdom

***Correspondence:**
Jorge F. S. Ferreira
jorge.ferreira@ars.usda.gov

Specialty section:
This article was submitted to Plant Biotechnology, a section of the journal Frontiers in Plant Science

Received: *23 December 2017*
Accepted: *06 July 2018*
Published: *13 August 2018*

Citation:
Ferreira JFS, Benedito VA, Sandhu D, Marchese JA and Liu S (2018) Seasonal and Differential Sesquiterpene Accumulation in Artemisia annua Suggest Selection Based on Both Artemisinin and Dihydroartemisinic Acid may Increase Artemisinin in planta. Front. Plant Sci. 9:1096. doi: 10.3389/fpls.2018.01096

Commercial *Artemisia annua* crops are the sole source of artemisinin (ART) worldwide. Data on seasonal accumulation and peak of sesquiterpenes, especially ART in commercial *A. annua*, is lacking while current breeding programs focus only on ART and plant biomass, but ignores dihydroartemisinic acid (DHAA) and artemisinic acid (AA). Despite past breeding successes, plants richer in ART are needed to decrease prices of artemisinin-combination therapy (ACT). Our results show that sesquiterpene concentrations vary greatly along the growing season and that sesquiterpene profiles differ widely among chemotypes. Field studies with elite Brazilian, Chinese, and Swiss germplasms established that ART peaked in vegetative plants from late August to early September, suggesting that ART is related to the photoperiod, not flowering. DHAA peaks with ART in Chinese and Swiss plants, but decreases, as ART increases, in Brazilian plants, while AA remained stable through the season in these genotypes. Chinese plants peaked at 0.9% ART, 1.6% DHAA; Brazilian plants at 0.9% ART, with less than 0.4% DHAA; Swiss plants at 0.8% ART and 1% DHAA. At single-date harvests, seeded Swiss plants produced 0.55–1.2% ART, with plants being higher in DHAA than ART; Brazilian plants produced 0.33–1.5% ART, with most having higher ART than DHAA. Elite germplasms produced from 0.02–0.43% AA, except Sandeman-UK (0.4–1.1% AA). Our data suggest that different chemotypes, high in ART and DHAA, have complementary pathways, while competing with AA. Crossing plants high in ART and DHAA may generate hybrids with higher ART than currently available in commercial germplasms. Selecting for high ART and DHAA (and low AA) can be a valuable approach for future selection and breeding to produce plants more efficient in transforming DHAA into ART *in planta* and during post-harvest. This novel approach could change the breeding focus of *A. annua* and other pharmaceutical species that produce more than one desired metabolite in the same pathway. Obtaining natural variants with high ART

content will empower countries and farmers who select, improve, and cultivate *A. annua* as a commercial pharmaceutical crop. This selection approach could enable ART to be produced locally where it is most needed to fight malaria and other parasitic neglected diseases.

Keywords: seasonal sesquiterpene accumulation, sesquiterpene-based selection, sesquiterpene seasonal peak, high-DHAA germplasm selection, different chemotypes

INTRODUCTION

Active pharmaceutical ingredients (APIs) based on artemisinin (ART), such as artemether and artesunate, are key components of the most effective antimalarial drugs. The Nobel Assembly at Karolinska Institute awarded the Nobel Prize in Physiology or Medicine to Prof. Youyou Tu in 2015 in recognition of her early work in the late 1960s and 70s that culminated with the discovery of ART, the most effective natural anti-malarial medicine after quinine. Currently, all ART that is used as raw material for the production of artemisinin-combination therapy (ACT) is obtained from the plant *Artemisia annua* (Family: Asteraceae). Although other plants and microorganisms have been engineered with ART-pathway genes, tobacco was only able to produce artemisinic acid (AA) at 0.12% of leaf dry weight (DW) (Fuentes et al., 2016), and ART at less than 0.0007% of leaf DW (Farhi et al., 2011); transgenic moss produced ART at 0.021% of leaf DW (Khairul Ikram et al., 2017). These yields are 47 (moss) to 1,400 times (tobacco) less than an *A. annua* plant that produces 1% ART. Also, moss is not a feasible alternative considering its low biomass yield. Although baker's yeast produced 25 g of AA per liter of culture (Paddon et al., 2013), derivatization of AA to ART is further needed, making the process economically unfeasible compared to plant-based ART (Peplow, 2016). The low yields of ART in tobacco may be in part due to the fact that ART is phytotoxic (Duke et al., 1987) and must be stored extracellularly, inside epicuticular spaces of glandular trichomes (Duke et al., 1994; Ferreira and Janick, 1995b). Although other Artemisia species can produce ART (Mannan et al., 2010), their ART shoot concentrations are not large enough to justify commercialization. The no-cost/no-profit price of semi-synthetic ART by Sanofi is estimated to range from US$350 to 400 kg^{-1}, which is well above the US$250 kg^{-1} for the naturally-produced ART (Peplow, 2016). Although heterologous systems are valuable to improve the knowledge of the ART pathway, more efficient ways to stabilize market prices and reduce ACT costs are urgently needed. Rather than pursuing ART production in heterologous systems, more viable approaches to increase plant-based ART supply should focus on: (1) breeding plants that are higher in ART than the currently reported average of approximately 1.5% ART, (2) producing cultivars that are less variable in plant-to-plant ART concentrations, (3) producing cultivars that are higher in DHAA and able to convert DHAA into ART more efficiently, (4) improving ART commercial extraction to over 70% efficiency, and (5) recycling DHAA from ART commercial waste to produce more ART.

Since the initial plant screenings by the Chinese government in the late 1960s, plants have been selected only for their high biomass and ART leaf content. In 1985, Chinese accessions were reported to range from 0.01 to 0.5% ART, with plants from the Sichuan and Chongqing provinces being the highest in ART (Klayman, 1985), and those north of the Huaihe river bank reported to have 0.1% ART or less (Li et al., 2017). Only a few breeding programs managed to increase ART shoot concentration from 0.5 to 1.5% or higher. Because *A. annua* has a high degree of self-incompatibility (allogamy) that precludes self-pollination, and the word "hybrid" often used does not denote true hybrids generated from homozygous parents, but rather the F_1 progeny of two distinct, highly heterozygous, parents. The oldest breeding program with published reports in English and French is from the company Mediplant (Conthey, Switzerland). In the early 1990s this program produced several crossings that generated plants with over 1% ART (Debrunner et al., 1996; Magalhães et al., 1999). Later, Mediplant reported a new line named "Hybrid 1" with up to 1.8% ART and 2.9 tons of dry leaves ha^{-1} (Simonnet et al., 2008), but we are not sure whether "Hybrid 1" was ever available commercially or to breeding programs destined to generate high-ART plants for humanitarian purposes. The Brazilian breeding program, in collaboration with Mediplant, developed hybrids named "CPQBA," the acronym (in Portuguese) for the Multidisciplinary Center for Chemical and Biological Research (Campinas, Brazil) with seeds that sold for US$40 g^{-1}, with 12–15 thousand seeds g^{-1}. Despite the fact that plants from both Mediplant and CPQBA selections were late flowering in the environment where they were selected (Nicolas Delabays, personal communication), they flowered prematurely and produced little biomass when planted close to the equator (5–7° latitude) due to a short day length that inhibit vegetative development and accelerated the reproductive stage (Ferreira et al., 2005). Selected plants from this Swiss (Mediplant) cultivar named Artemis® produced from 0.65 to 1.9% ART when cultivated in an Appalachian Gilpin soil (Beaver, WV, 37°44′N 81°8′W) from May to August in a Quonset greenhouse under a mild potassium stress (Ferreira, 2007). Most recently, the cross "Hyb8001r" was developed and introduced by the Centre for Novel Agricultural Products (CNAP) in the UK, which is now commercialized by East-West Seed International. In field trials worldwide, "Hyb8001r" produced shoot ART up to 1.44% (g/100 g DW) and up to 4.4 tons/ha of dry leaf biomass, with a theoretical ART yield of 54 kg/ha (Suberu et al., 2016). In their work, "Hyb8001r" is referred to as CNAP8001, with seeds available to growers linked to the ACT raw material supply chain (https://www.artemisiaf1seed.org/hyb8001r/).

The literature provides evidence that *A. annua* plants accumulate not only ART, but also its biosynthetic precursor DHAA and AA (Wallaart et al., 2000; Ferreira, 2007; Ferreira

and Luthria, 2010). After artemisinic aldehyde (AO), the ART pathway diverts into either AA, arteannuin B, and artemisitene (AT) or into DHAA, dihydroartemisinic hydroperoxide (DHAHP), and ART (Kjær et al., 2013; Bryant et al., 2015) (**Figure 1**). Despite the fact that AA can be the main sesquiterpene produced (over 1% of leaf DW) by certain chemotypes of *A. annua* (Ro et al., 2006), the chemotype used for commercial purposes produce mainly ART, with DHAA as its main precursor (Wallaart et al., 1999b; Brown and Sy, 2004; Ferreira and Luthria, 2010). Contrary to previous reports of that *in vitro* photooxidative conversion of DHAA into ART could occur with almost 27% efficiency in organic solvents and with the presence of chlorophyll *a* (Acton and Roth, 1992; Wallaart et al., 1999a). Recent work suggests enzymatic action in the final stages of the pathway (Zhu et al., 2014; Bryant et al., 2015).

It was originally postulated that ART was produced and sequestered in glandular trichomes of leaves (Duke et al., 1994) and flowers (Ferreira and Janick, 1995a,b); and that the isolation of enzymes from these trichomes would confirm this hypothesis (Ferreira and Janick, 1995a). Since then, ART biosynthetic enzymes have been isolated from glandular trichomes (Olofsson et al., 2012; Tan et al., 2015; Chen et al., 2017). However, although the pathway produces AA, DHAA, and ART simultaneously, the two main chemotypes found in the literature either accumulate mainly AA (Elhag et al., 1992; Ro et al., 2006) or mainly DHAA and ART (Wallaart et al., 1999b, 2000; Ferreira, 2008). Detailed experiments based on the use of synthetically-produced radio-labeled precursors fed to plants also concluded that, compared to AA, DHAA is more cost-effective to produce ART in genetically-engineered yeast (Brown, 2010). A two-step auto-photooxidation step is postulated to occur in plants to convert DHAA into ART while plants senesce, or are dried under oven, shade, or sun (Brown and Sy, 2004; Ferreira and Luthria, 2010). Sun drying for 1–3 weeks was the most efficient way to convert DHAA into ART (over 90%), whereas forced-air oven drying (45°C from 12 to 16 h) only achieved a 40% conversion (Ferreira and Luthria, 2010). These findings suggest that drying plants in a forced-air oven illuminated with UV light may convert DHAA into ART more efficiently than in a dark oven. The average content of ART in plants used for industrial extraction has been reported to be 0.7% based on leaf dry weight (Malcolm Cutler, personal communication). However, ART yields can be maximized if the plants are harvested at the time ART reaches its seasonal peak, which is prior to flowering (Delabays et al., 2001; Ferreira, 2008). Swiss plants field-cultivated in West Virginia and harvested toward the end of their vegetative stage (no flowers), in early September, produced 0.7% ART and an average of 450 g dry leaves plant^{-1}, or 4.5 tons ha^{-1} for a plant density of 1 plant m^{-2} (Ferreira, 2007).

A. annua plants increased ART production in response to abiotic stresses, such as potassium deficiency (Ferreira, 2007), drought (Marchese et al., 2010), post-harvest drying (Ferreira and Luthria, 2010), senescence (Lommen et al., 2007), and salinity (Qureshi et al., 2005; Qian et al., 2007; Yadav et al., 2017). Interestingly, environmental stresses such as drought, wound, and cadmium (Xiao et al., 2016), and application of the hormones JA and cytokinin (Maes et al., 2011) increased trichome density in *A. annua*. Trichome development and ART biosynthesis have been linked through the transcription factor TAR1 and its role in upregulating ADS, CYP71AV1,

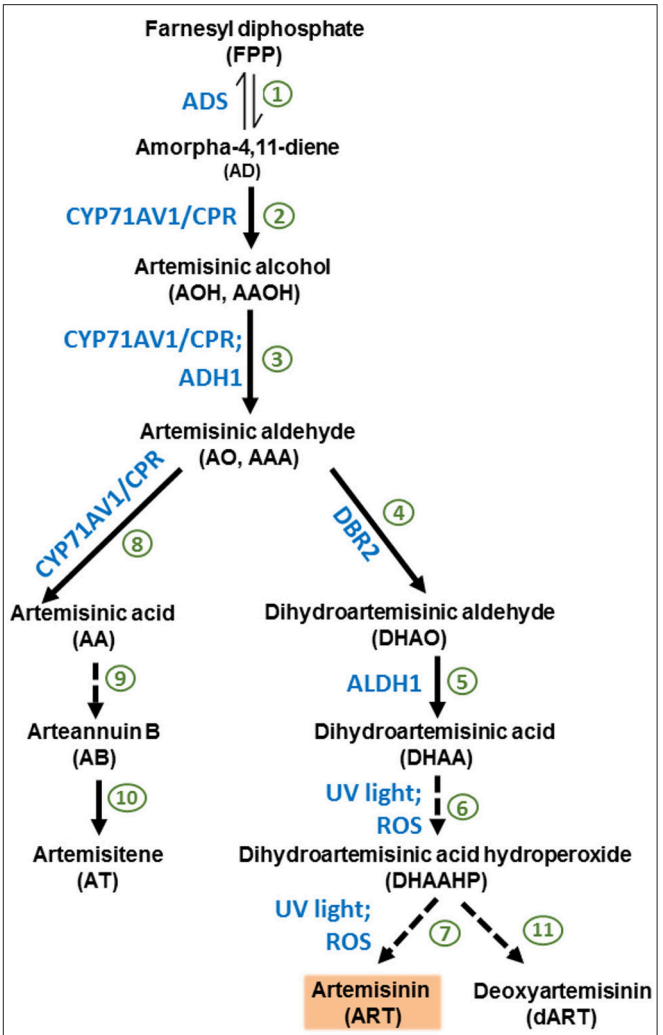

FIGURE 1 | Biosynthetic pathway of artemisinin starting from farnesyl diphosphate (FPP). 1. Amorpha-4,11-diene synthase (ADS) synthesizes the first committed product of the artemisinin pathway, AD. 2. Cytochrome P450 monooxygenase CYP71AV1 oxidizes AD to AA in three successive reactions (2, 3, and 8). CYP71AV1 is the main rate-limiting enzyme of the committed artemisinin pathway. Cytochrome P450 reductase (CPR) restores the active state of CYP71AV1. 3. AO can be produced by CYP71AV1/CRP enzymatic system, and alcohol dehydrogenase 1 (ADH1) can also make AO using AOH as a substrate. 4. AO is utilized by the enzyme artemisinic aldehyde Δ11(13) reductase (DBR2), which generates DHAO, as well as the third reaction of CYP71AV1 (7), which generates AA. 5. Aldehyde dehydrogenase 1 (ALDH1) converts DHAO to DHAA. 6–7. The conversion of DHAA into ART through the intermediate DHAAHP is postulated to be non-enzymatic, but induced only by ultraviolet light and oxygen. 8. The third reaction of CYP71AV1 converts AO into AA, diverting the pathway from producing ART and DHAA. 9. AA can be converted non-enzymatically into AB. 10. AB can be converted into AT. 11. DHAAHP may also generate DART. Once extracted from plants and purified, ART is derivatized into dihydroartemisinin (dART), then into other antimalarial drugs (e.g., artemether and artesunate), which the body metabolizes to the bioactive DART.

and ART biosynthesis (Tan et al., 2015) and several other genes, reviewed elsewhere (Xiao et al., 2016). The literature also suggests that reactive oxygen species (ROS) triggered by stress may lead to the transformation of DHAA into ART, although that has not yet been shown *in planta* through direct correlation between quantified ROS build-up and the increased conversion of DHAA into ART. Also, although potassium deficiency stress increased ART leaf concentration by 75%, it had no apparent effect on the concentrations of either DHAA and AA (Ferreira, 2007). Thus, the simple effect of photooxidation seems more plausible at this point, although it is unknown how DHAA is converted into ART as the plant metabolism shuts down during senescence and drying. For instance, compared to freeze dried sub-samples, shade, oven, and sun dried shoots had significantly higher concentrations of ART and decreased concentrations of DHAA and AA, and sun drying was more efficient in converting DHAA into ART (Ferreira and Luthria, 2010). Although it is currently debatable whether the last steps of the pathway (leading from DHAA to ART and deoxyartemisinin (dART) through dihydroartemisinic acid hydroperoxide (DHAAHP) are enzymatic or not, if selection and breeding focus exclusively on optimizing ART yields (and neglects DHAA), the potential to increase ART production *in planta* through the conversion of DHAA into ART during post-harvest drying will be wasted.

In order to validate their production potential, promising elite germplasm should be tested in areas with similar edaphoclimatic conditions of potential commercial production. A new cultivar ("Artemis®") developed in Conthey, Switzerland (46°13′N 7°17′E, elevation 485 m above sea level - asl), and another ("A3") developed by the University of Campinas, Brazil (22°48′S, 47°07′W, 749 m asl) have been tested in Kenya, Tanzania, and Nigeria, and produced from 0.7 to over 1% ART DW. However, a Chinese genotype from Chongqing, China (29.43°N, 106.91°E, 238 m asl) was grown only in China and Vietnam until its field trials in West Virginia (37°45′N 80°50′W, 890 m asl) reported here. Further selections of the Brazilian cultivar better adapted to lowland humid tropics resulted in plants with higher ART (1% w/w) and leaf dry biomass (3 ton/ha) than the Chinese, Indian, and U.S. clones (0.4–0.5% ART, 1.5–2 ton/ha of dry leaf biomass) in Calabar, Nigeria (4.96°N 8.3°E, 50 m asl) (Brisibe et al., 2012). To our knowledge, there are no current breeding programs engaged in producing *A. annua* genotypes that are rich in both ART and DHAA, or with a less variable ART yield from plant to plant.

The aims of this work are to: (1) show the seasonal and differential accumulation of ART, DHAA, and AA of elite Brazilian, Chinese, and Swiss cultivars cultivated in a West Virginian field of similar latitude and altitude to Chongqing (China), where approximately 90% of the world's *A. annua* is cultivated for ART extraction; (2) provide evidence that a high-ART genotype can also be high in DHAA, which should be considered as an important sesquiterpene and biochemical marker that can be used in the selection and breeding to produce new high-ART *A. annua* lines.

MATERIALS AND METHODS

Plant Material and Field Cultivation

The three main high-ART cultivars used in this study to evaluate seasonal and individual accumulation of sesquiterpenes, were donated by Mediplant (Switzerland, cv. Artemis®), Centro Pluridisciplinar de Pesquisas (CPQBA-Sao Paulo, Brazil, cv. 3M), and Holley Pharma (Chongqing, China, cultivar not identified). Another cultivar (Sandeman Seeds, UK) with high concentration of AA, but low ART and DHAA, was donated by a colleague (Dr. Dae-Kyun Ro). Plants from Brazilian, Chinese, and Sandeman cultivars were started from seeds, while a Swiss selection was cloned in a Quonset greenhouse under long-day photoperiod before transferring to the field. From here on, these genotypes will be mainly referred to as Brazilian, Chinese, Sandeman, and Swiss. For all field experiments reported here, all genotypes were transferred to the field in the first week of June 2006, 2007, or 2009 on an Appalachian soil (Gilpin silt loam—fine-loamy, mixed, mesic Typic Hapludults) at the Richmond School Farm, Beaver, WV (37°45′N 80°50′W, 890 m asl) and provided twice with 45 kg N, 20 kg P, and 37 kg K per hectare during the five-six months of cultivation (June to October/November). Soil pH was 5.8 and plants were irrigated for the first month, until established, with further irrigation only provided by rain. Soil analysis is provided elsewhere (Ferreira, 2007). To determine the seasonal accumulations of ART, DHAA, and AA, Chinese and Brazilian plants were field cultivated in 2006 and 2007, respectively, with three seed-generated plants of each genotype sampled bi-weekly (non-destructively) throughout the season. Seeds of the Swiss genotype (Artemis®), were cultivated in West Virginia and quantified for ART, DHAA, and AA. One selection (named MDP-11) was cloned in 2006 to generate enough plants for the determination of seasonal peak ART. Thus, for the Swiss genotype, three plants of the cloned MDP-11 were harvested at each collection date, the whole plant was oven dried, and a dry sample from the bottom, middle, and top part of each plant was pooled for HPLC-UV analysis. To evaluate the natural segregation of ART, DHAA, and AA in both Swiss and the Brazilian genotypes, approximately 100 plants generated from seeds were transferred to the field, and 55–65 plants were harvested at random on August 24, 2007 (Brazilian) and August 18/19, 2008 (Swiss). Dried leaves were separated from stems, ground to 0.5 mm particle size in a Wiley mill, and saved in a −20°C freezer until extraction for HPLC-UV analysis of underivatized ART and its precursors (Ferreira and Gonzalez, 2009).

Extraction of ART, its Precursors, and HPLC Analysis

ART, deoxyartemisinin (co-synthesized with ART), DHAA, and AA were extracted from 500 mg of *A. annua* dry leaf samples, refluxed with 50 mL of petroleum ether (45°C) for 1 h, transferred to beakers and left to dry overnight in a fume hood. Next day, samples were reconstituted in 20 mL of acetonitrile (two washes of 10 mL each), filtered through a 0.45 μm nylon filter attached to a 10-mL luer-lock syringe and transferred

to a 20-mL scintillation vial. Samples were transferred to 1.8 mL HPLC vials and 10 μL were injected by an HPLC auto-sampler into the system (Agilent 1100 series). ART, DHAA, and AA were quantified by HPLC-UV (Ferreira and Gonzalez, 2009). Standards of ART were purchased from Sigma/Aldrich (sigmaaldrich.com) and standards of DHAA and AA were donated by Amyris (Amyris.com). To better follow results and discussion, and the roles of ART, DHAA, and AA and their competing pathways, see **Figure 1**.

Relationship Among Sesquiterpenes in *A. annua*

The mathematical model formula used to evaluate ART leaf concentration (ART%) in relation to shoot concentration of AA (AA%) in **Figures 4**, **5** is shown in Equation 1, and is equivalent to a log-normal distribution fit, where *ln* = Napierian logarithm and *e* is Euler number =2.1718.

$$ART(\%) = \frac{0.36 \pm 0.06}{AA(\%)} \times e^{\left(-0.5 \times \left(\frac{\ln\left(\frac{AA(\%)}{0.34 \pm 0.03}\right)}{\ln(0.19 \pm 0.01)}\right)^2\right)} \quad (1)$$

RESULTS

Differential Seasonal Sesquiterpene Accumulation in *A. annua*

In West Virginia, the seasonal peak of ART concentration for the Brazilian, Chinese, and Swiss cultivars occurred between the end of August and the first week of September, declining steadily thereafter (**Figure 2**). All Plants of these three cultivars were high in ART and DHAA, but low in AA. The Brazilian cultivar had lower DHAA than ART, the Swiss cultivar had DHAA in similar or slightly higher concentrations than ART, and the Chinese cultivar had higher DHAA than ART. The Chinese cultivar displayed the highest concentrations of DHAA, reaching 1.6% DHAA and 0.95% ART at its seasonal peak (Sept 1). The Swiss plants that were asexually propagated as clones, expectedly showed a small plant-to-plant variation in sesquiterpene content than the Brazilian or Chinese plants generated from seeds (**Figure 2**). At the peak, the Brazilian and Swiss plants produced an average ART concentration of 0.75%, but a few plants reached 1.5% ART (data not shown). The peak for DHAA concentration coincided with ART in the Chinese and Swiss plants, whereas DHAA was lower than ART during most of the season in Brazilian plants. Plants peaked in their DHAA concentration at 0.6% (July 23, first harvest), 1.58% (Sept 1), and 1.25% (Sept 08) for the Brazilian, Chinese and Swiss plants, respectively. The Brazilian, Chinese, and Swiss genotypes were all low in AA, ranging from 0.1-0.2% and remained fairly constant throughout the whole experiment (**Figure 2**).

Sesquiterpene Profiling of Different *A. annua* Chemotypes

Due to the phenotypical segregation observed for DHAA accumulation in 2006, when over 50 seed-generated plants of the Brazilian cultivar were field grown and analyzed (data not shown), three segregating individual plants were cloned and harvested weekly to originate the data in **Figure 2**. Data for each segregating clone (3M-8, 3M-43, and 3M-49) are shown in **Figure 3** regarding the seasonal differences in ART, DHAA, and AA concentrations. Relative concentrations of ART, DHAA, and AA were clearly different among the three genotypes throughout the growing season (**Figure 3**). ART concentration ranged from 0.2 to 0.9% with maximum and minimum concentrations on August 28th and October 30th, respectively. All three plants peaked in ART concentration on August 28th. Opposite to the Chinese and Swiss genotypes, DHAA content starts high and decreases throughout the growing season in all three Brazilian (3M) clones (**Figure 3**). AA content was largely unchanged in each of the genotypes throughout the growing season. Genotypes 3M-8 and 3M-43 were most similar in their chemical profiles for

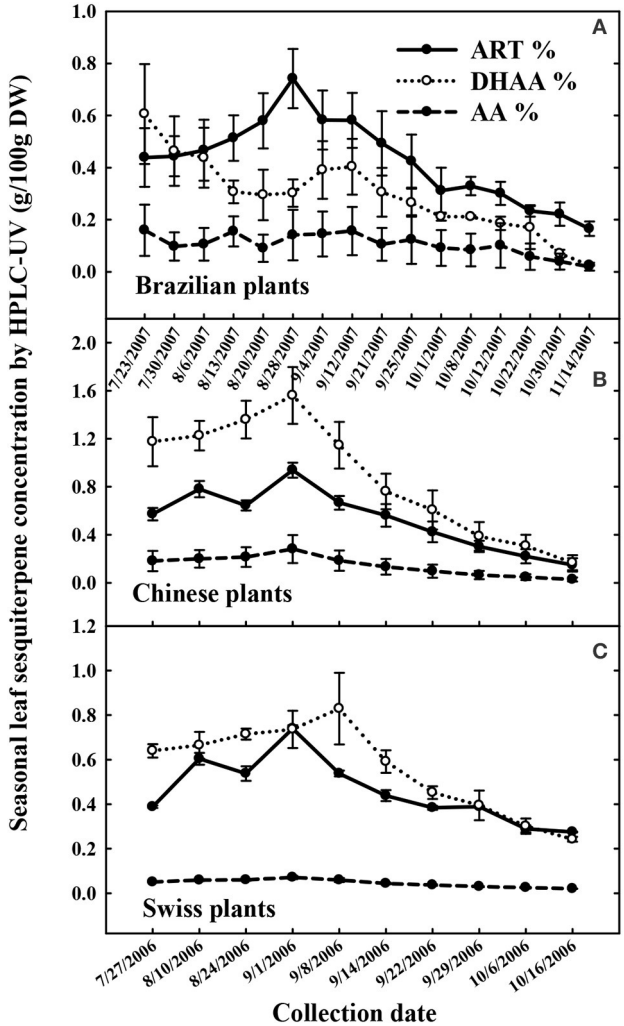

FIGURE 2 | Seasonal accumulation of artemisinin (ART), dihydroartemisinic acid (DHAA), and artemisinic acid (AA) in field cultivated *Artemisia annua* genotypes from Brazil **(A)**, China **(B)**, and Switzerland **(C)** field-cultivated in 2006, and 2007 in West Virginia, USA. All cultivars reached peak ART in late August to early September.

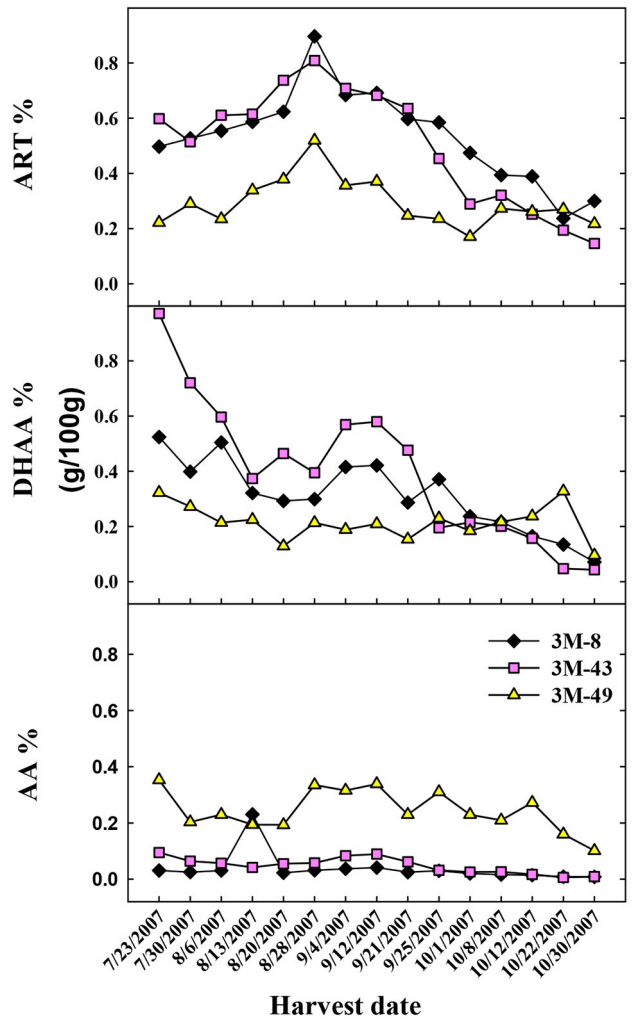

FIGURE 3 | Shoot concentration (g/100 g DW) of the sesquiterpenes, artemisinin (ART%), dihydroartemisinic acid (DHAA%), and artemisinic acid (AA%) in three seed-derived plants from the Brazilian cultivar (3M). Each plant was sampled [**top**, **middle** and **bottom**] weekly and processed for sesquiterpene extraction and HPLC-UV analysis.

all three sesquiterpenes, whereas the 3M-49 displayed lower ART and DHAA content and higher AA content as compared to the other two genotypes for most of the growing season (**Figure 3**).

In 2008, 50 seed-originated Brazilian and Swiss plants were cultivated in a West Virginia field and in 2009, some seed-originated Sandeman plants were cultivated in the same field. The data for the three elite cultivars and the Sandeman cultivar were grouped for shoot artemisinin concentration (ART %) and artemisinic acid concentrations (AA%) and evaluated through a three-parameter non-linear fit (**Eq. 1**).

The data were also grouped for leaf ART% and leaf DHAA% and presented as both Pearson (r, $n = 95$) and linear coefficient of determination (R^2, $n = 95$) (**Figure 4**). When these 95 sexually propagated (37 Brazilian, 48 Swiss, and 10 Sandeman) plants were randomly collected on Aug 18–19, 2008 (Brazilian and Swiss) and 2009 (Sandeman), the Brazilian plants ranged from 0.25 to 1.3% ART, 0.2–1.5% DHAA, and 0.02–0.12 AA, whereas the Swiss plants ranged from 0.58–1% ART, 0.9–1.6% DHAA, and 0.1–0.43 AA, and the Sandeman plants from 0.07–0.2% ART, 0.01–0.12% DHAA, and 0.41–1.18% AA (**Figure 4**). Data modeling analysis of these 95 plants of four different genotypes (based on leaf sesquiterpene concentrations) resulted in highly significant Pearson ($r = -0.56^{***}$, $n = 95$) and a linear coefficient of determination (or fit) of $R^2 = 0.31^{***}$. However, a higher, and highly significant, non-linear fit of $R^2 = 0.57^{***}$ was obtained for the observed *vs.* predicted relationship between ART% vs. AA% (**Figure 4A**) according to the model in **Eq. 1**. The root mean square error for the ART% predictions, or the diversion of the observed data from the prediction by the model presented in **Eq. 1** was only 0.18%. Interestingly, the range of AA concentration in the sexually propagated progenies was 0.02–0.12% for Brazilian, 0.1–0.43% for Swiss, and 0.41–1.18% for Sandeman plants (**Figure 4A**).

When correlating ART to DHAA in the three elite cultivars plus the Sandeman plants, both Pearson ($r = 0.74^{***}$, $n = 95$) and the linear fit ($R^2 = 0.54^{***}$, $n = 95$) were highly significant (**Figure 4B**). There was no significant correlation between ART and either AA or DHAA, or between AA and DHAA, for the sexually-propagated Sandeman plants (correlations not shown). The implications of these comparisons across germplasms is explored in the Discussion section.

The several years of HPLC-UV (Ferreira and Gonzalez, 2009) quantification of ART, DHAA, and AA in greenhouse and field-grown plants allowed for a selection of several Brazilian and Swiss clones with contrasting concentrations of all three sesquiterpenes, including a genotype from Sandeman Seeds (UK) that produces over 1% AA and 0.2% or less of either ART or DHAA (**Figure 5**). The Swiss clones were relatively high in DHAA and ART as compared to the Brazilian and Sandeman plants (**Figure 5**). For these selected genotypes, DHAA presented significant and high correlation with ART, while AA did not show a significant correlation with ART (**Figures 5B,C**). Although the Brazilian clones were lower in DHAA than the Swiss clones, three clones that were high in DHAA (3M13, 3M39, and 3M85) were also high in ART (**Figure 5A**).

DISCUSSION

Our field data revealed that, regardless of genotype, plants from different origins planted in the same location will reach their ART and DHAA peaks at the same time in the season (**Figure 2**). The ART peak was not related to flowering and agrees with reports that ART in Swiss plants peaked at the end of August also in Conthey, Switzerland, independently of the physiological state for the hybrid cultivar Artemis® (Delabays et al., 2001). Our results suggest that plants of elite germplasms, regardless of their origins, allocated more resources toward DHAA and ART accumulation, while AA remained below 0.43%, and stable, during the whole season. DHAA biosynthesis was favored in Chinese, similar to ART in Swiss, and lower than ART in Brazilian plants, while AA biosynthesis (opposite to ART or DHAA) was favored in Sandeman plants. Results

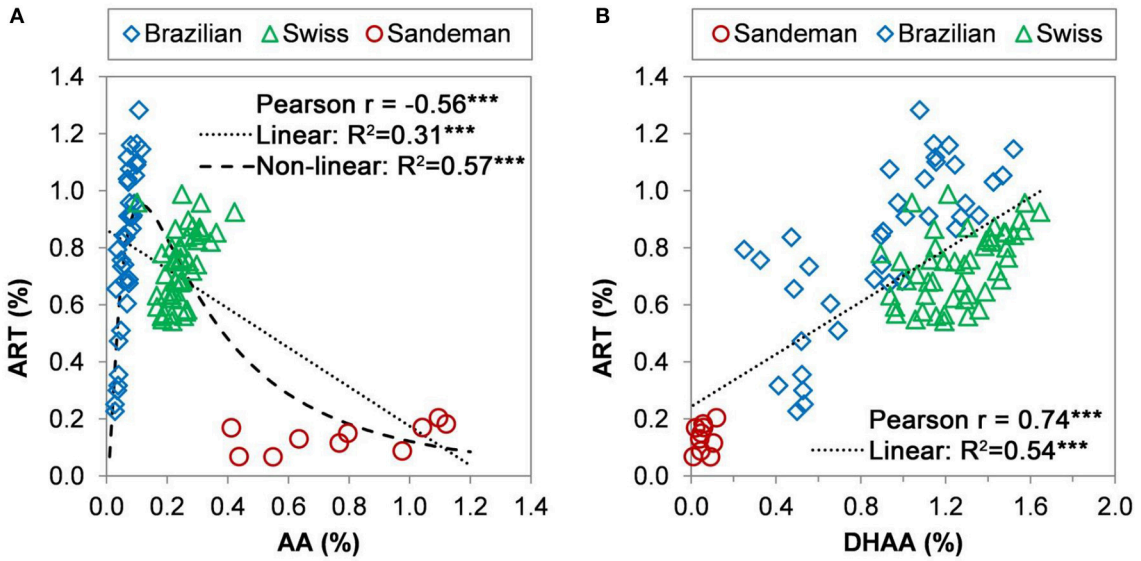

FIGURE 4 | Pearson coefficient correlation between the shoot concentration (g/100 g DW) of dihydroartemisinic acid (DHAA) and artemisinin (ART) (top panels), and of artemisinic acid (AA) and ART (bottom panels) of 38 Brazilian (left) and Swiss (right) seed-derived plants. Plants were grown in the field and collected randomly on August 18–19, 2008, for HPLC-DAD analysis. Correlation between artemisinin and (AA) or (DHAA).

showed that Brazilian plants produce more ART than DHAA, whereas Chinese plants accumulated more DHAA than ART (**Figure 2**). Comparing Brazilian to Chinese plants, and accepting the possibility that the conversion of DHAA to ART may involve enzymes (Zhu et al., 2014; Bryant et al., 2015), besides photooxidation, it is possible that the pathway in the Chinese genotype may have enzyme isoforms that are less efficient to convert DHAA into ART, while the Brazilian genotype has isoforms that are very efficient in converting DHAA to ART. A recent report (Czechowski et al., 2018) involving Swiss plants that were either high in ART (Artemis®), or low in ART (NCV) and high in AA, arteannuin B (AB), and artemisitene (AT), confirmed previous (Ferreira, 2007) and our current results of high biosynthesis of ART and DHAA in Swiss plants (Artemis®). Czechowski et al. (2018) remarked that competing pathways had enzymes that produced ART and derivatives, all having a methyl group (CH_3) on carbon 11, while the other side of the pathway (for AA, AB, and AT) had similar compounds, but with an ethyl group (CH_2) on carbon 11. These authors hypothesized that the existence of different isoforms of the amorpha-4,11-diene C-12 oxidase (CYP71AV1- steps 2 and 3 of the pathway in **Figure 1**), may be associated with high- and low-ART plants. They also concluded that the enzyme DBR2 (Step 4, **Figure 1**) was highly expressed on Artemis® plants that are high in ART and DHAA and that, although no enzyme may be involved, AA somehow converts rather to AB than to AT. Similarly, we have observed during our HPLC-UV analysis that DHAA and DHAAHP, which may (Zhu et al., 2014; Bryant et al., 2015) or may not (Czechowski et al., 2018) be enzyme-substrates, converted preferentially to ART, with very little conversion to dART (Ferreira and Luthria, 2010). Based on this evidence, if we infer that there could be isoforms of aldehyde dehydrogenase (ALDH1) with different efficiencies in converting dihydroartemisinic aldehyde (Step 5, **Figure 1**) to DHAA, but with low conversion of DHAA to ART, we would have plants such as the Chinese or Swiss (higher DHAA than ART). Alternatively, for high efficiency of conversion of DHAA to ART (higher ART than DHAA), we would have Brazilian plants. Thus, the cross of Brazilian and Chinese would be expected to produce plants with higher ART than either parent.

During the direct quantification of ART and its precursors in the Swiss Artemis® (Ferreira and Gonzalez, 2009), plants produced from 0.65 to 1.9% ART, but no AT or AB. Also, field-grown (Illinois, USA) Brazilian (3M) plants harvested on September 13, 2003 (Peng et al., 2006), produced neither AT or AB, as confirmed by mass spectrometry. These previous results with high-ART Swiss and Brazilian genotypes agree with Czechowski et al. (2018) in that AB and AT may be produced only in low-ART plants, such as their NCV plants (Czechowski et al., 2018).

Considering that plants with high concentrations of DHAA, and low AA, may lead to high ART% in leaves *in planta* or after drying, our data reflects the fact that Chinese, Brazilian, and Swiss plants vary in their accumulation of DHAA and ART, with Brazilian plants having higher ART than DHAA, Swiss plants having similar concentrations of ART and DHAA, and Chinese plants having almost twice as much DHAA as ART (**Figure 2**). Swiss plants showed a narrower range of both traits compared to the Brazilian clones, and were higher than Brazilian plants in DHAA, while Brazilian plants were higher than the Swiss in ART (**Figures 2, 4,** and **5**). Data from **Figure 4** and the sesquiterpene analyses from 63 and 55 seeded plants from Swiss (0.56–1.2% ART) and Brazilian (0.33–1.5% ART) genotypes, respectively, (**Supplementary Figures 1**, **2**) prove that the Brazilian genotype

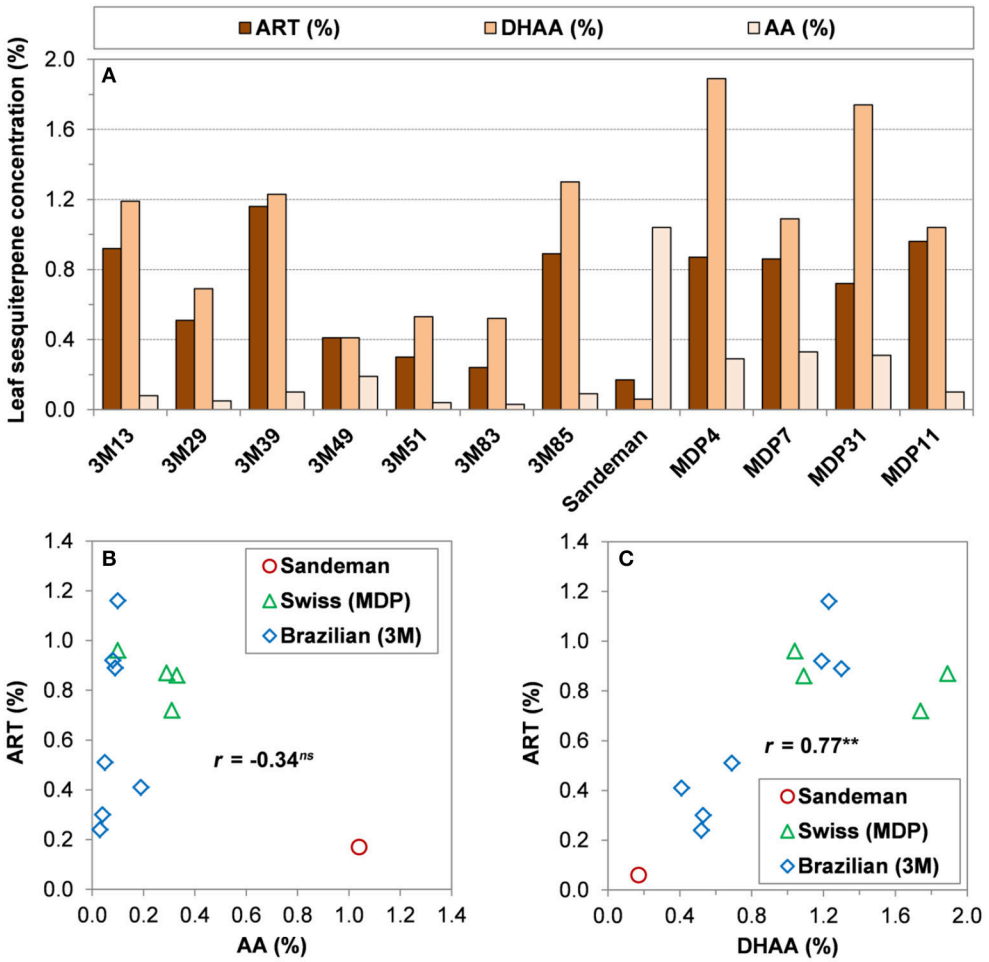

FIGURE 5 | Relationship among three sesquiterpenes present in leaves of different *A. annua* genotypes. **(A)** Leaf concentrations (g/100 g DW) of artemisinin (ART%), dihydroartemisinic acid (DHAA%), and artemisinic acid (AA%) from selected genotypes of Brazilian (3M), Sandeman Seeds UK (Sandeman), and Swiss (Artemis or MDP), maintained at West Virginia University; **(B)** Linear regression between ART% and AA%; **(C)** Linear regression between ART% and DHAA%. Shoot concentrations from greenhouse-grown plants will be slightly higher when grown in the field and collected late August/early September (e.g., 3M-39 = 1.9% ART and MDP 11 = 1.0% ART) in West Virginia.

has a broader genetic base compared to the Swiss genotype. This broad base in ART (0.23–0.78% ART) was also previously reported from 16 Brazilian (3M) plants (Peng et al., 2006). This implies that further selection of high-ART Brazilian plants and their crossing with high-DHAA Chinese or Swiss plants may result in progenies with higher ART concentrations than either genotype can currently afford separately. Our data also suggest that these plants should have AA leaf concentrations lower than 0.2% because as AA increases the concentrations of ART and DHAA decrease, as seen for Brazilian plant 3M-49 (**Figure 3**) and Sandeman plants (**Figures 4**, **5**). Swiss plants had AA over 0.2%, a fair concentration of DHAA and ART, but not as high as Brazilian plants (**Figure 4**).

Previously, and without knowing their DHAA concentration, Chinese plants have been successfully used as parents to increase ART in Swiss plant developed by Mediplant (Delabays et al., 1993), and that may also explain why these plants have high concentrations of DHAA despite their levels of AA over 0.2% (**Figure 5**). Later on, the use of Vietnamese plants selected for ART% as high as 1.3%, but with unknown concentrations of DHAA, was also mentioned as a good source of parents to increase ART% in new crosses (Delabays et al., 1995). On the onset of ART research in China, an ART-rich *A. annua*, originally from the Sichuan Province, was used in "Project 523" to afford high-ART extraction (Tu, 2011). It is interesting to note that a recent publication involving a Sichuan Province genotype reported control sesquiterpene concentrations of 0.6% ART, 2% DHAA, and 0.06% AA (Wang et al., 2010). These sesquiterpene ratios are similar to the ones reported in this work for the Chinese genotype (average of 0.9% ART, 1.6% DHAA, 0.02% AA) (**Figure 2**). We assume that Vietnamese plants, originally imported from China, may also be high in DHAA, and a good parent source to breed high-ART plants. Thus, the differences in ART and DHAA contents found between

the Brazilian and both Swiss and Chinese plants (both high in DHAA) can be explored to breed novel genetic recombinants high in ART. The enzymatic ability to convert most of the DHAA into ART can be genetically acquired from the Brazilian plants. The excess DHAA, not converted to ART *in vivo*, could still be converted into ART during drying (Ferreira and Luthria, 2010), suspending the irrigation to stress the plants close to harvest (Marchese et al., 2010), extracted to be converted into ART semi-synthetically (Kopetzki et al., 2013), or extracted from ART commercial waste as raw material for ART semi-synthesis (Liu et al., 2017).

Previous studies proved that the broad-sense heritability was high ($H^2 > 0.98$) for the ART trait (Ferreira et al., 1995). This was later confirmed by narrow-sense heritability (Delabays et al., 2001) suggesting that additive effects play a major role in the total genetic variance, and that selection for both ART and DHAA traits will be highly and efficiently conserved, leading to further increase in ART leaf concentration of new hybrids. An individual Brazilian clone (3M-49, **Figure 3**) and 10 seed-generated Sandeman plants (**Figure 4**) illustrate that a genotype that produces AA as the main sesquiterpene will produce ART and DHAA in low concentrations, and vice-versa, therefore confirming that DHAA/ART and AA are in two competing branches of the biosynthetic pathway and should be considered for their additive (ART and DHAA) or negative (AA) effects when breeding new high-ART genotypes. Data generated from the 10 Sandeman-UK seeded plants clearly shows that plants with high leaf concentrations of AA should not be used to generate new genotypes high in ART and DHAA. Confirming this line of thought, a previous attempt to select high-ART clones using tissue culture-, greenhouse-, and field-propagated plants of unknown origin produced plants with 0.4 to 1.0% AA, but with only 0.03–0.06% ART (Elhag et al., 1992). Their *A. annua* plants, field-cultivated in Saudi Arabia, produced a very similar picture to that reported in our work for Sandeman plants cultivated in West Virginia in 2009 (0.41–1.18% AA, 0.01–0.12% DHAA, and 0.07–0.2% ART, **Figure 4**). Although reported from different sites and in different years, these similar results attest to the fact that these populations, possibly unrelated, maintain their characteristic pathways leading to plants that are mostly high in AA and very low in ART and DHAA.

Our yearly records for the Brazilian and Swiss clones strongly support that plants high in ART and DHAA are lower in AA and vice-versa and individual plant sesquiterpene profiles and Pearson coefficients in **Figure 5** ($r = -0.34^{ns}$ for AA vs. ART and $r = 0.77^{**}$ for DHAA vs. ART, $n = 12$) mirror the sesquiterpene profile and coefficients of their seed-generated 95 plants from the same germplasm ($r = -0.56^{***}$ for AA vs. ART and $r = 0.74^{***}$ for DHAA vs. ART, $n = 95$) in **Figures 4A,B**. The highly significant non-linear fit ($R^2 = 0.57^{***}$) obtained between AA% and ART% reflects the fact that Brazilian plants were higher in ART but had a very low leaf concentration of AA. As the AA% rises to 0.2% or higher (Swiss plants), ART started to decrease and when AA% was from 0.4 to 1.18% (Sandeman plants), leaf ART% was never higher than 0.2% (**Figure 4**). Again, these Pearson coefficients suggest a negative correlation between AA and ART ($r = -0.56^{***}$ and -0.34^{ns}, **Figures 4**, **5**, respectively) as they are biosynthesized in competing sides of the same pathway.

An *A. annua* germplasm collection encompassing twelve genetically diverse clones (**Figure 5**) was established at the USDA-ARS Appalachian Farming Systems Research Center, Beaver, WV was clonally propagated and maintained for approximately five years at the USDA-ARS in Beaver, and is currently maintained at the Evansdale Greenhouse (West Virginia University, Morgantown, WV). This collection holds clones with distinct chemotypes from Brazil and Switzerland, plus a clone originated from a commercial nursery (Sandeman Seeds, UK) that is high in AA, but low in ART and DHAA (**Figure 5**). These plants have maintained their concentrations of the sesquiterpenes they were selected for.

For the ten plants generated from Sandeman seeds, the lack of significant correlation between any of the sesquiterpenes reflects the fact that AA is not a precursor of ART, but may be a precursor of AB and AT in its side of the pathway (**Figure 1**). Plants high in DHAA may produce even higher ART yields if stressed by abiotic factors such as drought, potassium deficiency, and salinity, or during commercial drying, as previously reported (Brown and Sy, 2004; Ferreira, 2007; Ferreira and Luthria, 2010; Marchese et al., 2010; Yadav et al., 2017). However, more research is needed to determine the extent, and which stress may increase ART without compromising biomass yield. In the meanwhile, new different systems for the *in vitro* conversion of DHAA into ART or its antimalarial derivatives (e.g., artemether and artemotil) have been recently reviewed and reported encouraging yields of up to 65% (Lévesque and Seeberger, 2012; Howard et al., 2017).

Remarkably, the step involved in converting DHAA into ART is thought to be mediated by photooxidation instead of through an enzymatic catalysis (Brown, 2010; Czechowski et al., 2018). This suggests that the photooxidation step may be differentially regulated by an unknown mechanism between the Chinese and Brazilian plants. Alternatively, as the conditions for chemical reaction used for semi-synthetic synthesis of ART may not exist in plants, there is the possibility that an unknown biochemical process is involved in the DHAA conversion to ART (Xie et al., 2016) and, surprisingly, it could even involve an enzyme *in vivo* (Zhu et al., 2014; Bryant et al., 2015). However, one should keep in mind that the reported non-enzymatic conversion of DHAA to ART had only a 23% overall yield (Acton and Roth, 1992) and that even with optimized conditions and the addition of 0.24 nmol of chlorophyll *a*, it took 129 h to convert 26.8% of the DHAA into ART (Wallaart et al., 1999b). However, drying plant material for 12–16 h in a forced-air oven (in the dark) at 40°C allowed an estimated 40% conversion of DHAA to ART, while sun drying from 1 to 3 weeks resulted in a 94% conversion (Ferreira and Luthria, 2010). Also, suspending irrigation in field plants 38 h before harvest resulted in an ART increase of 29% compared to the irrigated control (Marchese et al., 2010). The higher conversions achieved by oven, drought and sun drying, compared to conversions in organic solvents reported by Acton and Wallaart's research teams, indicate that either ROS produced by heat stress are rapidly being used to convert DHAA into ART or that the conversion could, at least partially, involve enzymes. Freeze dried plant samples had significantly higher concentrations of DHAA and lower concentrations of ART (Ferreira and Luthria, 2010) as if the

conversion had been blocked by either the freezing of enzymes or by the absence of oxygen during the freeze drying process, or both. A similar low concentration of ART was reported for both freeze drying and microwave drying compared to open-air drying (Ferreira et al., 1992). In addition, oven drying leaves at 20–40°C, for at most 25 h of drying, did not alter artemisinin concentration in dried leaves, while drying at 90°C for 5 hours significantly decreased ART% in leaves (Xavier Simonnet, personal communication). Thus, it seems that although some conversion of DHAA to ART can happen without enzymes, it does not rule out the participation of enzymes that could speed up the conversion of DHAA into ART as the plant dies, which could work simultaneously with photooxidation to assure the highest amount of ART in glandular trichomes during plant death.

CONCLUSIONS

Our field data shows for the first time that, regardless of the genotype, plants consistently reach their ART peaks during the same approximate time of the year, toward the end of their vegetative stage, suggesting that the ART is related to photoperiod, not flowering, and confirming reports for peak ART in vegetative Swiss plants (Artemis®) cultivated in Conthey, Switzerland. Over the years, this seasonal peak remained true regarding the sesquiterpene profile of cloned plants maintained in a greenhouse under long days during the winter. This propagation strategy and reliable ART concentration were also used by an *A. annua* breeding program at Rutgers University that used one of our Brazilian (3M) selections from Illinois (USA), which was reported to produce 1.5% ART (Wang et al., 2005). Plants left in the field flowered and died as days got shorter in the winter. Our results reiterate previous reports that ART and DHAA compete for substrate with the AA side of the pathway, and that DHAA is the main precursor of ART in high-artemisinin chemotypes. Although concentrations of AA may correlate to ART concentration in the same cultivar, it remained low and unchanged throughout the season in all cultivars studied for seasonal ART peak. Thus, for breeding purposes, using a genotype high in AA will not lead to plants high in ART or DHAA as previously published (Elhag et al., 1992), and confirming our results with the Sandeman cultivar. Field studies with several seed-originated plants of selected Brazilian genotype (3M, CPQBA) and Swiss genotype (Artemis®, Mediplant) (**Figure 4**) indicated that the Swiss hybrids have parents with an allelic composition less diverse related to the ART trait than Brazilian plants. Both, Brazilian and Swiss plants varied in their ART and DHAA contents, but homogeneously produced plants with as much as 1.8% DHAA (Swiss, **Supplementary Figure 1**) and 1.5% ART (Brazilian, **Supplementary Figure 2**) and that were either higher in ART than DHAA (Brazilian) or vice-versa (Chinese and Swiss). Chinese plants had the highest levels of DHAA and these plants could provide suitable alleles for breeding, as they also contributed to generate the Swiss cultivar Artemis® in 1999. Our results confirmed the reports by Wallaart et al. (2000) that cultivars that have higher concentrations of DHAA than ART are low in AA, and vice-versa, recently also confirmed by Czechowski et al. (2018). Plants that have higher DHAA than ART (Chinese) may be crossed with plants that have higher ART than DHAA (Brazilian) to generate plants with even higher ART than either parent, as these genotypes may have an ideal combination of enzymatic systems needed to transform DHAA into ART. Although the cross could not be genetically confirmed, but based on their low selfing rate, crosses between Brazilian and Chinese plants, done by pairing plants synchronized to flower in Indiana (Purdue), and selected in Georgia were recently reported to produce 2.16% ART (Wetzstein et al., 2018). Alternatively, genotypes with high DHAA may be genetically engineered to overexpress enzymes needed to convert DHAA into ART, if eventually demonstrated that indeed enzymes are involved in the end of the ART pathway *in vivo* (Zhu et al., 2014).

Based on the evidence provided by several years of metabolomics study of three elite germplasms of *A. annua* and by cross referencing of previous published literature, this work presents strong evidence and a novel approach that suggests that future *A. annua* breeding programs should consider plants of different chemotypes that are high in both, ART and DHAA and low in AA. If the *in planta* conversion of DHAA into ART is indeed non-enzymatic and only requires photooxidation, the role of ROS in this conversion and the use of both light and oxygen during either pre-harvest water stress or post-harvest drying may prove to be useful to increase leaf concentration of ART. Finally, plants that are high in DHAA can also provide this compound as a precursor for the semi-synthesis of ART in continuous flow systems that have so far proved efficient for the *in vitro* conversion of DHAA into ART.

AUTHOR CONTRIBUTIONS

JF conceived the experiments involving seasonal sesquiterpene accumulation and relationship, based on HPLC analysis of sesquiterpenes and participated actively in all drafts of the manuscript. JF, VB, and DS collaborated in the discussion of results and potential use of elite germplasms high in ART and DHAA to increase artemisinin. VB has propagated and kept the germplasm selections presented in **Figure 5** for the past 6 years. JM contributed with critical comments in most drafts of the manuscript. SL read and commented on the initial drafts.

FUNDING

All the Work was funded by the USDA-ARS.

ACKNOWLEDGMENTS

To Dr. Pedro Melillo de Magalhães (CPQBA, Brazil), Dr. Nicolas Delabays and Dr. Xavier Simonnet (Mediplant, Switzerland), Dr. Kevin Mak (Holley Pharma, China), and Dr. Dae-Kyun Ro for providing seeds of the Brazilian, Chinese, Sandeman, and Swiss cultivars used in this work. Thanks are also due to Mrs. Barry Harter and Bob Arnold for their valuable help during greenhouse

clonal propagation, field work, and sample preparation for HPLC-UV analyses. Special thanks to Dr. Elia Scudiero (UC-Riverside, California) for his suggestions to analyze combined germplasm data for **Figures 4**, **5** with a non-linear mathematical model.

SUPPLEMENTARY MATERIAL

The Supplementary Material for this article can be found online at: https://www.frontiersin.org/articles/10.3389/fpls.2018.01096/full#supplementary-material

Supplementary Figure 1 | Sesquiterpene profile of Swiss cultivar ("Artemis," Mediplant) in 63 seed-generated plants, field-cultivated in West Virginia, and harvested on 08/18/2008. All plants contained higher dihydroartemisinic acid (DHAA) in shoots than artemisinin (ART). Subplots show correlation between ART and DHAA concentrations in g/100g DW (%).

Supplementary Figure 2 | Sesquiterpene profile of Brazilian cultivar (3M, CPQBA) in 55 seed-generated plants cultivated in field. The majority of the plants contained higher artemisinin (ART) in shoots than dihydroartemisinic acid (DHAA). Subplots show correlation between ART and DHAA concentrations in g/100g DW (%). Concentration of AA for plants 3M-49 (0.28%) and 3M-49 (0.4%), harvested on August 20 and August 28, respectively, were removed not to throw off correlation as they were higher in AA than all the other plants.

REFERENCES

Acton, N., and Roth, R. J. (1992). On the conversion of dihydroartemisinic acid into artemisinin. *J. Org. Chem.* 57, 3610–3614. doi: 10.1021/jo00039a020

Brisibe, E. A., Udensi, O., Chukwurah, P. N., De Magalhães, P. M., Figueira, G. M., and Ferreira, J. F. S. (2012). Adaptation and agronomic performance of *Artemisia annu*a L. under lowland humid tropical conditions. *Ind. Crop. Prod.* 39, 190–197. doi: 10.1016/j.indcrop.2012.02.018

Brown, G. D. (2010). The biosynthesis of artemisinin (Qinghaosu) and the phytochemistry of *Artemisia annua* L. (Qinghao). *Molecules* 15, 7603–7698. doi: 10.3390/molecules15117603

Brown, G. D., and Sy, L. K. (2004). *In vivo* transformations of dihydroartemisinic acid in *Artemisia annua* plants. *Tetrahedron* 60, 1139–1159. doi: 10.1016/j.tet.2003.11.070

Bryant, L., Flatley, B., Patole, C., Brown, G. D., and Cramer, R. (2015). Proteomic analysis of *Artemisia annua* – towards elucidating the biosynthetic pathways of the antimalarial pro-drug artemisinin. *BMC Plant Biol.* 15:175. doi: 10.1186/s12870-015-0565-7

Chen, M., Yan, T., Shen, Q., Lu, X., Pan, Q., Huang, Y., et al. (2017). Glandulra trichome-specific WRKY 1 promotes artemisinin biosynthesis in *Artemisia annua*. *New Phytol.* 214, 304–316. doi: 10.1111/nph.14373

Czechowski, T., Larson, T. R., Catania, T. M., Harvey, D., Wei, C., Essome, M., et al. (2018). Detailed phytochemical analysis of high- and low artemisinin-producing chemotypes of *Artemisia annua*. *Front. Plant Sci.* 9:641. doi: 10.3389/fpls.2018.00641

Debrunner, N., Dvorak, V., Magalhaes, P., and Delabays, N. (1996). "Selection of genotypes of *Artemisia annua* L. for the agricultural production of artemisinin," in *International Symposium on Breeding Research on Medicinal Plants*, ed F. Pank (Quedlinburg), 222–225.

Delabays, N., Benakis, A., and Collet, G. (1993). Selection and breeding for high artemisinin (quinghaosu) yielding strains of *Artemisia annua*. *Acta Hort.* 330, 203–207. doi: 10.17660/ActaHortic.1993.330.24

Delabays, N., Jenelten, U., and Dvorak, V. (1995). New high artemisinin yielding hybrids of *Artemisia annua* L. *Rev. suisse Vitic. Arboric. Hortic.* 19.

Delabays, N., Simonnet, X., and Gaudin, M. (2001). The genetics of artemisinin content in *Artemisia annua* L. and the breeding of high yielding cultivars. *Curr. Med. Chem.* 8, 1795–1801. doi: 10.2174/0929867013371635

Duke, M. V., Paul, R. N., Elsohly, H. N., Sturtz, G., and Duke, S. O. (1994). Localization of artemisinin and artemisitene in foliar tissues of glanded and glandless biotypes of *Artemisia annua* L. *Int. J. Plant Sci.* 155, 365–372. doi: 10.1086/297173

Duke, S. O., Vaughn, K. C., Croom, E. M. J., and Elsohly, H. N. (1987). Artemisinin, a constituent of annual wormwood (*Artemisia annua*), is a selective phytotoxin. *Weed Sci.* 35, 499–505.

Elhag, H. M., El-Domiaty, M. M., El-Feraly, F. S., Mossa, J. S., and El-Olemy, M. M. (1992). Selection and micropropagation of high artemisinin producing clones of *Artemisia annua* L. *Phytother. Res.* 6, 20–24. doi: 10.1002/ptr.2650060106

Farhi, M., Marhevka, E., Ben-Ari, J., Algamas-Dimantov, A., Liang, Z., and Zeevi, V. (2011). Generation of the potent anti-malarial drug artemisinin in tobacco. *Nat. Biotechnol.* 29, 1072–1074. doi: 10.1038/nbt.2054

Ferreira, J. F. (2007). Nutrient deficiency in the production of artemisinin, dihydroartemisinic acid, and artemisinic acid in *Artemisia annua* L. *J. Agric. Food Chem.* 55, 1686–1694. doi: 10.1021/jf063017v

Ferreira, J. F. S. (2008). Seasonal and post-harvest accumulation of artemisinin, artemisinic acid, and dihydroartemisinic acid in three accessions of *Artemisia annua* cultivated in West Virginia, USA. *Planta Med.* 74, 310–311. doi: 10.1055/s-2008-1075155

Ferreira, J. F. S., and Janick, J. (1995a). "Distribution of artemisinin in *Artemisia annua*," in *Progress in New Crops*, ed J. Janick (Arlington, VA: ASHA), 578–584.

Ferreira, J. F. S., and Janick, J. (1995b). Floral morphology of *Artemisia annua* with special reference to trichomes. *Int. J. Plant Sci.* 156, 807–815. doi: 10.1086/297304

Ferreira, J. F. S., Laughlin, J. C., Delabays, N., and Magalhães, P. M. (2005). Cultivation and genetics of *Artemisia annua* for increased production of the anti-malarial artemisinin. *Plant Gen. Resour.* 3, 206–229. doi: 10.1079/PGR200585

Ferreira, J. F. S., and Luthria, D. L. (2010). Drying affects artemisinin, dihydroartemisinic acid, artemisinic acid, and the antioxidant capacity of *Artemisia annua* L. leaves. *J. Agric. Food Chem.* 58, 1691–1698. doi: 10.1021/jf903222j

Ferreira, J. F. S., Simon, J. E., and Janick, J. (1995). Relationship of artemisinin content of tissue-cultured, greenhouse-grown, and field-grown plants of *Artemisia annua*. *Planta Med.* 61, 351–355. doi: 10.1055/s-2006-958098

Ferreira, J. F., Charles, D., Simon, J. E., and Janick, J. (1992). Effect of drying methods on the recovery and yield of artemisinin from A*rtemisia annua* L. *HortScience* 27:650.

Ferreira, J. F., and Gonzalez, J. M. (2009). Analysis of underivatized artemisinin and related sesquiterpene lactones by high-performance liquid chromatography with ultraviolet detection. *Phytochem. Anal.* 20, 91–97. doi: 10.1002/pca.1101

Fuentes, P., Zhou, F., Erban, A., Karcher, D., Kopka, J., and Bock, R. (2016). A new synthetic biology approach allows transfer of an entire metabolic pathway from a medicinal plant to a biomass crop. *Elife* 5:e13664. doi: 10.7554/eLife.13664

Howard, J. L., Schotten, C., and Browne, D. L. (2017). Continuous flow synthesis of antimalarials: opportunities for distributed autonomous chemical manufacturing. *React. Chem. Eng.* 2, 281–287. doi: 10.1039/C7RE00034K

Khairul Ikram, N. K. B., Kashkooli, A. B., Peramuna, A. V., Van Der Krol, A. R., Bouwmeester, H., and Simonsen, H. T. (2017). Stable production of the antimalarial drug artemisinin in the moss *Physcomitrella patens*. *Front. Bioeng. Biotechnol.* 5:47. doi: 10.3389/fbioe.2017.00047

Kjær, A., Verstappen, F., Bouwmeester, H., Ivarsen, E., Fretté, X., Christensen, L. P., et al. (2013). Artemisinin production and precursor ratio in full grown *Artemisia annua* L. plants subjected to external stress. *Planta* 237, 955–966. doi: 10.1007/s00425-012-1811-y

Klayman, D. L. (1985). Qinghaosu (artemisinin): an antimalarial drug from China. *Science* 228, 1049–1055. doi: 10.1126/science.3887571

Kopetzki, D., Lévesque, F., and Seeberger, P. H. (2013). A continuous-flow process for the synthesis of artemisinin. *Chemistry* 19, 5450–5456. doi: 10.1002/chem.201204558

Lévesque, F., and Seeberger, P. H. (2012). Continuous-flow synthesis of the anti-malaria drug artemisinin. *Angew. Chem.* 51, 1706–1709. doi: 10.1002/anie.201107446

Li, L., Josef, B. A., Liu, B., Zheng, S., Huang, L., and Chen, S. (2017). Three-dimensional evaluation on ecotypic diversity of traditional Chinese medicine: a case study of *Artemisia annua* L. *Front. Plant Sci.* 8:1225. doi: 10.3389/fpls.2017.01225

Liu, S., Ferreira, J. F. S., Liu, L., Tang, Y., Tian, D., Liu, Z., et al. (2017). Isolation of dihydroartemisinic acid from the *Artemisia annua* L. by-product by combining ultrasound-assisted extraction with response surface methodology. *Chem. Pharm. Bull.* 65, 746–753. doi: 10.1248/cpb.c17-00192

Lommen, W. J., Elzinga, S., Verstappen, F. W., and Bouwmeester, H. J. (2007). Artemisinin and sesquiterpene precursors in dead and green leaves of *Artemisia annua* L. crops. *Planta Med.* 73, 1133–1139. doi: 10.1055/s-2007-981567

Maes, L., Van Nieuwerburgh, F. C. W., Zhang, Y., Reed, D. W., Pollier, J., Vande Casteele, S. R. F., et al. (2011). Dissection of the phytohormonal regulation of trichome formation and biosynthesis of the antimalarial compound artemisinin in *Artemisia annua* plants. *New Phytol.* 189, 176–189. doi: 10.1111/j.1469-8137.2010.03466.x

Magalhães, P. M. D., Pereira, B., Sartoratto, A., Oliveira, J. D., and Debrunner, N. (1999). New hybrid lines of the antimalarial species *Artemisia annua* L. *Acta Hort.* 502, 377–381. doi: 10.17660/ActaHortic.1999.502.62

Mannan, A., Ahmed, I., Arshad, W., Asim, M., Qureshi, R., Hussain, I., et al. (2010). Survey of artemisinin production by diverse Artemisia species in northern Pakistan. *Malar. J.* 9:310. doi: 10.1186/1475-2875-9-310

Marchese, J. A., Ferreira, J. F. S., Rehder, V. L. G., and Rodrigues, O. (2010). Water deficit effect on the accumulation of biomass and artemisinin in annual wormwood (*Artemisia annua L.*, Asteraceae). *Braz. J. Plant Physiol.* 22, 1–9. doi: 10.1590/S1677-04202010000100001

Olofsson, L., Lundgren, A., and Brodelius, P. E. (2012). Trichome isolation with and without fixation using laser microdissection and pressure catapulting followed by RNA amplification: expression of genes of terpene metabolism in apical and sub-apical trichome cells of *Artemisia annua* L. *Plant Sci.* 183, 9–13. doi: 10.1016/j.plantsci.2011.10.019

Paddon, C. J., Westfall, P. J., Pitera, D. J., Benjamin, K., Fisher, K., and Mcphee, D. (2013). High-level semi-synthetic production of the potent antimalarial artemisinin. *Nature* 496, 528–532. doi: 10.1038/nature12051

Peng, C. A., Ferreira, J. F. S., and Wood, A. J. (2006). Direct analysis of artemisinin from *Artemisia annua* L. using high-performance liquid chromatography with evaporative light scattering detector, and gas chromatography with flame ionization detector. *J. Chromatogr. A* 1133, 254–258. doi: 10.1016/j.chroma.2006.08.043

Peplow, M. (2016). Synthetic malaria drug meets market resistance: first commercial deployment of synthetic biology for medicine has modest impact. *Nature* 530, 389–390. doi: 10.1038/530390a

Qian, Z., Gong, K., Zhang, L., Lv, J., Jing, F., Wang, Y., et al. (2007). A simple and efficient procedure to enhance artemisinin content in *Artemisia annua* L. by seeding to salinity stress. *Afr. J. Biotechnol.* 6, 1410–1413. Available online at: https://www.ajol.info/index.php/ajb/article/view/57560/45940

Qureshi, M. I., Israr, M., Abdin, M. Z., and Iqbal, M. (2005). Responses of *Artemisia annua* L. to lead and salt-induced oxidative stress. *Environ. Exper. Bot.* 53, 185–193. doi: 10.1016/j.envexpbot.2004.03.014

Ro, D.-K., Paradise, E. M., Ouellet, M., Fisher, K. J., Newman, K. L., Ndungu, J. M., et al. (2006). Production of the antimalarial drug precursor artemisinic acid in engineered yeast. *Nature* 440, 940–943. doi: 10.1038/nature04640

Simonnet, X., Quennoz, M., and Carlen, C. (2008). "New Artemisia annua hybrids with high artemisinin content," in *XXVII International Horticultural Congress-IHC2006: International Symposium on Asian Plants with Unique Horticultural Potential* (Leuven: Acta Horticulturae), 371–373.

Suberu, J., Gromski, P. S., Nordon, A., and Lapkin, A. A. (2016). Multivariate data analysis and metabolic profiling of artemisinin and related compounds in high yielding varieties of *Artemisia annua* field-grown in Madagascar. *J. Pharm. Biomed. Anal.* 117, 522–531. doi: 10.1016/j.jpba.2015.10.003

Tan, H., Xiao, L., Gao, S., Li, Q., Chen, J., Xiao, Y., et al. (2015). TRICHOME AND ARTEMISININ REGULATOR 1 Is required for trichome development and artemisinin biosynthesis in *Artemisia annua*. *Mol. Plant* 8, 1396–1411. doi: 10.1016/j.molp.2015.04.002

Tu, Y.-Y. (2011). The discovery of artemisinin (qinghaosu) and gifts from Chinese medicine. *Nat. Med.* 17, 1217–1220. doi: 10.1038/nm.2471

Wallaart, T. E., Pras, N., Beekman, A. C., and Quax, W. J. (2000). Seasonal variation of artemisinin and its biosynthetic precursors in plants of *Artemisia annua* of different geographical origin: proof for the existence of chemotypes. *Planta Med.* 66, 57–62. doi: 10.1055/s-2000-11115

Wallaart, T. E., Pras, N., and Quax, W. J. (1999a). Isolation and identification of dihydroartemisinic acid hydroperoxide from *Artemisia annua*: a novel biosynthetic precursor of artemisinin. *J. Nat. Prod.* 62, 1160–1162. doi: 10.1021/np9900122

Wallaart, T. E., Van Uden, W., Lubberink, H. G. M., Woerdenbag, H. J., Pras, N., and Quax, W. J. (1999b). Isolation and identification of dihydroartemisinic acid from *Artemisia annua* and its possible role in the biosynthesis of artemisinin. *J. Nat. Prod.* 62, 430–433. doi: 10.1021/np980370p

Wang, H. H., Ma, C. F., Li, Z. Q., Ma, L. Q., Wang, H., Ye, H. C., et al. (2010). Effects of exogenous methyl jasmonate on artemisinin biosynthesis and secondary metabolites in *Artemisia annua* L. *Ind. Crop. Prod.* 31, 214–218. doi: 10.1016/j.indcrop.2009.10.008

Wang, M., Park, C., Wu, Q., and Simon, J. E. (2005). Analysis of artemisinin in *Artemisia annua* L. by LC-MS with selected ion monitoring. *J. Agric. Food Chem.* 53, 7010–7013. doi: 10.1021/jf051061p

Wetzstein, H. Y., Porter, J. A., Janick, J., Ferreira, J. F. S., and Mutui, T. M. (2018). Selection and clonal propagation of high artemisinin genotypes of *Artemisia annua*. *Front. Plant Sci.* 9:358. doi: 10.3389/fpls.2018.00358

Xiao, L., Tan, H., and Zhang, L. (2016). *Artemisia annua* glandular secretory trichomes: the biofactory of antimalarial agent artemisinin. *Sci. Bull.* 61, 26–36. doi: 10.1007/s11434-015-0980-z

Xie, D.-Y., Ma, D.-M., Judd, R., and Jones, A. L. (2016). Artemisinin biosynthesis in *Artemisia annua* and metabolic engineering: questions, challenges, and perspectives. *Phytochem. Rev.* 15, 1093–1114. doi: 10.1007/s11101-016-9480-2

Yadav, R. K., Sangwan, R. S., Srivastava, A. K., and Sangwan, N. S. (2017). Prolonged exposure to salt stress affects specialized metabolites-artemisinin and essential oil accumulation in *Artemisia annua* L.: metabolic acclimation in preferential favour of enhanced terpenoid accumulation accompanying vegetative to reproductive phase transition. *Protoplasma* 254, 505–522. doi: 10.1007/s00709-016-0971-1

Zhu, J., Yang, J., Zeng, Z., Zhang, W., Song, L., Wen, W., et al. (2014). Inducing effect of dihydroartemisinic acid in the biosynthesis of artemisinins with cultured cells of *Artemisia annua* by enhancing the expression of genes. *Sci. World J.* 2014:293190. doi: 10.1155/2014/293190

Conflict of Interest Statement: The authors declare that the research was conducted in the absence of any commercial or financial relationships that could be construed as a potential conflict of interest.

The reviewer TL and handling editor declared their shared affiliation.

frontiers in Plant Science

ORIGINAL RESEARCH
published: 30 July 2019
doi: 10.3389/fpls.2019.00984

Flavonoid Versus Artemisinin Anti-malarial Activity in *Artemisia annua* Whole-Leaf Extracts

Tomasz Czechowski[1†], Mauro A. Rinaldi[1†], Mufuliat Toyin Famodimu[2], Maria Van Veelen[3], Tony R. Larson[1], Thilo Winzer[1], Deborah A. Rathbone[1,4], David Harvey[1], Paul Horrocks[2,3] and Ian A. Graham[1]*

[1] Centre for Novel Agricultural Products, Department of Biology, University of York, York, United Kingdom, [2] Institute for Science and Technology in Medicine, Keele University, Keele, United Kingdom, [3] School of Medicine, Keele University, Keele, United Kingdom, [4] Biorenewables Development Centre, Dunnington, United Kingdom

Artemisinin, a sesquiterpene lactone produced by *Artemisia annua* glandular secretory trichomes, is the active ingredient in the most effective treatment for uncomplicated malaria caused by *Plasmodium falciparum* parasites. Other metabolites in *A. annua* or related species, particularly flavonoids, have been proposed to either act as antimalarials on their own or act synergistically with artemisinin to enhance antimalarial activity. We identified a mutation that disrupts the CHALCONE ISOMERASE 1 (CHI1) enzyme that is responsible for the second committed step of flavonoid biosynthesis. Detailed metabolite profiling revealed that *chi1-1* lacks all major flavonoids but produces wild-type artemisinin levels, making this mutant a useful tool to test the antiplasmodial effects of flavonoids. We used whole-leaf extracts from *chi1-1* and mutant lines impaired in artemisinin production in bioactivity *in vitro* assays against intraerythrocytic *P. falciparum* Dd2. We found that *chi1-1* extracts did not differ from wild-type extracts in antiplasmodial efficacy nor initial rate of cytocidal action. Furthermore, extracts from the *A. annua cyp71av1-1* mutant and RNAi lines impaired in amorpha-4,11-diene synthase gene expression, which are both severely compromised in artemisinin biosynthesis but unaffected in flavonoid metabolism, showed very low or no antiplasmodial activity. These results demonstrate that *in vitro* bioactivity against *P. falciparum* of flavonoids is negligible when compared to that of artemisinin.

Keywords: malaria, *Artemisia annua*, artemisinin, flavonoids, *Plasmodium falciparum*, chalcone isomerase

OPEN ACCESS

Edited by:
Goetz Hensel, Leibniz-Institut für Pflanzengenetik und Kulturpflanzenforschung (IPK), Germany

Reviewed by:
Qifang Pan, Shanghai Jiao Tong University, China
De-Yu Xie, North Carolina State University, United States

***Correspondence:**
Ian A. Graham
ian.graham@york.ac.uk

[†]These authors have contributed equally to this work

Specialty section:
This article was submitted to Plant Biotechnology, a section of the journal Frontiers in Plant Science

Received: *08 March 2019*
Accepted: *12 July 2019*
Published: *30 July 2019*

Citation:
Czechowski T, Rinaldi MA, Famodimu MT, Van Veelen M, Larson TR, Winzer T, Rathbone DA, Harvey D, Horrocks P and Graham IA (2019) Flavonoid Versus Artemisinin Anti-malarial Activity in Artemisia annua Whole-Leaf Extracts. Front. Plant Sci. 10:984. doi: 10.3389/fpls.2019.00984

INTRODUCTION

Malaria is one of the most prevalent infectious diseases with 219 million cases and 435,000 deaths reported in 2017 (World Health Organization [WHO], 2018). The WHO recommends the use of artemisinin-based combination therapies (ACTs) for treatment of uncomplicated malaria caused by the *Plasmodium falciparum* parasite (World Health Organization [WHO], 2018). ACTs consist of fast-acting and stable artemisinin derivatives, such as artesunate, co-formulated with a different class of drug to reduce the emergence of resistance and increase treatment efficacy (Petersen et al., 2011). The main source of the sesquiterpene artemisinin is currently the medicinal plant *Artemisia annua*, which has achieved a yield of 1.5% dry leaf weight through breeding (Townsend et al., 2013). Additionally, a semi-synthetic alternative has been developed through precursor biosynthesis in yeast and chemical conversion to artemisinin (Peplow, 2016).

Artemisia annua accumulates artemisinin together with a wide range of secondary metabolites in the extracellular subapical cavity of glandular secretory trichomes, specialized 10-cell structures on the surfaces of aerial tissues (Brown, 2010; Lange, 2015; Czechowski et al., 2018). This wide range of metabolites has led to speculation that perhaps other compounds in *A. annua* or related species might act as antimalarials or potentially enhance the antimalarial activity of artemisinin. Therefore, several groups have tried to isolate and identify metabolites from *A. annua* and related species that might function as antimalarials (O'Neill et al., 1985; Elford et al., 1987; Liu et al., 1989, 1992; Cubukcu et al., 1990; Mueller et al., 2000; Bhakuni et al., 2001; Kraft et al., 2003).

Recent publications have reported that *A. annua* whole-plant preparations are more effective than artemisinin alone (not ACTs) in treating rodent malaria (Elfawal et al., 2012) and reducing the development of resistance (Elfawal et al., 2015), and that whole-plant preparations may be effective in treating artesunate-resistant malaria patients (Daddy et al., 2017). These results suggest that *A. annua* produces metabolites that might act together with artemisinin and thus whole-plant preparations have been proposed as replacement treatments for ACTs (Weathers et al., 2014). In particular, flavonoids have been singled out as the likely synergistic metabolites (Elfawal et al., 2012, 2015; Weathers et al., 2014; Daddy et al., 2017) mainly because there is some evidence that they may improve the antimalarial activity of artemisinin *in vitro* (Elford et al., 1987; Liu et al., 1989, 1992; Ferreira et al., 2010).

Flavonoids are a diverse class of plant and fungal secondary metabolites with over 6500 different flavonoid products described from the secondary metabolism of various plant species (Ververidis et al., 2007). Flavonoid biosynthesis starts from primary metabolism precursors: phenylalanine and malonyl-CoA. Phenylalanine is used to produce 4-coumaroyl-CoA which is then combined with malonyl-CoA by chalcone synthase to yield the two-phenyl ring backbone common to all chalcones. A key step in flavonoid synthesis is the conjugate ring-closure of chalcones catalyzed by chalcone-flavanone isomerase (CHI), which results in the three-ringed structure of a flavone. The phenylpropanoid metabolic pathway contributes a series of enzymatic modifications that yield flavanones, dihydroflavonols, and eventually anthocyanins. Many products can be derived from this pathway including flavonols, flavan-3-ols, proanthocyanidins (tannins) and a host of other various polyphenolics (Ververidis et al., 2007). Flavonoids have been classified according to the position of the linkage of the aromatic ring to the benzopyrano moiety into four classes: major flavonoids (2-phenyl benzopyrans), which include flavonols, flavonones, flavanonols, flavones, anthocyanins and anthocyanidines; isoflavonoids (3-benzopyrans), which contain isoflavanons, isoflavanones and isoflavanonols; neo-flavonoids (4-benzopyrans) which include neoflavenes and 4-arylcoumarins; and finally, minor flavonoids which include aurones, auronols, 2′OH chalcones and 2′OH dihydrochalcones (Ververidis et al., 2007).

In the present work we report an *A. annua* loss-of-function mutation of the trichome-specific *CHALCONE ISOMERASE 1* (*CHI1*) gene. Levels of all major flavonoids in the *chi1-1* mutant were reduced to undetectable levels. We used *chi1-1* to test the antimalarial effects of flavonoids. We extended the bioassays to include whole-leaf extracts from *A. annua* silenced in amorpha-4,11-diene synthase (*AMS*), which encodes the enzyme that catalyzes the first committed step of artemisinin biosynthesis (Catania et al., 2018), and the *cyp71av1-1* mutant, impaired in the second committed step of artemisinin biosynthesis (Czechowski et al., 2016). The *AMS* silenced line has dramatically reduced artemisinin production (5% of the wild-type levels) and accumulates the sesquiterpene precursor farnesyl pyrophosphate in trichomes (Catania et al., 2018). *cyp71av1-1* completely abolishes artemisinin production and redirects the artemisinin pathway to the synthesis of arteannuin X, a novel sesquiterpene epoxide (Czechowski et al., 2016). Both the *AMS* silenced and *cyp71av1-1* mutant lines produce wild-type levels of major flavonoids. We have performed a comparative analysis of whole-leaf extracts from *chi1-1*, the *AMS* silenced line, *cyp71av1-1*, and wild-type *A. annua* in *in vitro P. falciparum* Dd2 kill assays (Ullah et al., 2017) to determine the antiplasmodial efficacy and initial cytocidal activity of these extracts.

MATERIALS AND METHODS

Plant Material

For wild-type plant material we used the Artemis F1 hybrid variety of *A. annua* developed by Mediplant (Conthey, Switzerland), obtained by crossing C4 and C1 parental lines of East Asia origin (Delabays et al., 2001). Seeds were sown in 4-inch pots filled with Levington modular compost and grown in a glasshouse under long-day conditions (16-h day/8-h night) at 17–22°C for 12 weeks.

RNA Isolation and Semi-Quantitative RT-PCR

Total RNA was isolated from eight *A. annua* tissues: meristems, cotyledons, trichomes, young leaves, expanded leaves, mature leaves, stems, and flowers as previously described (Graham et al., 2010) and quantified using the NanoDrop 8000 (NanoDrop products, Wilmington, DE, United States). 5 μg of total RNA was digested with RQ1 RNase-free DNase (Promega, United Kingdom) according to the manufacturer's protocol. 1st strand cDNA synthesis was performed using 2.5 μg of DNaseI digested RNA with oligo dT(18) primers and SuperScript™ II Reverse Transcriptase (Thermo Fisher, United Kingdom) according to manufacturer's protocols. 3 μL of the first strand cDNA was used for PCR amplification using the following gene specific primers: CHI1_For: 5′-TGGCAACACCACCTTCAGC TACC-3′ (left), CHI1_Rev: 5′-GTTGTGAAGAGAATAGAG GCG-3′ (right), CHI2_For: 5′-ATGGCTAAGCTTCATTCCTCC AC-3′ (left), CHI2_Rev: 5′-CAGGTATGATACCATCTCTA GC-3′ (right), CHI3_For 5′-CTGGAGCAATTCCCAGATC AG-3′ (left), CHI3_Rev 5′-AGAATGTTTTGCCATCAACATC TC-3′ (right), Ubiquitn_For: 5′-GTCGGCTAATGGAGAAG ACAAGAAG-3′ (left) and Ubiquitn_Rev: 5′-GAAAGCA CGACCAGATTCATAGC-3′ (right) using GoTaq™ *Taq* polymerase (Promega, United Kingdom). The PCR program used to amplify the target sequences was: 94°C, 2 min; followed

by 10 cycles of "touch down": 94°C, 30 sec; 65°C (−1°C/cycle); 72°C, 1 min, followed by 20 cycles of 94°C, 30 sec; 55°C, 30 sec; 72°C, 1 min, followed by a final extension at 72°C for 5 min. 10 μL of PCR product was resolved on 1% agarose gels. Predicted product sizes for each gene are: 466 bp for *CHI1*, 520 bp for *CHI2*, 507 bp for *CHI3*, and 454 bp for *UBQ*.

chi1-1 Mutant Isolation and Characterization

An ethyl methanesulfonate-mutagenized *A. annua* population was established as described before (Graham et al., 2010; Czechowski et al., 2016). Screening of the self-fertilized M2 population was performed as previously described (Czechowski et al., 2016) with the following modifications. DNA was isolated from 30 to 50 mg of fresh leaf material harvested from individual 4 to 6-week-old M2 plants, using the BioSprint 96 system (Qiagen, Hilden, Germany) according to the manufacturer's protocol. DNA was quantified fluorometrically using Hoechst 33258 dye and a plate reader (Fuoromax, United Kingdom). DNA samples were normalized to 5 ng/μL using the Freedom EVO® 200 workstation (Tecan United Kingdom Ltd.) and arranged in four-fold pools for reverse genetic screening. The full-length genomic DNA sequence of the Artemis *A. annua CHI1* gene for TILLING was obtained by PCR using gene-specific primers designed based on Gene Bank-deposited sequence EZ246664. A 937-bp fragment of CHI1 was amplified in a two-step PCR reaction. The first step was carried out with unlabeled primers: 5′-TGGCAACACCACCTTCAGCTACC-3′ (left) and 5′-CTGTGGTTGCTTTCTCATCAAAATGG-3′ (right) on 12.5 ng of pooled gDNA in 10 μL volumes. Nested PCR and labeling with IR dyes were performed on a 1/10 dilution of the first PCR with a mixture of unlabeled M13-tailed primers (5′-TGTAAAACGACGGCCAGTCGACAGCAACTAGTAATGG TAAACTG-3′ (left) and 5′-AGGAAACAGCTATGACCACAT AAGATCTGAAAGTCTTGAAGCC-3′ (right), and with M13 left primer (5′-TGTAAAACGACGGCCAGT-3′) labeled with IRDye700 and M13 right primer (5′-AGGAAACAGCTATGACC AT-3′) labeled with IRDye 800 (MWG, Ebersberg, Germany). Heteroduplex formation, CEL I nuclease digestion and analysis on the LI-COR 4300 DNA sequencer platform were carried out as previously described (Till et al., 2006). All mutants found on the TILLING gels were verified by Sanger sequencing of both DNA strands of PCR-amplified fragments using the following primers: 5′-GCAATAATGCTATGTGTTGGTGC-3′ (left) and 5′-CACAATGTTTGCAGCTTCAGGTATG-3′ (right). Two segregating M3 mutant populations were obtained by crossing M2 siblings that were heterozygous for the *chi1-1* mutation.

KASP™ SNP Assay for *chi1-1* Mutation Status

Twenty nanograms of DNA was used for 10 μL KASPar assay reactions containing: 1 × KASP V4.0 low ROX master mix (LGC Genomics); a concentration of 167 nM of each of the two allele-specific primers: chi1-1_ForC: 5′-GAAG GTGACCAAGTTCATGCTCAATGATACTACCATTAACTGGT AAGC-3′ and chi1-1_ForT: 5′-GAAGGTCGGAGTCAACGGAT TGACAATGATACTACCATTAACTGGTAAGT-3′ and 414 nM universal primer chi1-1_Rev 5′-CTCCAACGCACATTTCAGA CACCTT-3′, according to the manufacturer's recommendations. Allelic discrimination runs and allelic discrimination analysis were performed on Viia7 system (Life Technologies Ltd.) according to the manufacturer's recommendations.

Metabolite Analysis by UPLC-and GC-MS

Plants were grown from five cuttings from each genotype and metabolic profiles were generated from 10 to 50 mg FW pooled samples of leaves at different developmental stages: 4–6 (counting from the apical meristem) representing the young stage; leaves 11–13 representing the mature, expanded stage and three leaves taken just above first senescing leaves representing old leaves. Fresh leaf samples were stored at −80°C. Trichome-specific metabolites were extracted as described previously (Czechowski et al., 2016) and analyzed by UPLC-MS as previously described (Graham et al., 2010; Czechowski et al., 2016). Dry leaf material was obtained from 14-week-old plants, cut just above the zone of senescing leaves and dried for 14 days at 40°C. Leaves were stripped from the plants, and leaf material sieved through 5 mm mesh to remove small stems. Metabolite extractions from 10 mg of the dry leaf material and UPLC-MS analysis were performed as previously described (Graham et al., 2010; Czechowski et al., 2016). Number of the biological replicates measured was as follows: young and mature wild-type leaves $n = 49$, old wild-type leaves $n = 60$, dry wild-type leaves $n = 21$; young-, mature- and old heterozygous *chi1-1* leaves $n = 94$, dry heterozygous *chi1-1* leaves $n = 37$; young, mature and old homozygous *chi1-1* leaves $n = 63$, dry heterozygous *chi1-1* leaves $n = 32$. The experiments comparing trichome vs. whole-leaf metabolites were performed on leaves 14–16 harvested from five individuals grown from cuttings ($n = 5$). Trichome-specific metabolites were first extracted from the fresh mature leaves as described above. The remaining leaf material was washed three times with 500 μL of chloroform and solvent removed by pipetting. Leaf tissue was ground to a fine powder in TissueLyser II (Qiagen, United Kingdom), extracted and quantified by UPLC-MS. GC-MS analysis was performed on the same dipped and ground-leaf extracts as described before (Czechowski et al., 2016). To evaluate method suitability for detecting flavonoids, comparative extracts of dry material were made with either 9:1 chloroform:ethanol (v/v; used throughout this study) vs. 85:15 methanol:water (v/v; typically used to extract polar flavonoids from plant material). These extracts were then separated on an extended UPLC gradient (starting conditions modified to 100% of aqueous solvent A), to avoid any potentially highly polar flavonoids being lost in the void volume.

Whole-Leaf Extraction for *P. falciparum* Kill Rate Assays

Fourteen-week-old plants were cut above the area of senescing leaves and dried for 14 days at 40°C. Leaves were separated from the rest of the dry plants and sieved through 5-mm mesh to remove small stems. Dry leaves were stored long

term in a humidity-controlled cabinet at 4°C. For whole-leaf extracts, 1 g dry leaves was ground to a fine powder and extracted in 9:1 chloroform and ethanol solution overnight, centrifuged at 4,700 rpm for 20 min and the supernatant was filtered through Wattman paper. An aliquot was taken for quantification by UPLC-MS. The solvent was evaporated until only an oily residue remained and re-suspended in DMSO to reach a final concentration of 5 mg/ml artemisinin (or to reach a casticin concentration equivalent to that of the wild type in the *AMS* RNAi line, or equivalent to heterozygous *cyp71av1-1* in homozygous *cyp71av1-1*).

In vitro Plasmodium falciparum Assays

The *in vitro* screening of antiplasmodial activity of extracts was carried out starting with trophozoite stage (24–32 h post infection) intraerythrocytic stages of the *P. falciparum* Dd2 strain using a 48 h (one complete cycle of intraerythrocytic development) Malaria Sybr Green I Fluorescence assay as previously described (Smilkstein et al., 2004; Ullah et al., 2017). The mean percentage growth ± StDev (n = 9 from three independent biological repeats) was plotted against $\log_{10}$-transformed drug concentration and a non-linear regression (sigmoidal concentration–response/variable slope equation) in GraphPad Prism v5.0 (GraphPad Software, Inc., San Diego, CA, United States) used to estimate the 50% effective concentration (EC_{50}) and the 95% confidence intervals.

Determination of the relative initial cytocidal activity against trophozoite stage intraerythrocytic stages of the *P. falciparum* $Dd2^{luc}$ (Wong et al., 2011) were carried out using the Bioluminescence Relative Rate of Kill assay as described (Ullah et al., 2017). All assays were carried out over 6 h using a $9 \times EC_{50}$ to $0.33 \times EC_{50}$ concentration series. The mean ± StDev bioluminescence signal, normalized to an untreated control, are plotted (n = 9 from three biological repeats) and compared to the benchmark standards of dihydroartemisinin (DHA), chloroquine (CQ), mefloquine (MQ) and atovaquone (ATQ). Stock solutions of atovaquone (10 mM in DMSO), chloroquine (100 mM in deionized water), dihydroartemisinin (50 mM in methanol), and mefloquine (50 mM in DMSO) were made (Sigma-Aldrich) and stored at −20°C. In all experiments, the maximum final concentration of solvent was 0.6% (v/v).

RESULTS

Isolation and Characterisation of a *CHI1* Mutant Impaired in Flavonoid Biosynthesis

Casticin and other polymethoxylated flavonoids accumulate in leaf and flower trichomes of the *A. annua* Artemis variety, some to high levels comparable to those of artemisinin (Czechowski et al., 2016, 2018). We previously identified three putative *CHI* genes using *A. annua* transcriptome data (Graham et al., 2010). *CHI1* is expressed in young leaf and flower bud trichomes whereas *CHI2* is expressed in young and mature leaf trichomes and *CHI3* is expressed most highly in meristems and cotyledons (Graham et al., 2010). Further quantitative RT-PCR-based expression profiling, extended to other tissues, revealed that *CHI1* expression is the most trichome specific of the three genes tested, whereas *CHI2* is more generally expressed in several tissues and *CHI3* expression is not detected in trichomes (**Figure 1A**). The 229 amino acid-long predicted protein sequence for CHI1 is most similar to CHI characterized in other organisms than it is to the other two putative CHI proteins we previously identified from *A. annua* (**Supplementary Figure S1A**; Jez et al., 2000). Amino acid sequence alignment of CHI homologs shows that CHI2 and CHI3 are missing a number of highly conserved residues including those required for substrate binding (**Supplementary Figure S1A**; Jez et al., 2000). In contrast CHI1 contains all of the conserved residues, suggesting that it is the only one of the three CHI homologs from *A. annua* that produces a functional chalcone isomerase enzyme.

Using an established ethyl methanesulfonate-mutagenized population of *A. annua* (Czechowski et al., 2016) we performed a TILLING screen of the single-copy *CHI1* gene that resulted in an allelic series of five mutants, including three with intronic mutations, one with a silent mutation and one with a nonsense mutation that created a C1567 to T transition in the third exon of *CHI1* (**Figure 1B** and **Supplementary Figure S1B**). The latter mutation, which we designate *chi1-1*, gave a predicted change of amino acid Gln107 in the polypeptide to a stop codon that would result in a major truncation of the enzyme and loss of most of the putative substrate-binding site (**Figure 1C** and **Supplementary Figure S1A**). CHI is a functional monomer and residues that are important for substrate binding and the active site in other species lie beyond the residue corresponding to *A. annua* CHI1 Q107 (**Figure 1C** and **Supplementary Figure S1A**; Jez et al., 2000),

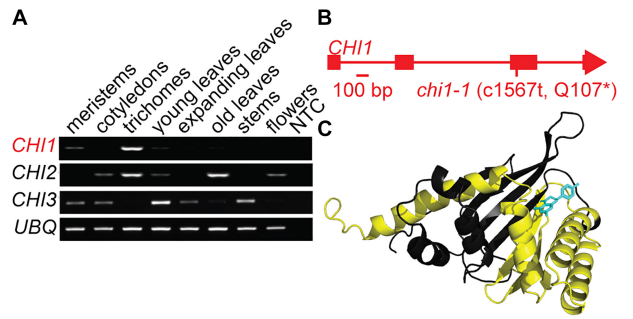

FIGURE 1 | Discovery and characterization of the *chi1-1* mutation. **(A)** *Artemisia annua CHI1*, *CHI2* and *CHI3* expression in meristems, cotyledons, young leaf trichomes, young leaves, fully expanded leaves, mature leaves, stems, flowers, and no template control (NTC) were determined by semi-quantitative PCR. *UBQ* (Putative ubiquitin-like protein, GQ901904) was used as a loading control. **(B)** Gene schematic of *CHI1* indicates the position of the *chi1-1* mutation. **(C)** The *A. annua* CHI1 protein structure was modeled by I-TASSER (Yang et al., 2015) on the 10 most closely related structural analogs. The parts of the structure expected to be missing in the *chi1-1* mutant are highlighted in yellow, naringenin (enzyme product) bound to CHI1 is shown in blue.

which suggested the truncation would result in a complete loss of CHI function.

In order to investigate the effects of the *chi1-1* mutation on artemisinin and flavonoid biosynthesis we analyzed three leaf developmental stages: young (leaves 4–6 as counted down from the apical meristem), mature (leaves 11–13) and old (3 leaves preceding the first senescing leaves). To generate material for this analysis we performed two crosses of heterozygous *chi1-1* M2 siblings originating from a self-fertilized M1 individual and performed DNA marker-based selection of wild type (WT) and heterozygous and homozygous *chi1-1* individuals from the segregating M3 population using the KASP^{TM} SNP assay. We observed a strong segregation distortion from the expected 1:2:1 (WT:heterozygous:homozygous mutation) in both M3 populations. The first cross resulted in 30 individuals of which 24 were heterozygous and 6 homozygous for the *chi1-1* mutation whereas the second cross resulted in 54 individuals of which 36 were heterozygous and 18 homozygous for the *chi1-1* mutation, but we could not identify segregating wild-type individuals. Such segregation distortion is not unusual for *A. annua*, which naturally outcrosses, and has been reported for the populations coming from self-fertilized individuals (Graham et al., 2010). In the absence of any segregating M3 wild–type individuals we used non-mutagenized *Artemis* F1 as wild type for metabolic profiling.

CHI disruption or suppression has previously been reported to result in discoloration and/or decreased flavonol levels in *Arabidopsis thaliana*, petunia, carnation, onion and tobacco (van Tunen et al., 1991; Shirley et al., 1992; Itoh et al., 2002; Kim et al., 2004; Nishihara et al., 2005) whereas petunia *CHI* overexpression leads to increased flavonol accumulation in tomato (Muir et al., 2001). *A. annua* produces the polymethoxylated flavonoids casticin, artemetin, chrysoplenetin, chrysosplenol-D, and cirsilineol (Bhakuni et al., 2001). Whereas the wild type and the *chi1-1* heterozygote produced similar amounts of casticin, chrysoplenol C, dehydroxycasticin and artemetin none of these flavonoids were detectable in homozygous *chi1-1* individuals (**Figures 2Ai–iv**). These results demonstrate that *chi1-1* is a null allele. Flavonoids in the wild type and heterozygous *chi1-1* are most abundant in young, followed by mature and old leaves (**Figure 2A**). Noteworthy, *chi1-1* accumulated a compound with an m/z ratio of 273.0757 that was not detectable in the wild type or the *chi1-1* heterozygote (**Figure 2Av**). The UPLC-MS profile of this compound suggests it represents the molecular ion of naringenin chalcone (MW = 272.26 g/mol), the substrate of chalcone isomerase, which would be expected to accumulate in the *chi1-1* null mutant.

We initially devised our chloroform:ethanol extraction method to be optimal for artemisinin extraction, which has a logP of 2.8. Chloroform has a logP value of ∼2.3, which is also quite closely matched to the calculated logP values of *A. annua* methoxylated flavonoids (2.1–3.4, using structures reported by Ferreira et al., 2010). We compared our 9:1 chloroform:ethanol extraction method used throughout this study with a solvent more typically used for flavonoid extraction (85:15 methanol:water) by extracting WT and homozygous *chi1-1* dry material (**Supplementary Table S4**). The UPLC method was also extended so that the elution conditions at the start of the run were much more aqueous, to ensure that any polar flavonoids (if present) were not eluted in the void volume. Peaks were picked and identified according to our standard high-resolution accurate mass protocols, and additionally matched against formula hits for 40 previously reported flavone and flavonol compounds from *A. annua* (Ferreira et al., 2010). The results show, from dry material, that 142 peaks could be resolved of which only six potential flavonoids could be identified; all six of these compounds were extracted in both solvent systems, and were in fact best extracted in our standard chloroform:ethanol solvent (**Supplementary Table S4**). As expected, highly polar phenolic compounds such as scopolin and scopoletin (PubChem xlogP values of −1.1 and 1.5, respectively) extracted better in the methanolic solvent and could be resolved using the adapted UPLC method. All 40 flavonoids reported by Ferreira et al. (2010) have predicted xlogP values in the range −1.3–3.5, so we would expect to detect these in the modified UPLC method, if present in any of the extracts. From this comparison we conclude that our chloroform:ethanol extraction solvent is sufficient to extract the full suite of flavonoids present in the various *A. annua* genotypes used in the present study, which all derive from the F1 Artemis commercial variety (Delabays et al., 2001) which serves as the wild type in the current study. In a detailed metabolite analysis of high- and low- artemisinin-producing chemotypes of *A. annua,* which involved both MS and NMR based detection and identification we found similarly low numbers of flavonoids (Czechowski et al., 2018). We note that the much larger number of flavonoids reported in the review by Ferreira et al. (2010) are based to an extent on HPLC-UV analysis of *A. annua* material obtained from Yunnan Herbarium, China (Lai et al., 2007). Future work involving comparative metabolite analysis of different cultivars grown under identical conditions should help establish the basis of the difference in the numbers of flavonoids being reported in these different studies.

Finally, artemisinin levels were consistently decreased in all homozygous *chi1-1* leaf material types compared to heterozygous *chi1-1* and the wild type (**Figure 2Avi**). DHAA levels were simultaneously reduced in young leaves of homozygous *chi1-1* when compared to heterozygous *chi1-1* and the wild type (**Supplementary Table S1**). We also observed a mild reduction in the level of dihydroartemisinic acid tertiary allylic hydroperoxide in all leaf types of homozygous *chi1-1* when compared to heterozygous *chi1-1* and the wild type. On the other hand, levels of DHAA-derived 11,13-dihydroamorphanes such as dihydro-epi-deoxy arteannuin B, deoxyartemisinin, arteannuin I/J, arteannuin M/O and 11-hydroxy-arteannuin remained unchanged in homozygous *chi1-1* (**Supplementary Table S1**).

To further confirm the specificity of the effects of the *chi1-1* mutation on trichomes, we analyzed metabolites in trichomes and leaves separately. Fresh mature leaves were dipped in chloroform to disrupt the trichomes and release the contents (dip), as previously described (Graham et al., 2010), and the remaining leaf material was ground, extracted and analyzed separately (ground leaves). Known trichome-specific compounds such as artemisinin, DHAA or camphor were found in extracts from the dip treatment but not in the post-dip ground leaf extracts (**Figures 2Bi,iii** and **Supplementary Table S2**),

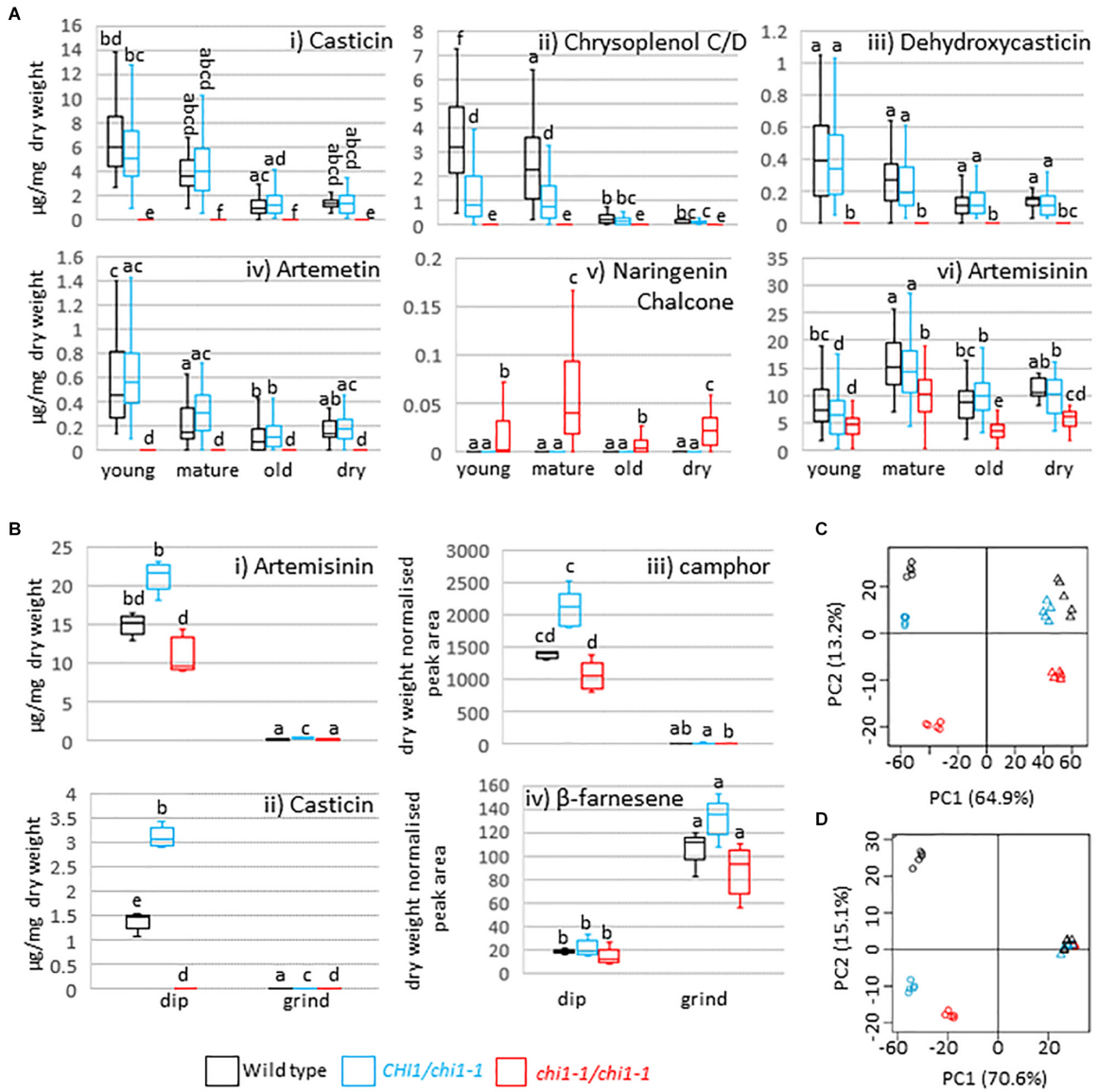

FIGURE 2 | Effects of the *chi1-1* mutation on the metabolite profile of *Artemisia annua*. Box and whisker plots showing levels of **(A)** four major flavonoids, putative naringenin chalcone and artemisinin as measured by UPLC-MS in young (leaves 1–5 as counted from the apical meristem), mature (leaves 11–13), old (three leaves above first senescing leaf) and dry (oven-dried) leaf material harvested from 12 to 14-week-old plants of the *Artemis* wild type (black), heterozygous (blue) and homozygous *chi1-1* mutant (red) and **(B)** selected flavonoids, sesquiterpenes and monoterpenes in the extracts from dipped (dip) or ground leaf material for the wild type (black) and heterozygous (blue) and homozygous (red) *chi1-1* mutant. Metabolite concentrations measured by GC- or UPLC-MS **(A,B)** are expressed as a proportion of the residual dry leaf material following extraction. Groups not sharing letters representing Tukey's range test results indicate statistically significant differences ($p < 0.05$). Each box is represented by minimum of 20 **(A)** or by five **(B)** biological replicates. **(C,D)** Principal component analysis of 83 UPLC-MS identified peaks **(C)** and of 58 GC-MS identified peaks **(D)** from dipped and ground leaf material from wild type (black) and heterozygous (blue) and homozygous *chi1-1* (red). Dip leaf extracts are represented by circles and ground leaf extracts by triangles. Principal component analysis was performed on log-scaled and mean-centered data.

consistent with previous morphological studies (Duke et al., 1994) and the trichome-specific expression of the relevant biosynthetic pathway enzymes (Olsson et al., 2009; Graham et al., 2010; Olofsson et al., 2011; Soetaert et al., 2013). Casticin, chrysoplenol C/D, dehydroxycasticin and artemetin were also found in extracts from dip treatments but not in post-dip ground leaf extracts from heterozygous *chi1-1* or the wild type, but were completely absent in homozygous *chi1-1* dip and post-dip ground leaf extracts (**Figure 2Bii** and **Supplementary Table S2**). β-farnesene, germacrene-D, *trans*-caryophyllene and squalene were found mostly in post-dip ground leaf extracts (**Figure 2Biv** and **Supplementary Tables S2**, **S3**). This is consistent with the previous metabolite studies on gland bearing vs. glandless biotypes of *A. annua*

TABLE 1 | Artemisinin and flavonoid levels and antimalarial efficacy of plant extracts.

	Artemisinin (mg/mL)	Casticin (mg/mL)	Dehydroxycasticin (mg/mL)	Cirsilineol (mg/mL)	Chrysoplenol C (mg/mL)	Artemetin (mg/mL)	Total detected flavonoid (mg/mL)	EC_{50} (ng/mL) [95% CI]
Wild type	5.00 ± 0.80^{b}	0.51 ± 0.07^{c}	0.09 ± 0.01^{c}	0.11 ± 0.04^{b}	0.004 ± 0.003^{a}	0.00^{a}	0.71 ± 0.12^{c}	15.6 [14.5–16.8]
chi1-1 het	5.00 ± 0.28^{b}	0.36 ± 0.02^{b}	0.042 ± 0.009^{b}	0.00^{a}	0.005 ± 0.002^{a}	0.00^{a}	0.40 ± 0.03^{b}	34.6 [31.7–37.9]
chi1-1 hom	5.00 ± 0.44^{b}	0.00^{a}	0.00^{a}	0.00^{a}	0.00^{a}	0.00^{a}	0.00^{a}	25.7 [25.1–26.4]
AMS silenced line	0.062 ± 0.007^{a}	0.50 ± 0.06^{c}	0.021 ± 0.007^{ab}	0.006 ± 0.002^{a}	0.00^{a}	0.12 ± 0.01^{c}	0.65 ± 0.08^{c}	350.4 [303.1–405.1]
cyp71av1-1 het	5.00 ± 0.55^{b}	0.69 ± 0.04^{d}	0.15 ± 0.02^{d}	0.00^{a}	0.074 ± 0.012^{b}	0.00^{a}	0.91 ± 0.05^{d}	14.1 [13.5–14.7]
cyp71av1-1 hom	0.00^{a}	0.61 ± 0.14^{cd}	0.31 ± 0.05^{e}	0.00^{a}	0.00^{a}	0.08 ± 0.01^{b}	1.00 ± 0.19^{d}	4220 [3820–4665]

Mean concentrations and standard deviations from the mean of five technical replicates are shown. Total detected flavonoid is the sum of the five listed flavonoids. Letters represent Tukey's range test results after one way ANOVA for each metabolite or total detected flavonoids. Genotypes not sharing letters indicate statistically significant differences ($p < 0.05$). EC_{50} is the 50% effective concentration of extract needed to inhibit growth of the Plasmodium falciparum parasites. Artemisinin concentrations have been normalized to 5 mg/ml in wild type, chi1-1 het, chi1-1 hom and cyp71av1-1 as detailed in section "Whole-Leaf Extraction for P. falciparum Kill Rate Assays."

(Tellez et al., 1999) and with the ubiquitous expression of the relevant terpene synthases in *A. annua* (Graham et al., 2010; Olofsson et al., 2011). A principal component analysis for 83 of the UPLC-MS (**Figure 2C**) and 58 of the GC-MS (**Figure 2D**) detectable metabolites revealed that homozygous *chi1-1* more strongly diverged from the wild type and heterozygous *chi1-1* in extracts from dip treatment, but less so in post-dip ground leaf extracts, where ground material clustered together. These findings suggested that the *chi1-1* mutant is mainly disrupted in trichome metabolism and that *CHI1* is needed for flavonoid synthesis specifically in trichomes.

Flavonoids Do Not Contribute Antimalarial Activity in Whole-Leaf Extracts

The *chi1-1* line allowed for a direct comparison of *A. annua* extracts with and without flavonoids to evaluate the contribution of the cytocidal effects of these compounds on *Plasmodium* parasites *in vitro*. To evaluate whether there were changes from the potent and rapid cytocidal effects expected from artemisinin-containing extracts, the metabolites from wild type, and heterozygous and homozygous *chi1-1* extracts were quantified and re-suspended to the same artemisinin concentration (**Table 1**). The antiplasmodial activity against asexual intraerythrocytic stages of *P. falciparum* indicated that the effective concentration required to inhibit growth by 50% (EC_{50}) was essentially the same, between 15 and 35 ng/ml for the wild type and heterozygous and homozygous *chi1-1* (**Figure 3A** and **Table 1**). We also performed an evaluation of the initial cytocidal activity of the same extracts using a Bioluminescence Relative Rate of Kill (BRRoK) assay (Ullah et al., 2017). Here, asexual intraerythrocytic stages of *P. falciparum* are exposed to multiples (0.33 to 9X) of EC_{50} of extract, or benchmark antimalarial drugs of a known order of rate of kill, for 6 h. This assay allows a compound/extract to be compared to fast cytocidal drugs like artemisinin, the derivative dihydroartemisinin and chloroquine; slower cytocidal drugs like mefloquine; and cytostatic drugs such as atovaquone (Ullah et al., 2017). When performing BRRoK assays, the three samples were indistinguishable from one another and most similar to dihydroartemisinin (the active metabolite of artemisinin compounds) in the concentration *v.* loss of bioluminescence plot (**Figure 3B**). These results indicate that flavonoids in the wild-type extracts did not alter the fast cytocidal activity of artemisinin in the samples.

Artemisinin-Reduced Whole-Leaf Extracts Lack Potent and Rapid Antiplasmodial Activity

To test for the potential antiplasmodial activity of artemisinin-unrelated compounds in *A. annua*, we used the artemisinin-reduced *AMS* silenced plant line (Catania et al., 2018). Samples from this line were prepared alongside the other genetic variants and re-suspended to match the wild-type casticin levels, which resulted in a 100-fold reduction in artemisinin levels compared to the wild type (**Table 1**). Determination of the EC_{50} in the *AMS* silenced line revealed a greater than 20-fold reduction in potency when compared to the wild-type (**Figure 3A**). Moreover, samples from the *AMS* silenced line in the BRRoK assay lacked the rapid initial cytocidal activity of the wild type and heterozygous and homozygous *chi1-1* samples and were only apparently cytocidal at concentrations above $3xEC_{50}$ (**Figure 3B**).

We also used a *cyp71av1-1* mutant shown to be completely deficient in the synthesis of artemisinin (Czechowski et al., 2016) to investigate potential antiplasmodial effects of flavonoids (and other *A. annua* compounds) in the absence of artemisinin. As a control we used heterozygote *cyp71av1-1* that accumulates wild-type artemisinin levels. In extracts from *cyp71av1-1* antiplasmodial activity was reduced ∼300 fold compared to extracts from heterozygous *cyp71av1-1* (**Figure 3C**). The initial cytocidal activity of the control heterozygote *cyp71av1-1* extracts were comparable to those of the wild type and *chi1-1* extracts, whereas cytocidal activity was reduced in the *cyp71av1-1* mutant (**Figure 3D**). It is noteworthy that extracts from *cyp71av1*-1 homozygous lines are among the highest in total flavonoid content of the material used for anti-plasmodial assays (**Table 1**). Taken together these results represent convincing evidence that *A. annua* flavonoids do not exhibit anti-plasmodial activity in *in vitro* assays. These results also suggest that the sesquiterpene epoxide artennuin X, one of the most abundant metabolites produced by *cyp71av1-1* in the absence of artemisinin

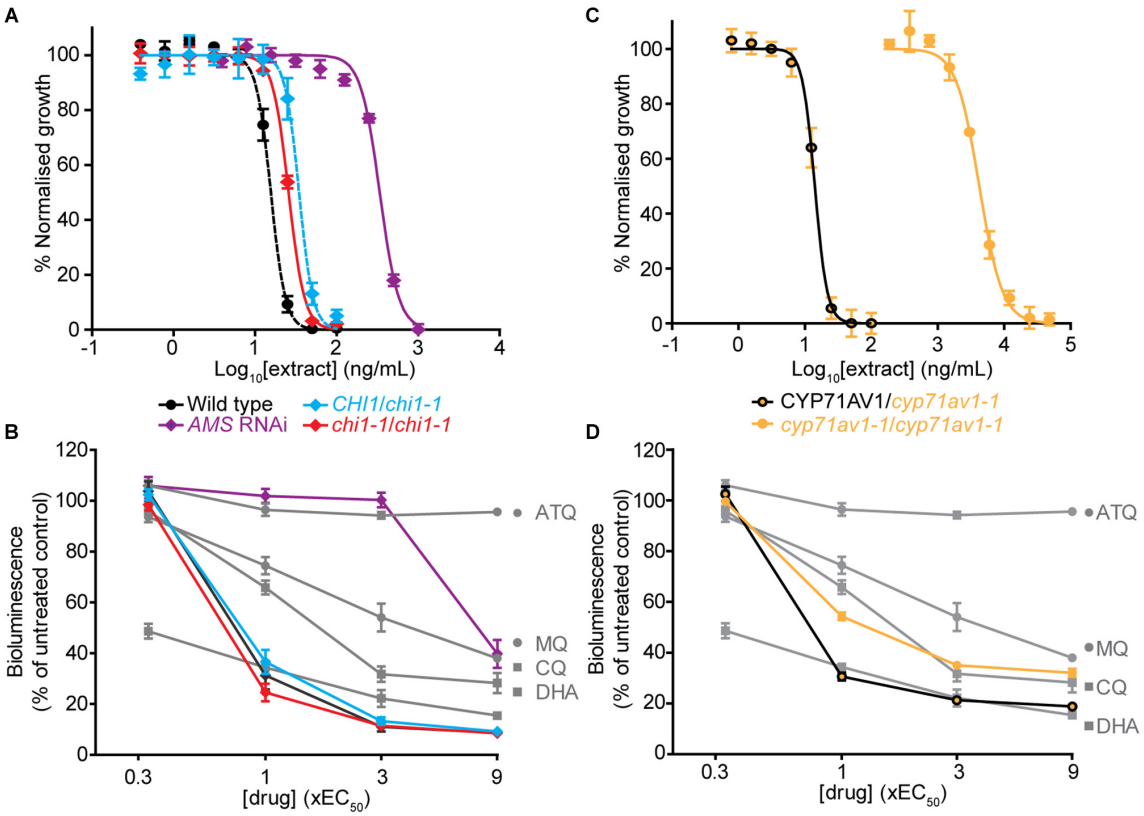

FIGURE 3 | Comparison of *in vitro* antiplasmodial activity of leaf extracts from *Artemisia annua* wild type, mutant and antisense lines with altered flavonoid and artemisinin content. **(A,C)** Log concentration-normalized response curves of *Plasmodium falciparum* parasites after 48 h of treatment with extracts used to determine the EC_{50} (50% effective concentration of extract needed to inhibit growth of the *P. falciparum* parasites) of the indicated extracts. **(B,D)** Bioluminescent Relative Rate of Kill (BRRoK) assays to determine the initial (6 h) cytocidal action, compared to an untreated control after exposure to extracts of wild type, heterozygous and homozygous *chi1-1*, and the *AMS* silenced line **(B)** or heterozygous and homozygous *cyp71av1-1* **(D)** at multiples of the EC_{50} alongside dihydroartemisinin (DHA) > chloroquine (CQ) > mefloquine (MQ) > atovaquone (ATQ) benchmark controls. Error bars represent standard deviations from the means of three biological replicates.

(Czechowski et al., 2016), also does not have appreciable antiplasmodial activity. This is not really surprising as arteannuin X does not carry an endoperoxide bridge (Czechowski et al., 2016), which is thought to be crucial for antiplasmodial activity of sesquiterpene lactones such as artemisinin.

DISCUSSION

CHI1 Is Necessary for Trichome-Specific Flavonoid Synthesis

We report the identification and characterization of an *A. annua* mutant in *CHI1*, which encodes the enzyme that catalyzes the second committed step of the flavonoid biosynthesis pathway. The *chi1-1* mutation is predicted to result in a truncation that would preclude a sizable portion of the CHI1 functional monomer, including sections that may interact with the product naringenin (**Figure 1C** and **Supplementary Figure S1A**). Indeed, *chi1-1* failed to produce all four major polymethoxylated flavonoids, usually detected in young, mature and dry *A. annua* leaves (**Figures 2Ai–iv**). Flavonoid levels in heterozygous *chi1-1* were comparable with wild type (Artemis), which indicates that *chi1-1* is a recessive mutation (**Figures 2Ai–iv**). Expression profiling in various tissues of wild-type *A. annua* demonstrated that *CHI1* seems to be specifically expressed in trichomes (**Figure 1A**). In fact, we showed that the effect of the *chi1-1* mutation on metabolite levels is clearly trichome-specific (**Figures 2B–D** and **Supplementary Table S2**) which is consistent with the *CHI1* expression pattern (**Figure 1A**). The fact that two other *CHI* gene homologs expressed in *A. annua* (*CHI2* and *CHI3*) did not compensate for the lack of flavonoids in trichomes of *chi1-1* strongly suggests that CHI1 is the main enzyme responsible for flavonoid biosynthesis in *A. annua* trichomes.

The precursors of all secondary or specialized metabolites in higher plants are derived from primary metabolism. Phenylpropanoid biosynthesis leading to flavonoids relies on the synthesis of L-phenylalanine from chorismate, sourcing carbon precursors from the pentose phosphate pathway of primary metabolism. Terpenoid biosynthesis on the other hand starts from the common precursors supplied by the plastidic MEP and the cytosolic mevalonate pathways, which both rely on carbon sourced from glycolysis. Crosstalk between the phenylpropanoid

and terpenoid biosynthetic pathways occurs, therefore, at the level of early carbon precursors, such as glyceraldehyde 3-phosphate and acetyl-CoA, and with reducing power provided by NAD(P)H and energy released from ATP hydrolysis. We had therefore speculated that artemisinin biosynthesis may be improved by specific blockage of flavonoid biosynthesis in *A. annua* trichomes, due to more carbon precursors becoming available for farnesyl pyrophosphate biosynthesis. However, we did not observe any increase in levels of artemisinin or related precursors in homozygous *chi1-1* mutants disrupted in flavonoid production (**Figures 2Aiv,Bi**). On the contrary, artemisinin levels in all *chi1-1* leaf ages were lower when compared to heterozygous *chi1-1* and the wild type (**Figures 2Aiv,Bi**). The reduction of artemisinin levels in *chi1-1* might be explained by lower DHAA levels (**Supplementary Table S1**), which could be due to either decreased DHAA synthesis or enhanced DHAA degradation, but the connection to the *chi1-1* mutation is unclear. The crosstalk between phenylpropanoid and terpenoid metabolism is further highlighted by the report that overexpression of the *A. annua CINNAMYL ALCOHOL DEHYDROGENASE* results in an increase in lignin and coumarin and a reduction in artemisinin and other sesquiterpenes (Ma et al., 2018).

Flavonoids Had No Effect on the *in vitro* Antiplasmodial Activity of *A. annua* Extracts

Flavonoids have been suggested as candidates for increasing antiplasmodial activity and potentially slowing the emergence of resistance in whole-plant preparations, relative to artemisinin alone (Weathers et al., 2014; Elfawal et al., 2015). It has been proposed that these attributes may arise due to flavonoids enhancing artemisinin action by increasing artemisinin solubility in water (Mueller et al., 2000) or through the action of some flavonoids, such as casticin, in increasing artemisinin binding to hemin, one potential target of artemisinin action (Bilia et al., 2002). Artemisinin action *in vitro* against intraerythrocytic stages of *P. falciparum* typically provides an EC_{50} of 3–5 nM (Liu et al., 1992; Hasenkamp et al., 2013). Casticin, the most abundant flavonoid in *A. annua*, has an EC_{50} of 65 μM and 5 μM casticin reduced the artemisinin EC_{50} some 3–5 fold (Liu et al., 1992). Artemetin also reduces the artemisinin EC_{50}, although to a lesser degree than casticin (Elford et al., 1987). In another report, the flavonoids artemetin, casticin, chrysoplenetin, chrysosplenol-D, cirsilineol and eupatorin have an IC_{50} that is 100 times that of artemisinin (Liu et al., 1992). When combining 5 μM of these flavonoids with artemisinin, the artemisinin IC_{50} is reduced to as much as half (Liu et al., 1992). However, the interactive mode of action of these compounds is unclear. In an isobologram analysis of compound interactions, casticin has an antagonistic antimalarial activity with artemisinin in a 3:1 combination (Suberu et al., 2013) but is apparently synergistic at a 10–10,000:1 combination (Elford et al., 1987; Liu et al., 1992). Therefore, additional compounds in whole-plant preparations could have synergistic or antagonistic effects with artemisinin depending on the relative concentration in the plant. Results of our *in vitro* antiplasmodial activity assays using *Artemisia* whole-leaf preparations do not show any synergistic effects between flavonoids and artemisinin, in contrast to previous reports (Ferreira et al., 2010; Suberu et al., 2013). We observed no appreciable differences between the artemisinin-producing heterozygous *chi1-1* (flavonoid containing) and homozygous *chi1-1* (flavonoid lacking) in terms of their EC_{50} potency or initial rate of cytocidal activity (**Figure 3B**). We therefore conclude that flavonoids do not appreciably contribute to the *in vitro* antiplasmodial activity beyond that provided by the artemisinin content, at least in the concentrations at which they are present in leaves of Artemis, a commercial F1 hybrid of *A. annua* (Delabays et al., 2001).

The *in vitro* Antimalarial Activity of *A. annua* Extracts Is Predominantly Due to Artemisinin

Several groups have investigated compounds in *A. annua* extracts to find new sources of antimalarial activities other than artemisinin, or explore the possibility that *A. annua* compounds aid artemisinin (O'Neill et al., 1985; Elford et al., 1987; Liu et al., 1989, 1992; Mueller et al., 2000; Bhakuni et al., 2001). *A. annua* compounds having antimalarial activity have been reported but with EC_{50} values that are over three orders of magnitude higher than artemisinin (Suberu et al., 2013). In *in vitro* assays, arteannuin B and artemisinic acid have been shown to have additive antimalarial activity with artemisinin, whereas DHAA has antagonistic antimalarial activity with artemisinin (Suberu et al., 2013). Furthermore, some artemisinin precursors isolated from *A. annua* tea, including 9-epi-artemisinin and artemisitene, while being reported to have antimalarial activity themselves, can act antagonistically with artemisinin, possibly because they could have similar molecular targets in the malarial parasite (Suberu et al., 2013). However, artemisinin related compounds reported to either act by themselves or aid artemisinin are present in *A. annua* at much lower concentrations than required for antimalarial activity based on the EC_{50} (Elford et al., 1987; Bhakuni et al., 2001; Suberu et al., 2013), and therefore would perhaps not be expected to have an effect in whole-leaf extracts.

Our data suggests that the artemisinin-reduced extracts prepared so that they have wild-type casticin levels (**Table 1**), and likely the same concentration of non-artemisinin related compounds as wild-type extracts, had no *in vitro* antiplasmodial activity beyond that provided by the residual artemisinin in the homozygous *chi1-1* extracts (**Figures 3A,B**). We extended our studies to include the use of *cyp71av1-1* mutant extracts, which has been shown to completely lack artemisinin (Czechowski et al., 2016). Whereas the *cyp71av1-1* heterozygote control extract was essentially indistinguishable from those of the wild type and the *chi1-1* homozygote (**Figures 3C,D**), extracts of the *cyp71av1-1* homozygote were some 350–1000 fold less potent in their antiplasmodial activity. Whilst the *cyp71av1-1* homozygote did demonstrate a moderate to good initial cytocidal activity (**Figure 3D**), the BRRoK assay of these extracts used at least 10 times a greater concentration of extract than any other sample by virtue of these assays using multiples of the EC_{50}.

While our results clearly demonstrate that flavonoids from *A. annua* plant extracts do not play a role in enhancing antiplasmodial activity relative to artemisinin in *in vitro* assays, the possibility remains that these compounds could have *in vivo* effects (Elfawal et al., 2012, 2015). It has been postulated that flavonoids could increase artemisinin solubility or inhibit activity of the cytochrome P450s responsible for degradation of artemisinin (Elfawal et al., 2012). *A. annua* extracts have been shown to result in higher artemisinin concentration in mice blood than the same concentration of artemisinin alone and this effect was attributed to arteannuin B (Cai et al., 2017). However, it should be noted that artemisinin is known to dissolve poorly in water and has a short serum half-life (Elfawal et al., 2012). Consequently, artemisinin is typically chemically converted to dihydroartemisinin, artesunate or artemether to improve solubility and increase its half-life in human serum (Petersen et al., 2011). These improved artemisinin-based compounds are combined with a companion drug from a different class to formulate ACTs - the WHO recommended method of treatment for patients with malaria. Companion drugs include lumefantrine, mefloquine, amodiaquine, sulfadoxine/pyrimethamine, piperaquine and chlorproguanil/dapsone. This combination contributes to high efficacy, fast action and reduction in the likelihood of resistance developing for ACTs. *In vivo* investigations into the effectiveness of whole plant extracts for the treatment of malaria should use approved artemisinin-related compounds with improved solubility and lifetime in human serum or indeed ACTs, rather than artemisinin alone, as a proper comparator in studies to investigate the potential of whole-leaf extracts from *A. annua*. We conclude that endogenous flavonoids present in whole-leaf extracts of *A. annua* have no appreciable effect on the antimalarial activity of artemisinin as determined by quantitative *in vitro* assays.

DATA AVAILABILITY

All datasets generated for this study are included in the manuscript and/or the **Supplementary Files**.

AUTHOR CONTRIBUTIONS

TC, MR, DR, TW, TL, PH, and IG conceived and designed the research. TC, MR, DR, TW, DH, MF, and MV performed the experiments. TC, MR, TL, MF, MV, PH, and IG analyzed the data. TC, MR, PH, and IG wrote the manuscript.

FUNDING

We acknowledge financial support for this project from The Bill and Melinda Gates Foundation (grant number OPGH5210) as well as from The Garfield Weston Foundation. This work was also supported by Tertiary Education Trust Fund, Nigeria (to MF) and a British Society for Antimicrobial Chemotherapy Vacation Scholarship (to MV).

ACKNOWLEDGMENTS

We thank A. Fenwick for the assistance in horticulture, C. Calvert for the help in project management, and X. Simonnet and Médiplant for providing access to the Artemis variety.

SUPPLEMENTARY MATERIAL

The Supplementary Material for this article can be found online at: https://www.frontiersin.org/articles/10.3389/fpls.2019.00984/full#supplementary-material

REFERENCES

Bhakuni, R. S., Jain, D. C., Sharma, R. P., and Kumar, S. (2001). Secondary metabolites of *Artemisia annua* and their biological activity. *Curr. Sci.* 80, 35–48.

Bilia, A. R., Lazari, D., Messori, L., Taglioli, V., Temperini, C., and Vincieri, F. F. (2002). Simple and rapid physico-chemical methods to examine action of antimalarial drugs with hemin: its application to *Artemisia annua* constituents. *Life Sci.* 70, 769–778. doi: 10.1016/s0024-3205(01)01447-3

Brown, G. D. (2010). The biosynthesis of artemisinin (Qinghaosu) and the phytochemistry of *Artemisia annua* L. (Qinghao). *Molecules* 15, 7603–7698. doi: 10.3390/molecules15117603

Cai, T. Y., Zhang, Y. R., Ji, J. B., and Xing, J. (2017). Investigation of the component in *Artemisia annua* L. leading to enhanced antiplasmodial potency of artemisinin via regulation of its metabolism. *J. Ethnopharmacol.* 207, 86–91. doi: 10.1016/j.jep.2017.06.025

Catania, T. M., Branigan, C., Stawniak, N., Hodson, J., Harvey, D., Larson, T. R., et al. (2018). Silencing amorpha-4,11-diene synthase genes in *Artemisia annua* leads to FPP accumulation with little effect on endogenous terpenes. *Front. Plant Sci.* 29:547. doi: 10.3389/fpls.2018.00547

Cubukcu, B., Bray, D. H., Warhurst, D. C., Mericli, A. H., Ozhatay, N., and Sariyar, G. (1990). *In vitro* antimalarial activity of crude extracts and compounds from *Artemisia abrotanum* L. *Phytother. Res.* 4, 203–204. doi: 10.1002/ptr.2650040510

Czechowski, T., Larson, T. R., Catania, T. M., Harvey, D., Brown, G. D., and Graham, I. A. (2016). *Artemisia annua* mutant impaired in artemisinin synthesis demonstrates importance of nonenzymatic conversion in terpenoid metabolism. *Proc. Natl. Acad. Sci. U.S.A.* 113, 15150–15155. doi: 10.1073/pnas.1611567113

Czechowski, T., Larson, T. R., Catania, T. M., Harvey, D., Wei, C., Essome, M., et al. (2018). Detailed phytochemical analysis of high- and low artemisinin-producing chemotypes of *Artemisia annua*. *Front. Plant Sci.* 9:641. doi: 10.3389/fpls.2018.00641

Daddy, N. B., Kalisya, L. M., Bagire, P. G., Watt, R. L., Towler, M. J., and Weathers, P. J. (2017). *Artemisia annua* dried leaf tablets treated malaria resistant to ACT and i.v. artesunate: case reports. *Phytomedicine* 32, 37–40. doi: 10.1016/j.phymed.2017.04.006

Delabays, N., Simonnet, X., and Gaudin, M. (2001). The genetics of artemisinin content in *Artemisia annua* L. and the breeding of high yielding cultivars. *Curr. Med. Chem.* 8, 1795–1801. doi: 10.2174/0929867013371635

Duke, M. V., Paul, R. N., Elsohly, H. N., Sturtz, G., and Duke, S. O. (1994). Localization of artemisinin and artemisitene in foliar tissues of glanded and glandless biotypes of *Artemisia annua* L. *Int. J. Plant Sci.* 155, 365–372. doi: 10.1086/297173

Elfawal, M. A., Towler, M. J., Reich, N. G., Golenbock, D., Weathers, P. J., and Rich, S. M. (2012). Dried whole plant *Artemisia annua* as an antimalarial therapy. *PLoS One* 7:e52746. doi: 10.1371/journal.pone.0052746

Elfawal, M. A., Towler, M. J., Reich, N. G., Weathers, P. J., and Rich, S. M. (2015). Dried whole-plant *Artemisia annua* slows evolution of malaria drug resistance

and overcomes resistance to artemisinin. *Proc. Natl. Acad. Sci. U.S.A.* 112, 821–826. doi: 10.1073/pnas.1413127112

Elford, B. C., Roberts, M. F., Phillipson, J. D., and Wilson, R. J. (1987). Potentiation of the antimalarial activity of qinghaosu by methoxylated flavones. *Trans. R. Soc. Trop. Med. Hyg.* 81, 434–436. doi: 10.1016/0035-9203(87)90161-1

Ferreira, J. F., Luthria, D. L., Sasaki, T., and Heyerick, A. (2010). Flavonoids from *Artemisia annua* L. as antioxidants and their potential synergism with artemisinin against malaria and cancer. *Molecules* 15, 3135–3170. doi: 10.3390/molecules15053135

Graham, I. A., Besser, K., Blumer, S., Branigan, C. A., Czechowski, T., Elias, L., et al. (2010). The genetic map of *Artemisia annua* L. identifies loci affecting yield of the antimalarial drug artemisinin. *Science* 327, 328–331. doi: 10.1126/science.1182612

Hasenkamp, S., Merrick, C. J., and Horrocks, P. (2013). A quantitative analysis of *Plasmodium falciparum* transfection using DNA-loaded erythrocytes. *Mol. Biochem. Parasitol.* 187, 117–120. doi: 10.1016/j.molbiopara.2013.01.001

Itoh, Y., Higeta, D., Suzuki, A., Yoshida, H., and Ozeki, Y. (2002). Excision of transposable elements from the chalcone isomerase and dihydroflavonol 4-reductase genes may contribute to the variegation of the yellow-flowered carnation (*Dianthus caryophyllus*). *Plant Cell Physiol.* 43, 578–585. doi: 10.1093/pcp/pcf065

Jez, J. M., Bowman, M. E., Dixon, R. A., and Noel, J. P. (2000). Structure and mechanism of the evolutionarily unique plant enzyme chalcone isomerase. *Nat. Struct. Biol.* 7, 786–791. doi: 10.1038/79025

Kim, S., Jones, R., Yoo, K. S., and Pike, L. M. (2004). Gold color in onions (*Allium cepa*): a natural mutation of the chalcone isomerase gene resulting in a premature stop codon. *Mol. Genet. Genomics* 272, 411–419. doi: 10.1007/s00438-004-1076-7

Kraft, C., Jenett-Siems, K., Siems, K., Jakupovic, J., Mavi, S., Bienzle, U., et al. (2003). *In vitro* antiplasmodial evaluation of medicinal plants from Zimbabwe. *Phytother. Res.* 17, 123–128. doi: 10.1002/ptr.1066

Lai, J.-P., Lim, Y. H., Su, J., Shen, H.-M., and Ong, C. N. (2007). Identification and characterization of major flavonoids and caffeoylquinic acids in three compositae plants by LC/DAD-APCI/MS. *J. Chrom. B.* 848, 215–225. doi: 10.1016/j.jchromb.2006.10.028

Lange, B. M. (2015). The evolution of plant secretory structures and emergence of terpenoid chemical diversity. *Annu. Rev. Plant Biol.* 66, 139–159. doi: 10.1146/annurev-arplant-043014-114639

Liu, K. C., Yang, S. L., Roberts, M. F., Elford, B. C., and Phillipson, J. D. (1992). Antimalarial activity of *Artemisia annua* flavonoids from whole plants and cell cultures. *Plant Cell Rep.* 11, 637–640. doi: 10.1007/BF00236389

Liu, K. C. S., Yang, S. L., Roberts, M. F., Elford, B. C., and Phillipson, J. D. (1989). The contribution of flavonoids to the antimalarial activity of *Artemisia annua*. *Planta Med.* 55, 654–655. doi: 10.1055/s-2006-962242

Ma, D., Xu, C., Alejos-Gonzalez, F., Wang, H., Yang, J., Judd, R., et al. (2018). Overexpression of *Artemisia annua* cinnamyl alcohol dehydrogenase increases lignin and coumarin and reduces artemisinin and other sesquiterpenes. *Front. Plant Sci.* 19:828. doi: 10.3389/fpls.2018.00828

Mueller, M. S., Karhagomba, I. B., Hirt, H. M., and Wemakor, E. (2000). The potential of *Artemisia annua* L. as a locally produced remedy for malaria in the tropics: agricultural, chemical and clinical aspects. *J. Ethnopharmacol.* 73, 487–493. doi: 10.1016/S0378-8741(00)00289-0

Muir, S. R., Collins, G. J., Robinson, S., Hughes, S., Bovy, A., Ric De Vos, C. H., et al. (2001). Overexpression of petunia chalcone isomerase in tomato results in fruit containing increased levels of flavonols. *Nat. Biotechnol.* 19, 470–474. doi: 10.1038/88150

Nishihara, M., Nakatsuka, T., and Yamamura, S. (2005). Flavonoid components and flower color change in transgenic tobacco plants by suppression of chalcone isomerase gene. *FEBS Lett.* 579, 6074–6078. doi: 10.1016/j.febslet.2005.09.073

Olofsson, L., Engström, A., Lundgren, A., and Brodelius, P. E. (2011). Relative expression of genes of terpene metabolism in different tissues of *Artemisia annua* L. *BMC Plant Biol.* 11:45. doi: 10.1186/1471-2229-11-45

Olsson, M. E., Olofsson, L. M., Lindahl, A. L., Lundgren, A., Brodelius, M., and Brodelius, P. E. (2009). Localization of enzymes of artemisinin biosynthesis to the apical cells of glandular secretory trichomes of *Artemisia annua* L. *Phytochemistry* 70, 1123–1128. doi: 10.1016/j.phytochem.2009.07.009

O'Neill, M. J., Bray, D. H., Boardman, P., Phillipson, J. D., and Warhurst, D. C. (1985). Plants as sources of antimalarial drugs part. 1. *In vitro* test method for the evaluation of crude extracts from plants. *Planta Med.* 51, 394–398. doi: 10.1055/s-2007-969529

Peplow, M. (2016). Synthetic biology's first malaria drug meets market resistance. *Nature* 530, 389–390. doi: 10.1038/530390a

Petersen, I., Eastman, R., and Lanzer, M. (2011). Drug-resistant malaria: molecular mechanisms and implications for public health. *FEBS Lett.* 585, 1551–1562. doi: 10.1016/j.febslet.2011.04.042

Shirley, B. W., Hanley, S., and Goodman, H. M. (1992). Effects of ionizing radiation on a plant genome: analysis of two Arabidopsis transparent testa mutations. *Plant Cell* 4, 333–347. doi: 10.1105/tpc.4.3.333

Smilkstein, M., Sriwilaijaroen, N., Kelly, J. X., Wilairat, P., and Riscoe, M. (2004). Simple and inexpensive fluorescence-based technique for high-throughput antimalarial drug screening. *Antimicrob. Agents Chemother.* 48, 1803–1806. doi: 10.1128/aac.48.5.1803-1806.2004

Soetaert, S. S., Van Neste, C. M., Vandewoestyne, M. L., Head, S. R., Goossens, A., Van Nieuwerburgh, F. C., et al. (2013). Differential transcriptome analysis of glandular and filamentous trichomes in *Artemisia annua*. *BMC Plant Biol.* 13:220. doi: 10.1186/1471-2229-13-220

Suberu, J. O., Gorka, A. P., Jacobs, L., Roepe, P. D., Sullivan, N., Barker, G. C., et al. (2013). Anti-plasmodial polyvalent interactions in *Artemisia annua* L. aqueous extract – possible synergistic and resistance mechanisms. *PLoS One* 8:e80790. doi: 10.1371/journal.pone.0080790

Tellez, M. R., Canel, C., Rimando, A. M., and Duke, S. O. (1999). Differential accumulation of isoprenoids in glanded and glandless *Artemisia annua* L. *Phytochemistry* 52, 1035–1040. doi: 10.1016/s0031-9422(99)00308-8

Till, B. J., Zerr, T., Comai, L., and Henikoff, S. (2006). A protocol for TILLING and ecotilling in plants and animals. *Nat. Protoc.* 1, 2465–2477. doi: 10.1038/nprot.2006.329

Townsend, T., Segura, V., Chigeza, G., Penfield, T., Rae, A., Harvey, D., et al. (2013). The use of combining ability analysis to identify elite parents for *Artemisia annua* F1 hybrid production. *PLoS One* 8:e61989. doi: 10.1371/journal.pone.0061989

Ullah, I., Sharma, R., Biagini, G. A., and Horrocks, P. (2017). A validated bioluminescence-based assay for the rapid determination of the initial rate of kill for discovery antimalarials. *J. Antimicrob. Chemother.* 72, 717–726. doi: 10.1093/jac/dkw449

van Tunen, A. J., Mur, L. A., Recourt, K., Gerats, A. G., and Mol, J. N. (1991). Regulation and manipulation of flavonoid gene expression in anthers of petunia: the molecular basis of the Po mutation. *Plant Cell* 3, 39–48. doi: 10.1105/tpc.3.1.39

Ververidis, F., Trantas, E., Douglas, C., Vollmer, G., Kretzschmar, G., and Panopoulos, N. (2007). Biotechnology of flavonoids and other phenylpropanoid-derived natural products. Part I: chemical diversity, impacts on plant biology and human health. *Biotechnol. J.* 2, 1214–1234. doi: 10.1002/biot.200700084

Weathers, P. J., Towler, M., Hassanali, A., Lutgen, P., and Engeu, P. O. (2014). Dried-leaf *Artemisia annua*: a practical malaria therapeutic for developing countries? *World J. Pharmacol.* 3, 39–55.

World Health Organization [WHO] (2018). *World Malaria Report 2018*. Geneva: World Health Organization.

Wong, E. H., Hasenkamp, S., and Horrocks, P. (2011). Analysis of the molecular mechanisms governing the stage-specific expression of a prototypical housekeeping gene during intraerythrocytic development of *P. falciparum*. *J. Mol. Biol.* 408, 205–221. doi: 10.1016/j.jmb.2011.02.043

Yang, J., Yan, R., Roy, A., Xu, D., Poisson, J. and Zhang, Y. (2015). The I-TASSER Suite: protein structure and function prediction. *Nat. Methods* 12, 7–8. doi: 10.1038/nmeth.3213

Conflict of Interest Statement: The authors declare that the research was conducted in the absence of any commercial or financial relationships that could be construed as a potential conflict of interest.

frontiers in Plant Science

ORIGINAL RESEARCH
published: 26 June 2020
doi: 10.3389/fpls.2020.00950

AaABCG40 Enhances Artemisinin Content and Modulates Drought Tolerance in *Artemisia annua*

*Xueqing Fu, Hang Liu, Danial Hassani, Bowen Peng, Xin Yan, Yuting Wang, Chen Wang, Ling Li, Pin Liu, Qifang Pan, Jingya Zhao, Hongmei Qian, Xiaofen Sun and Kexuan Tang**

Joint International Research Laboratory of Metabolic & Developmental Sciences, Key Laboratory of Urban Agriculture (South) Ministry of Agriculture, Plant Biotechnology Research Center, Fudan-SJTU-Nottingham Plant Biotechnology R&D Center, Shanghai Jiao Tong University, Shanghai, China

The phytohormone Abscisic acid (ABA) regulates plant growth, development, and responses to abiotic stresses, including senescence, seed germination, cold stress and drought. Several kinds of researches indicate that exogenous ABA can enhance artemisinin content in *A. annua*. Some transcription factors related to ABA signaling are identified to increase artemisinin accumulation through activating the artemisinin synthase genes. However, no prior study on ABA transporter has been performed in *A. annua*. Here, we identified a pleiotropic drug resistance (PDR) transporter gene *AaPDR4/AaABCG40* from *A. annua*. *AaABCG40* was expressed mainly in roots, leaves, buds, and trichomes. GUS activity is primarily observed in roots and the vascular tissues of young leaves in *proAaABCG40*: *GUS* transgenic *A. annua* plants. When *AaABCG40* was transferred into yeast AD12345678, yeasts expressing *AaABCG40* accumulated more ABA than the control. The *AaABCG40* overexpressing plants showed higher artemisinin content and stronger drought tolerance. Besides, the expression of *CYP71AV1* in OE-*AaABCG40* plants showed more sensitivity to exogenous ABA than that in both wild-type and i*AaABCG40* plants. According to these results, they strongly suggest that AaABCG40 is involved in ABA transport in *A. annua*.

Keywords: *Artemisia annua*, artemisinin, pleiotropic drug resistance (PDR) transporter, drought tolerance, abscisic acid

OPEN ACCESS

Edited by:
Tomasz Czechowski, University of York, United Kingdom

Reviewed by:
Lei Zhang, Second Military Medical University, China
Yi Shang, Yunnan Normal University, China

***Correspondence:**
Kexuan Tang
kxtang@sjtu.edu.cn

Specialty section:
This article was submitted to Plant Biotechnology, a section of the journal Frontiers in Plant Science

Received: *20 February 2020*
Accepted: *10 June 2020*
Published: *26 June 2020*

Citation:
Fu X, Liu H, Hassani D, Peng B, Yan X, Wang Y, Wang C, Li L, Liu P, Pan Q, Zhao J, Qian H, Sun X and Tang K (2020) AaABCG40 Enhances Artemisinin Content and Modulates Drought Tolerance in Artemisia annua. Front. Plant Sci. 11:950. doi: 10.3389/fpls.2020.00950

INTRODUCTION

Artemisinin, isolated from the traditional Chinese medicine *A. annua*, is extensively used for the treatment of malaria (Weathers et al., 2006). Artemisinin Combination Therapies (ACTs) are presently recommended by WHO (World Health Organization) as the preferred drug to fight the malaria (World Health Organization, 2017). Considerable effort has been expended to determine the artemisinin biosynthetic pathway (**Figure S1**). The mevalonate (MVA) pathway and the methylerythritol phosphate (MEP) pathway produce the precursors isopentenyl diphosphate (IPP) and its isomer dimethylallyl diphosphate (DMAPP) (Vranová et al., 2013). Farnesyl diphosphate synthase (FPS) catalyzes IPP and DMAPP to synthesize farnesyl diphosphate (FPP) (Schramek et al., 2010). After that, amorpha-4, 11-diene synthase (ADS) catalyzes the cyclization

reaction using FPP as the substrate to synthesize amorpha-4, 11-diene (Bouwmeester et al., 1999; Mercke et al., 2000). Then amorpha-4, 11-diene is oxidized to artemisinic alcohol, and further catalyzed into artemisinic aldehyde by the cytochrome P450 monooxygenase (CYP71AV1) (Ro et al., 2006; Teoh et al., 2006). Artemisinic aldehyde D11 (13) reductase (DBR2) catalyzes artemisinic aldehyde to form dihydroartemisinic aldehyde (Zhang et al., 2008). Then dihydroartemisinic aldehyde is converted into the direct precursor of artemisinin, dihydroartemisinic acid (DHAA), catalyzed by aldehyde dehydrogenase (ALDH1) (Teoh et al., 2009). Subsequently, artemisinin is synthesized *via* a nonenzymatic reaction (Brown and Sy, 2004). Alternatively, CYP71AV1 and ALDH1 catalyze the artemisinic aldehyde to form artemisinic acid (Ro et al., 2006; Teoh et al., 2009). Artemisinic acid synthesized arteannuin B *via* a nonenzymatic photo-oxidized reaction (Brown and Sy, 2007). In addition, artemisinin biosynthesis occurs in the glandular trichomes of *A. annua*, containing two stalk, two basal, and three pairs of secretory cells (Duke and Paul, 1993; Olsson et al., 2009).

The limited supply of artemisinin which is due to its low content (0.1%-1.0% dry weight) in *A. annua* has urged its production improvement through developing a new kind of *A. annua* plant with higher content of artemisinin (Tang et al., 2014). It is well-known that the artemisinin content is enhanced by the treatment of exogenous ABA (Abscisic acid) in *A. annua* (Jing et al., 2009). The phytohormone ABA is a phytohormone with the sesquiterpene structure, that plays important roles in several biological processes, such as senescence, seed germination, and root elongation, as well as responses to cold stress, drought and salt (Finkelstein et al., 2002; Zhu, 2002; De Smet et al., 2006; Bi et al., 2017; Sun et al., 2018). More studies showed that ABA was mainly synthesized in leaves (Hartung et al., 2002). McAdam et al. propose that the decline in leaf water status causes ABA biosynthesis, that regulates the stomatal closure. Then ABA is transported from the leaves to the roots to promote root growth (McAdam et al., 2016a; McAdam et al., 2016b). The biosynthesis of ABA was also autonomously occurred in guard cells and triggered stomatal closure (Endo et al., 2008; Bauer et al., 2013). In the past several decades, research on ABA has focused on the mechanism of ABA regulating artemisinin biosynthesis in *A. annua* (Zhang et al., 2013; Zhang et al., 2015; Zhong et al., 2018). Several studies indicated that ABA transporter is crucial for the ABA function (Taylor et al., 2000; Boursiac et al., 2013; Zhang et al., 2014). However, the molecular basis of ABA transport is currently unknown in *A. annua*.

Several ABA transporters in plants have been recently reported, some of which belong to ATP-binding-cassette (ABC) transporter family. ABC transporters are one of the biggest protein families in plants, which act as ATP-driven transporters for a wide range of substrates, including terpenoids, lipids, vitamins, organic acids, and ions (Theodoulou, 2000; Lee et al., 2005; Sugiyama et al., 2006; Kang et al., 2010; Fu et al., 2017). In plants, ABC transporters are divided into eight subfamilies (Verrier et al., 2008). In particular, the pleiotropic drug resistance (PDR) transporters are the essential branch of the ABCG subfamily (Rea, 2007). In *Arabidopsis*, AtPDR12/AtABCG40, a member of PDR subfamily of ABC transporters, mediated cellular ABA uptake and involved in the detoxification of Pb^{2+} (Lee et al., 2005; Kang et al., 2010). Subsequently, *AtABCG25* was isolated from *Arabidopsis* and encoded an ABCG subfamily transporter. These results suggested that AtABCG25 functioned as an exporter of ABA and also controlled the intercellular ABA signaling in *Arabidopsis* (Kuromori et al., 2010). AtABCG22, an ABCG transporter closely related to AtABCG25, was identified to be associated with stomatal regulation in *Arabidopsis* and considered as a candidate ABA transporter, the functions of which have not been demonstrated in the ABA signaling and biosynthesis pathways (Kuromori et al., 2011). In the process of ABA signaling, AtABCG25 acts as a mediator in exporting ABA from vascular tissues, while AtPDR12/AtABCG40 plays a role in importing ABA into guard cells (Kang et al., 2010; Kuromori et al., 2010). Simultaneously, *AtDTX50* encoded a Multidrug and Toxic Compound Extrusion (MATE) protein, which was identified and found to be expressed in both guard cells and vascular tissues of *Arabidopsis thaliana*. When *AtDTX50* was expressed in both *Escherichia coli* and *Xenopus oocyte*, it functioned as an ABA efflux transporter (Zhang et al., 2014). In addition, the function of an NRT1.2 in the nitrate transporter (AIT1) as a regulator is to control the ABA pool size at the primary site of ABA synthesis (Kanno et al., 2012). Here, we report that a PDR transporter AaPDR4/AaABCG40 was cloned from *A. annua*. AaABCG40 was involved in ABA transport. Overexpressing *AaABCG40* could enhance artemisinin content and drought tolerance.

EXPERIMENTAL PROCEDURES

Plant Materials

A. annua seeds (Huhao 1) obtained from Chongqing province, were developed by our group in Shanghai. Plants were grown under a 16/8 h light/dark photoperiod at 25°C in the greenhouse. Tobacco (*Nicotiana benthamiana*) was grown under the same conditions as *A. annua* (Shen et al., 2016).

Isolation and Characterization of *AaABCG40*

ABC transporter proteins were identified by using the HMM model (PF00005.27) from Pfam (http://pfam.xfam.org/) for searching against *A. annua* protein databases and reduced sequence redundancy by CD-HIT (Shen et al., 2018). *A. annua* ABC transporters were analyzed using the Conserved Domain Database (CDD) (Çakır and Kılıçkaya, 2013). The phylogenetic tree analysis was performed using MEGA7 *via* the neighbor-joining method, and the bootstrap analysis was performed using 1000 replicates (Kumar et al., 2016). The ABC transporter protein sequences from *A. annua* were aligned with ClustalX. The Heatmap was generated using the MultiExperiment Viewer (MeV). The full-length of *AaABCG40* sequence was predicted from the *A. annua* genome database. 500 ng total RNA isolated from the leaves of *A. annua* was used to synthesize cDNA, and

the full-length of *AaABCG40* was amplified using the specific primers (**Table S1**).

Real-Time Quantitative PCR

To check the expression level of the putative genes, total RNA was extracted using the RNeasy Kit (Qiagen, Germany). Fresh leaves, roots, and aerial tissues of 5-month-old *A. annua* were collected at various developmental stages and grounded to powder in liquid nitrogen with mortar and pestle (Fu et al., 2017). Before cDNA synthesis, DNase (DNase I Kit, Takara, Japan) treatment was applied to digest the genomic DNA. Subsequently, cDNA was reverse transcribed using a reverse transcription kit (Promega, USA). RT-qPCR was carried out using the Roche Lightcycler ® 96 (Roche, Mannheim, Germany) with Fast Start Universal SYBR Green Master Mix (Roche Diagnostics, Germany) as described previously (He et al., 2017). qRT-PCR was performed in three independent experimental replicates. Calculation of the relative expression level was performed using the $2^{-\Delta\Delta ct}$ method (Livak and Schmittgen, 2001). **Table S1** summarizes the primers.

Construction and Transformation of *A. annua*

To construct the RNAi lines, the 300 bp non-conservative domain coding sequence of *AaABCG40* cDNA was cloned in pENTR gateway cloning vector and further inserted into pHELLSGATE12 *via* LR recombination reaction (Invitrogen, Carlsbad, CA, USA). Alternatively, the *AaABCG40* open reading frame was inserted into pHB-GFP overexpression vector. Both overexpressed and knocked down vectors were transformed into *A. annua* using *Agrobacterium*-mediated transformation (*Agrobacterium tumefaciens* strain EHA105). Empty pHB-GFP and pHELLSGATE12 were used as negative controls. After 3-4 months the transgenic lines were shifted to pots and transferred to the greenhouse.

Subcellular Localization of AaABCG40

The recombinant plasmid (pHB-*AaABCG40-GFP*) was transferred into *A. tumefaciens* strain GV3101 for *Nicotiana benthamiana* leaves transient expression (Voinnet et al., 2003). The fusion protein AaABCG40-GFP and PIP1-mCherry protein locate at the plasma membrane were injected into tobacco leaf together to confirm the localization of AaABCG40 (Siefritz et al., 2002). After 2-3 days, the GFP fluorescence could be observed using Leica TCS SP5-II confocal laser microscopy (Leica, Wetzlar, Germany).

Molecular Cloning of *AaABCG40* Promoter and Promoter-GUS Fusions in Transgenic *A. annua*

The promoter of *AaABCG40* was predicted from *A. annua* genomic databases (Shen et al., 2018). The promoter region of *AaABCG40* was amplified with *AaABCG40*-specific primers using the genomic DNA of the *A. annua* leaves as the template (**Table S1**). The promoter region was amplified containing *Pst*I and *BamH*I restriction sites and inserted into pCAMBIA1391Z vector. Subsequently, the recombinant plasmid (pCAMBIA1391Z-proAaABCG40-GUS) was transferred into *A. tumefaciens* strain EHA105 for the plant transformation. All the primers mentioned in this experiment are listed in **Table S1**. Histochemical staining for GUS activity in transgenic plants was performed according to previous protocol (Jefferson, 1987).

Artemisinin Content Analysis by HPLC-ELSD

To measure the artemisinin content of both overexpressed and RNAi line, fresh leaves were collected and stored at 45°C for 48 h, dried leaves were powdered, and 0.1 g/sample was extracted twice with 1 ml methanol and disrupted by an ultrasonic processor (Shanghai Zhisun Instrument Co. Ltd model JYD-650) at 40°C and 55 Hz for 30 min. Centrifuging at 12,000 rpm for 10 min, the supernatant was collected and moved to a new 2 ml tube. The above steps were carried out one more time to maximize the total extraction. The samples were then passed through a nitrocellulose 0.25 μm pore size Sartorious ® membrane. The samples were then injected into a Waters Alliance 2695 HPLC system coupled with a Waters 2420 ELSD detector (Milford, MA, USA) using pure artemisinin as standard (sigma). The HPLC condition was as described previously (Chen et al., 2012). Three biological repeats were applied for each sample.

Measurement of ABA Concentration

The ABA concentration was measured using a Phytodetek ABA enzyme immunoassay test kit (Elisa, Agdia, Elkhart, USA). Fresh leaves were ground into powder in liquid nitrogen. Then 100 mg powder of each sample was extracted with 8 ml solution (80% methanol, 100 mg/L butylated hydroxytoluene, and 0.5 g/L citric acid monohydrate), and stirred overnight at 4°C in the dark. The culture was centrifuged at 12,000 rpm for 10 min at 4°C. Subsequently, the supernatant was collected in a new tube and dried. The residue was dissolved in 100 μl methanol and 900 μl of TBS buffer (50 mM Tris, 0.1 mM $MgCl_2{\cdot}6H_2O$, 0.15 M NaCl, pH 7.8) and analyzed as described previously (Zhang et al., 2014).

Functional Analysis of AaABCG40 in Yeast Cells

The CDS of *AaABCG40* was inserted into the *Spel*I and *Pst*I sites of pDR196. *AtPDR12* was cloned and inserted into the *Spel*I and *Pst*I sites of pDR196 vector as the positive control. The recombinant plasmids (pDR196-AaABCG40 and pDR196-AtPDR12) were respectively introduced into the strain AD12345678 using the lithium acetate method. The yeast transformant was incubated in 50 ml Synthetic Dextrose (SD) medium (-uracil) at 29°C with shaking at 180 rpm until OD_{600} reached at 1.0, subsequently suspended using 50 ml half-strength SD medium (-uracil) containing 50 μM ABA (Sigma-Aldrich). The cells were cultivated with shaking at 180 rpm at 29°C and collected by centrifuging at the indicated times, respectively. The cells were washed twice using the sterilized water, and followed by disrupted in methanol for 15 min at 30 Hz using acid-washed

glass beads (Yu and De Luca, 2013). The supernatants were collected and filtered for ABA contents analysis. Three biological repeats were applied for each sample.

Abscisic Acid Treatment and Drought Treatment

For hormone treatments, 100 μM ABA was used, whereas water with 1% of ethanol was used as a mock treatment. The cutting seedlings of OE-*AaABCG40* transgenic plants, i*AaABCG40* transgenic plants, and wild-type *A. annua* plants were sprayed with 100 ml ABA (100 μM), respectively, followed by sampling at 0, 1, 3, 6, 9, and 12 h for RNA extraction to analyze the gene expression. Two-month-old cutting seedlings of OE-*AaABCG40* transgenic plants, i*AaABCG40* transgenic plants, and wild-type *A. annua* plants were cultivated in pots and watered well in the growth chamber under a 16-h light/8-h dark cycle at 25°C for a week. Then the water supply was absolutely stopped. For drought treatment, water was withheld for a period of 14 days. After 14 days, the condition of all the plants was observed and recorded. The water loss was performed according to previous study (Zhang et al., 2014).

RESULTS

Isolation and Characterization of *AaABCG40*

ABA treatment enhanced the artemisinin content through increasing the expression of artemisinin biosynthetic genes (Jing et al., 2009). In Arabidopsis, ABA transporter AtPDR12, belonging to PDR subfamily, was strongly expressed in root (Kang et al., 2010). Therefore, we want to clone and identify ABA transporter. We identified 93 ABC transporter proteins from *A. annua* by HMM research using Pfam mold (PF00005.27). Then these sequences of ABC proteins were analyzed using the Conserved Domain Database of NCBI. Identified ABC transports were aligned using ClustalW program, and the phylogenetic analysis was generated to classify them into different subfamilies. Eight PDR transporters were screened from *A. annua* (**Figure S2**). The Heatmap analysis showed that a PDR transporter gene (Aannua00284S063360) was predominately expressed in root (**Figure S3**). Therefore, this PDR transporter was further examined as the candidate transporter, that might be involved in ABA transport. The full-length cDNA of Aannua00284S063360 was cloned and assigned as *AaPDR4/AaABCG40*. *AaABCG40* is 4299 bp and encodes a protein of 1432 amino acids. The phylogenetic tree analysis with AaABCG40 and other PDR transporters, including *Arabidopsis* PDR transporters, AaPDR3, NpPDR1, NtPDR1, and SpTUR2 was performed, showing that AaABCG40 was similar to that of PDR proteins (AtPDR12, AaPDR3, NpPDR1, NtPDR1, and SpTUR2) involved in terpene transport (Van Den Brûle et al., 2002; Stukkens et al., 2005; Kang et al., 2010; Crouzet et al., 2013; Fu et al., 2017) (**Figure 1A**). AaABCG40 belongs to the full-length size PDR subfamily and contains two nucleotide-binding domains (NBD) and two transmembrane domains (TMD) (**Figure 1B**). Compared to the conserved domain of known PDR transporters involved in terpene transport, it exhibited the high conservation in plants (**Figure 1C**).

Expression Patterns of *AaABCG40* Gene in *A. annua*

To analyze the expression pattern of *AaABCG40*, the different tissues were collected for RNA extraction from *A. annua*. RT-qPCR results showed that *AaABCG40* highly expressed in both trichomes and roots, and poorly in old leaves (**Figure 1D**). Subsequently, the *AaABCG40* expression patterns in leaves at different developmental stages were analyzed. The highest expression level in the youngest leaf (leaf 0) was observed, following a rapid reduction with the leaves aging (**Figure 1E**).

To further analyze the expression pattern of *AaABCG40* in *A. annua,* the predicted promoter sequence from the genome database was cloned and inserted into the vector pCAMBIA1391Z carrying *GUS* reporter gene. The recombinant plasmid was further introduced into *A. annua* plants. The GUS staining was mainly active in the vascular tissues of leaves and roots in transgenic plants, following with high expression in trichomes (**Figure 2**). Similarly, GUS staining was primarily restricted to the hypocotyls, roots, and vascular veins of leaves in the *pAtABCG25-GUS* transgenic plants (Kuromori et al., 2010). It was also observed that the GUS signals of the *pAtABCG40-GUS* transgenic plants was predominantly active in roots and the leaves of young plantlets (Kang et al., 2010).

AaABCG40 Was a Plasma Membrane-Localized Protein

To determine the subcellular localization of AaABCG40 protein, we performed a construct that produced the green fluorescent protein (GFP) fused to the C-terminal domain of AaABCG40 under control of the CaMV35S promoter. Subsequently, the *AaABCG40-GFP* recombinant plasmid was transiently co-expressed in tobacco leaves together with the reported plasma membrane marker PIP1 (Siefritz et al., 2002). Subcellular localization of the AaABCG40-GFP fusion protein was observed in plasma membrane with PIP1-mCherry (**Figure 3**). The results showed that AaABCG40 was a plasma membrane-localized protein, implying that AaABCG40 functioned as a transport through the cellular membrane.

Overexpression of *AaABCG40* Increases Artemisinin Biosynthesis

To further explore the function of AaABCG40, 35S::*AaABCG40* transgenic *A. annua* lines were generated. In the *AaABCG40*-overexpressing transgenic plants, the transcript levels of *AaABCG40* were markedly increased to 2.6-4.7 folds compared with the WT (**Figure 4A**). Therefore, we selected three independent lines for further analysis. The artemisinin content was measured from three independent transgenic plants by HPLC. According to our data, 35S:: *AaABCG40* transgenic *A. annua* lines tested produced about 1.54-2.03-fold artemisinin content than the control (**Figure 4B**). RT-qPCR results showed that the expression of the artemisinin biosynthetic enzyme genes *ADS*, *CYP71AV1*, *DBR2,* and *ALDH1* was increased to 2.3-2.5-,

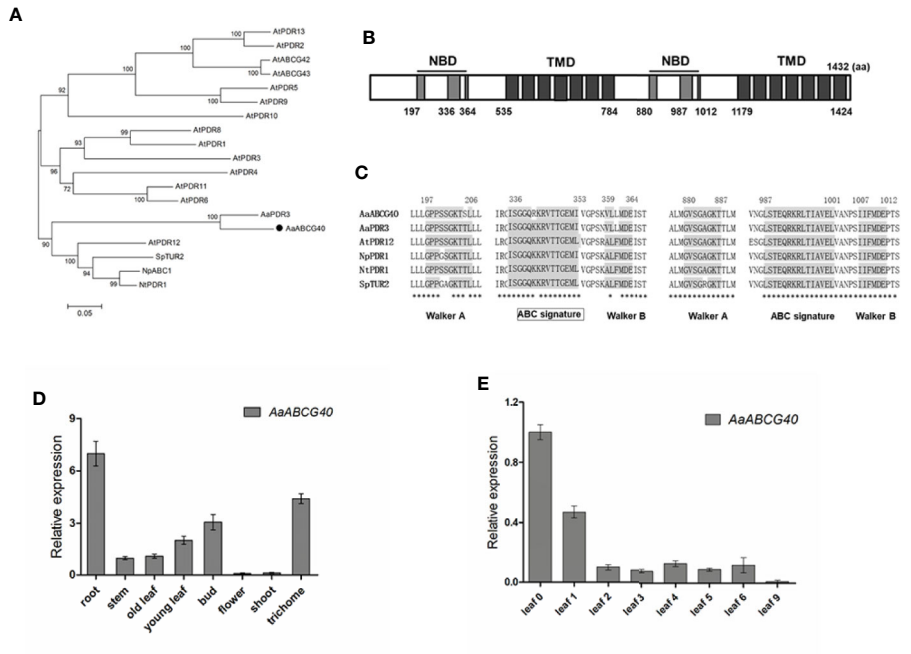

FIGURE 1 | Sequence analysis of AaABCG40. **(A)** Phylogenetic analysis of AaABCG40 from *A. annua* and some known PDR transporters from *Arabidopsis*, *A. annua* AaPDR3, *N. plumbaginifolia* NpPDR1, *N. tabacum* NtPDR1, and *S. polyrrhiza* SpTUR2. The tree presented here is a neighbor-joining tree based on amino acid sequence alignment. **(B)** The structure of AaABCG40 was predicted by scanning the deduced amino acid sequence. NBD and TMD indicate the predicted location of NBDs and TMDs, respectively. **(C)** Multiple alignment of the conserved domain of known PDR transporters involved in terpene transport has the high conservation in plants. The Walker A, Walker B and ABC signature motifs are shown with shading. The identical amino acid residues in are marked by asterisks. **(D)** Relative expression of *AaABCG40* in root, stem, old leaf, young leaf, bud, flower, shoot and trichome. **(E)** Relative expression of *AaABCG40* in leaves of different developmental ages of *A. annua*. *ACTIN* was used as internal control. The error bars represent the means ± SD (standard deviation) from three biological replicates.

2.8-4.6-, 1.9-2.9-, and 2.2-3.5-fold in *OE-AaABCG40*-2, 11, 26 transgenic plants, respectively (**Figure 4C**).

To further analyze the function of AaABCG40, we downregulated the *AaABCG40* expression in *A. annua*. Investigation of *AaABCG40* transcript levels by RT-qPCR showed that the *AaABCG40* expression was significantly decreased in *AaABCG40*-RNAi lines. Three independent transgenic lines (i*AaABCG40*-12, 13, 23) exhibiting a 54%-68% reduction of *AaABCG40* transcript levels were chosen for the further experiments (**Figure 4D**). In order to analyze whether other ABCG genes are affected or not, the expression levels of ABCG transporter genes from *A. annua*, which have high homology with *AaABCG40*, were analyzed by qRT-PCR. These results showed that the expression of ABCG subfamily genes of the transgenic plants had no significant difference with those of both wild type and empty vector plants (**Figure S4**). The content of artemisinin was slightly decreased, and the lowest artemisinin content was merely decreased by 17.4% of the control (**Figure 4E**). RT-qPCR results showed the transcript levels of *CYP71AV1* and *DBR2* were generally reduced to 44%-80% and 76%-77% of the control, while the transcript levels of *ADS* and *ALDH1* were not significantly downregulated (**Figure 4F**). Taken together, these data demonstrated that the change of the substrate content transported by AaABCG40 enhanced the artemisinin accumulation through activating the expression of the artemisinin synthase genes in *A. annua*.

AaABCG40 Was an ABA Influx in Yeast Strain AD1-8

In higher plants, ABA is synthesized in leaves, and accumulated in guard cells and vascular tissues, which is then transported to other tissues (Cheng et al., 2002; Koiwai et al., 2004; Endo et al., 2008). In *Arabidopsis*, AtABCG40/AtPDR12 localized at plasma membrane was identified to function as ABA transporter (Kang et al., 2010). AaABCG40 cloned from *A. annua* had the closest evolutionary relationship to AtPDR12, and also the similar expression pattern with AtPDR12, which suggested that AaABCG40 might have a similar function in *A. annua*. Besides, ABA treatment enhanced the artemisinin accumulation through activating the expression of the synthase genes in artemisinin biosynthesis (Jing et al., 2009). Therefore, we expressed *AaABCG40* cDNA in a heterologous system, the yeast mutant strain AD12345678 (Decottignies et al., 1998). The recombinant plasmid (pDR196-AtPDR12) was introduced into the strain AD12345678 as the positive control. The

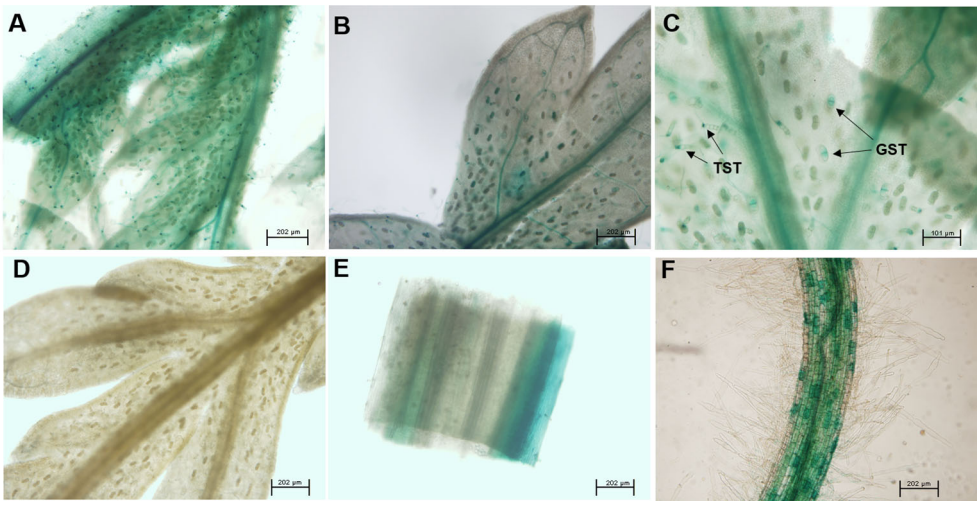

FIGURE 2 | *AaABCG40* is mainly expressed in trichomes and roots. The expression of the *pro AaABCG40*-GUS was observed in **(A)** the first leaf, **(B)** the second leaf, **(C)** trichomes and vascular tissue of young leaf, **(D)** the ninth leaf, **(E)** stem and **(F)** the lateral root. GST: glandular secretory trichome; TST, T-shaped trichome.

yeast cells of *AaABCG40* transformant, *AtPDR12* transformant and the control (transformed with the empty vector pDR196) were incubated in half-strength SD medium containing 50 μM ABA, respectively, and the intracellular contents were determined. Yeast-expressing *AaABCG40* exhibited higher ABA content, with 1.7-4.8 folds of that detected in the control at the same time point (**Figure 5**). And the positive control (*AtPDR12* transformant) also accumulated more ABA than that of empty vector control (**Figure 5**). The yeast cells expressing *AaABCG40* showed more efficiency in ABA uptake and took up ABA faster than the control. These results indicate that AaABCG40 was an ABA transporter in yeast.

Overexpression of AaABCG40 and Its Effects on ABA Regulating the Artemisinin Biosynthesis

In *A. annua*, the artemisinin content was enhanced with ABA treatment through promoting the expression level of the artemisinin biosynthetic genes (Jing et al., 2009). Great progress has been made to reveal the molecular mechanism on ABA regulation of the artemisinin biosynthesis. Previously,

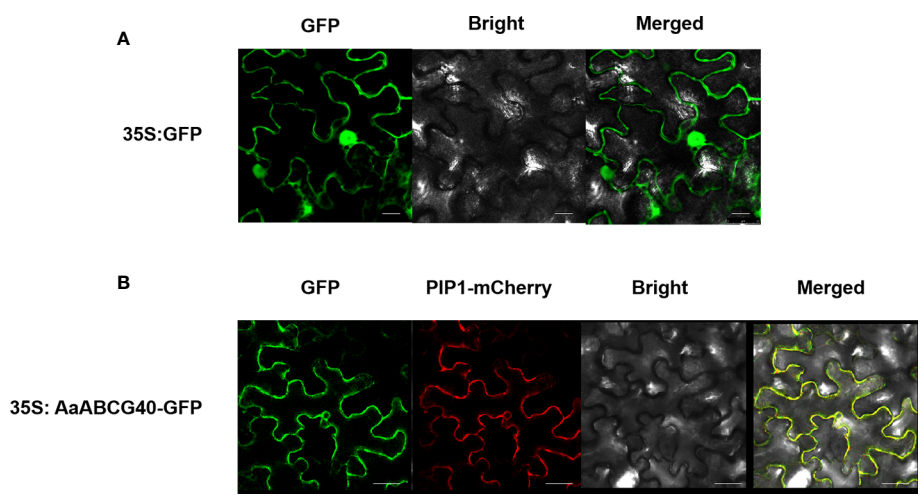

FIGURE 3 | The subcellular localization of AaABCG40. **(A)** Localization of 35S: GFP in tobacco leaves. **(B)** AaABCG40 protein co-localized with plasma membrane integral protein PIP1 on the plasma membrane of tobacco leaves determined through confocal microscopy. Bars = 40 μm.

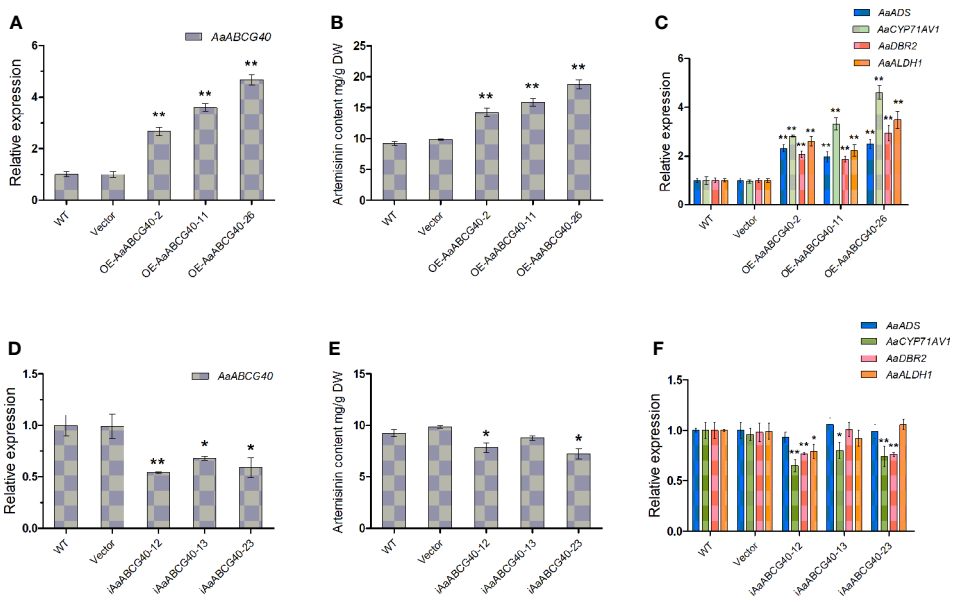

FIGURE 4 | Comparative analyses of *AaABCG40* gene expression and artemisinin analyses in wild type (WT), plants transformed with the empty vector (EV), *AaABCG40*-overexpression and *AaABCG40*-RNAi plants. **(A)** Relative expression of *AaABCG40* in WT, EV and *AaABCG40*-overexpression transgenic *A. annua* lines. **(B)** The contents of artemisinin in WT, EV, and *AaABCG40*-overexpression transgenic *A. annua* lines. **(C)** Relative expression of *AaADS*, *AaCYP71AV1*, *AaDBR2,* and *AaALDH1* in WT, EV and *AaABCG40*-overexpression transgenic *A. annua* lines. **(D)** Relative expression of *AaABCG40* in WT, EV, and *AaABCG40*-RNAi transgenic *A. annua* lines. **(E)** The contents of artemisinin in WT, EV, and *AaABCG40*-RNAi transgenic *A. annua* lines. **(F)** Relative expression of *AaADS*, *AaCYP71AV1*, *AaDBR2,* and *AaALDH1* in WT, EV, and *AaABCG40*-RNAi transgenic *A. annua* lines. All data represent the means ± SD of three replicates. **P < 0.05, *P < 0.01, student's *t*-test.

AabZIP1 was identified from *A. annua* and proved to activate *ADS* and *CYP71AV1* expressions by binding to their promoters (Zhang et al., 2015). In addition, AaABF3 was reported to positively regulate the artemisinin biosynthesis through directly binding to *ALDH1* promoter (Zhong et al., 2018). To further identify the function of AaABCG40 in *A. annua*, the OE-*AaABCG40*-26, *iAaABCG40*-12 and wild type cutting seedlings were prepared to be treated by exogenous ABA. Subsequently, the transcription level of *CYP71AV1* was measured by RT-qPCR. The results showed that the transcription level of *CYP71AV1* increased rapidly after the ABA treatment and peaked at 6 h, the expression of *CYP71AV1* in wild type increased 1.83-fold (**Figure S5**). The *CYP71AV1* transcription level in OE-*AaABCG40*-26 increased 2.27-fold at 6 h, while the *CYP71AV1* transcription level in i*AaABCG40-12* increased 1.58-fold at 6 h (**Figure S5**), suggesting that *CYP71AV1* in OE-*AaABCG40* plants showed more sensitive to exogenously ABA than that in both wild-type and *iAaABCG40* plants. Taken together, AaABCG40 might be involved in ABA transport in *A. annua*.

AaABCG40-Overexpression Plants Showed More Tolerant to Drought in *A. annua*

The phytohormone ABA participates in many physiological processes, such as photosynthesis, abiotic stress, seed germination and stomatal regulation (Savouré et al., 1997; Zhou et al., 2006; Cutler et al., 2010; Kim et al., 2012). In particular, drought improves ABA biosynthesis and results in the closure of stomata in plants (Zhang et al., 2001; Shinozaki and Yamaguchi-shinozaki, 2007). As described above, AaABCG40 functioned as ABA importer might be involved in drought-stress response in *A. annua*. We prepared the OE-*AaABCG40*-26, *iAaABCG40*-12 and wild type cutting seedlings to test the ability of tolerance to drought. We found that leaves of the OE-*AaABCG40* plant wilted more slowly than those of the control under drought stress (**Figure 6**). And *iAaABCG40*-12 transgenic plants exhibited more rapid wilting than those of the control (**Figure S6**). Taken together, these results indicated that overexpression of *AaABCG40* significantly improved drought tolerance in *A. annua*.

DISCUSSION

AaABCG40 Was Involved in ABA Transport

ABA plays an important role in responses to environmental changes, such as drought stress, the regulation of stomatal guard-cell and seed germination. In plants, ABA is predominantly synthesized in vascular tissues, and delivered to the stomatal guard-cell (Hartung et al., 2002; Koiwai et al., 2004; Weathers et al., 2006; Endo et al., 2008). Many molecules involved in ABA transport have been identified. In *Arabidopsis*, pleiotropic drug resistance transporter PDR12 (AtPDR12)/AtABCG40 was reported to act as ABA importer (Kang et al., 2010). AtPDR12

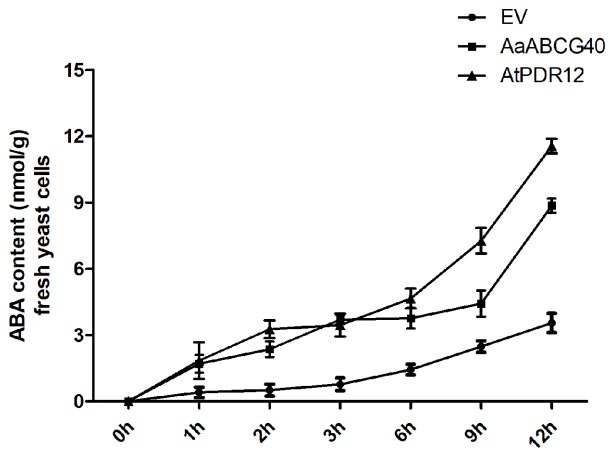

FIGURE 5 | Time-dependent uptake of ABA by AD1-8 yeast cells expressing *AaABCG40* and transformed with the empty vector (EV). Yeast was incubated in half-strength SD medium containing 50 μM ABA at pH 5.9. The error bars represent the means ± SD from three biological replicates. The recombinant plasmid (pDR196-AtPDR12) was introduced into the strain AD12345678 as the positive control.

was mainly expressed in the young leaves, and also in primary and lateral roots. When *AtABCG40* was expressed in both YMM12 yeast and tobacco BY2 cells, the results indicated that AtABCG40 functioned as ABA transporter. Besides, *atabcg40* mutants wilted faster than those of control and exhibited a strongly delayed response to ABA.

Here, we characterized a PDR transporter AaPDR4/AaABCG40 from *A. annua*. RT-qPCR showed that *AaABCG40* was mainly expressed in trichomes, young leaves and roots (**Figure 1D**). Notably, the GUS staining also exhibited that AaABCG40 was active in the vascular tissues of leaves, trichomes, stems, and roots (**Figure 2**). Interestingly, ABA is predominantly produced in the vascular tissues (Cheng et al., 2002; Koiwai et al., 2004; Endo et al., 2008). If AaABCG40 acted as a carrier for the delivery of ABA into cells, it would be localized to plasma membrane in plants. AaABCG40 fused GFP protein was localized to plasma membrane with the marker protein in tobacco (**Figure 3**), indicating that AaABCG40 had the ability to transport ABA into the cells. In conclusion, we hypothesis that AaABCG40 located at the plasma membrane is important factor in the ABA transport. A heterologous yeast expression system is a useful method for identifying the function of transporters (Morita et al., 2009; Yu and De Luca, 2013; Fu et al., 2017). To assess whether AaABCG40 functions as an ABA transporter or not, *AaABCG40* cDNA was expressed in the yeast strain AD12345678. The results showed that yeast expressing AaABCG40 consistently accumulated more ABA than controls containing the empty vector along the same time course (**Figure 5**). In addition, when OE-*AaABCG40*-26, *iAaABCG40*-12 and wild type cutting seedlings were treated by exogenous ABA, OE-*AaABCG40* plant showed more sensitive to exogenously ABA (**Figure 4**). Besides, we analyzed ABA content in the transgenic lines using an ABA ELISA kit. The results revealed that leaves of *AaABCG40*-overexpression transgenic *A. annua* plants contained a higher level of ABA than wild type (**Figure S7**). On the contrary, ABA content in leaves of *AaABCG40*-RNAi transgenic *A. annua* plants was reduced, compared with wild type (**Figure S7**).

In our investigation, these data preferentially suggest that AaABCG40 would be involved in ABA transport based on four findings: *i*) the amino acid sequence of AaABCG40 belonging to the full-length size PDR subfamily, contains two NBDs (nucleotide-binding domains) and two TMDs (transmembrane domains) (**Figure 1B**), *ii*) AaABCG40 is localized to plasma membrane and active in trichomes, the vascular tissues of leaves and roots, where ABA is mainly biosynthesized (**Figures 2** and **3**), *iii*) when *AaABCG40* was transferred into yeast AD1-8, yeast expressing *AaABCG40* could accumulate ABA faster than controls containing the empty vector (**Figure 5**), *iiii*) the *AaABCG40*-overexpression transgenic plant showed a higher expression of *CYP71AV1* with the exogenous ABA treatment (**Figure S5**). Taken together, these results indicated that AaABCG40 was involved in ABA transport.

Effects of AaABCG40 on ABA Regulating the Artemisinin Biosynthesis

To identify the function of AaABCG40, we generated *AaABCG40*-RNAi and *AaABCG40*-overexpression transgenic *A. annua* plants. The artemisinin contents of the leaves in *AaABCG40* overexpressing and *AaABCG40* RNAi transgenic lines measured by HPLC were significantly higher and lower, respectively, than that of wild type plants (**Figures 4B, E**). As we know, exogenous ABA treatment enhances artemisinin accumulation in *A. annua* (Jing et al., 2009). Overexpression of an ABA receptor gene *AaPYL9* also observably enhanced the artemisinin production in *A. annua* (Zhang et al., 2013). Besides, AabZIP1 and AaABF3 involved in ABA signaling were reported to positively regulate the artemisinin biosynthesis. Overexpression of *AabZIP1* and *AaABF3* respectively increased the artemisinin contents, while reducing the expression of *AabZIP1* and *AaABF3* respectively resulted in a decrease in artemisinin contents (Zhang et al., 2015; Zhong et al., 2018). We analyzed the expression level of *AabZIP1* and *AaABF3* in *AaABCG40*-RNAi and *AaABCG40*-overexpression transgenic *A. annua* plants. The results showed that the expression of both *AaZIP1* and *AaABF3* were reduced in *AaABCG40* RNAi lines, while overexpressing *AaABCG40* significantly increased the transcript levels of *AaZIP1* and *AaABF3* in *AaABCG40*-overexpression transgenic lines (**Figure S8**). RT-qPCR analysis also showed that the expressions of *ADS*, *CYP71AV1*, *DBR2,* and *ALDH1* were increased in *AaABCG40*-overexpression transgenic lines (**Figure 4C**). And we also noticed that the transcript level of *ADS* and *ALDH1* were not downregulated in *AaABCG40*-RNAi transgenic lines (**Figure 4F**). In plants, several ABA transporters are synergistically responsible for ABA transport. ABA content in leaves of *AaABCG40*-RNAi transgenic *A. annua* plants was slightly lower than that in the wild type plants. Moreover, the artemisinin biosynthesis has the very complex regulatory

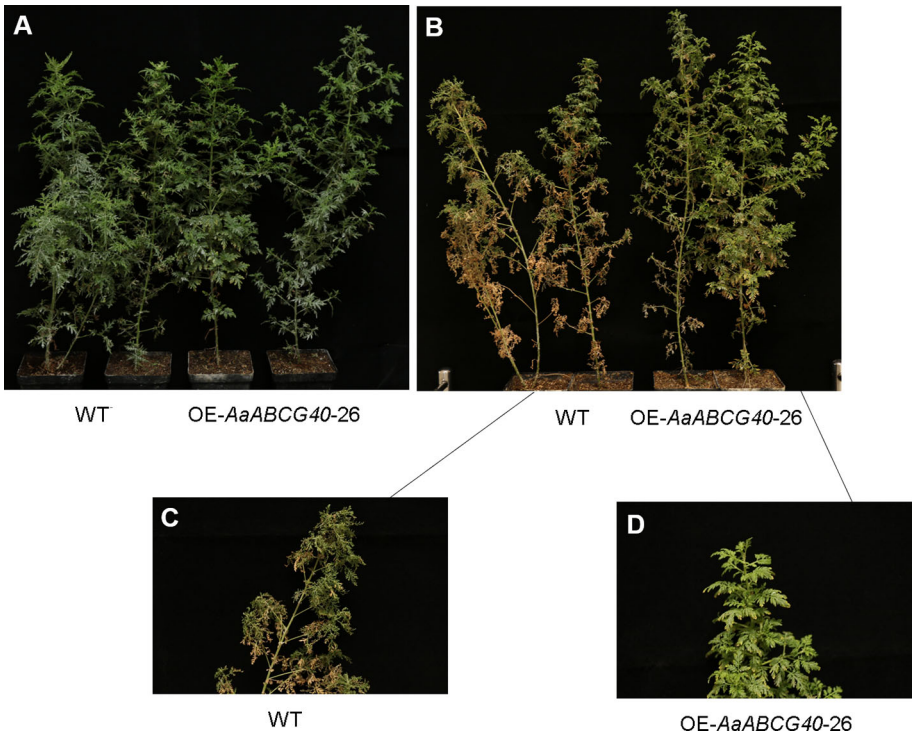

FIGURE 6 | *AaABCG40*-overexpression transgenic *A. annua* showed better tolerance under drought stress. **(A)** Two-month-old cutting seedlings of OE-*AaABCG40* transgenic plants and wild-type *A. annua* plants were cultivated in pots and watered well in the growth chamber under a 16-h light/8-h dark cycle at 25°C for a week. **(B)** Water was withheld for 14 days. **(C)** Wild-type *A. annua* plant was cultivated after water supply was absolutely stopped for 14 days. **(D)** OE-*AaABCG40* transgenic plant was cultivated after water supply was absolutely stopped for 14 days.

network. Previous research indicated that both biotic factors and abiotic factors observably influence the artemisinin biosynthesis in *A. annua*. According to these results, we speculated that overexpressing *AaABCG40* increased ABA accumulation, which activated the expression of the transcription factor genes in ABA signaling pathway to promote the artemisinin biosynthesis in *AaABCG40*-overexpression transgenic lines.

AaABCG40 Modulates Drought Tolerance

ABA is rapidly accumulated when plants are exposed to drought stress (Leung and Giraudat, 1998). If AaABCG40 functioned as ABA importer, AaABCG40 would be involved in drought-stress response in plants. We detected the ability of drought resistance using OE-*AaABCG40*-26, *iAaABCG40*-12, and wild type cutting seedlings. As expected, the leaves of OE-*AaABCG40*-26 seedlings wilted more slowly than those of wild type (**Figure 6**). In addition, the next generation of *iAaABCG40-12* and OE-*AaABCG40*-26 transgenic plants were analyzed the ability of drought resistance and the water loss. The seeds of *iAaABCG40-12,* OE-*AaABCG40-26* transgenic plant and wild-type *A. annua* plants were cultivated in pots and watered well in the growth chamber under a 16-h light/8-h dark cycle at 25°C for 1 month. Then the water supply was absolutely stopped. For drought treatment, water was withheld for a period of 20 days. As **Figure S9** shown, the seedlings of OE-*AaABCG40*-26 transgenic plants wilted more slowly and also lost water more slowly than wild type and *iAaABCG40-12* seedlings. These results suggested that the leaves of OE- *AaABCG40*-26 seedlings accumulated more ABA than those of wild type, and repression the expression of *AaABCG40* impaired the ability of rapid response to drought stress.

DATA AVAILABILITY STATEMENT

All datasets generated for this study are included in the article/ **Supplementary Material**. Accession Numbers: AaABCG40 (KR559559.1), AaPDR3 (KR153482), AtPDR12 (NM_001332173.1), AtPDR13 (NM_001341001.1), NpPDR1 (Q949G3.1), NtPDR1 (Q76CU2.1), SpTUR2 (O24367.1).

AUTHOR CONTRIBUTIONS

XF and KT designed the research. XF and HL performed the experiments. XF, DH, BP, XY, and YW carried out vector construct, expression analysis, transgene plant generation,

subcellular localization and yeast assay. XF and KT drafted the manuscript. CW, PL, QP, JZ, HQ, and XS revised the manuscript. All authors contributed to the article and approved the submitted version.

FUNDING

This research was supported by the National Science Foundation of China (18Z103150043); China Postdoctoral Science Funding (2018M630435).

ACKNOWLEDGMENTS

We thank Masakazu Niimi (Otago University, New Zealand), André Goffeau (Université Catholique de Louvain, Belgium), and Mohan Gupta (Chicago University, USA) for providing the yeast AD12345678 strain. No conflict of interest declared.

SUPPLEMENTARY MATERIAL

The Supplementary Material for this article can be found online at: https://www.frontiersin.org/articles/10.3389/fpls.2020.00950/full#supplementary-material

REFERENCES

Bauer, H., Ache, P., Lautner, S., Fromm, J., Hartung, W., Al-Rasheid, K. A. S., et al. (2013). The stomatal response to reduced relative humidity requires guard cell-autonomous ABA synthesis. *Curr. Biol.* 23, 53–57. doi: 10.1016/j.cub.2012.11.022

Bi, B., Tang, J., Han, S., Guo, J., and Miao, Y. (2017). Sinapic acid or its derivatives interfere with abscisic acid homeostasis during *Arabidopsis thaliana* seed germination. *BMC Plant Biol.* 17 (1), 99. doi: 10.1186/s12870-017-1048-9

Boursiac, Y., Léran, S., Corratgé-Faillie, C., Gojon, A., Krouk, G., and Lacombe, B. (2013). ABA transport and transporters. *Trends Plant Sci.* 18, 325–333. doi: 10.1016/j.tplants.2013.01.007

Bouwmeester, H. J., Wallaart, T. E., Janssen, M. H., van Loo, B., Jansen, B. J., Posthumus, M. A., et al. (1999). Amorpha-4, 11-diene synthase catalyses the first probable step in artemisinin biosynthesis. *Phytochemistry* 52, 843–854. doi: 10.1016/s0031-9422(99)00206-x

Brown, G. D., and Sy, L.-K. (2004). In vivo transformations of dihydroartemisinic acid in *Artemisia annua* plants. *Tetrahedron* 60, 1139–1159. doi: 10.1016/j.tet.2003.11.070

Brown, G. D., and Sy, L.-K. (2007). In vivo transformations of artemisinic acid in *Artemisia annua* plants. *Tetrahedron* 63, 9548–9566. doi: 10.1016/j.tet.2007.06.062

Çakır, B., and Kılıçkaya, O. (2013). Whole-genome survey of the putative atp-binding cassette transporter family genes in *Vitis vinifera*. *PloS One* 8, e78860. doi: 10.1371/journal.pone.0078860

Chen, Y. F., Shen, Q., Wang, Y. Y., Wang, T., Wu, S. Y., Zhang, L., et al. (2012). The stacked over-expression of *FPS*, *CYP71AV1* and *CPR* genes leads to the increase of artemisinin level in *Artemisia annua* L. *Plant Biotechnol. Rep.* 7, 287–295. doi: 10.1007/s11816-012-0262-z

Cheng, W. H., Endo, A., Zhou, L., Penney, J., Chen, H. C., Arroyo, A., et al. (2002). A unique short-chain dehydrogenase/reductase in *Arabidopsis* glucose signaling and abscisic acid biosynthesis and functions. *Plant Cell* 14, 2723–2743. doi: 10.1105/tpc.006494

Crouzet, J., Roland, J., Peeters, E., Trombik, T., Ducos, E., Nader, J., et al. (2013). NtPDR1, a plasma membrane ABC transporter from *Nicotiana tabacum*, is involved in diterpene transport. *Plant Mol. Biol.* 82, 181–192. doi: 10.1007/s11103-013-0053-0

Cutler, S. R., Rodriguez, P. L., Finkelstein, R. R., and Abrams, S. R. (2010). Abscisic acid: emergence of a core signaling network. *Annu. Rev. Plant Biol.* 61, 651–679. doi: 10.1146/annurev-arplant-042809-112122

De Smet, I., Zhang, H., Inzé, D., and Beeckman, T. (2006). A novel role for abscisic acid emerges from underground. *Trends Plant Sci.* 11, 434–439. doi: 10.1016/j.tplants.2006.07.003

Decottignies, A., Grant, A. M., Nichols, J. W., de Wet, H., McIntosh, D. B., and Goffeau, A. (1998). ATPase and multidrug transport activities of the overexpressed yeast ABC protein *Yor1p*. *J. Biol. Chem.* 273, 12612–12622. doi: 10.1074/jbc.273.20.12612

Duke, S. O., and Paul, R. N. (1993). Development and fine structure of the glandular trichomes of *Artemisia annua* L. *Int. J. Plant Sci.* 154, 107–118. doi: 10.1086/297096

Endo, A., Sawada, Y., Takahashi, H., Okamoto, M., Ikegami, K., Koiwai, H., et al. (2008). Drought induction of Arabidopsis 9-cis-epoxycarotenoid dioxygenase occurs in vascular parenchyma cells. *Plant Physiol.* 147, 1984–1993. doi: 10.1104/pp.108.116632

Finkelstein, R. R., Gampala, S. S. L., and Rock, C. D. (2002). Abscisic acid signaling in seeds and seedlings. *Plant Cell* 14 Suppl, S15. doi: 10.1105/tpc.010441

Fu, X. Q., Shi, P., He, Q., Shen, Q., Tang, Y. L., Pan, Q. F., et al. (2017). AaPDR3, a PDR transporter 3, is involved in sesquiterpene β-Caryophyllene transport in *Artemisia annua*. *Front. Plant Sci.* 8, 723. doi: 10.3389/fpls.2017.00723

Hartung, W., Sauter, A., and Hose, E. (2002). Abscisic acid in the xylem: where does it come from, where does it go to? *J. Exp. Bot.* 53, 27–32. doi: 10.1093/jexbot/53.366.27

He, Q., Fu, X. Q.., Shi, P., Liu, M., Shen, Q., and Tang, K. X. (2017). Glandular trichome-specific expression of alcohol dehydrogenase 1 (ADH1) using a promoter-GUS fusion in *Artemisia annua* L. *Plant Cell Tiss. Org.* 130, 61–72. doi: 10.1007/s11240-017-1204-9

Jefferson, R. A. (1987). Asaying chimeric genes in plants: The GUS gene fusion system. *Plant Mol. Biol. Rep.* 5, 387–405. doi: 10.1007/BF02667740

Jing, F. Y., Zhang, L., Li, M. Y., Tang, Y. L., Wang, Y. Y., Wang, Y., et al. (2009). Abscisic acid (ABA) treatment increases artemisinin content in *Artemisia annua* by enhancing the expression of genes in artemisinin biosynthetic pathway. *Biologia* 64, 319–323. doi: 10.2478/s11756-009-0040-8

Kang, J., Hwang, J. U., Lee, M., Kim, Y. Y., Assmann, S. M., Martinoia, E., et al. (2010). PDR-type ABC transporter mediates cellular uptake of the phytohormone abscisic acid. *P. Natl. Acad. Sci. U.S.A.* 107, 2355–2360. doi: 10.1073/pnas.0909222107

Kanno, Y., Hanada, A., Chiba, Y., Ichikawa, T., Nakazawa, M., Matsui, M., et al. (2012). Identification of an abscisic acid transporter by functional screening using the receptor complex as a sensor. *P. Natl. Acad. Sci. U.S.A.* 109, 9653–9658. doi: 10.1073/pnas.1203567109

Kim, H., Hwang, H., Hong, J. W., Lee, Y. N., Ahn, I. P., Yoon, I. S., et al. (2012). A rice orthologue of the ABA receptor, OsPYL/RCAR5, is a positive regulator of the ABA signal transduction pathway in seed germination and early seedling growth. *J. Exp. B.* 63, 1013–1024. doi: 10.1093/jxb/err338

Koiwai, H., Nakaminami, K., Seo, M., and Mitsuhashi, W. (2004). Tissue-specific localization of an abscisic acid biosynthetic enzyme, AAO3, in *Arabidopsis*. *Plant Physiol.* 134, 1697–1707. doi: 10.1093/jxb/err338

Kumar, S., Stecher, G., and Tamura, K. (2016). MEGA7: molecular evolutionary genetics analysis version 7.0 for bigger datasets. *Mol. Biol. Evol.* 33, 1870–1874. doi: 10.1093/molbev/msw054

Kuromori, T., Miyaji, T., Yabuuchi, H., Shimizu, H., Sugimoto, E., Kamiya, A., et al. (2010). ABC transporter AtABCG25 is involved in abscisic acid transport and responses. *P. Natl. Acad. Sci. U.S.A.* 107, 2361–2366. doi: 10.4161/psb.5.9.12566

Kuromori, T., Sugimoto, E., and Shinozaki, K. (2011). Arabidopsis mutants of *AtABCG22*, an ABC transporter gene, increase water transpiration and drought susceptibility. *Plant J.* 67, 885–894. doi: 10.1093/molbev/msw054

Lee, M., Lee, K., Lee, J., Noh, E. W., and Lee, Y. (2005). AtPDR12 contributes to lead resistance in *Arabidopsis*. *Plant Physiol.* 138, 827–836. doi: 10.2307/4629886

Leung, J., and Giraudat, J. (1998). Abscisic acid signal transduction. *Annu. Rev. Plant Biol.* 49, 199. doi: 10.1146/annurev.arplant.49.1.199

Livak, K. J., and Schmittgen, T. D. (2001). Analysis of relative gene expression data using real-time quantitative PCR and the 2(-Delta Delta C(T)) Method. *Methods* 25, 402–408. doi: 10.1006/meth.2001

McAdam, S. A., Brodribb, T. J., and Ross, J. J. (2016a). Shoot-derived abscisic acid promotes root growth. *Plant Cell Environ.* 39 (3), 652–659. doi: 10.1111/pce.12669

McAdam, S. A., Manzi, M., Ross, J. J., Brodribb, T. J., and Gómez-Cadenas, A. (2016b). Uprooting an abscisic acid paradigm: Shoots are the primary source. *Plant Signal Behav.* 11 (6), e1169359. doi: 10.1080/15592324.2016.1169359

Mercke, P., Bengtsson, M., Bouwmeester, H. J., Posthumus, M. A., and Brodelius, P. E. (2000). Molecular cloning, expression, and characterization of amorpha-4,11-diene synthase, a key enzyme of artemisinin biosynthesis in *Artemisia annua* L. *Arch. Biochem. Biophys.* 381, 173–180. doi: 10.1006/abbi.2000.1962

Morita, M., Shitan, N., Sawada, K., Van Montagu, M. C., Inzé, D., Rischer, H., et al. (2009). Vacuolar transport of nicotine is mediated by a multidrug and toxic compound extrusion (MATE) transporter in *Nicotiana tabacum*. *P. Natl. Acad. Sci. U. S. A.* 106, 2447–2452. doi: 10.1073/pnas.0812512106

Olsson, M. E., Olofsson, L. M., Lindahl, A. L., Lundgren, A., Brodelius, M., and Brodelius, P. E. (2009). Localization of enzymes of artemisinin biosynthesis to the apical cells of glandular secretory trichomes of *Artemisia annua* L. *Phytochemistry* 70, 1123–1128. doi: 10.1016/j.phytochem.2009.07.009

Rea, P. A. (2007). Plant ATP-binding cassette transporters. *Annu. Rev. Plant Biol.* 58, 347–375. doi: 10.1146/annurev.arplant.57.032905.105406

Ro, D. K., Paradise, E. M., Ouellet, M., Fisher, K. J., Newman, K. L., Ndungu, J. M., et al. (2006). Production of the antimalarial drug precursor artemisinic acid in engineered yeast. *Nature* 440, 940–943. doi: 10.1038/nature04640

Savouré, A., Hua, X. J., Bertauche, N., Montagu, M. V., and Verbruggen, N. (1997). Abscisic acid-independent and abscisic acid-dependent regulation of proline biosynthesis following cold and osmotic stresses in *Arabidopsis thaliana*. *Mol. Gen. Genet.* 254, 104–109. doi: 10.1007/s004380050397

Schramek, N., Wang, H., Romischmargl, W., Keil, B., Radykewicz, T., Winzenhorlein, B., et al. (2010). Artemisinin biosynthesis in growing plants of *Artemisia annua.* A $13CO_2$ study. *Phytochemistry* 71, 179–187. doi: 10.1016/j.phytochem.2009.10.015

Shen, Q., Lu, X., Yan, T. X., Fu, X. Q., Lv, Z. Y., Zhang, F. Y., et al. (2016). The jasmonate-responsive AaMYC2 transcription factor positively regulates artemisinin biosynthesis in *Artemisia annua*. *New Phytol.* 210, 1269–1281. doi: 10.1111/nph.13874

Shen, Q., Zhang, L. D., Liao, Z. H., Wang, S., Yan, T. X., Shi, P., et al. (2018). The genome of *Artemisia annua* provides insight into the evolution of Asteraceae family and artemisinin biosynthesis. *Mol. Plant* 11 (6), 776–788. doi: 10.1016/j.molp.2018.03.015

Shinozaki, K., and Yamaguchi-shinozaki, K. (2007). Gene networks involved in drought stress response and tolerance. *J. Exp. Bot.* 58, 221. doi: 10.1093/jxb/erl164

Siefritz, F., Tyree, M. T., Lovisolo, C., Schubert, A., and Kaldenhoff, R. (2002). PIP1 plasma membrane aquaporins in tobacco: from cellular effects to function in plants. *Plant Cell* 14, 869–876. doi: 10.1105/tpc.000901

Stukkens, Y., Bultreys, A., Grec, S., Trombik, T., Vanham, D., and Boutry, M. (2005). NpPDR1, a pleiotropic drug resistance-type ATP-binding cassette transporter from *Nicotiana plumbaginifolia*, plays a major role in plant pathogen defense. *Plant Physiol.* 139, 341–352. doi: 10.1104/pp.105.062372

Sugiyama, A., Shitan, N., Sato, S., Nakamura, Y., Tabata, S., and Yazaki, K. (2006). Genome-wide analysis of ATP-binding cassette (ABC) proteins in a model legume plant, *Lotus japonicus*: comparison with Arabidopsis ABC protein family. *DNA Res.* 13, 205–228. doi: 10.1093/dnares/dsl013

Sun, L. R., Wang, Y. B., He, S. B., and Hao, F. S. (2018). Mechanisms for abscisic acid inhibition of primary root growth. *Plant Signal Behav.* 13 (9), e1500069. doi: 10.1080/15592324.2018.1500069

Tang, K. X., Shen, Q., Yan, T. X., and Fu, X. Q. (2014). Transgenic approach to increase artemisinin content in *Artemisia annua* L. *Plant Cell Rep.* 33, 605–615. doi: 10.1007/s00299-014-1566-y

Taylor, I. B., Burbidge, A., and Thompson, A. J. (2000). Control of abscisic acid synthesis. *J. Exp. B.* 51, 1563. doi: 10.1093/jexbot/51.350.1563

Teoh, K. H., Polichuk, D. R., Reed, D. W., Nowak, G., and Covello, P. S. (2006). *Artemisia annua* L. (Asteraceae) trichome-specific cDNAs reveal CYP71AV1, a cytochrome P450 with a key role in the biosynthesis of the antimalarial sesquiterpene lactone artemisinin. *FEBS Lett.* 580, 1411–1416. doi: 10.1016/j.febslet.2006.01.065

Teoh, K. H., Polichuk, D. R., Reed, D. W., and Covello, P. S. (2009). Molecular cloning of an aldehyde dehydrogenase implicated in artemisinin biosynthesis in *Artemisia annua*. *Botany-botanique* 87, 635–642. doi: 10.1139/B09-032

Theodoulou, F. L. (2000). Plant ABC transporters. *BBA-Biomembranes* 1465, 79–103. doi: 10.1016/S0005-2736(00)00132-2

Van Den Brûle, S., Müller, A., Fleming, A. J., and Smart, C. C. (2002). The ABC transporter SpTUR2 confers resistance to the antifungal diterpene sclareol. *Plant J.* 30, 649–662. doi: 10.1046/j.1365-313X.2002.01321.x

Verrier, P. J., Bird, D., Burla, B., Dassa, E., Forestier, C., Geisler, M., et al. (2008). Plant ABC proteins - a unified nomenclature and updated inventory. *Trends Plant Sci.* 13, 151–159. doi: 10.1016/j.tplants.2008.02.001

Voinnet, O., Rivas, S., Mestre, P., and Baulcombe, D. (2003). An enhanced transient expression system in plants based on suppression of gene silencing by the p19 protein of tomato bushy stunt virus. *Plant J.* 33, 949–956. doi: 10.1046/j.1365-313X.2003.01676.x

Vranová, E., Coman, D., and Gruissem, W. (2013). Network analysis of the MVA and MEP pathways for isoprenoid synthesis. *Annu. Rev. Plant Biol.* 64, 665–700. doi: 10.1146/annurev-arplant-050312-120116

Weathers, P. J., Elkholy, S., and Wobbe, K. K. (2006). Artemisinin: The biosynthetic pathway and its regulation in *Artemisia annua*, a terpenoid-rich species. *Vitro Cell Dev-Pl.* 42, 309–317. doi: 10.1079/IVP2006782

World Health Organization (2017). *World Malaria Report 2017*. Available at: http://www.who.int/malaria/publications/world-malaria-report-2017/report/en/

Yu, F., and De Luca, V. (2013). ATP-binding cassette transporter controls leaf surface secretion of anticancer drug components in *Catharanthus roseus*. *P. Natl. Acad. Sci. U. S. A.* 110, 15830–15835. doi: 10.1073/pnas.1307504110

Zhang, X., Zhang, L., Dong, F. C., Gao, J. F., Galbraith, D. W., and Song, C. P. (2001). Hydrogen peroxide is involved in abscisic acid-induced stomatal closure in *Vicia faba*. *Plant Physiol.* 126, 1438–1448. doi: 10.1104/pp.126.4.1438

Zhang, Y., Teoh, K. H., Reed, D. W., Maes, L., Goossens, A., Olson, D. J., et al. (2008). The molecular cloning of artemisinic aldehyde Delta11(13) reductase and its role in glandular trichome-dependent biosynthesis of artemisinin in. *Artemisia Ann. J. Biol. Chem.* 283, 21501–21508. doi: 10.1074/jbc.M803090200

Zhang, L., Jing, F. Y., Li, F., Li, M. Y., Wang, Y. Y., Wang, G. F., et al. (2009). Development of transgenic *Artemisia annua* (Chinese wormwood) plants with an enhanced content of artemisinin, an effective anti-malarial drug, by hairpin-RNA-mediated gene silencing. *Biotech. Appl. Biochem.* 52, 199–207. doi: 10.1042/BA20080068

Zhang, F. Y., Lu, X., Lv, Z. Y., Zhang, L., Zhu, M. M., Jiang, W. M., et al. (2013). Overexpression of the *Artemisia* orthologue of ABA receptor, AaPYL9, enhances ABA sensitivity and improves artemisinin content in *Artemisia annua* L. *PloS One* 8, e56697. doi: 10.1371/journal.pone.0056697

Zhang, H. W., Zhu, H. F., Pan, Y. J., Yu, Y. X., Luan, S., and Li, L. G. (2014). A DTX/MATE-type transporter facilitates abscisic acid efflux and modulates ABA sensitivity and drought tolerance in Arabidopsis. *Mol. Plant* 7, 1522–1532. doi: 10.1093/mp/ssu063

Zhang, F. Y., Fu, X. Q., Lv, Z. Y., Lu, X., Shen, Q., Zhang, L., et al. (2015). A basic leucine zipper transcription factor, AabZIP1, connects abscisic acid signaling with artemisinin biosynthesis in *Artemisia annua*. *Mol. Plant* 8, 163–175. doi: 10.1016/j.molp.2014.12.004

Zhong, Y. J., Li, L., Hao, X. L., Fu, X. Q., Ma, Y. N., Xie, L. H., et al. (2018). AaABF3, an abscisic acid-responsive transcription factor, positively regulates artemisinin biosynthesis in *Artemisia annua*. *Front. Plant Sci.* 9, 1777. doi: 10.3389/fpls.2018.01777

Zhou, B. Y., Guo, Z. F., and Lin, L. (2006). Effects of abscisic acid application on photosynthesis and photochemistry of stylosanthes guianensis under chilling stress. *Plant Growth Regul.* 48, 195–199. doi: 10.1007/s10725-006-0005-7

Zhu, J. K. (2002). Salt and drought stress signal transduction in plants. *Annu. Rev. Plant Biol.* 53, 247–273. doi: 10.1146/annurev.arplant.53.091401.143329

Conflict of Interest: The authors declare that the research was conducted in the absence of any commercial or financial relationships that could be construed as a potential conflict of interest.

The reviewer LZ declared a past co-authorship with several of the authors XF, LL, KT to the handling Editor.

Advantages of publishing in Frontiers

OPEN ACCESS
Articles are free to read for greatest visibility and readership

FAST PUBLICATION
Around 90 days from submission to decision

HIGH QUALITY PEER-REVIEW
Rigorous, collaborative, and constructive peer-review

TRANSPARENT PEER-REVIEW
Editors and reviewers acknowledged by name on published articles

Frontiers
Avenue du Tribunal-Fédéral 34
1005 Lausanne | Switzerland

Visit us: www.frontiersin.org
Contact us: info@frontiersin.org | +41 21 510 17 00

REPRODUCIBILITY OF RESEARCH
Support open data and methods to enhance research reproducibility

DIGITAL PUBLISHING
Articles designed for optimal readership across devices

FOLLOW US
@frontiersin

IMPACT METRICS
Advanced article metrics track visibility across digital media

EXTENSIVE PROMOTION
Marketing and promotion of impactful research

LOOP RESEARCH NETWORK
Our network increases your article's readership